University of Sheffield

Exploring the role of αB-crystallin in resistance to anti-angiogenic therapies

A thesis submitted in partial fulfilment of the requirements for the degree of Doctor of Philosophy by

Marwa Abdullah Alsharif

The University of Sheffield

Faculty of Medicine, Dentistry and Health

Department of Oncology and Metabolism

January 2023

Acknowledgements

First, praise is to Almighty Allah for providing me with the strength, determination and patience to complete my study.

This thesis would not have been accomplished without the supervision of Professor Penelope Ottewell. I want to thank her for supervising me halfway through my PhD. Her support, understanding and immense knowledge helped to complete my practical work and write my thesis. I am deeply indebted to my second supervisor Dr Chryso Kanthou for her constant professional and personal support throughout my PhD study. In particular, I would like to thank her for teaching me how to perform several experiments and for her feedback and corrections to my thesis. I sincerely appreciate Professor Nicola Brown for her valuable orientation, feedback and corrections to my thesis. Dr Chryso Kanthou and Professor Nicola Brown had their retirement halfway through my PhD. However, they were incredibly kind to keep monitoring me and assisting me in reaching this life milestone. Thank you is not enough to express my gratitude to them. I would also like to thank my government for giving me this great opportunity and funding my project.

During my PhD journey, I was lucky to work with great scientists who helped me in several experiments; thank you to Jiabao Zhou, Lubaid Saleh, Ruth Thomas, Margherita Puppo and Diane Lefley. My special thanks to Matthew Fisher and Maggie Glover for their help in my *in vivo* work and immunohistochemistry.

With all love, my special thanks go to my husband Feras for his love, understanding, sacrifices and unwavering support. I would be remiss in not mentioning my parents; your belief in me has given me the courage and patience to complete my study. My little ones, the ones who have witnessed every single day in this journey, Ola and Faisal, thank you for your motivating words, assistance, and tolerance on the hard days. I sincerely appreciate the support that comes from my parents-in-law; thank you for your prayers and support. I am thankful to my siblings Bushra, Safa, Seba, Bader, Omer, and Rufaida for their prayers and emotional support. Also, I express my thanks to my friends, Nashwa and Haifa, for their advice and help during my study.

Abstract

Anti-VEGF therapies have not improved the overall survival in breast cancer and many patients show no response to these treatments. The causes of this innate resistance need to be investigated so that they can be targeted in order improve the efficacy of these treatments. Additionally, identification of biomarkers can be utilised to select patients who are more likely to respond to treatments. αB-crystallin is a small heat shock protein encoded by the *CRYAB* gene and known to function as a chaperone protein. Its function is to protect misfolded proteins from degradation and apoptosis under stress conditions. αB-crystallin is thought to protect VEGF from degradation and support its stability. αB-crystallin is significantly upregulated in tumour vasculature during angiogenesis and after anti-VEGF treatment. Protecting VEGF from degradation and increasing its stability may stimulate tumour growth and contribute to resistance to anti-VEGF therapies. Therefore, this project tests the hypothesis that αB-crystallin contributes to the resistance to anti-VEGF therapies in breast cancer. To test this hypothesis, I made transgenic triple negative, MDA-MB-231, breast cancer cells that produce different levels of αB-crystallin (MDA-MB-231/*CRYAB*) and control cells that do not produce αB-crystallin (MDA-MB-231/WT). These cells were compared with triple negative breast cancer cells that naturally produce high amounts of αB-crystallin (MDA-MB-468) and MDA-MB-468 cells in which levels of αB-crystallin have been reduced by siRNA. *In vitro,* VEGF production from breast cancer cells expressing different levels of αB-crystallin were measured by ELISA after heat shock (42°C/24h), or hypoxia (0.1% O_2/24h) and sensitivity to doxorubicin induced apoptosis was measured by flow cytometry. *In vivo*: MDA-MB-231/WT and MDA-MB-231/*CRYAB* cells were administered by intra-ductal injection into BALB/c nude mice 7-days prior to PBS (control), 4 mg/kg/week doxorubicin, 7.5 mg/kg/3X per week bevacizumab or a combination of both. Tumour growth was measured using callipers, tumour/microenvironmental VEGF analysed by ELISA and tumour microvascular density (MVD) was assessed following CD31 and CD34 immunohistochemistry. The data showed that under heat shock and hypoxia, overexpression of *CRYAB* in MDA-MB-231 cells reduced VEGF expression compared to wild-type cells, whereas the knockdown of *CRYAB* in MDA-MB-468 resulted in more VEGF compared to wild-types cells. *In vivo*: MDA-MB-231/WT tumours grew more rapidly and produced more VEGF compared with MDA-MB-231/*CRYAB* tumours. Bevacizumab alone reduced tumour growth in MDA-MB-231/WT cells but not in MDA-MB-

231/*CRYAB* cells. However, resistance to Bevacizumab was overcome by the addition of doxorubicin with the combination of doxorubicin and bevacizumab synergistically reducing tumour volume and VEGF levels of MDA-MB-231/*CRYAB* tumours but not MDA-MB-231/WT tumours. Furthermore, vascular marker expression was very low in MDA-MB-231/*CRYAB* tumours compared to MDA-MB-231/WT tumours. The *in vitro* and *in vivo* results suggest that αB-crystallin negatively regulates VEGF and breast cancer growth and angiogenesis. Overall, αB-crystallin may act as a tumour suppressor protein in our system by inactivating VEGF production. This needs further investigation to reveal its role in oncogenic-related pathways.

Table of Contents

List of Figures

List of Tables

List of Abbrevations

ABC-HRP	Horseradish peroxidase-conjugated avidin-biotin complex
APS	Ammonium persulfate
Bax	Bcl-2-associated X protein
BCA	Bicinchoninic acid assay
BCL2	B-cell lymphoma 2
cDNA	Complimentary DNA
CEPs	Circulating endothelial progenitor cells
CPCs	Circulating progenitor cells
CT	Computerised tomography
DAB	3,3'-diaminobenzidine
DMEM	Dulbecco's Modified Eagle Medium
DMSO	Dimethyl sulfoxide
DTT	Dithiothreitol
EDTA	Ethylenediaminetetraacetic acid
EGFR	Epidermal growth factor receptor
ELISA	Enzyme-linked immunosorbent assay
EMEA	European Medicines Agency
EMT	Epithelial mesenchymal transition
EPCs	Endothelial progenitor cells
ER	Oestrogen receptor
ERK	Extracellular signal-regulated kinases
EtOH	Ethanol
FBS	Fetal bovine serum
FDA	Federal Drug Agency
FDA	Food and Drug Administration
FFPE	Formalin fixed paraffin embedded (FFPE)
FGF	Fibroblast growth factors
FGFR	Fibroblast growth factor receptor
FSC	Forward scatter
H&E	Haematoxylin and eosin (H & E)
HCC	Hepatocellular carcinoma
HDBEC	Human Dermal Blood Endothelial Cells
HER2	Human dermal receptor 2
HIER	Heat-induced epitope retrieval
HIF-1	Hypoxia-inducible transcription factor 1
HNSCCs	Head and neck squamous cell carcinomas
HSPs	Heat shock proteins
I.v	Intra-venous injection
IC50	Half maximal inhibitory concentration
IGF	Insulin like Growth Factor
IHC	Immunohistochemistry
IMS	Industrial methylated spirit
IP	Intraperitoneal injection
kDa	Kilo Dalton

mAb	Monoclonal antibody
MAPK	Mitogen-activated protein kinase
mCRC	Metastatic colorectal cancer
MDA-MB-231	M.D. Anderson- Metastasis Breast cancer
MDA-MB-231/*CRYAB*	MDA-MB-231/*CRYAB*
MDA-MB-231/WT	MDA-MB-231/ Wild type
miRNA	Micro RNA
MRI	Magnetic resonance imaging
mRNA	Messenger RNA
MVD	Microvessel density
NGS	Next generation sequencing
NGS	Nottingham Grading System
NPC	Nasopharyngeal carcinoma
NPI	Nottingham Prognostic Index
NSCLC	Non-small cell lung cancer
NSCLC	Non-squamous non-small cell lung carcinoma
NST	Invasive Carcinoma of No Special Type
NST	Invasive Carcinoma of No Special Type
OS	Osteosarcoma
OV	Overall survival
PBS	Phosphate buffered saline
PD-1	programmed cell death 1 (PD-1)
PDGF	Platelet-derived growth factor
PD-L1	programmed cell death ligand 1
PFS	progression-free survival
PI3K	Phosphatidylinositol 3-kinase
PIGF	Placenta growth factor
PKC	Protein kinase C
PLCγ	Phospholipase Cγ
PR	Progesterone receptor
RCC	Renal cell carcinoma
RIPA	Radioimmunoprecipitation assay
RPE	Retinal pigment epithelium
rpm	Revolutions per minute
RTK	Receptor tyrosine kinase
SDF1 α	Stromal cell-derived factor 1α
SDS	Sodium dodecyl sulphate
SDS-PAGE	Sodium Dodecyl Sulfate Polyacrylamide Gel Electrophoresis.
SEM	Standard error of the mean
SFM	Serum free medium
sHSPs	Small heat shock proteins
siRNA	Short interfering RNA
SSC	Side scatter
TAF	Tumour angiogenic factors
TAF	Tumour associated fibroblasts
TBS	Tris-buffered saline
TBT-T	Tris-buffered saline-Tween

TEMED	Tetramethylethylenediamine
TGFβ	Transforming growth factor-β
TKI	Tyrosine kinase inhibitor
TNBC	Triple negative breast cancer
VDAs	Vascular disrupting agents
VEGF	Vascular endothelial growth factor
VEGF	Vascular endothelial growth factor A
VEGF-B	Vascular endothelial growth factor B
VEGF-C	Vascular endothelial growth factor C
VEGF-D	Vascular endothelial growth factor D
VEGF-E	Vascular endothelial growth factor E
VEGF-F	Vascular endothelial growth factor F
VEGFR	Vascular endothelial growth factor receptor
VEGFR	Vascular endothelial growth factor receptor
VEGFR1	Vascular endothelial growth factor receptor 1
VEGFR2	Vascular endothelial growth factor receptor 2
VEGFR3	Vascular endothelial growth factor receptor 3

Chapter1 **Introduction**

Angiogenesis is the formation of new blood vessels from existing ones and is a critical process associated with several physiological functions, including embryonic development and wound healing. Angiogenesis also plays an important role in pathological conditions such as tumour growth and progression. Vascular endothelial growth factor (VEGF) is a major inducer of tumour angiogenesis and anti-angiogenic treatments that target VEGF have been used in treating many cancers, including breast cancer. The use of these treatments, have differential outcomes, depending on the cancer type. In breast cancer, anti-angiogenic agents are used in combination with chemotherapies in treating metastatic disease. However, many patients do not respond to these treatments and often the initial responsive patients develop resistance. There is an urgent need to understand why patients develop resistance to these treatments, so that resistance can be targeted. In addition, identifying the patients who are more likely to respond to combination therapy with antiangiogenic agents is another approach to maximise clinical benefit.

αB-crystallin is a heat shock protein that is highly expressed in aggressive types of breast cancer such as basal like and triple negative breast cancer. αB-crystallin acts as anti-apoptotic protein that prevents aggregation of proteins under stress conditions. In addition to heat, it is upregulated by chemotherapeutic agents. Importantly, αB-crystallin stabilises VEGF and promotes its secretion and is thought to act to promote angiogenesis in cancer. It is hypothesised that αB-crystallin, through its protective function on VEGF, confers resistance to anti-VEGF treatments. This introduction will start with a background on the various subtypes of breast cancer, followed by a description of how angiogenesis develops in cancer, the role of VEGF in tumour angiogenesis and how VEGF and angiogenesis can be targeted with anti-angiogenic drugs. Mechanisms of resistance to anti-VEGF treatments and the current approaches to overcome resistance will also be discussed. In addition, the role of αB-crystallin as an anti-apoptotic and proangiogenic factor in breast cancer and its potential contribution to resistance to anti-angiogenic treatments will be discussed.

1.1 Breast cancer

Between 2016 and 2018, there were around 55,920 new cases of breast cancer diagnosed in the UK, and breast cancer is the most common cancer among females (UK 2018) . Breast cancer is a heterogeneous disease that mainly arises from breast tissue that lines the milk ducts or the lobules (Sharma *et al.* 2010).The traditional classification of breast cancer was based on histological characteristics and tumour grade (Weigelt and Reis-Filho 2009). Following the evolution of microarrays, breast cancers are classified according to their molecular characteristics, which are based on gene expression patterns.

1.1.1 Histopathological classification

Histopathological classification divides breast cancer into two types; *in situ* (ductal and lobular) and invasive breast cancer. There are more than 21 subtypes of invasive breast carcinoma, and the most frequent type is Invasive Carcinoma of No Special Type (NST), also known as invasive ductal carcinoma. NST constitutes around 60–75% of all breast cancers (Eliyatkın *et al.* 2015) . The remaining tumour types are histological special types, which are morphologically distinct including invasive lobular, tubular, mucinous and metaplastic carcinoma, and carcinoma with medullary, neuroendocrine, or apocrine features and they all constitute about 20–25% of all breast cancers. Although the histological special types provide prognostic information, they are relatively uncommon (Eliyatkın *et al.* 2015).

Histological tumour grade is determined by the degree of differentiation of the tumour tissue. The grade is determined by assessing three morphological features: a) the degree of tubular formation, b) the degree of nuclear pleomorphism, and c) the mitotic count. Each feature is assigned a score and then combined to give a grade between 1-3, where grade 1 tumours are the most differentiated and grade 3 are the least. This grading system is known as Nottingham Grading System (NGS) and is combined with lymph node stage and tumour size to form prognostic indices: the Nottingham Prognostic Index (NPI) (Rakha *et al.* 2010, Vuong *et al.* 2014).

Histopathological classification of breast cancer has some drawbacks, such as it is widely subjective and depends on the pathologist's decision. The biological and prognostic variations of breast cancer and the development of gene expression techniques has resulted in the development of other taxonomy based on gene expression profiles.

1.1.2 Microarray-based gene expression profiling of breast cancer

The taxonomy is based on the variations of gene expression patterns of breast tumour tissues, using cDNA microarrays. Perou *et al.* (2000) first classified breast cancer based on molecular characteristics into Luminal-like breast cancer (Oestrogen receptor positive ER-positive), Human dermal receptor 2 (HER2) positive breast cancer, basal-like breast cancer, and normal-like breast cancer. A further study divided the luminal-like breast cancer into luminal A and Luminal B (Sørlie 2004). Outcomes of patients were associated with specific molecular subtypes, such as poor prognosis was associated with the basal-like subtype, suggesting that the molecular-based classification has improved the prognosis of breast cancer. In clinical practice, gene expression profiles are combined with other factors that can be identified by immunohistochemistry. For example, the proliferation marker such as Ki67 is used beside the gene expression profile to distinguish between luminal A and luminal B cancers. In addition, to differentiate between "luminal", HER2+, and basal-like breast cancer, basal cytokeratins (CK14 and CK5/6 and the epidermal growth factor receptor (EGFR) can also be used as markers (Eliyatkın *et al.* 2015).

1.1.2.1 Luminal-like breast cancer

Luminal-like breast cancer is oestrogen receptor positive (ER-positive) and is subdivided into Luminal A, and Luminal B. Around 50%-60% of all breast cancers are Luminal A and characterized by lower levels of Ki67, positive or negative of progesterone receptor (PR), low histological grade and are HER2-negative. Patients with Luminal A have an improved prognosis, and treatments are hormone based. Luminal B comprises 15-20% of all breast cancers, is of a higher-grade, PR-positive or negative, HER2-negative or positive and with high levels of Ki67. Luminal B is associated with poor prognosis and increased relapsed rate compared to luminal A. Treatments are also hormonal, however, Luminal B are less responsive to hormonal therapy compared to Luminal A (Vuong *et al.* 2014, Yersal and Barutca 2014).

1.1.2.2 Human dermal receptor 2 HER2 positive breast cancer

HER2-positive tumours account for 15-20% of breast cancer subtypes. They are characterised by the high expression of the HER2 gene. These tumours have a poor prognosis and confer

more aggressive biological characteristics. They are highly proliferative and have a high histological grade (Eliyatkın *et al.* 2015).

1.1.2.3 Basal Like breast cancer

Basal-like breast cancer represents between 8% to 37% of all breast cancers, and are aggressive tumours, mostly grade 3. They are known with triple negative breast cancer due to the lack of hormone receptors and HER2. They are characterised by high expression of high-molecular-weight cytokeratins CK 5/6, CK14 and epidermal growth factor receptor (EGFR) (Yersal and Barutca 2014). Triple negative breast cancer is not always a synonym of basal-like breast cancer. Triple-negative breast cancer can be identified by immunohistochemistry and has some subgroups that do not express basal cytokeratin genes, whereas the term “basal-like breast cancer” is based on the gene expression profile. (Kreike *et al.* 2007). Claudin-low tumours are another aggressive sub-type that show several common features with basal-like-like tumours. This sub-type was identified by low expression of genes involved in tight junctions and cell-cell adhesion, including Claudins 3, 4, 7, Occludin, and E-cadherin (Herschkowitz *et al.* 2007).

1.1.2.4 Normal-like breast cancer

These tumours account for about 5%-10% of all breast carcinomas. They are classified as triple-negative as they lack the expression of ER, PR and HER2, but they are not basal-like cancer because they are negative for CK5 and EGFR (Yersal and Barutca 2014).

1.2 Next generation sequencing (NGS)

The development of NGS has advanced the genetics and genomes of breast cancer and has revolutionised breast cancer prognosis. NGS involves sequencing the whole-genome, whole-exome sequencing, cancer derived gene sequencing, and hotspot sequencing, which sequences specific regions or regions with recurrent mutations of genes of interest. NGS has been used to characterise genomic alterations such as copy number changes, loss/gain, and mutations. It also helps to identify sub clonal mutations and in separating the "driver" mutations that are thought to be important in the development of cancer from the "passenger" mutations that do not appear to be important in the progression of the disease (Yersal and Barutca 2014).

1.3 Development of a blood vessel network: embryonic vasculogenesis and angiogenesis

Primitive blood vessels are formed from mesoderm during the embryonic development by the differentiation of mesodermal stem cells called angioblasts that form the primary capillary plexus. This process is referred to as vasculogenesis (Risau and Flamme 1995). The established capillary plexus undergoes differentiation and remodelling to generate new blood vessels through a process called angiogenesis (Chung and Ferrara 2011, Kolte *et al.* 2016). Angiogenesis is an active pathway during the developmental stage and becomes quiescent in healthy adult tissues. However, in certain pathologies such as diabetic retinopathy and proliferating tumours, the formation of new blood vessels increases (Chung and Ferrara 2011). Angiogenesis is mediated by binding of proangiogenic factors to their receptors on endothelial cells. The main mediator of angiogenesis is VEGF through its binding to vascular endothelial growth factor receptor 2 (VEGFR2) as well as other VEGF receptors. In addition, there are other pathways involve in the regulation of angiogenesis which will be discussed in the subsequent section. Angiogenesis can occur by at least two mechanism; sprouting angiogenesis and Intussusceptive angiogenesis (Risau 1997).

1.3.1 Sprouting angiogenesis

Sprouting angiogenesis is the formation of new capillary vessels out of pre-existing ones (Figure 1.1 A) (Hillen and Griffioen 2007, Styp-Rekowska *et al.* 2011). It starts with binding of proangiogenic factors with their receptors on endothelial cells. This activates a series of steps, starting with degradation of the extracellular matrix and the basement membrane surrounding the endothelial cells. This allows the migration of endothelial through the matrix. Following this, the endothelial cells proliferate, form a lumen and create a new extracellular matrix (Hillen and Griffioen 2007). In healthy tissues, angiogenesis is controlled by a balance between pro-angiogenic molecules such as VEGF, fibroblast growth factors (FGFs), platelet-derived growth factor (PDGF), epidermal growth factor (EGF), and antiangiogenic factors such as thrombospondin-1, endostatin, tumstatin and canstatin (Bergers and Benjamin 2003, Hillen and Griffioen 2007). The stimulation of angiogenesis starts with binding of proangiogenic factor to its receptor on endothelial cells. The main mediator of this pathway is VEGF through its binding to VEGFRs on endothelial cells. During this process, endothelial cells differentiate into different phenotypes. Initially, endothelial cells differentiate into tip cells that act to guide the migrating cells into an emerging sprout toward the proangiogenic

gradient. Following this, the endothelial cells called stalk cells migrate and proliferate along the sprout, forming a lumen (Blanco and Gerhardt 2013). This process is controlled by the Notch pathways that regulates endothelial cell fate determination. Tip cells migrate toward the VEGF gradient and express high levels of delta-like ligand 4 (DLL-4) that binds to Notch in adjacent stalk cells. This interaction leads to downregulation of VEGFR2 expression in these cells. This is an important regulatory step to prevent the formation of new tip cells and favours their differentiation into stalk cells. In addition, stalk cells express Jagged-1, which is a proangiogenic factor that antagonises the DII4 Notch pathway. Stalk cells also express high level of vascular endothelial growth factor receptor-1 (VEGFR1) which traps VEGF and prevents the formation of new tip cells. Stalk cells then proliferate and migrate into the emerging sprout, forming a lumen, a basement membrane and recruit mural cells (pericytes) for stabilisation of the blood vessel. This pathway of Notch is thought to be transient and tip cells then change into a phalanx phenotype, which integrate into the endothelial cell lining of adjacent capillaries in a process called anastomosis (Risau 1997, Thurston and Kitajewski 2008, Chung and Ferrara 2011, Ribatti and Crivellato 2012, Blanco and Gerhardt 2013).

1.3.2 Intussusceptive angiogenesis

Intussusceptive angiogenesis is a type of angiogenesis that is distinct from sprouting (Figure 1.1 B) (Styp-Rekowska *et al.* 2011). This process involves splitting of pre-existing vessels into two new vessels by the formation of a transvascular tissue pillar into the lumen of the vessel. This type of angiogenesis starts by splitting of the blood vessels by transluminal pillars, which are then covered by pericytes and myofibroblasts. At the final stage, the endothelial cells retract, the pillars enlarge, and two separated vessels are produced (Hillen and Griffioen 2007, Ribatti and Crivellato 2012).

1.4 Tumour Angiogenesis

In 1971, there was a significant advancement in tumour angiogenesis research through the seminal research of Judah Folkman, who hypothesised that a tumour is dependent on angiogenesis for continued growth. He also predicted that tumour cells produce diffusible tumour angiogenic factors (TAFs) and proposed the idea of antiangiogenesis with a TAF antibody, as a form of cancer treatment (Folkman 1971, Folkman 2008).

1.4.1 Angiogenic switch

Folkman proposed that tumours do not grow beyond few millimetre in the absence of a vasculature and remain dormant (Folkman 1971). Tumours become vascularised in response to growth factors produced by the cancer cells that lead to the differentiation and sprouting of endothelial cells. The rapid and continued growth of the tumour leads to an imbalance between oxygen supply and consumption and that causes hypoxia in the tumour microenvironment. Tumour angiogenesis is controlled by the balance between proangiogenic factors and antiangiogenic factors. To meet the metabolic demands of a hypoxic microenvironment, production of pro-angiogenic growth factors and activation of several downstream signalling factors increase, hence the angiogenic switch is established in the tumour microenvironment (Bergers and Benjamin 2003, Verheul *et al.* 2004). VEGF signalling pathways are upregulated to activate the sprouting of new blood vessels. Blood vessel proliferation and sprouting in the tumour microenvironment results in an increase in the permeability of tumour blood vessels. Endothelial cells in the tumour microenvironment continuously remodel and differentiate, vessels become leaky and more permeable, which can attract platelets and activate them. Activated platelets then release growth factors, for instance platelet derived growth factor (PDGF) (Bergers and Benjamin 2003) that support further angiogenesis and tumour growth. The increasing rate of these sequential events generate weak vessels with less abundant perivascular cells (pericytes). The perivascular coverage is important in blood vessel maturation. However, the perivascular cells in the tumour vasculature associate loosely with the endothelial cells and do not function properly (Morikawa *et al.* 2002). The disruption of these functions mediates irregular blood flow in the tumour. In addition, other growth factors are recruited to tumour site such as FGF. Furthermore, inflammatory cells start to deposit in the stroma as a response to this inflammation where they release cytokines and growth factors (Bergers and Benjamin 2003, Komohara and Takeya 2017). In contrast to the normal physiological function of angiogenesis, the tumour vasculature continues growing and remodelling and losses the balance between the positive and negative control, hence it is described as a ‘wound that never heals’ (Dvorak 1986, Bergers and Benjamin 2003).

1.4.2 Structural and functional characteristics of tumour blood vessels

As a consequence of aberrant angiogenesis, tumour blood vessels are different from normal blood vessels in terms of their structure, organisation and function (Fukumura and Jain 2007). Unlike the normal vasculature which is arranged in a hierarchical order with well-differentiated arterioles, capillaries, and venules, the tumour vasculature is disorganised, chaotic, dilated, and tortuous. Normal vasculature has dichotomous branching with even diameters, but tumour vasculature has trifurcations and branches with variable sizes. The pericytes in tumour blood vessels exhibit aberrant shape and show less association with blood vessels. In addition, the tumour vasculature has widened and weak inter-endothelial junctions, an increased number of fenestrations, vesicles, and vesico-vacuolar channels, and lacks a normal basement membrane (Dvorak 2002, Azzi *et al.* 2013). Because of these characteristics, tumour blood vessels are often described as immature, and their function is abnormal. The defective tumour vessels exhibit hyperpermeability due to their poor endothelial junctions and poor pericyte coverage and the constant production of proangiogenic factors. VEGF which is a potent pro-angiogenic factor is also known for its vascular permeability inducing properties. Aberrant expression of VEGF in the tumour contributes to the immature and abnormal characteristics of the tumour blood vessels. In addition, tumour blood flow is poorly distributed, changes over time and can stop altogether, and flow can even reverse direction in some vessels. (Fukumura and Jain 2007). As a consequence, regions with poor or no perfusion are prevalent, which results in hypoxia in the tumour microenvironment (Azzi *et al.* 2013). In addition to the defective blood vessels, the tumour microenvironment lacks or has non-functional lymphatic vessels, which can lead to poor drainage of fluid and interstitial proteins from the tumour tissue, which increase the interstitial fluid pressure (Heldin *et al.* 2004). Taken together, the abnormal morphology and characteristics of tumour vasculature contribute to non-functional blood vessels and the hypoxic nature of the tumour microenvironment.

1.5 Hypoxia and hypoxia inducible factors

It is well known that most solid tumours develop hypoxia, which results from the imbalance created due to the low oxygen supply and high oxygen and nutrient consumption by growing tumour cells. The dysfunctional vasculature in the tumour microenvironment impairs blood

flow and increases hypoxia. Hypoxia leads to a complex microenvironment and is considered as a poor prognosis factor.

In a hypoxic microenvironment, hypoxia-inducible transcription factor 1 (HIF-1) is induced and activates different gene targets, including *VEGF* (Harris 2002). HIF-1 is a heterodimeric protein consisting of HIF-α and HIF-1β subunits. HIF-1β is present in tissues under all oxygen levels, while HIF-α is found under hypoxic conditions. HIF-α levels must be induced, for the HIF-1 transcriptional complex to be functional. The Sp1 transcription factor is primarily responsible for the constitutive expression of the *HIF-1* gene. Other transcription factor binding sites, such as AP-1 and 2, NF-1, and NF-KB, can also be found in the promoter region of the *HIF-1* gene. Oxygen levels influence the stability of the HIF1-α subunit. Under normal oxygen levels, three specific oxygen-dependent proline-hydroxylases (PHD 1–3) hydroxylate two key proline residues in HIF1-α within its oxygen-dependent degradation domain. The hydroxylated HIF1-α is recognised by the von Hippel–Lindau tumour suppressor protein (pVHL) and E3 ubiquitin ligase complex, which leads to ubiquitylation of HIF-1α, hence leading to its proteasomal degradation. In hypoxic conditions, the PHD enzymes are inhibited due to the lack of oxygen, therefore HIF1-α is not targeted for degradation. Once stabilised, HIF1-α transfers to the nucleus and can dimerise with HIF-1β. The HIF-1 heterodimer that is formed then binds to hypoxic response elements in the promoter regions of its target genes such as *VEGF*, activating their expression. In addition, HIF-α can be hydroxylated by factor inhibiting HIF-1 (FIH) at an asparagine residue and this inhibits its interaction with the coactivator p300/CBP, therefore inhibiting transcriptional activation (Déry et al. 2005, Ziello et al. 2007, Jing et al. 2019).

HIF-1 also undergoes hypoxia-independent regulation (Maxwell *et al.* 1999, Richard *et al.* 1999, Semenza 2003, Déry *et al.* 2005, Tanaka *et al.* 2006, Ziello *et al.* 2007). For example, phosphorylation by p42/p44-mitogen-activated protein kinases results in increased transcriptional activity of the HIF-1 complex (Richard *et al*. 1999). Moreover, HIF-1 can also accumulate due to excessive translation (Déry *et al*. 2005). The increase in protein translation appears to be sufficient to tip the balance between synthesis and degradation in favour of normoxic HIF-1 accumulation (Déry et al. 2005). Genetic alteration in von Hippel-Lindau (VHL), which encodes the von Hippel-Lindau tumour suppressor protein (pVHL), has been reported to be responsible for the stabilization of HIF-1α subunits (Maxwell *et al.* 1999). This led to the

hypoxia-independent activation of HIF-1 in two VHL-deficient renal carcinoma cell lines, RCC4 and 786-O. Consequently, this activation upregulated mRNAs responsible for encoding hypoxically inducible proteins such as VEGF and glucose transporter 1 in these tumour cells (Maxwell *et al.* 1999). The PI3K/Akt and MAPK signalling pathways activate mammalian target of rapamycin and the protein-synthesizing machinery, which in turn promotes HIF-1 expression and activation. HIF-1 can be activated by autocrine processes since it transactivates growth factor genes such as VEGF, insulin-like growth factor 2, and transforming growth factor, the products of which can activate PI3K/Akt and MAPK signalling (Semenza 2003). HIF-1 expression was significantly reduced in mouse hepatocellular carcinoma (HCC) cell lines after treatment with the PI3K inhibitor LY294002, demonstrating that HIF-1 expression is dependent on PI3K/Akt signalling (Tanaka *et al.* 2006).

1.6 Methods of tumour vascularisation other than angiogenesis

In addition to angiogenesis, tumours can acquire a blood vessel network through other mechanisms. These include vessel co-option, vasculogenic mimicry and vasculogenesis (Figure 1.1).

1.6.1 Vessel co-option

Vessel co-option occurs when the tumour cells do not induce an angiogenic response, but instead grow along the pre-existing vessels of normal tissues and/or tumour cells may invade the space between the pre-existing vasculature, leading to the incorporation of blood vessels into the tumour mass (Figure 1.1 C). This vascular phenotype was observed with tumours in highly vascularised organs to facilitate in the metabolic demand and potential for metastasis without inducing angiogenesis (Holash *et al.* 1999, Stessels *et al.* 2004, Hillen and Griffioen 2007). Vessel co-option has been observed in various primary and metastatic cancers such as breast cancer that metastasised to liver, melanomas, and lung carcinoma (Döme *et al.* 2002, Stessels *et al.* 2004, Travis *et al.* 2011). Vessel co-option was detected in a glioma model in which tumour cell early growth utilized co-option followed by an angiogenic response. Initially, tumour cells were co-opted to the existing host blood vessels (Holash *et al.* 1999). The co-opted vessels then underwent high regression, which is thought to be a host defensive mechanism. The remaining tumour cells then activated an angiogenic response (Holash *et al.* 1999). This process in which co-option is followed by angiogenesis is only one form of co-option and the process is highly varied dependent on the cancer cell type or the site of vessel

co-option. Another form of co-option was observed in bronchoalveolar carcinoma, a non-small cell lung cancer subtype, where lung cancer cells were observed to grow along the alveolar walls and replaced the alveolar epithelium, but preserved the alveolar walls (Travis *et al.* 2011).

1.6.2 Vasculogenic mimicry

Vasculogenic mimicry is another mechanism that tumour cells exploit to induce a blood supply (Figure 1.1 D). This process has been observed in aggressive malignancies in which tumour cells generate a vasculogenic network lined with non-endothelial cells and composed of extracellular matrix. Maniotis *et al.* (1999) described microcirculatory channels combined with extracellular matrix in aggressive melanomas. These channels were lined with tumour cells; expressed endothelial cell associated genes and differentiated into vasculogenic-like networks. This vasculogenic network is thought to act independently or alongside other form of vascularisation to support blood perfusion and dissemination of cancer cells (Maniotis *et al.* 1999, Hendrix *et al.* 2003, Williamson *et al.* 2016).

1.6.3 Tumour vasculogenesis

Vasculogenesis is another mechanism through which tumours become vascularised through new blood vessels formation and the recruitment of endothelial progenitor cells (EPCs) also known as angioblasts into the tumour site (Figure 1.1 E). This process is regulated by several growth factors and cytokines that are produced during tumour progression. Tumour vasculogenesis is a multistep process and each step is regulated by growth factors and cytokines, which induce the recruitment of EPCs. It starts with chemoattraction and mobilisation of EPCs from bone marrow into the circulation. The EPCs then home via the angiogenic vasculature before they differentiate into endothelial cells (Hillen and Griffioen 2007, Ding *et al.* 2008). The proangiogenic growth factor VEGF activates the differentiation of EPCs into endothelial cells, whereas platelet-derived growth factor-BB (PDGF-BB) attracts mural cells that contribute to the maturation and maintenance of stabilised blood vessels (Miyata *et al.* 2005).The involvement of EPCs in the tumour vasculature remains controversial. There are studies demonstrating a substantial role of EPCs in the tumour vasculature, whereas there are other reports of a modest contribution of EPCs in developing of tumour blood vessels (Asahara *et al.* 1999, Machein *et al.* 2003) . For instance, mice transplanted with bone marrow cells that highly express β-galactosidase (lacZ) cells under the transcriptional

regulation of fetal liver kinase-1 (Flk-1) and Tie-2 (endothelial-specific promoters) were used to study the contribution of EPCs in the vasculature of colon cancer. The study demonstrated that there are abundant Flk-1 or Tie-2 expressing EPCs at the tumour periphery and in the vascularised region of developing tumours, suggesting that these EPCs were mobilised and recruited to contribute to tumour vascularisation (Asahara *et al.* 1999). Tie-2 progenitor cells integrate at the tumour periphery in the vascular bed, however, they minimally contributed to vessel formation in a murine glioma tumour model (Machein *et al.* 2003). Taken together, these conflicting studies suggest that EPCs incorporate into tumour vasculature of specific tumours, but the mechanism of this is as yet undetermined.

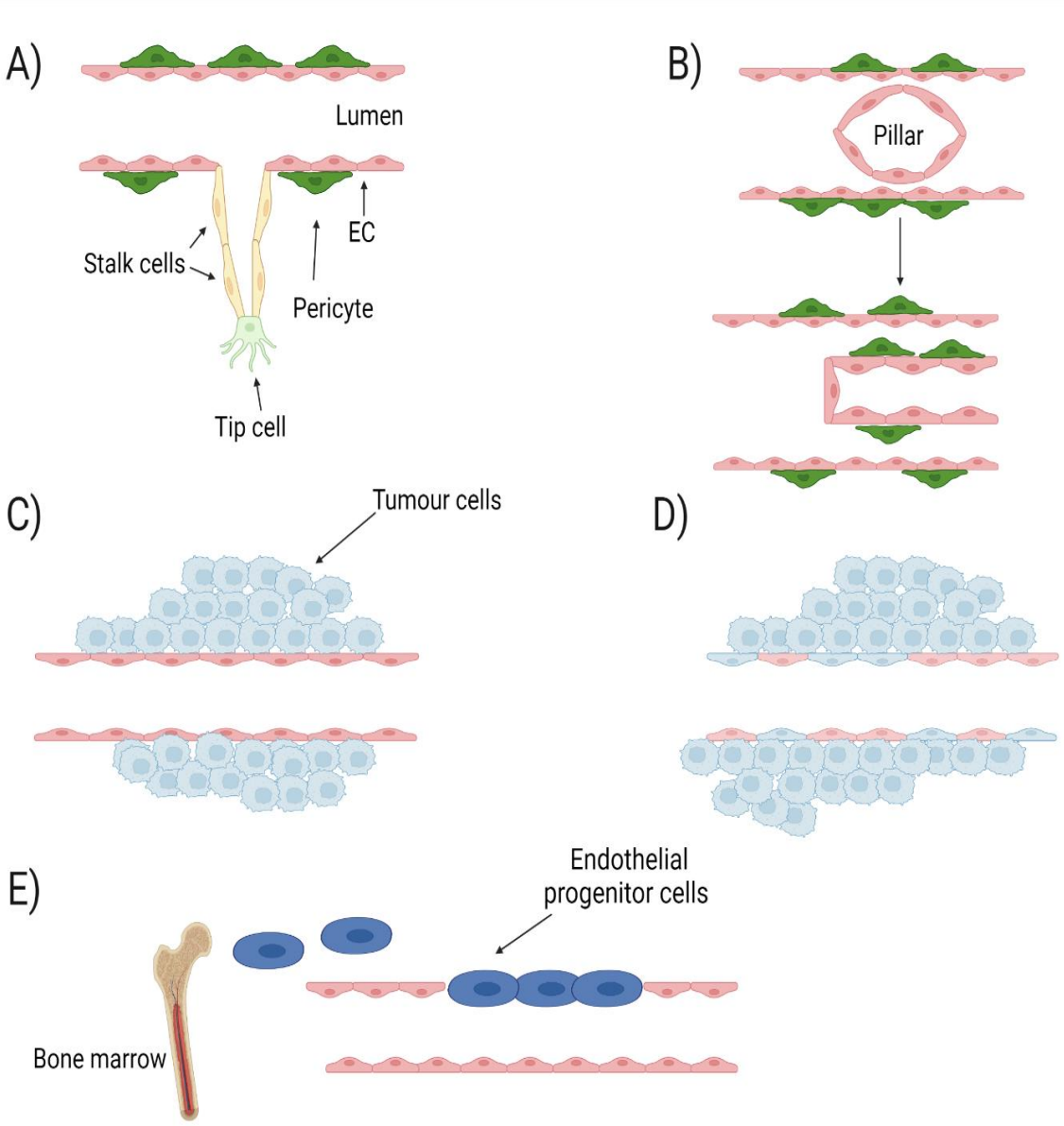

Figure 1.1 Different methods of tumour vascularisation. Tumours induce blood vessel formation through different mechanisms. **A)** New blood vessels are formed from pre-existing ones by sprouting angiogenesis. **B)** Intussuceptive angiogenesis in which a new transvascular pillar is formed and then it splits into a new lumen. **C)** Tumours can co-opt and grow along a pre-existing vessel of normal tissues. **D)** Vasculogenic mimicry in which tumour cells mimic the endothelial cells and generate a vasculogenic network lined with tumour cells. **E)** Tumour vasculogenesis involves the recruitment of endothelial progenitor cells from bone marrow and their differentiation into endothelial cells.

1.7 Vascular endothelial growth factor (VEGF)

VEGF is the most potent angiogenic factor and is essential in physiological and pathological angiogenesis. The VEGF family consists of several members including VEGF-A, VEGF-B, VEGF-C, VEGF-D and placenta growth factor (PIGF) (Ferrara *et al.* 2003, Vempati *et al.* 2014, Ahmad and Nawaz 2022). VEGF-A is a key regulator of angiogenesis, while lymphangiogenesis is regulated by VEGFC and VEGFD (Ferrara *et al.* 2003, Apte *et al.* 2019, Ahmad and Nawaz 2022). The various VEGF family members bind to tyrosine kinase VEGF receptors VEGFR-1, VEGFR-2 and VEGFR-3 expressed by endothelial cells in an overlapping pattern to activate signal transduction and various biological functions (Figure 1.2) (Li and Eriksson 2001). VEGF-A (referred to as VEGF) triggers multiple functions in endothelial cells, including proliferation, migration and vascular permeability (Hicklin and Ellis 2005). VEGF is a prognostic factor in several malignancies as high levels of VEGF are associated with the progression of disease and poor survival (George *et al.* 2001, Bando *et al.* 2005, Hsu *et al.* 2009). The *VEGF-A* gene generates at least six different isoforms (by alternative splicing), including isoforms with 121, 165, 189, and 206 amino acids in the human and 120, 164, 188, and 205 in mice (Hicklin and Ellis 2005). The isoforms differ in the presence of a heparin binding domain which is encoded by exon 6 and exon 7. The heparin binding domain ensures their binding to the extracellular matrix on the cell surface. For example, VEGF121 is diffusible and not bound to the extracellular matrix due to the absence of the heparin binding domain. VEGF189 has a high affinity to heparin sulphate proteoglycans and can bind to cell surface glycosaminoglycans. VEGF165 has intermediate properties in terms of matrix binding. The different isoforms differ in terms of their activities and give rise to different vascular structures with different branching patterns during embryonic development (Hicklin and Ellis 2005). The different roles of the isoforms in also directing tumour blood vessel development have been evaluated by Tozer *et al* using fibrosarcoma cell lines that each express only one of the major isoforms of VEGF ie VEGFA120, VEGFA164 or VEGFA188 (Tozer *et al.* 2008). The study revealed different functions of VEGF isoforms in vascular growth and morphology during fibrosarcoma growth. When implanted into mice the VEGF188 fibrosarcoma cells developed into tumours with a more stabilized and mature vascular phenotype compared to those developed by VEGF164 and VEGF120 expressing fibrosarcoma cells. VEGFA120 expressing- fibrosarcomas had leaky vessels and developed haemorrhage (Tozer *et al.* 2008). Therefore, it appears that VEGF

isoforms play an essential role in tumour angiogenesis as well as normal vascular development in the embryo.

1.7.1 Regulation of VEGF expression, secretion, and degradation

VEGF is a potent growth factor that is regulated at the transcriptional, post-transcriptional and post-translational levels (Pagès and Pouysségur 2005). In the tumour microenvironment, hypoxia is a key factor responsible for transcriptional regulation of VEGF but also various effectors including growth factors, hormones, cytokines, oncogenes, tumour suppressors and cellular stress are known to promote VEGF transcription. Hypoxia, through the activation of HIF-1, is a main regulator of VEGF gene expression (Pagès and Pouysségur 2005). As described in section 1.5, the HIF-1 heterodimer binds to the hypoxia-responsive element (HRE) site on the VEGF promoter to upregulate VEGF transcription (Richard *et al.* 1999, Maxwell *et al.* 2001, Loureiro and D'Amore 2005). The mitogen activated protein kinase p42/p44 MAP pathway, itself activated by many growth factors, cytokines and oncogenes such as RAS was reported to activate the gene expression of VEGF (Berra *et al.* 2000). In non-hypoxic conditions p42/p44 MAP activates VEGF promoter by recruiting Sp1/AP-2 transcription factors that bind and upregulate the expression of VEGF. Moreover, in hypoxia, p42/p44 MAP induces the phosphorylation of HIF-1, which activates the transcriptional- expression of VEGF (Berra *et al.* 2000). TNF-α is a macrophage/monocyte derived cytokine that is found to induce angiogenesis through activation of the gene expression of VEGF as well as other pro-angiogenic factors including interleukin-8 (IL-8) and bFGF (Yoshida *et al.* 1997). In human microvascular endothelial cells that were treated with TNF-α, mRNA of these growth factors and their receptors increased. In addition, anti-IL-8, anti-VEGF, and anti-bFGF antibodies all decreased TNF-dependent tubular morphogenesis in vascular endothelial cells, and coadministration of all three antibodies almost totally blocked tubular formation indicating reduced angiogenic activity (Yoshida *et al.* 1997). In terms of hormonal regulation of VEGF, oestrogen and androgens were shown to stimulate VEGF expression by increasing the gene transcription and mRNA stability (Ruohola *et al.* 1999).

At the post-transcriptional level, VEGF is regulated by the alternative splicing of mRNA as described in the previous section. At the post-translational level, VEGF undergoes different post-translation regulations such as glycosylation. VEGF is glycoprotein contains N-glycosylation site (Kang *et al.* 2013). VEGF Glycosylation has been reported to increase VEGF

bioactivity and secretion (Brandner *et al.* 2006, Kang *et al.* 2013). Moreover, the proteolytic processing of VEGF by matrix metalloproteinases (MMPs) plays a critical role in VEGF regulation. MMPs are a class of zinc-dependent extracellular matrix (ECM) remodelling endopeptidases that may degrade nearly every ECM component (Cabral-Pacheco *et al.* 2020). Specifically for the extracellular-bound long VEGF isoforms, MMPs cleave ECM and process VEGF and help to release it from the matrix and enhance its bioavailability (Lee *et al.* 2005). Lee *et al,* 2005 showed that MMP-cleaved VEGF induced a distinct blood vessels structure that differ from MMP resistant-VEGF constructs, suggesting that MMPs are key regulators of VEGF bioavailability (Lee *et al.* 2005). As described in the previous section, VEGF isoforms differ in their affinities to heparan sulfate proteoglycans. The longer VEGF isoforms with heparan binding affinity, when they are secreted, they remain sequestered in the ECM and remain more protected from proteolytic degradation (Vempati *et al.* 2014). VEGF can be targeted by endogenous inhibitors, such as soluble receptor- VEGFR1, a secreted isoform of the membrane VEGF receptor VEGFR1. This soluble VEGFR1 is considered as a key regulatory factor that can lead to inactivation of VEGF and limit its activity, hence promoting vascular quiescence (Vempati *et al.* 2014). High circulating soluble VEGF1 levels have been found to be associated with better prognosis in cancer patients (Aoyagi *et al.* 2010). Loss of VEGF can also occur through clearance and degradation and these are also important mechanisms for limiting VEGF activity. Relevant pathways include lymphatic drainage, transvascular transfer into the bloodstream, proteolytic breakdown and cellular endocytosis; however, their relative relevance in cancer is unknown (Vempati *et al.* 2014).

1.7.2 VEGF receptors

VEGF binds to tyrosine kinase receptors that consist of seven extracellular immunoglobulin domains, and a tyrosine-kinase site in the cytoplasmic domain (Hicklin and Ellis 2005, Apte *et al.* 2019, Ahmad and Nawaz 2022). VEGFR-1 and VEGFR-2 are identified mainly on the cell membrane of endothelial cells and hematopoietic cells, and VEGFR-3 is primarily expressed by lymphatic endothelial cells (Figure 1.2). VEGF also binds to neuropilin-1, neuropilin-2 that act as co-receptors and the longer VEGF isoforms also bind to heparin-sulphate proteoglycan. Interactions of VEGF with the neuropilins enhance its binding to the tyrosine kinase VEGFRs and alter VEGF signalling (Hicklin and Ellis 2005, Apte *et al.* 2019). It should be noted that different VEGF ligands bind to different VEGFRs with different affinities. For example, VEGF-

A has high binding affinity for VEGFR1 and VEGFR2, VEGF-B and PIGF interact with VEGFR1, whilst VEGFC and VEGFD bind to VEGFR3 in lymphatic vessels (Figure 1.2). The biological response of the interactions between VEGFRs and their ligands transduce signals for cell proliferation, cell survival, and cell migration. However, the transduced biological responses are different between VEGFRs owing to differences in the responses of the ligand binding. VEGFR2 is a key mediator of angiogenesis; additionally the kinase activity of VEGFR2 is stronger than VEGFR1 (Shibuya and Claesson-Welsh 2006). Binding of VEGF leads to the dimerization of the VEGF receptor followed by kinase activation and auto phosphorylation of specific tyrosine residues, and many cytoplasmic proteins. Several effectors are then activated and bind to the phosphorylated tyrosine residues which results in signal transduction and biological functions including migration, proliferation, and cell survival (Kowanetz and Ferrara 2006).

1.7.2.1 VEGFR1

VEGFR1 is a receptor for VEGFA, VEGF- B and PIGF (Figure 1.2). Binding to VEGFA induces signal transduction for growth and survival of endothelial cells. VEGFR1 is important for vascular organisation during embryogenesis. Fong *et al* demonstrated that VEGFR1 knock out leads to vascular malformations in mouse embryos (Fong *et al.* 1995) . However, VEGFR1 triggers weak mitogenic effects in endothelial cells. A study by Gille *et al* investigated the signal transduction produced by both VEGF1 and VEGFR2 (Gille *et al.* 2000). They used engineered VEGF-A to bind selectively to either VEGR1 or VEGFR2, and demonstrated that migration, differentiation, and proliferation of endothelial cells was transduced mainly through VEGFA binding to VEGFR2, but not VEGFR1. Cells other than endothelial cells also express VEGF receptors such as for example monocytes that express VEGFR1 which stimulates their migration through binding to VEGF-A (Gille *et al.* 2000, Matsumoto and Claesson-Welsh 2001). It is worth noting that VEGFR1 may serve as a negative regulator of angiogenesis by binding VEGF, hence decreasing its binding to VEGFR2, thus resulting in downregulation of angiogenic signalling (Koch and Claesson-Welsh 2012).

1.7.2.2 VEGFR2

VEGFR2 binds VEGFA, VEGFC, VEGFD and VEGFE (Figure 1.2). The effector molecules bind via their Src homology-2 domain with the autophosphorylated binding site in tyrosine residues,

and this interaction leads to different biological functions. VEGFR2 has a crucial role in haematopoiesis and the formation of blood vessels during embryogenesis. Shalby and colleagues demonstrated this finding using mice with a mutation in VEGFR2 (Shalaby *et al.* 1995). They reported that mutated embryos die between 8.5 and 9.5 days due to the absence of blood vessels in the yolk sac and the decreased number of haematopoietic progenitors. This finding indicates that VEGFR2 has an essential role in vascular formation during the embryogenesis (Shalaby *et al.* 1995). The physiological and pathological effects of VEGFA on endothelial cells, mediated by interactions with VEGFR2 include proliferation, migration, survival, and vascular permeability. VEGFR2 induces proliferation via the phosphorylation of tyrosine 1175 that triggers the PLC-γ pathway and then activation of the protein kinase C (PKC) pathway leading to inositol trisphosphate generation and calcium mobilization. Additionally, this pathway activates PKCβ, which in turn stimulates many effectors such as Raf, MEK, and MAPK involved in DNA synthesis and cell proliferation. In addition, VEGFR2 activates the Akt/PKB via the tyrosine pathway which promotes cell survival by inhibiting the activity of proapoptotic proteins B-cell lymphoma 2 (Bcl-2)-associated death promoter homologue (Maksimiuk *et al.*) and Caspase 9 (Gerber *et al.* 1998, Cross *et al.* 2003, Shibuya and Claesson-Welsh 2006). In addition, Tyrosine kinase 1175 phosphorylation triggers binding and activation of Shb adapter protein which regulate the focal adhesion and migration of endothelial cells (Holmqvist *et al.* 2004) . Activation of AKT/PKB pathways is also implicated in the increase of vascular permeability through stimulation of endothelial nitric oxide synthase (eNOS) which generates nitric oxide and activation of cellular permeability (Dimmeler *et al.* 1999, Shibuya and Claesson-Welsh 2006). Moreover, binding of VEGF to VEGFR2 regulates the migration of endothelial cells through the phosphorylation of tyrosine 951 (Matsumoto *et al.* 2005). Tyrosine 951 Phosphorylation activates the binding of T cell specific adapter (TSAd) protein. Activation of TSAD pathway induces actin stress fibre formation, mediating endothelial cell migration (Figure 1.2) (Matsumoto *et al.* 2005).

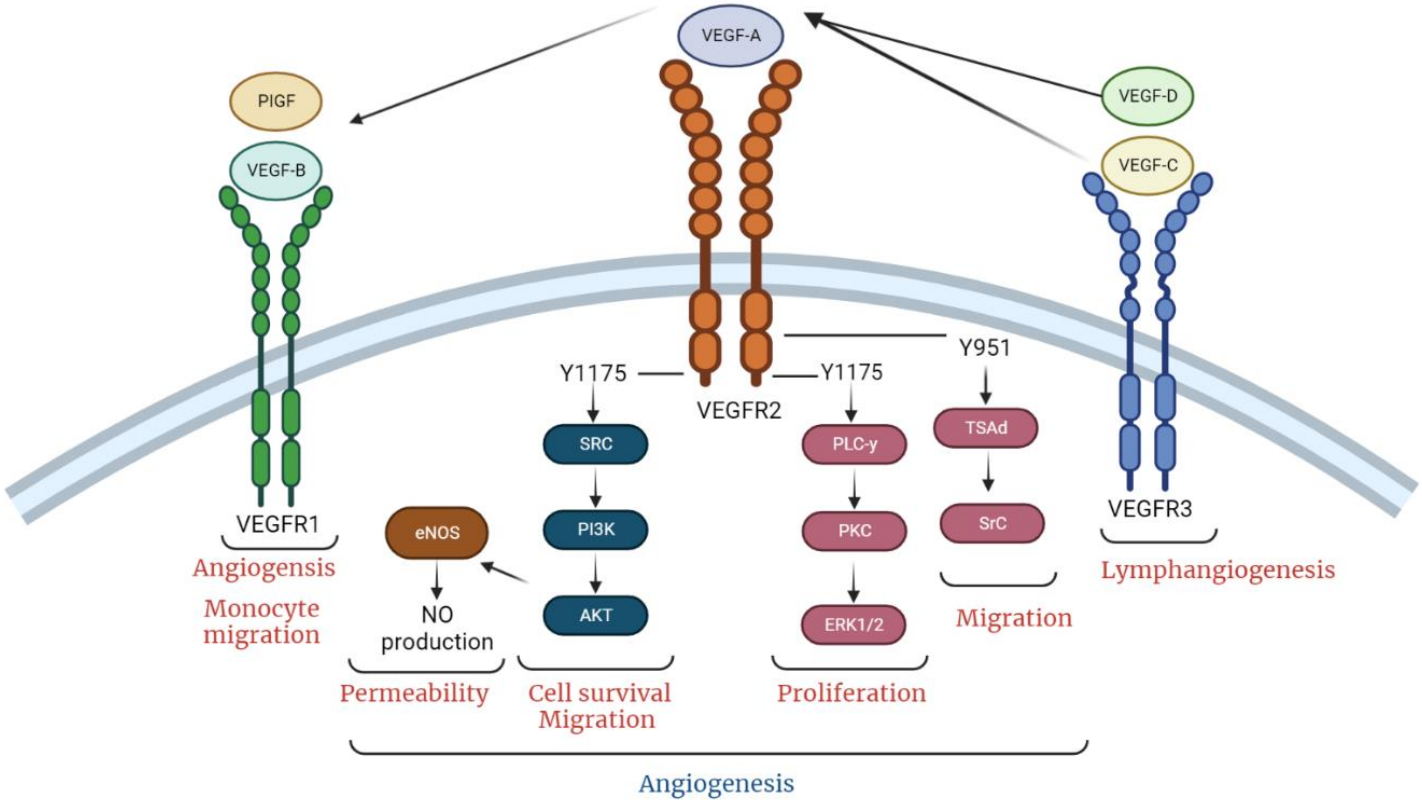

Figure 1.2 Biological functions mediated by VEGF receptors. The regulation of angiogenesis occurs mainly through VEGF-VEGFR2 binding and signalling. VEGF-A binds to VEGFR2 and activates different tyrosine residues which in turn activate several functions in endothelial cells including proliferation, survival, migration and vascular permeability. The phosphorylation of tyrosine 1175 (Y1175) triggers proliferation, survival, migration and permeability. Migration of endothelial cells can also be activated through phosphorylation of tyrosine 951 (Y951). VEGFR1 stimulates monocyte migration through binding to VEGF-A, VEGF-B and PLGF. Lymphangiogenesis is regulated by VEGF-C and VEGF-D binding to VEGFR3.

1.8 Anti-VEGF therapies

Targeting VEGF became an attractive therapeutic strategy after the role of VEGF as an angiogenic growth factor was established (Ferrara 2005). Kim *et al*, 1993 investigated the role of VEGF as a tumour angiogenic factor *in vivo*. They tested the effect of an antibody that neutralized VEGF on the growth of human tumour xenografts of rhabdomyosarcoma, and glioblastoma multiform. The antibody inhibited both tumour growth and angiogenesis in a dose dependent manner (Kim *et al.* 1993). The antibody was later humanised (known as bevacizumab) and was tested in clinical trials (Presta *et al.* 1997). The US FDA first approved bevacizumab for treating previously untreated metastatic colorectal cancer in February 2004 (Hurwitz *et al.* 2004). Subsequently, FDA and regulatory bodies in other countries approved bevacizumab for up to six malignancies, including non-squamous non-small cell lung carcinoma (NSCLC), glioblastoma multiforme, renal cell carcinoma (RCC), cervical cancer, ovarian cancer and breast cancer. Several other agents were developed later to target the VEGF pathway, including VEGF receptor tyrosine kinase inhibitors (TKIs), an antibody targeting VEGFR2 activity and a chimeric soluble VEGF receptor (Apte *et al.* 2019). There are some of these agents are used in combination with chemotherapeutic agents and some are used as a single agent (Table 1.1) (Kanthou and Tozer 2018, Jászai and Schmidt 2019).

Table 1-1 FDA- approved anti-VEGF agents for cancer treatment, their targets and indications

Antiangiogenic agent/Class	Target	Indication	Clinical use	Year of FDA approval	References
Bevacizumab/monoclonal Ab	VEGF	Metastatic CRC	With chemotherapy, first and second line	2004, 2006	(Hurwitz *et al.* 2004, Cohen *et al.* 2007)
		Recurrent or metastatic NSCLC	With chemotherapy, first line	2006	(Cohen *et al.* 2007)
		Recurrent glioblastoma	With chemotherapy	2009	(Garcia *et al.* 2020)
		Recurrent ovarian, fallopian or peritoneal cancer.	With chemotherapy	2014	(Pujade-Lauraine *et al.* 2014)
		Metastatic RCC.	With interferon alfa 2b, single agent	2009	(Escudier *et al.* 2010, Garcia *et al.* 2020)
		Recurrent or metastatic cervical cancer.	With chemotherapy	2014	(Tewari *et al.* 2014)
Ramucirumab/monoclonal Ab	VEGFR 2	Metastatic CRC	With FOLFIRI chemotherapy	2015	(Goel *et al.* 2016)
		Metastatic NSCLC	With docedaxel	2014	(Das and Wakelee 2014)
		Metastatic gastric or gastroesophageal	Single agent or combined with paclitaxel in advanced	2014	(Casak *et al.* 2015)

		junction adenocarcinoma	disease		
Ziv-aflibercept/VEGF Trap Recombinant fusion protein	VEGF-A, VEGF-B, PlGF	Metastatic CRC	With FOLFIRI chemotherapy	2012	(Ricci *et al.* 2015)
Sorafenib/RTKi	VEGFR-2, 3 PDGFRs, RAF, KIT, FLT-3	RCC	Single agent	2005	(Wilhelm *et al.* 2006)
		HCC (Unresectable)	Single agent	2007	(Kim *et al.* 2017)
		metastatic thyroid carcinoma	Single agent	2013	(McFarland and Misiukiewicz 2014)
Pazopanib/ RTKi	VEGFR 1-3 FGFRs, KIT	Advanced soft tissue carcinoma	Single agent	2012	(Van Der Graaf *et al.* 2012, Lee *et al.* 2019)
		Advanced RCC	Single agent	2009	(Ward and Stadler 2010)
Sunitinib	VEGFR 1-3 PDGFR FGFR1 KIT, RET, FLT3	Metastatic gastrointestinal stromal tumours	Single agent	2006	(Adams and Leggas 2007)
		Metastatic RCC	Single agent	2006	(Adams and Leggas 2007)
		Metastatic/progressive pancreatic cancer	Single agent	2011	(Raymond *et al.* 2011)

Axitinib	VEGFR 1-3	Advanced RCC	Single agent	2012	(Tyler 2012)
Vandetanib	VEGFR 1-3, Tie-2, EGFR, RET	Advanced/metastatic medullary thyroid cancer	Single agent	2011	(Chau and Haddad 2013)
Cabozantinib-S-malate	VEGFRs, RET, MET, Tie-2, FLT-3	Metastatic medullary thyroid cancer	Single agent	2012	(Weitzman and Cabanillas 2015)
		Advanced RCC	Single agent	2016	(Escudier *et al.* 2016)
		HCC	Single agent	2019	(Personeni *et al.* 2019)
Regorafenib	VEGFR 1-3 , FGFR, PDGFR, KIT, TIE-2, Raf	Refractory and metastatic CRC	Single agent	2012	(Cai *et al.* 2018)
		HCC	Single agent	2017	(Heo and Syed 2018)
		Locally advanced, unresectable or metastatic gastrointestinal stromal tumour	Single agent	2013	(Crona *et al.* 2013)
Lenvatinib RTKi	VEGFR-1-3 FGFR-1, PDGFRs, KIT	Differentiated and refractory to radioactive iodine thyroid carcinoma	Single agent	2015	(Nair *et al.* 2015)
		Unresectable HCC	Single agent	2018	(Hao and Wang 2020)
		RCC	With everolimus	2016	(Li *et al.* 2020)
		endometrial carcinoma	With pembrolizumab	2019	(Walker *et al.* 2023)

AB, Antibody; CRC, colorectal cancer; HCC, hepatocellular carcinoma; NSCLC, non-small cell lung cancer; RCC, renal cell carcinoma; EGFR, epidermal growth factor receptor; FGFR, fibroblast growth factor receptor; mTOR, mammalian target of rapamycin; FLT-3, fms like tyrosine kinase 3; KIT, v-kit Hardy–Zuckerman 4 feline sarcoma viral oncogene homolog; MET, mesenchymal-epithelial transition proto-oncogene; PlGF, placental growth factor; PDGFR, platelet-derived growth factor receptor; TIE2, tyrosine kinase with immunoglobulin-like and EGF-like domains 2; RET, receptor tyrosine kinase proto-oncogene; VEGF, vascular endothelial growth factor; VEGFR, vascular endothelial growth factor receptor.

1.8.1 Anti- VEGF therapies for breast cancer

Bevacizumab was the first anti-VEGF therapy used to treat breast cancer patients. This is a monoclonal antibody that binds VEGF and was approved for the treatment of human epidermal growth factor receptor type 2 (HER2)–negative breast cancer, in combination with paclitaxel, a chemotherapeutic agent The combination showed a significant increase in progression-free survival (PFS) compared to using chemotherapy alone (Miller *et al.* 2007, Ayoub *et al.* 2022). This led to the European Medicines Agency (EMEA) and Food and Drug Administration (FDA) approval of using bevacizumab as a treatment for HER2-negative breast cancer in 2007 and 2008 respectively. Despite this, little or no improvement has been made in terms of overall survival for patients using paclitaxel plus bevacizumab versus paclitaxel alone (Kristensen *et al.* 2014) . Another significant issue with this drug is the high toxicity and adverse effects for patients, including hypertension, bleeding events and proteinuria. Subsequently, bevacizumab is no longer used in the United States for treatment of HER2–negative breast cancer, as the FDA withdrew the approval. Contrary to this, EMEA has maintained the approval (Kristensen *et al.* 2014). Different chemotherapy regimens have been combined with bevacizumab (Avastin), such as Avastin plus Docetaxel (AVADO) trial (Miles *et al.* 2010) and RIBBON-1 (Regimens in Bevacizumab for Breast Oncology) trial (Robert *et al.* 2011). All these trials showed a significant benefit in the PFS but not in overall survival of breast cancer patients (Sledge 2015). A recent clinical trial analysed data of two identical clinical trials tested the addition of bevacizumab to endocrine therapy as first-line treatment in metastatic hormone receptor-positive breast cancer. The addition of bevacizumab to endocrine therapy improved PFS but not the OS compared to endocrine therapy alone. However, patients displayed high toxicity with combination treatment (Martin *et al.* 2019).

In addition to using antibodies, other types of anti VEGF treatments inhibit tyrosine kinase activity of VEGFR2. Sunitinib is a TKI that targets VEGF receptors and platelet derived growth factor (PDGFR), c-kit (KIT), and Flt-3 receptors (Barrios *et al.* 2010). Sunitinib was used as a monotherapy for treating HER2-negative breast cancer in a phase III trial. Sunitinib did not improve PFS and was associated with higher severities of many common adverse events compared with a chemotherapeutic agent (Barrios *et al.* 2010).

Sorafenib, another TKI was used in combination with anti-hormone therapy for treating metastatic breast cancer in a phase II clinical trial. The combination showed improvement in

clinical benefit rate , but significant toxicity of treatment resulted in discontinuing treatment in many patients (Isaacs *et al.* 2011). A recent clinical trial demonstrated that no benefit in terms of survival outcomes for the addition of sorafenib to letrozole (hormone therapy) and cyclophosphamide (chemotherapeutic agent) in locally advanced HER2 negative breast cancer patients. In addition, large number of patients who received combination therapies containing sorafenib displayed disease progression (Ianza *et al.* 2020).

It is widely acknowledged that VEGF inhibitors have considerable benefits in many patients, including metastatic colorectal cancer and renal cell carcinoma (Jain *et al.* 2009, Sledge 2015). However, the outcomes of anti-VEGF treatments in breast cancer are modest (Jain *et al.* 2009, Sledge 2015). It is unclear the reasons for good response in some types of cancer and not in other types and this represents one of the challenges in the use of anti-VEGF inhibitors. Another challenge with using anti-VEGF treatments is the resistance observed to this type of treatment. Some patients show an initial transitory response, in the form of tumour regression. However, the initial response is followed by tumour regrowth and sign of toxicities while other patients showed no response at all (Bergers and Hanahan 2008, Jayson *et al.* 2016, Oguntade *et al.* 2021). Understanding mechanisms of resistance could explain the reasons of no response or relapse in a large proportion of patients.

1.9 Resistance to anti-VEGF treatments

Resistance to VEGF pathway inhibitors has become the topic of extensive research. There is an initial response, which may be followed by adaptive resistance; this could be referred as acquired resistance (evasive). On the other hand, there are some patients who do not show any response, indicating that an intrinsic (pre-existing) resistance may exist (Bergers and Hanahan 2008, Loges *et al.* 2010, Weathers and De Groot 2014) .

Experimental work has suggested several mechanisms through which resistance to antiangiogenic agents may be acquired (Bergers and Hanahan 2008). These include upregulation of alternative proangiogenic signalling pathways, and recruitment of bone marrow derived progenitor cells that can activate VEGF-independent angiogenesis. In addition, increased tumour growth but also metastasis and invasion are likely because of hypoxia (Bergers and Hanahan 2008). Moreover, tumours become less dependent on VEGF by increasing the pericyte coverage of the tumour vasculature, which decreases the activation

of VEGF signalling (Bergers and Hanahan 2008, Weathers and De Groot 2014). Antiangiogenic therapies if given for extended periods, cause extensive destruction of the tumour blood vessels, which led to hypoxia and subsequent activation of proangiogenic growth factors (Jain 2005, Ribatti *et al.* 2019).

1.9.1 Evasive (adaptive) resistance

1.9.1.1 Upregulation of alternative proangiogenic signalling pathways

In this situation, tumour cells and stromal cells may use VEGF-independent angiogenesis using alternative proangiogenic factors such as PDGF, FGF, IL-8 and Insulin like Growth Factor (IGF) to induce tumour vessel growth. For instance, IL-8 is a proangiogenic chemokine and was found to be upregulated after the knockdown of HIF-1α in mice (Mizukami *et al.* 2005) . HIF-1α is the main regulator of VEGF signalling pathway. The partial blockade of the hypoxic induction of VEGF led to compensatory activation of proangiogenic pathway via IL-8 (Mizukami *et al.* 2005). Another study reported an increase in PIGF and VEGFD in colorectal cancer patients during the progression phase of the disease after treatment with bevacizumab combined with chemotherapy, suggesting that tumours utilised alternative proangiogenic pathways (Lieu *et al.* 2013). A clinical investigation reported that glioblastoma patients treated with the VEGFR inhibitor AZD2171 demonstrated a response phase followed by a relapse. FGF and stromal cell-derived factor 1α (SDF1 α) levels were found to be higher in the blood during the relapse phase compared to that during the response phase in the same patients, suggesting the upregulation of alternative proangiogenic pathways. This study proposed FGF and SDF1α as biomarkers and suggested targeting these molecules in combination with AZD2171 to maximise benefit (Batchelor *et al.* 2007). Human glioblastoma-associated endothelial cells showed resistance to both VEGFR inhibitor (ki8751) and the VEGF blocking antibody (B20) (Liu *et al.* 2018) . Notably, these cells were found to express less VEGFR-2 compared to normal endothelial cells, suggesting a mechanism of resistance to anti-VEGF therapy. Interestingly, it was found that these cells acquired the characteristics of mesenchymal cells. PDGF was implicated in acquiring the cells the mesenchymal phenotype and in the downregulation of VEGFR-2 in glioblastoma-endothelial cells. Therefore, PDGF renders glioblastoma-endothelial cells resistant to anti-VEGF treatments by these mechanisms. Combining the PDGFR inhibitor (crenolanib) with VEGFR-2 (ki8751), inhibited endothelial cell viability. Similarly, in a glioblastoma mouse model, dual inhibition using the

two treatments demonstrated anti-tumour effect in terms of increased mouse survival and inhibition of tumour growth, suggesting that PDGF inhibition renders the glioblastoma endothelial cells sensitive to anti-VEGF treatment (Liu *et al.* 2018).

1.9.1.2 Excessive vessel pruning and hypoxia.

Most antiangiogenic therapies aim to 'normalize' the abnormal tumour vasculature. This process initially leads to pruning and remodelling of the small and leaky blood vessels, leaving the mature and functional blood vessels. Consequently, this partially alleviates interstitial hypertension and leads to a normal vasculature, which is better oxygenated. Enhanced oxygenated areas in a tumour can improve delivery of chemotherapeutic drugs and improve the radiation response. Therefore, it is thought that combining these conventional therapies (chemotherapy and radiotherapy) with antiangiogenic agents may act in a synergistic manner. However, the process of "vascular normalisation" could be reversed, and hence the antiangiogenic treatments can increase a hypoxic microenvironment due to continued and extensive destruction of the tumour blood vessels. In addition, chemotherapy and radiotherapy may be less effective. Excessive vessel pruning impairs oxygen delivery to the tumour and promotes hypoxia and leads to increased production of angiogenic growth factors as well as selection for more aggressive malignant cells (Winkler *et al.* 2004, Jain 2005, Batchelor *et al.* 2007, El Alaoui-Lasmaili and Faivre 2018). For instance, VEGF levels and interleukin-8/CXCL8, pro-angiogenic factors were increased in renal cell carcinomas (RCCs) after treatment with bevacizumab compared with normal tissues. In addition, treatment with bevacizumab in nude mice enhanced the growth of RCCs *in vivo*, with selection of tumour cells with a high growth capacity (Grepin *et al.* 2012). Furthermore, hypoxia enhanced the invasion and metastasis of tumour cells to distant sites once tumour cells escaped from the initial treatment (Grepin *et al.* 2012). Several studies have reported metastasis following the development of resistance to anti-VEGF therapy. Shojaei *et al* investigated metastatic induction after treatment with sunitinib in several tumour cell lines including breast, lung and colorectal cell lines, with metastasis demonstrated in breast and colorectal cell lines, suggesting that sunitinib- induced metastasis is tumour dependent (Shojaei *et al.* 2012). Furthermore, one study investigated invasion and metastasis of tumour cells in a mouse model of pancreatic neuroendocrine carcinoma after treatment with a VEGF receptor inhibitor (DC101) (Pàez-Ribes *et al.* 2009). After an initial anti-tumour response, tumours

adapted to the treatment, and invaded and metastasised to a distant site. This study observed hypoxia in the metastatic tumour microenvironment after treatment with angiogenesis inhibitors compared with untreated tumours, suggesting that hypoxia may be implicated in this treatment resistance (Pàez-Ribes *et al.* 2009).

1.9.1.3 Recruitment of bone marrow progenitor cells

Hypoxia induced after treatment with anti-VEGF inhibitors, stimulates release of pro-angiogenic factors and cytokines from both tumour and stromal cells that promote neo-vascularisation by recruitment of bone marrow derived cells (Giuliano and Pagès 2013). Several studies have detected progenitor cells after antiangiogenic treatment. Circulating endothelial progenitor cells (CEPs) have been shown to accumulate in the viable tumour rim after treatment of tumour-bearing mice with vascular disrupting agents (VDAs) (Gaya and Rustin 2005). The VDAs caused acute destruction of existing blood vessels leading to a rapid necrosis and then hypoxia (Gaya and Rustin 2005). Tumour regrowth and mobilization of CEPs were demonstrated rapidly after VDA treatment. This study proposed that recruitment of CEPs might contribute to the rapid growth of tumours and development of resistance (Shaked *et al.* 2006). Furthermore, AZD2171 a tyrosine kinase inhibitor against VEGFR used in recurrent glioblastoma patients, showed an increase in circulating progenitor cells (CPCs) after treatment and suggested that the CPCs might be CEPs and may consequently contribute to revascularisation (Batchelor *et al.* 2007). These data collectively suggest that an adaptive response is activated post treatment with antiangiogenic agents. Furthermore, HIF1α activation during hypoxia leads to downstream signalling of chemokine stromal-cell derived factor-1 SDF1α that triggers the recruitment of CXCR4+VEGFR1+ hematopoietic cells. CXCR4+VEGFR1+ hematopoietic cells supports the neo-vascularization of tumour growth and ischemic tissues (Petit *et al.* 2007). Hypoxia post anti-VEGF treatment may induce the SDF-1–CXCR4 pathway that facilitates the revascularisation of tumours.

1.9.1.4 Escaping the anti-angiogenic treatments by increasing pericyte coverage

Pericytes are an important constituent for vessel maturation. The pericytes cover endothelial cells, leading to maturation and stabilisation of newly formed vascular structures. The endothelial cells at this stage inhibit proliferation and become quiescent. In contrast, in tumour tissues this process is aberrant due to the continuous secretion of proangiogenic

factors from the growing tumour. Notably, as the anti-VEGF treatments target the proliferating endothelial cells in the tumour microenvironment, tumours can escape anti-VEGF treatments by increasing the coverage of pericytes, making blood vessels more stable, quiescent, and less susceptible to targeting by anti-VEGF treatments (Bergers and Hanahan 2008, Zarrin *et al.* 2017). This concept was explained in a study which found that SU5416 an inhibitor of VEGFRs has an effect on the tumour at an early stage but not at late stage tumours with functional pericyte-covered blood vessels (Bergers *et al.* 2003). Tumour regrowth was detected in tumour mouse models after treatment with a VEGF receptor signalling inhibitor AG-013736 or AG-028262 (Mancuso *et al.* 2006). Although the treatments caused a massive reduction in blood vessels, pericytes and basement membrane remained behind intact and restored the tumour vasculature within 7 days after treatment stopped. Interestingly, the regrown tumour vasculature re-induced VEGF-dependent angiogenesis, suggesting that tumours may also utilize pericytes as a scaffold for inducing new sprouts (Mancuso *et al.* 2006).

1.9.2 Intrinsic resistance

In intrinsic resistance, tumour cells themselves activate intrinsic resistance mechanisms during their progression. These mechanisms are developed independent to treatments and contribute to non-responsive outcome. The complex tumour microenvironment with redundancy of growth factors produced by tumour cells or stromal cells represents one of these mechanisms. When the tumour cells or surrounding stroma activate a plethora of proangiogenic signalling pathways, blocking the VEGF signalling pathway may not be sufficient to halt angiogenesis and tumour growth. Tumour stroma consists of several cells that trigger redundancy of proangiogenic signalling pathways. Therefore, a tumour can survive after blockade of one proangiogenic pathway (Bergers and Hanahan 2008, Loges *et al.* 2010, Huijbers *et al.* 2016) . A study on breast cancer tissues showed high expression levels of different proangiogenic factors, including FGF, Placenta growth factor (PIGF) when compared to normal tissues (Relf *et al.* 1997). It has been reported that PIGF expression increased in different tumour models and was expressed by tumour cells and stromal cells. Targeting PIGF in tumour but not in healthy tissues led to decreased angiogenesis suggesting that PIGF is a major proangiogenic factor in tumours (Fischer *et al.* 2007).

The components of tumour stroma have a major role in the refractoriness to antiangiogenic therapies. Tumour stroma consists of different cell types, including tumour-associated fibroblasts (TAF), pericytes, endothelial progenitor cells and inflammatory cells such as myeloid cells. Preclinical and clinical data showed the involvement of these cells in resistance to antiangiogenic treatments. This is because tumour stroma induces several proangiogenic signalling pathways that contribute to angiogenesis (Orimo *et al.* 2005, Shojaei and Ferrara 2008, Crawford and Ferrara 2009, Loges *et al.* 2010, Jászai and Schmidt 2019). TAF produce angiogenic factors that stimulate angiogenesis. TAF isolated from a tumour resistant to an anti-VEGF treatment, expressed high levels of platelet-derived growth factor C (PDGF-C) that was found to stimulate angiogenesis. Combining anti-VEGF with PDGF-C-neutralizing antibodies inhibited angiogenesis (Crawford *et al.* 2009). Beside stimulation of angiogenesis, TAFs produce SDF1 that stimulates the recruitment of bone marrow derived EPCs which in turn promotes vasculogenesis (Orimo *et al.* 2005). In addition, accumulation of fibroblasts increases the secretion of extracellular proteins, causing desmoplasia. Desmoplasia is also characterised by lack of vasculature, which contributes to resistance to anti-VEGF therapies and other conventional therapies. The lack of vasculature and accumulation of stroma cells impede the blood flow in tumour parenchyma, hence the treatments cannot be easily delivered into the tumour. Pancreatic cancer is known to be highly desmoplastic, and the outcome of anti-angiogenic therapies is poor in pancreatic cancer. The lack of response to antiangiogenic therapies is proposed to be because of desmoplasia (Tamburrino *et al.* 2013, Li *et al.* 2019). Taken together, it is tempting to speculate that tumour stroma with abundant fibroblasts may represent a challenge and cause resistance to anti-angiogenic therapies via different mechanisms.

Moreover, accumulation of inflammatory cells in tumour stroma which fuel the tumour with growth factors and cytokines mediate angiogenesis. For instance, a preclinical experiment using murine- transplanted tumours showed an increase in CD11b+Gr1+ myeloid cells in a subset of tumours, which showed no response to an anti-VEGF monoclonal antibody (G6.23). Notably, the accumulation of CD11b+Gr1+ myeloid cells was independent of treatment, suggesting that the mechanism of resistance in this case is inherent (Shojaei *et al.* 2007).

Some tumours are refractory to anti-angiogenic therapies because they do not rely on the tumour vasculature that is ideal target of anti-angiogenic treatments. Instead, they co-opt to

pre-existing established host vessels. This kind of resistance was observed in a clinical study on colorectal cancer liver metastases patients treated with bevacizumab. In patients who showed poor response to bevacizumab in terms of overall survival, tumour cells were found to co-opt to sinusoidal blood vessels. The study also found that breast cancer liver metastatic tumours showed the same pattern of angiogenesis, suggesting a potential explanation of resistance to bevacizumab in breast cancer patient may be in part as a result of inducing co-option vasculature (Frentzas *et al.* 2016).

1.10 Current approaches to overcome resistance to anti-angiogenic treatments.

Currently, multiple approaches have been suggested to overcome resistance to anti-VEGF treatments or to increase their efficacy. Combining conventional radiotherapy or chemotherapy treatments with antiangiogenic agents can result in improved responses through different mechanisms. Chemotherapy and radiotherapy kill the cancer directly and the antiangiogenic drugs starve the tumours of oxygen and therefore kill the cancer cells indirectly (Teicher 1996). Combining antiangiogenic treatments with conventional therapies may be more effective especially if given during the normalisation phase (Jain 2005, Carmeliet and Jain 2011). Establishing the “normalisation window” is therefore a proposed approach to evaluate the benefit from conventional therapies (Jain 2005, Batchelor *et al.* 2007, El Alaoui-Lasmaili and Faivre 2018). The normalisation window refers to the period after antiangiogenic therapies when the treatment prunes the dysfunctional and leaky blood vessels and remodel the remaining ones. As a result, remaining vessels are normalised with improved blood flow and oxygen delivery. They are better invested with pericytes, enabling enhanced delivery of cytotoxic agents and better response to radiotherapy, which requires oxygen for the generation of reactive oxygen species to kill cancer cells. However, if the antiangiogenic treatments are prolonged, massive destruction in the vasculature can occur, leading to hypoxia and poor blood flow (Jain 2005). In glioblastoma xenograft models, radiotherapy was found to be most effective when administered during the "normalisation window" (Winkler *et al.* 2004). Giving radiation therapy between days 4 and 6 after starting DC101 (a VEGFR2-specific monoclonal antibody) resulted in a significant delay in tumour growth. This effect was found to be due to a significant decrease in hypoxia and improved tumour oxygenation induced by DC101. The best timing for radiation coincided with the peak tumour oxygenation during DC101 treatment (Winkler *et al.* 2004). It is important to assess normalisation after

antiangiogenic therapy in human cancers and imaging approaches are being employed. A Phase II clinical trial in recurrent glioblastomas, used MRI to assess vessel architecture and caliber and found that treatment with the antiangiogenic agent cediranib increased oxygen saturation, and reduced vessel caliber, suggesting normalisation of blood vessels (Emblem *et al.* 2013). Additionally, the patients with these responses experienced prolonged survival (Emblem *et al.* 2013). In another clinical trial, MRI was used to measure relative vessel size and permeability, and edema-associated parameters (Batchelor et al. 2007). The data showed that AZD2171, a tyrosine kinase antiangiogenic agent, induced blood vessel normalisation one day after starting treatment and lasted up to 28 days, which was proposed to be the optimal timing for combining with a cycle of concurrent chemotherapy or radiotherapy. The blood vessel normalisation was evident with the alleviation of brain edema and significant decrease in blood vessel size. Nevertheless, new abnormal vessels were developed following drug withdrawal in cases of toxicities, but returned to a normalised state when drug treatment was resumed. (Batchelor et al. 2007). Measuring vessel size, vessel permeability and blood flow by medical imaging methods such as MRI computerized tomography (CT), positron emission tomography (PET) are therefore proposed for establishing the optimal dose and schedule of antiangiogenic treatments (Jain 2005, Batchelor *et al.* 2007). However, the normalisation period can be different between patients and therefore, more studies are needed to validate this approach (Goel *et al.* 2011). In addition, it is challenging to confirm the accuracy of these methods, and often, different medical centres do not agree on the best ways to collect and analyse data for a particular end-point (O'connor *et al.* 2017).

Bevacizumab with several standard chemotherapeutic agents increased the PFS rate in HER2-negative metastatic breast cancer patients compared to chemotherapeutic agents alone (Robert *et al.* 2011). Bevacizumab in combination with chemotherapy increased the survival significantly in patients with metastatic colorectal cancer (Hurwitz *et al.* 2004). A study of breast and colon tumour mouse models used thalidomide an anti-angiogenic agent and showed that thalidomide inhibited the tumour growth, normalised blood vessels, and promoted blood vessels maturation. As part of the normalisation effect, thalidomide increased tumour perfusion and decreased vascular leakiness, increasing the delivery of chemotherapy (Cisplatin) (Shen *et al.* 2019).

Another promising approach to combat resistance to anti-VEGF therapies is to target proangiogenic factors other than VEGF. This is because tumours may utilize other proangiogenic factors to escape treatment against the VEGF pathways. An antibody against PIGF showed promising results and increased the effect of chemotherapy and VEGFR inhibitor (Fischer *et al.* 2007). PIGF was reported to be increased after treatment with antiangiogenic treatments and was suggested to contribute to re-vascularisation (Fischer *et al.* 2007, Lieu *et al.* 2013). Therefore, targeting alternative angiogenic factors may increase the efficacy of antiangiogenic treatments. Moreover, using agents that target multiple angiogenic pathways is another way to increase the efficacy of antiangiogenic agents. These agents aim to simultaneously target the pathways of multiple angiogenic factors (Ballas and Chachoua 2011, Zhao and Adjei 2015). For example, regorafenib targets the activity of VEGFR1/2/3, PIGFR and FGFR and has shown anti-tumour and anti-angiogenesis effects (Abou-Elkacem *et al.* 2013, Zhao and Adjei 2015). A pre-clinical study showed that regorafenib, a multikinase inhibitor, suppressed tumour growth, vascularisation and metastasis in a murine CT26 metastatic colon cancer model compared to the angiogenesis inhibitor DC101 (Abou-Elkacem *et al.* 2013). Regorafenib is now approved for use in the clinic for the treatment of metastatic colorectal cancer, hepatocellular carcinoma, and metastatic gastrointestinal stromal tumours (see Table 1) (Crona *et al.* 2013, Cai *et al.* 2018, Heo and Syed 2018). A novel decoy receptor VE-Trap fusion protein that binds to VEGF and bFGF, simultaneously showed synergistic anti-tumour effect in terms of inhibiting proliferation and migration of VEGF and FGF-induced endothelial cells. Similarly, in a mouse model, VE-Trap demonstrated a significant inhibition of renal and lung xenograft tumour growth compared to mice treated with either the single VEGF inhibitor or bFGF inhibitor (Li *et al.* 2016). Taken together, targeting multiple proangiogenic factors augments the effect of anti-VEGF inhibitors.

Another therapeutic target is combining the VEGF-pathway inhibitors with immunotherapies. This strategy has been applied in the clinic and has demonstrated anti-tumour responses. Angiogenic factors especially VEGF activates an immunosuppressive microenvironment through different mechanisms. VEGF inhibits the normal activation and maturation of dendritic cells, leading to immune evasion by tumours. Moreover, the abnormal tumour vasculature prevents the infiltration of cytotoxic T-cells. Additionally, VEGF triggers the infiltration of immunosuppressive cells such as T-regulatory cells and myeloid-derived

suppressor cells into the tumour (Khan and Kerbel 2018, Teleanu *et al.* 2019, Hack *et al.* 2020, Lopes-Coelho *et al.* 2021). Tumour cells have been shown to activate the programmed cell death 1 (PD-1) pathway an immune checkpoint pathway. PD-1 is a negative regulator of immune cells that mediate immune responses such as T cytotoxic cells, dendritic cells and natural killer cells. PD-1 receptor on these cells binds to their corresponding ligands PD-L1 that are expressed on tumour cells, endothelial cells and other immune cells. The activated pathway inhibits the anti-tumour response of T cells; hence, tumour cells evade targeting by T cells and progress. Inhibitors of the PD-1/PD-L1 pathway are immunotherapies designed to block this pathways, hence tumour cells can be targeted by T cytotoxic cells (Akinleye and Rasool 2019, Lopes-Coelho *et al.* 2021). Combining antiangiogenic therapies with immunotherapies demonstrated a profound anti-tumour effect (Khan and Kerbel 2018, Teleanu *et al.* 2019, Hack *et al.* 2020, Lopes-Coelho *et al.* 2021). Combining bevacizumab with anti-PD-L1 antibody atezolizumab was shown to prolong PFS in patients with hepatocellular carcinoma compared to atezolizumab alone (Lee *et al.* 2020). A recent phase III clinical trial demonstrated an improvement in both PFS and OS in metastatic non–small-cell lung cancer patients treated with standard chemotherapy plus bevacizumab and atezolizumab as a first line treatment compared to patients who only received bevacizumab with chemotherapy (Socinski *et al.* 2018). In addition, a phase III clinical trial showed that the combination of bevacizumab plus atezolizumab improved the PFS compared to sunitinib alone in metastatic renal cell carcinoma (mRCC) (Rini *et al.* 2019). Analysis of tumour tissues of mRCC patients post treatment with combination bevacizumab and atezolizumab showed an increase in the trafficking and infiltration of $CD8^+$ T cells, suggesting that this dual inhibition promotes anti-tumour immunity (Wallin *et al.* 2016). The increase in trafficking of anti-tumour immune cells was potentially mediated by the normalisation of tumour vasculature which enabled the infiltration of CD8+ T cells (Shigeta *et al.* 2020). In addition, there are other reported mechanisms of action of the combined anti-angiogenic and immunotherapy treatments. A preclinical study on hepatocellular carcinoma murine models showed that the combination of VEGFR-2 inhibitor (sorafenib) with anti-PD-1 antibody promoted anti-tumour immune microenvironment. The combination increased the anti-tumour M1 tumour-infiltrating macrophages and activation of T-cytotoxic cells. In addition, it reduced the pro-tumour M2 tumour infiltrating macrophages and T-regulatory cells, enabling anti-tumour immunity

(Shigeta *et al.* 2020). Taken together, the combination of both anti-angiogenic therapies and anti PD1/PD-L1 treatments increased the efficacy of response.

1.11 Biomarkers determining response to anti-VEGF therapy.

Given the inconsistent results found with antiangiogenic drugs in the clinic, the need to identify cellular and/or molecular biomarkers that help to select patients who are more likely to benefit from antiangiogenic treatments is urgent. However, until now, there is no one definitive biomarker and the need to identify more biomarkers is important. Moreover, there are no validated biomarkers identifying whether patients show resistance or response from treatment. The other main challenge for a number of the biomarkers is that they are agent and/or disease dependent (Jain *et al.* 2009).

Plasma VEGF has been proposed to be a biomarker in several cancer types (Oguntade *et al.* 2021). However, while VEGF is of prognostic value across different cancers, its value as a predictor of treatment outcome in response to antiangiogenic agents is not consistent across different clinical studies. A clinical trial evaluated the use of baseline VEGF for predicting response to bevacizumab in HER-2 negative metastatic breast cancer showed that there was no correlation between baseline VEGF-A and treatment benefit (Miles *et al.* 2017). However, in another clinical trial, high levels of circulating VEGF-A in HER-2 negative metastatic breast cancer patients were associated with a good response to bevacizumab (Miles *et al.* 2013). Furthermore, VEGF is also not validated as a biomarker of response. VEGF and PIGF were reported to be increased in patients who showed tumour progression during treatment with AZD2171, a TKI against the activity of VEGFR and PIGFR (Batchelor *et al.* 2007, Jain *et al.* 2009). In contrast, VEGF and PIGF increased in metastatic renal cell carcinoma patients who showed response to sunitinib, a TKI (DePrimo *et al.* 2007). It is possible to speculate from these conflicting findings that VEGF as a biomarker is agent and/or disease dependent. It is not clear yet from the literature why there is increase in VEGF and PIGF after treatment with TKI and it cannot be predicted if this represents an escape mechanism or a sign of tumour response. This question remains unanswered. A preclinical study using a mouse model found that VEGF expression increased after sunitinib (TKI) treatment in non-tumour-bearing mice, suggesting that the increase in VEGF is not a tumour-induced mechanism to escape the therapy (Ebos *et al.* 2007). Taken together, more research is needed to evaluate VEGF as a biomarker.

Other circulating proteins can also indicate resistance to treatments. An increase in alternative proangiogenic factors such as FGF, SDF1α, CECs and CPCs were associated with tumour progression in glioblastoma (Batchelor *et al.* 2007). Specifically, FGF and SDF1α increases were associated with a significant increase in vessel size, suggesting the induction of alternative proangiogenic pathways (Batchelor *et al.* 2007).

Different clinical studies have investigated the role of CEPs and CECs as potential surrogate biomarkers (Beaudry *et al.* 2005, Mancuso *et al.* 2006). CECs increased in breast cancer patients who were treated with metronomic chemotherapy, a therapeutic strategy associated with antiangiogenic activity. Their increase was associated with progression free survival and improved overall survival. The study found that most of these CECs were apoptotic cells and were suggested to result from the antiangiogenic effect on the tumour vasculature. However, in glioblastoma, an increase in viable CECs during the treatment with TKI were observed in patients who showed no response during the treatment (Mancuso *et al.* 2006, Batchelor *et al.* 2007). These conflicting results underline the need for more research to investigate the reason of different outcomes between cancer models.

Tumour microvascular density (MVD) was also assessed as a predictive biomarker for bevacizumab benefit in a clinical trial of ovarian cancer patients (Bais *et al.* 2017). Patients with high pre-treatment MVS showed a significant increase in PFS from the addition of bevacizumab to chemotherapy compared with patients with low MVD. However, MVS was not considered as a predictor factor of benefit from bevacizumab in metastatic colorectal cancer (Jubb *et al.* 2006).

The change in plasma Tie2 has also been identified as a response biomarker for bevacizumab in metastatic colorectal cancer and ovarian cancer (Zhou *et al.* 2016, Jayson *et al.* 2018). The patients with 50 % increase in Tie2 levels showed disease progression and loss of benefit from bevacizumab (Zhou *et al.* 2016, Jayson *et al.* 2018). Tie2 is a receptor expressed by endothelial and binds to Angiopoietin (Ang) ligands (Ang1 and Ang 2). Binding of Ang1 to Tie2 promotes the stability and maturation of blood vessels by increasing the attachment of pericytes to endothelial cells. Ang2 competes with Ang 1 for binding to Tie2. Tie2-Ang2 signalling pathway induces remodelling of vasculature and inhibited its stability and maturation (Zhang *et al.* 2019). This is because Ang2 promotes the detachment of pericytes to endothelial cells,

leading to less mature vasculature. During tumour angiogenesis, the expression of Ang2 is upregulated and indicates poor prognosis (Huang *et al.* 2010, Saharinen *et al.* 2011).

Another recent clinical trial investigating Tie2 as a vascular response marker in patients with advanced biliary tract cancer treated with the VEGF tyrosine kinase inhibitor cediranib, identified that 24% reduction in plasma Tie2 within 9 weeks is a vascular response to treatment (Zhou *et al.* 2022). Nevertheless, identifying the vascular response rate to VEGF inhibitors is not possible for some tumour types such as breast cancer. This is because that not all patients benefit from VEGF inhibitors (Zhou *et al.* 2022).

In summary, several biomarkers have been proposed to predict the outcome of antiangiogenic treatments. However, no one biomarker is validated yet, and many studies have reported conflicting outcomes.

1.12 Crystallins

Crystallins are predominant proteins in the eye lens and responsible for lens transparency. They are three types of crystallins, α, β, and γ, consisting of different subunits. α-crystallin is a major member of the family of crystallin proteins subdivided into two subtypes; acidic and basic, known as αA-crystallin and αB-crystallin, respectively. Members of the α-crystallin family act to protect proteins from aggregation under stress conditions. αA-crystallin is thought to be expressed mainly in the eye, whereas αB-crystallin is expressed in other tissues such as heart, skeletal muscle, skin, brain, spinal cord and lung (Meehan *et al.* 2004). The overexpression of αB-crystallin was found to be associated with several neurological diseases such as Alexander's disease, Alzheimer's disease and Parkinson's disease (Horwitz 2000). Importantly, several studies showed that αB-crystallin is overexpressed in many cancer cells such as gliomas, renal cell carcinoma, and invasive breast cancer. Its expression may contribute to the aggressive behaviour of many cancer cells (Chen *et al* . 2014; Lee *et al* . 2012; Moyano *et al* . 2006).

1.12.1 α-crystallins as "heat shock" proteins

α-crystallin proteins are members of the heat shock protein family (HSPs) and act as chaperone molecules. They prevent the aggregation of misfolded proteins, hence allowing them to retain their functional structure. The chaperone function of α-crystallin proteins was first identified by Horwitz (1992). He tested the ability of α-crystallin to prevent the

accumulation of heat-induced lens proteins and enzymes. There are several stimulants that activate the expression of heat shock proteins in addition to heat, including pH extremes, nutrient limitation, osmotic variation, hypoxia, chemotherapeutic agents and noxious chemicals. HSPs are classified into families according to subunit weight, including HSP90, HSP70 and HSP60. The small heat shock proteins (sHSPs) have a molecular weight less than 35 kDa and α-crystallin proteins belong to this protein family (Derham and Harding 1999). αA-crystallin and αB-crystallin are known as HSPB4 and HSPB5, respectively. Both proteins have an approximate molecular mass of 20 kDa. α-crystallins constitute 35% of the mammalian eye lens in which they confer important chaperone roles. They protect the proteins in fibre cells from aggregation, which result as a normal consequence of ageing. With aging, most of proteins in fibre cells convert from water soluble into water insoluble. As a result, they become prone to aggregation and hence cataracts may develop. α-crystallin binds selectively to denatured proteins and refold the misfolded proteins (Horwitz 2003).

1.12.2 The influence of phosphorylation on the function of α-crystallin

αB-crystallin undergoes phosphorylation as a normal consequence of dividing and differentiation of cells. In addition, stress stimulation such as oxidative agents, ischaemia and heat can induce the phosphorylation of αA and αB-crystallin. αA-crystallin is phosphorylated at Ser122, whereas the phosphorylation sites of αB-crystallin are Ser19, Ser45 and Ser59 (Thornell and Aquilina 2015). Phosphorylation is reported to reduce the oligomeric size of α-crystallin (Ito *et al.* 2001). It is also thought to increase its chaperone-like function; however, some studies showed that phosphorylation decreased it or has no effect on its chaperone-like function (Ecroyd *et al.* 2007, Ahmad *et al.* 2008, Muranova *et al.* 2018). The role of αB-crystallin phosphorylation has been studied extensively and it is suggested to be involved in the regulation of many cellular pathways such as stress response and apoptosis pathways (Kamradt *et al.* 2002, Launay *et al.* 2006, Launay *et al.* 2010). In response to various stresses, phosphorylation of αB-crystallin in Ser45 is triggered by P44/42 MAPK, whereas P38/ MAPKAP kinase 2 is responsible for Ser59 phosphorylation. (Launay *et al.* 2006).

The role of αB-crystallin phosphorylation in the regulation of apoptosis has been reported by Launay *et al.* (2010). The study investigated the phosphorylated status of αB-crystallin after treatment with the anti-cancer agent vinblastine in the breast cancer cell line MCF7. There was a correlation between the apoptosis and phosphorylation of αB-crystallin at Ser59. The

molecular mechanism is that the phosphorylated αB-crystallin binds to Bcl-2, an anti-apoptotic protein and prevents its translocation to the mitochondria. The study demonstrated that although αB-crystallin is anti-apoptotic , this function is downregulated by its phosphorylation at Ser 59 (Launay *et al.* 2010). Additionally, αB-crystallin was shown to be induced in C2C12 myoblasts that are resistant to differentiation-induced apoptosis, a function that is essential for their development. Thus αB-crystallin confers resistance to differentiation-induced apoptosis in C2C12 myoblasts (Kamradt *et al.* 2002). However, the phosphorylation of αB-crystallin leads to the loss of anti-apoptotic function of αB-crystallin in cardiomyocytes (Kamradt *et al.* 2002). Although these studies have suggested that ser59 phosphorylation inhibits the chaperone function of αB-crystallin others have shown that phosphorylation at this site results in an increase in chaperone activity (Morrison *et al.* 2003, Kase *et al.* 2010, Dong *et al.* 2016). Morrison *et al* (2003) demonstrated that phosphorylation of αB-crystallin at Ser59 protected cardiac myocytes from ischemia-induced apoptosis (Morrison *et al.* 2003). In addition, Kase *et al* found that Ser59 phosphorylated αB-crystallin increased in retinal pigment epithelial cells under hypoxic conditions and protected the newly formed blood vessels from apoptosis. This chaperone function of αB-crystallin to endothelial cells was due to αB-crystallin binding to VEGF and protecting it from degradation during ocular angiogenesis (Kase *et al.* 2010). Similarly, Ser59 phosphorylated αB-crystallin was upregulated in diabetic retinopathy and co-localised with VEGF in neovascular endothelial cells in diabetic retinopathy (Dong *et al.* 2016). It could be speculated from this finding that Ser59 phosphorylated αB-crystallin acts to chaperone VEGF during angiogenesis and therefore stimulates the survival of endothelial cells.

αB-crystallin also exerts a protective role in the regulation of cytoskeletal proteins. It has been reported that Ser59 phosphorylated αB-crystallin colocalized with cytoskeletal components and protected their integrity against extracellular stress, suggesting a protective role of Ser59 phosphorylated αB-crystallin. It should be noted that the phosphorylation of ser-59 on αB-crystallin is induced through the activation of MAPK p38 pathway (Launay *et al.* 2006).

In summary, these studies suggest that the phosphorylation of αB-crystallin may act as a negative or positive regulator, depending on the cellular pathway and/or the target protein.

1.13 αB-crystallin as an anti-apoptotic protein

Several studies have revealed an anti-apoptotic function of αB-crystallin via different mechanisms. One study carried out by Kamradt and colleagues reported that αB-crystallin prevented the proteolytic activation of caspase-3. This study suggested that αB-crystallin binds to the p24 of caspase-3 and prevents its autoproteolytic cleavage and hence acts as an inhibitor of the intrinsic and extrinsic apoptotic pathways (Kamradt *et al.* 2001). A similar finding was observed in H_2O_2 -treated primary astrocyte cultures where overexpression of αB-crystallin inhibited the activation of caspase-3 due to its binding to p24 (Shin *et al.* 2009). The anti-apoptotic function of αB-crystallin was reported in another study in which αB-crystallin inhibited oxidative stress induced apoptosis in mouse myogenic C2C12 cells (Mercatelli *et al.* 2010). In another study αB-crystallin was shown to sequester p53, a regulator of apoptosis and decreased its translocation from the cytoplasm to the mitochondrial membrane (Liu *et al.* 2007). In addition, αB-crystallin has an affinity to other proapoptotic proteins such as Bax and Bcl-XS and decreases their activity *in vitro* and *in vivo* by preventing their translocation to the mitochondria during staurosporine-induced apoptosis (Mao *et al.* 2004). αB-crystallin also plays a role in the regulation of apoptosis in blood vessel endothelial cells. Dimberg *et al* investigated the function of αB-crystallin during tubular morphogenesis in tumour vessels using small interfering RNA–mediated knockdown of αB-crystallin expression (Dimberg *et al.* 2008). They found that the inhibition of expression gave rise to weak tubular morphogenesis, activation of caspase-3 and apoptosis induction. All these findings suggest that αB-crystallin interferes with apoptotic mechanisms and acts as an anti-apoptotic mediator.

αB-crystallin may interfere with different cellular processes to enhance cell survival during stress conditions. Beside its inhibitor function in apoptosis pathways, αB-crystallin activates mitogen-activated protein kinase (MAPK) pathway in basal like tumours (Moyano *et al.* 2006, van de Schootbrugge *et al.* 2013). The MAPK pathway is responsible for many biological responses including cell survival through the activation of Ras/Raf/MEK/ERK intracellular signaling pathway (Li *et al.* 2016). However, in some cell systems, this pathway can lead to stress activated apoptosis. For example, it was shown to lead to UVA-induced apoptosis of lens epithelial cells instead of promoting survival (Liu *et al.* 2004, Li *et al.* 2005). Indeed, αB-crystallin prevented the UVA-induced apoptosis in lens epithelia through the suppression of UVA-induced activation of the RAF/MEK/ERK pathway and activation of the AKT pathway that

promoted survival (Liu *et al.* 2004, Li *et al.* 2005). The protective function of this protein is also demonstrated in cardiac myocytes.

1.14 αB-crystallin can promote metastasis and invasion of tumour cells

Several studies have focused on the function of this protein as a promotor of metastasis and invasion as its overexpression has been demonstrated in many cancers (Chelouche-Lev *et al.* 2004, Wettstein *et al.* 2012, Kim *et al.* 2015, Chen *et al.* 2018). For instance, it is known that EMT is an essential process in cancer metastasis. This involves loss of epithelial markers such as E-cadherin and the transition into amotile mesenchymal phenotype, with an increase in vimentin and desmin proteins that are expressed by mesenchymal cells. Through EMT, malignant cells acquire a migratory phenotype and, therefore, become invasive (Wettstein *et al.* 2012). One study revealed a potential role for αB-crystallin in invasion and metastasis of gastric cancer cells (Chen *et al.* 2018). This study reported the influence of this protein in mediating invasion through the activation of NF-κB, which is a nuclear transcription factor that regulates EMT. Overexpression of αB-crystallin in gastric cancer cells led to the activation of the NF-κB signalling pathway, while silencing αB-crystallin inactivated NF-κB signalling (Chen *et al.* 2018). As has been demonstrated by several studies, αB-crystallin overexpression is considered as a poor prognostic factor. The overexpression of this protein contributes to the progression of basal-like breast cancer and enhances the invasion and migration of malignant cells *in vitro*. Furthermore, αB-crystallin is strongly associated with invasive ductal carcinoma and indicates short overall survival (Kim *et al.* 2015). In addition, αB-crystallin was linked with the axillary lymph node involvement in breast carcinoma and hence a marker of poor prognosis (Chelouche-Lev *et al.* 2004). The potential implication of αB-crystallin in cancer metastasis has been studied *in vitro* using TNBC cell lines and *in vivo* models (Malin *et al.* 2014) . αB-crystallin enhanced brain metastasis and was associated with poor survival. αB-crystallin increased adhesion to human brain microvascular endothelial cells (HBMECs), transendothelial migration and the infiltration of tumour cells through the blood brain barrier (BBB). The remarkable finding of this study is that the overexpression of αB-crystallin in TNBC cells stimulated the adhesion of TNBC cells to HBMECs at least in part through interactions with α3β1 integrin which is implicated in metastasis. However, more studies are needed to investigate the interaction between αB-crystallin and α3β1 integrin in other types of cancers.

This evidence indicates that αB-crystallin may be associated with invasion and migration of malignant cells (Malin *et al.* 2014).

In contrast, αB-crystallin may impair metastasis in nasopharyngeal carcinoma (NPC) and acts as a tumour suppressor gene through the suppression of EMT markers and the progression of the malignant cells (Huang *et al.* 2012). In this study, Huang *et al* observed that αB-crystallin associated with E-cadherin and β-catenin and prevented the disruption of cadherin/catenin adherens junction, one of the EMT features. The mechanism of this function is that αB-crystallin inhibits E-cadherin cytoplasmic internalization that leads to the disruption of adherens junctions. Furthermore, the study proposed that the overexpression of αB-crystallin prevented the release of membrane-bound β-catenin into the cytoplasm and nucleus. β-catenin has oncogenic functions and activates transcription factors that stimulate tumour progression. αB-crystallin interacted with β-catenin and prohibited its translocation to the cytoplasm and nucleus, suggesting that αB-crystallin contributed to the cadherin/catenin adherens junction and supressed EMT in NPC cancer. Furthermore, overexpression of αB-crystallin in bladder cancer cells reduced phosphorylated ERK and AKT and inhibited the migration and invasion of bladder cancer cells (Ruan *et al.* 2020). The tumour suppressor function of αB-crystallin was revealed in another study that showed that αB-crystallin may act to promote apoptosis (Watanabe *et al.* 2009). αB-crystallin may act as a pro apoptotic protein and induce apoptosis through binding to p53 protein. The study demonstrated that the suppression of αB-crystallin expression prevented p53-induced apoptosis, hence αB-crystallin acted as a proapoptotic protein (Watanabe *et al.* 2009). p53 is a tumour suppressor gene and activates the expression of several genes involved in cell cycle arrest, cellular senescence, DNA repair and apoptosis in response to cellular stress. In the p53 dependent apoptosis pathway, p53 regulates the transcription of several proapoptotic genes such as bax, puma and noxa. In addition, in response to stress, p53 accumulates in the cytosol and in the mitochondria where it activates proapoptotic proteins and inhibits antiapoptotic proteins. p53 in the cytosol, triggers the mitochondrial translocation of proapoptotic proteins, including bax and bak (Fridman and Lowe 2003, Amaral *et al.* 2010). In general, the pro-apoptotic function of αB-crystallin needs to be elucidated in more studies. In summary, it appears that αB-crystallin acts differentially in different cancers and therefore more research is needed to explore its role in EMT and apoptosis in malignant cells.

1.15 αB-crystallin a novel oncoprotein associated with poor prognosis in breast cancer and its role in treatment resistance

αB-crystallin is overexpressed in metastatic breast carcinoma including metaplastic breast cancer, infiltrating ductal breast carcinomas and is considered to be a specific potent marker for basal like breast cancer and triple negative breast cancer (Sitterding *et al.* 2008, Travis *et al.* 2011, Kabbage *et al.* 2012, Tsang *et al.* 2012). Several studies have demonstrated that αB-crystallin is associated with poor prognostic factors like lymph node metastasis (Chelouche‐Lev *et al.* 2004, Travis *et al.* 2011). Intriguingly, αB-crystallin induced neoplastic-like changes in human mammary epithelial cells including enlarged masses with filled lumens, abnormalities in mammary acini and promoted the survival of the cells (Moyano *et al.* 2006). These studies suggest that αB-crystallin may act as an oncoprotein that predicts poor prognosis.

αB-crystallin is considered to be an independent poor prognostic factor in other cancer types including human hepatocellular carcinoma (HCC) (Tang *et al.* 2009), head and neck cancer (HNSCC) (Chin *et al.* 2005) and non-small cell lung cancer (NSCLC) (Qin *et al.* 2014). Furthermore, significant overexpression of αB-crystallin has been observed in laryngeal squamous cell carcinoma (SCC) tissue samples compared with normal tissue samples and was associated with tumour progression (Mao *et al.* 2012, Yilmaz *et al.* 2015). Therefore, αB-crystallin is suggested to be an effective prognostic factor to predict patient outcomes. As discussed previously, αB-crystallin prevents apoptosis induced by different stimuli and activates the ERK/MAPK pro-survival pathway in basal like tumours. These events may be associated with a poor prognosis via a link to αB-crystallin. Furthermore, αB-crystallin can be used to predict the effectiveness of treatment. Studies have demonstrated that the αB-crystallin is implicated in the resistance to conventional cancer treatments. For instance, αB-crystallin correlated with resistance to neoadjuvant chemotherapy in triple negative breast cancer (Ivanov *et al.* 2008). Furthermore, radiotherapy may increase the expression of αB-crystallin since one study using gene expression profiling data in radiation induced tumour cells showed upregulation of αB-crystallin (Bang *et al.* 2016). Additionally, it was suggested that αB-crystallin may contribute to resistance to combined preoperative trastuzumab and vinorelbine in HER2 positive breast cancer (Harris *et al.* 2007). Importantly, it has been suggested that αB-crystallin may contribute to the resistance against anti-VEGF therapy. The

mechanism proposed in this case is that the endothelial cells in the tumour microenvironment upregulate αB-crystallin to protect intracrine VEGF and promote angiogenesis (Ruan *et al.* 2011). αB-crystallin is a chaperone that prevents the aggregation of misfolded or unfolded proteins (Koletsa *et al.* 2014) and is considered as a key regulator of angiogenesis in tumour tissue (Dimberg *et al.* 2008). Ruan *et al* demonstrated that tumours do not depend only on the paracrine mode to stimulate angiogenesis and tumour growth. Initially the tumour cells can stimulate the vasculature in the microenvironment via the paracrine mode, through production of VEGF and other pro-angiogenic growth factors, but in turn, endothelial cells may also produce and release VEGF that can activate their own growth and that of adjacent tumour cells. In the Ruan *et al* study, αB-crystallin was induced in the endothelial cells by co-culture with TNBC cell lines and then it was further upregulated by anti-VEGF therapy, suggesting that the endothelial cells upregulated αB-crystallin to protect intacrine VEGF activity. While anti-VEGF treatments like bevacizumab are designed to act against secreted VEGF, intracrine VEGF is protected and can support the endothelial cells in the tumour. Taken together, the upregulation of αB-crystallin by endothelial cells following anti-VEGF treatment or other stress stimuli may represent a resistance mechanism (Ruan *et al.* 2011). The role of αB-crystallin in the resistance to anti-VEGF therapy has also been studied using sorafenib (Huang *et al.* 2013). Ectopic expression of αB-crystallin in HCC activated ERK phosphorylation, inducing EMT in HCC cells, which developed resistance to sorafenib. In fact, αB-crystallin formed a complex with 14-3-3f that prevented its degradation. This complex is thought to activate the ERK pathway which in turn promoted the survival and invasiveness of HCC cells and contributed to the resistance to sorafenib (Huang *et al.* 2013). Thus, αB-crystallin may be considered as a therapeutic target for cancers in which αB-crystallin is upregulated and potentially promotes their progression.

1.16 Targeting αB-crystallin

Several studies have demonstrated that αB-crystallin predicts a poor survival in multiple cancer types. Importantly, αB-crystallin may impair the activity of anti-angiogenesis drugs. Targeting αB-crystallin has been a focus of several studies. As previously discussed, αB-crystallin stabilizes and prevents the aggregation of intracrine VEGF under stress or after anti-VEGF treatment, potentially inducing the resistance to anti-VEGF inhibitors such as bevacizumab. Subsequently, targeting the interaction between αB-crystallin and VEGF may

lead to down-regulation of intracrine VEGF, hence increasing the sensitivity to anti-VEGF treatment. Chen *et al* studied the possibility of disrupting t this interaction in TNBC cells through identifying NCI-41356 as a small molecule inhibitor of VEGF/αB-crystallin interactions. The results revealed that NCI-41356 decreased VEGF levels and inhibited the proliferation and invasion of TNBC cells. NCI-41356 also decreased angiogenesis related responses in endothelial cells that were co-cultured with TNBC cells (MDA-MB-231). Moreover, administration of NCI-41356 in a breast cancer xenograft model resulted in a significant regression of tumour growth and angiogenesis (Chen *et al.* 2014). Furthermore, a more recent study developed purine-based agents to reduce the interaction between VEGF and αB-crystallin (Fosu-Mensah *et al.* 2019). These compounds have been evaluated in cell viability assays using TNBC cell lines and their efficacy to disrupt the interaction between αB-crystallin and VEGF was determined. Results showed a significant reduction in the viability of TNBC cell lines and a decrease in the amount of VEGF secreted by the cells by 40% (Fosu-Mensah *et al.* 2019). Although these studies achieved a significant goal of targeting the interaction between VEGF and αB-crystallin, further studies are needed to determine the mechanisms of this interaction.

1.17 Study rationale

Antiangiogenic therapy has been used in the clinic for several cancer types. However, these treatments fail to give prolonged benefits. Most patients experience tumour regrowth after treatment, and in some cases their tumours progressed in an aggressive manner. Different modes of resistance to anti-VEGF treatments have been identified by multiple studies. It is widely known that αB-crystallin is overexpressed in multiple cancer types including metastatic breast cancer subtypes. It interferes with several signalling pathways, contributes to the progression of breast cancer, and is associated with poor prognostic factors. There are several studies that suggest possible mechanisms whereby αB-crystallin prevents apoptosis, enhances tumour cell survival, and promotes metastasis. Moreover, αB-crystallin confers resistance to chemotherapy and there are two studies suggesting that it also contributes to resistance to anti-VEGF treatment (Ruan *et al.* 2011, Huang *et al.* 2013). αB-crystallin is a chaperone molecule that binds to misfolded proteins and prevents their degradation under cellular stress. Importantly, αB-crystallin binds to intracrine VEGF and enhances its stability and may therefore contribute to the resistance to anti-VEGF drugs. Disrupting the interaction

between αB-crystallin and VEGF represents a promising target and has resulted in a significant decrease in angiogenesis in a breast cancer tumour model (Chen *et al.* 2014). Nevertheless, more research is needed in order to identify the mechanisms that are involved in the αB-crystallin-VEGF interaction. Targeting these mechanisms may improve the outcome of anti-VEGF therapies.

1.18 Hypothesis

αB-crystallin protects VEGF from degradation and increases its secretion, hence contributes to resistance to anti-VEGF therapies in breast cancer. This hypothesis will be investigated throughout this study.

1.19 Aim of the study

- To investigate the effect of αB-crystallin overexpression on cell proliferation, response to a chemotherapeutic agent (doxorubicin) and on the production/secretion of VEGF in TNBC cells (Chapter 3)
- To investigate the effect of αB-crystallin knockdown in TNBC cells on the production/secretion of VEGF (Chapter 4).
- To determine the effect of conditioned media from TNBC cells with different levels of αB-crystallin on endothelial cells response in terms of expression of αB-crystallin and their migration (Chapter 5).
- To assess of the efficacy of bevacizumab, doxorubicin and the combination of both drugs on the growth and vasculature of high versus null αB-crystallin in xenograft breast cancer models (Chapter 6).

Chapter2 **Materials and Methods**

A list of reagents and suppliers can be found in the Appendix.

2.1 Cell lines & Cell culture

2.1.1 Cell culture

Cell culture refers to cell growth under control conditions, generally outside their natural environment. There are two types of cultures; primary cell culture, which represents cells that are derived directly from living tissues, and secondary cell culture that are derived from a cell line or cell strain that has already been established. The cells in primary cell culture have finite life spans this is because they lack the interactions with the local environment that are essential for long-term survival, including tissue hierarchy and renewal of differentiated cells through stem cell signalling, whereas cell lines have been immortalised and no longer need these interactions to survive.

2.1.2 Cell lines

MDA-MB-468 is a breast cancer cell line derived from a pleural effusion of a 51-year-old black woman with metastatic breast adenocarcinoma.

MDA-MB-231 is a breast carcinoma cell line that was derived from a pleural effusion of a 51-year-old Caucasian female with a metastatic mammary adenocarcinoma.

Both MDA-MB-468 and MDA-MB-231 are classified as TNBC cell lines as they lack oestrogen receptor (ER) and progesterone receptor (PR) expression, as well as HER2. Cells were stored in liquid nitrogen and used from passage P2 to P20 after thawing.

Primary Human Dermal Blood Endothelial Cells (HDBECs) are a subpopulation of the Human Dermal Endothelial Cells, isolated from the dermis of juvenile foreskin or adult skin (different locations) from a single donor. Cells were not used beyond passage 7 (P7).

All cells used in this study were purchased new and authenticated by their supplier. Mycoplasma testing was carried out monthly in the department. Cell lines used during this study and the composition of the media required for standard subculture are detailed in Table 2.1.

Table 2-1 Cell lines and their culture medium requirements

Cell type	Source	Culture media
MDA-MB-468	(ATCC® HTB-132™)	500 ml DMEM–Dulbecco's Modified Eagle Medium (Lonza; BE12-741F) 10% Fetal Bovine Serum (FBS) (Gibco; 10270-106), 2 mM Glutamine (Lonza; BE17-605E) 100 μg /ml Streptomycin 100 U/ml Penicillin (Lonza; DE17-603E)
MDA-MB-231	(ATCC® HTB-26™)	500 ml DMEM–Dulbecco's Modified Eagle Medium (Lonza; BE12-741F) 10% Fetal Bovine Serum (FBS) (Gibco; 10270-106), 2 mM Glutamine (Lonza; BE17-605E) 100 μg /ml Streptomycin 100 U/ml Penicillin (Lonza; DE17-603E
Primary Human Dermal Blood Endothelial Cells (HDBEC)	PromoCell, C-12211	500 ml Endothelial Cell Growth Medium MV. 0.05 ml / ml Fetal Calf Serum 0.004 ml / ml Endothelial Cell Growth Supplement 10 ng / ml Epidermal Growth Factor (recombinant human) 90 μg / ml Heparin 1 μg / ml Hydrocortisone

2.1.3 Cell subculture

Subculture of cell lines was performed when the cell lines covered 80% of the growth surface area. Medium, PBS and Trypsin EDTA were all pre-warmed in a 37^{o}C water bath for at least 30 minutes. Medium was removed from the flask and the cell monolayer was gently washed with 10 ml 1X PBS twice to remove excess serum as well as magnesium and calcium ions that aid cell adhesion. 0.25% trypsin (1 ml per 25 cm^2 of surface area) was added to the flask and then incubated for 1-2 min to promote the detachment of the cells. Trypsin is a proteolytic enzyme that should not be incubated with cells for a long time as it can cause damage. The cells were checked under the microscope and when detached from the flask surface, trypsin was then neutralised by serum-containing medium to stop the function of trypsin. The cell suspension was centrifuged at 1000 rpm for 5 minutes, the supernatant was discarded, and the cell pellet was resuspended in an appropriate volume of medium, depending on the desired cell density.

2.2 Cell counting

Cell counting is a fundamental step in cell culture through which the cell density is calculated. A glass haemocytometer is used to count the number of cells, and the total number of viable cells can be determined using a 1:2 ratio of trypan blue dye (which is excluded by viable cells but taken up by dead cells). The sample was prepared by mixing 100 µl of cell suspension and 100 µl of trypan blue dye. The mixture was then loaded in the space between the glass slide and the haemocytometer. The viable cells were observed under the microscope and counted in four large corner squares (1 mm^2 each) (Figure 2.1). Using the calculation below, cell concentration (number of cells per ml) can be established.

Cell concentration = Total number of cells/ number of squares x 10^4 x dilution factor.

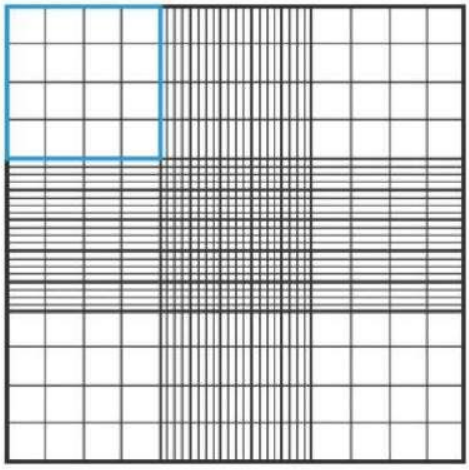

Figure 2.1 The haemocytometer four chambers as seen under the microscope. The cells are counted in four large corner squares

2.3 Freezing cell lines

Cell lines were frozen for long term storage enabling subsequent use of low passage aliquots. Cells were trypsinised and collected in a medium containing serum to neutralise trypsin, as described in section 2.1.3. The cells were syringed gently with a 27-gauge needle to dissociate the cell clumps and counted as explained in section 2.2. Once counted, cells were centrifuged and resuspended at 1000,000 cells/ml in a solution of complete medium/ 10% Dimethyl sulfoxide (DMSO). The cell suspension was divided into 1 ml aliquots in Stardstedt cyrovials and immediately placed in a "Mr Frosty" freezing container and stored at -80 ^{o}C overnight. The following day cryovials were transferred into liquid nitrogen for permanent storage.

2.4 Exposure of cells to heat shock and hypoxia.

αB-crystallin is one of the heat shock proteins that is induced in response to stress. To see the effect of heat shock on the induction of αB-crystallin, cells were exposed to 42^{o}C in a 5% CO_2 humidified incubator. For studying hypoxia, cells were placed in a humidified hypoxia chamber (Whitley H35 Hypoxyastation) set to of 0.1 % O_2. In parallel, control cultures were left in a normal humidified 37°C incubator.

2.5 Generation of cell-lines over expressing αB-crystallin.

Generation of αB-crystallin expressing cell lines was performed using plasmid DNA containing the CRYAB cDNA sequence (full sequence in the appendix). Stable transfection of CRYAB was performed into MDA-MB-231 cells which do not express this protein (see section 3.3.1). G418 is an analogue of neomycin and can be used as a selection factor by introducing the neomycin resistance gene (Neor) inside the plasmid (Figure 2.2). Therefore, this gene confers G418 resistance and only the cells that expressed the plasmid will survive, while the other cells will eventually die following treatment with the G418. Prior to transfecting MDA-MB-231 cells, a G418 dose response experiment was carried out to establish the lowest concentration of G418 antibiotic that killed all un-transfected cells (section 2.5.1). This concentration was subsequently used to isolate MDA-MB-231 cells that had successfully been transfected with the plasmid DNA before cloning.

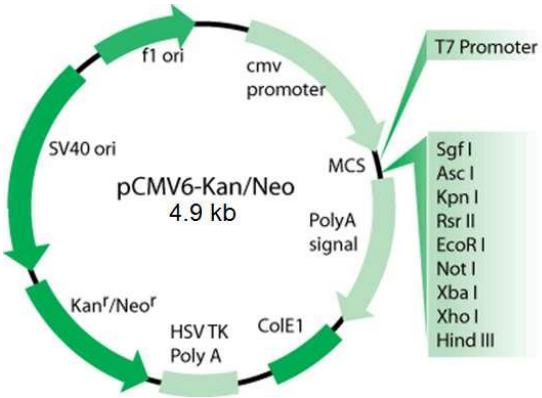

Figure 2.2 The cloning vector PCMV6-Kan/Neo of *CRYAB*. The multiple cloning site (MCS) within this plasmid contains *CRYAB* cDNA with restriction enzymes that are specific for the gene sequences in MCS, the CMV promoter consensus sequence drive protein expression in mammalian cells and an antibiotic selection cassette (Neor) which confers resistance to neomycin analogues in mammalian cells.

2.5.1 Generating G418 kill curves

MDA-MB-231 cells were seeded into 24 well plates at a density of 50,000 per well in 1 ml full growth medium. 24 h after plating, the full growth medium was replaced with medium containing G418 at concentrations between 100 to 1000 µg/ml. The control contained only full growth medium without G418. The cells were observed daily under the microscope. The lowest concentration of G418 that killed all the cells after two weeks of culture was used for determining successful transfection of cells in subsequent experiments.

2.5.2 Transfection efficiency using GFP plasmid DNA.

In order to check the efficiency of transfection in MDA-MB-231 cells, a GFP plasmid was used since the *CRYAB* plasmid did not express GFP or a similar reporter. The cells were seeded into 12 well plates at a density of 50,000 /well. On the following day, the medium was removed from all wells and was replaced with 1 ml of DMEM/ 10% FCS medium without antibiotics. The plate was placed in the incubator while the transfection mixture was being prepared. TransIT-X2 was used as the transfection reagent. 150 µl of 1X Optimem medium (reduced serum and antibiotic free medium) was added to each of 8 sterile Eppendorf tubes. 1 µg of GFP plasmid DNA was added to two tubes. Transfection reagent was added to three different tubes. Each tube containing plasmid DNA was then mixed with a tube containing transfection reagent. The third tube of transfection reagent was mixed with a tube containing Optimen alone to act as a test for transfection reagent toxicity. Finally, the two tubes containing only Optimem were mixed together, and this was used as control. Table 2.2 details the transfection procedure. All tubes were incubated for 20 min at room temperature to allow complexes of DNA and transfection reagent to form. After 20 min, each transfection mixture or control was added dropwise to a well containing cells. The plate was incubated overnight at 37^{o}C. On the following day, the cells were observed under a fluorescence microscope. Presence of green cells indicated that the cells were effectively transfected and GFP was expressed.

Table 2-2 Transfection parameters for determining the efficiency of TransIT-X transfection reagent of MDA-MB-231 cells.

Tube Number	1	2	3	4
Optimem	150 µl	150 µl	150 µl	150 µl
GFP DNA plasmid	1µg	1µg	-	-
Tube Number	5	6	7	8
Optimem	150 µl	150 µl	150 µl	150 µl
TransIT-X2	3 µl	3 µl	3 µl	-

2.5.3 Transfection using *CRYAB* plasmid DNA.

After the transfection efficiency was checked, MDA-MB-231 cells were transfected using the *CRYAB* plasmid. The cells were plated at a density of 50,000/well in 1 ml medium in a 12 well plate. The following day, the transfection mixture was prepared using 1 µg of *CRYAB* plasmid mixed with 3 µl of TransIT-X2. This mixture was applied to two wells. One well was used as a control in which only 3 µl of TransIT-X2 was added. The day after transfection, the medium was replaced with medium containing 750 µg/ml G418 which was the lowest concentration established to kill all the untransfected MDA-MB-213 cells. The medium was replaced every two days and the cells were checked regularly for any colonies produced. Once colonies were established, these were expanded, and the cells were screened by western blot for αB-crystallin expression.

2.5.4 Cell cloning

The MDA-MB-231 transfected cells that were established were expanded and frozen down as polyclonal lines. The transfected cells are heterogeneous in the amount of transgene. An increasing number of passages may lead to a reduction in the transgene expression overtime. Therefore, isolating a monoclonal cell population was undertaken using the limited dilution technique.

2.5.5 Methods for cloning MDA-MB-231 *CRYAB* transfected cells

A new vial of MDA-MB-231 *CRYAB* transfected cells was thawed and tested by western blot for αB-crystallin expression. If the cells were positive for αB-crystallin, they were used for cloning. Highly diluted cell suspensions were prepared to minimize the likelihood of having more than one cell per well. Therefore, when a cell formed a colony in the well, this would

have arisen from one cell and therefore could be considered as a monoclonal population. The cell suspensions were prepared after the cells were counted twice using the hemocytometer. The volume of suspension that was plated in each well was more likely to have one cell. In order to account for possible errors in the initial counting or plating efficiency, the cell suspensions that were prepared would give two cells per well, one cell per well and 0.5 cell per well. To do that, cells were trypsinised and counted accurately two times. Thereafter, serial dilutions of the cell suspension were prepared. The medium used was the G418 medium to maintain the selection of transfected cells. The cell suspensions were used to prepare one plate at 10 cells/ml cell density, one plate at 5 cells/ml cell density and one plate at 2.5 cells/ml cell density. Then, 200 µl of cell suspension was added into each well. The plates then were placed inside a 37 °C incubator. The plates were observed under the microscope after eight days to detect single colonies in the individual wells. The plates were left in the incubator until the grown colonies became confluent. Wells containing one single colony were marked and allowed to become confluent. The confluent colonies then were trypsinised and divided between two 12 well plates. One plate was used for culturing and expanding the cells. The other plate was used to extract the protein for analysis by western blot. The cells that are positive for αB-crystallin were expanded and frozen down.

2.6 Alamar blue viability assay

Alamar blue (resazurin) is a reagent used to monitor the activity of living cells to reduce the resazurin (blue) into the reduced form resorufin (pink). It quantitatively measures the viability of cell lines and helps determine the toxicity of novel agents (Al-Nasiry *et al.* 2007). The reduced form (resorufin) that is produced is pink and highly fluorescent, so the intensity of fluorescence produced is proportional to the number of living cells (Al-Nasiry et al. 2007). Cells were plated in 96 well plates. 10,000 cells/well were plated in 150 µl medium. The cells were allowed to adhere overnight. On the following day, the cells were treated with doxorubicin at different concentrations. The cells were incubated with drug for 48 h after which 20 µl of alamar blue (Thermo scientific, 88951) was added to each well and incubated with the cells for 24 h. The absorbance was measured at wavelengths of 570 nm and 600 nm. The percent difference in alamar blue reduction between treated and control cells was measured as follows (as provided from the manufacturer) (Thermo scientific, 88951)

Percentage difference between treated and control cells:

= (O2 x A1) - (O1 x A2) / (O2 x P1) - (O1 x P2) x 100

Where:

O1 = molar extinction coefficient (E) of oxidized alamar blue at 570 nm (80586)

O2 = E of oxidized alamar blue at 600 nm (117216)

A1 = absorbance of test wells at 570 nm

A2 = absorbance of test wells at 600 nm

P1 = absorbance of positive growth control well (cells plus alamar blue but no test agent) at 570 nm

P2 = absorbance of positive growth control well (cells plus alamar blue but no test agent) at 600 nm

2.7 Determining The IC50 of doxorubicin in MDA-MB231/WT and MDA-MB-231/*CRYAB*

Cell viability was measured by directly counting the cells after treatment with doxorubicin. This was done to determine the IC50 of doxorubicin in MDA-MB-231/WT and MDA-MB-231/*CRYAB*. The cells were plated at a density of 50,000 cells/well in 6-well plates. After 48 h, the cells were treated with different concentrations of doxorubicin. After 24 h, the cells were trypsinised and counted using a hemocytometer. The IC50 was determined using GraphPad prism software 8.0.2. First, the mean values of viable cells were normalised to percentages; the largest mean is defined as 100% viable cells and the lowest mean was defined as 0% viable cells. From the nonlinear regression dialog, inhibitor vs. normalised response -- variable slope model was used to obtain the IC50.

2.8 Doubling times and growth curves

The growth rate of MB-MDA-231/WT and MB-MDA-231/*CRYAB* overexpressing cells was measured by counting the cells every day for four days. MB-MDA-231/WT and MB-MDA-231/*CRYAB* were plated at a cell density of 50,000 cells/well in 6-well plates and incubated at 37˚C, 5% CO_2. At 24, 48, 72 and 96 hours after plating, cells from three wells per cell line were trypsinised, centrifuged at 1000 rpm for 5 min and the cell pellet resuspended in complete media. Viable cells were counted using the TC20 Automated Cell Counter. Doubling times

were calculated by plotting the log 2 of initial average end-point cell number/initial cell number (N/N0) and calculating the inverse slope at the linear part of the curve.

2.9 Short interfering RNA (siRNA) lipofection of MB-MDA-468 cells

The protein knockdown was carried out using the small interfering RNA (siRNA) technique. The synthetic double-strand RNA small fragments cause transient strong inhibition of targeted gene expression, resulting in suppression of protein production. *CRYAB* targeted siRNA transfection was carried out in *CRYAB* expressing MB-MDA-468 cells to further elucidate its role in breast cancer cells.

2.9.1 Lipid transfection

Lipid transfection, also known as lipofection or liposome-based transfection helps the delivery of genetic materials into cells. The lipid transfection uses a positively charged molecule called liposome that fuses with genetic materials to form a transfection complex. The complex then via the process of endocytosis passes the negatively charged cell membrane and travels to the nucleus.

2.9.2 siRNA transfection of MB-MDA-468 cells

MB-MDA-468 cells were plated at a density of 350,000 cells/well in 6-well plates in antibiotic-free full media and incubated at 37˚C, 5% CO_2 incubator overnight. After 24 h, 6 µl of Lipofectamine RNAiMAX transfection reagent (Thermo fisher, 13778150) was mixed with 150 µl of serum- free medium (SFM) for each well. Individual siRNAs or scrambled negative control siRNA duplex (see the duplex sequences in the appendix) were mixed with 150 µl SFM to give a final concentration of 10 nM per well, i.e. 1.15 µl of 20 µM siRNA per well. The diluted RNAiMAX was then combined with the siRNA mixture and incubated for 20 min before being added to the cells. Plates were rocked gently to mix and returned to the incubator. At 48 to 96 h post transfection cells were lysed with 1X RIPA lysis buffer, spun down at 13,000 rpm for 10 min and the supernatant was collected and stored at 80^{o}C for analysis by western blot to check the efficacy of αB-crystallin knockdown.

2.10 Flow cytometry analysis for cell viability using TOPRO3 and Annexin V

Flow cytometry is a powerful tool that is used to detect and measure specific populations of cells in a heterogenous sample based on their size, complexity, or fluorescence. Briefly, single cells pass through a laser beam or light source that leads to the production of light scatter or fluorescent light signals. The light signals are then converted by photo-multiplying tubes (PMTs), which is then processed to give a numerical signal.

2.10.1 Flow cytometry to detect apoptotic cells.

Annexin V and TOPRO3 were used as indicators of apoptotic cells. Annexin V binds to phosphatidylserine when it is translocated to the outer cell membrane during apoptosis (Van Engeland *et al.* 1998). TOPRO3 is a nucleic acid dye that is impermeable to live cells but penetrates compromised membranes characteristic of dead cells. Detection of apoptosis following treatment with doxorubicin was carried out by flow cytometry using Annexin V and TOPRP3. MDA-MB-231/WT and MDA-MB-231/*CRYAB* transfected cells were plated at a density of 50,000 cells/well in 6-well plates. After 48 h, the cells were treated with different concentrations of doxorubicin. The cells were incubated with the drug for 24 and 48 h, respectively. Media was aspirated from the wells and the cells were washed twice with 1 ml 1X PBS per well. The cells were harvested with 200 µl of 0.25% trypsin, and 800 µl of full medium was added to neutralise the trypsin reaction. All the media and washes were collected. The cells were spun down at 1100 rpm for 5 min before being resuspended in 250 µl of Annexin binding buffer. 1:50 of Annexin V was added to 5 mL round-bottomed polystyrene tubes and the samples were then added. The cells were vortexed and left for 10 min for Annexin V to bind. 5 µl of TOPRO 3 was added to the samples and the samples were run on the LSRII flow cytometer. Untreated cells were used as a control to adjust the voltage and amp gain and ensure that the cell population was visible on the SSC/FSC plot. A gate was drawn round the main cell population of the SSC/FSC plot to exclude debris from being analysed. Annexin V positive cells were detected by blue 530-30A channel, while TOPRO3 positive cells were detected by red 660-20-A channel. A gate was drawn to distinguish between viable cells (Q1), necrotic cells (Q3), early apoptotic cells (Q1) and late apoptosis (Q2) (Figure 2.3). Apoptosis percentage was calculated by adding the percentage of early and late apoptosis percentages. The data was analysed by FlowJo V10. 7.1 software.

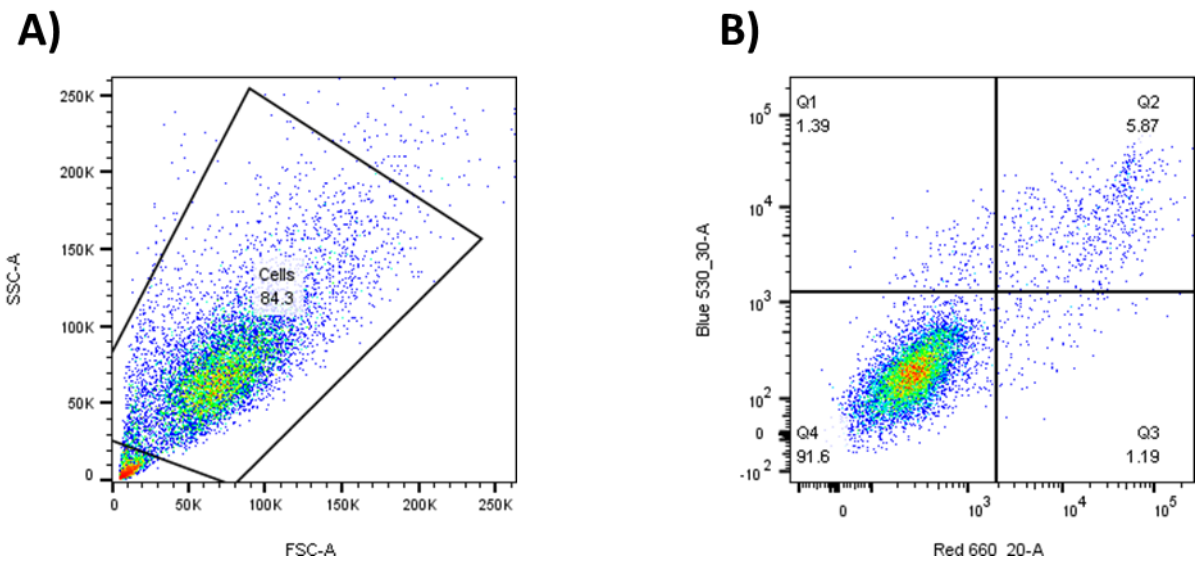

Figure 2.3 Gating strategy for apoptosis analysis. **A)** The first gate made around single cell populations of the SSC/FSC plot to exclude debris. **B)** Annexin V positive cells were detected by blue 530-30A channel, whereas TOPRO3 positive cells were detected by red 660-20-A channel. The gate was drawn to distinguish between viable cells (Q4), necrotic cells (Q3), early apoptotic cells (Q1) and late apoptosis (Q2). Apoptosis percentage was calculated by adding the percentage of early and late apoptosis percentages.

2.11 Co-culture model between αB-crystallin-expressing breast cancer cells and endothelial cells

Paracrine interactions between breast cancer cells with different levels of αB-crystallin on endothelial cell (HDBEC) response was assessed after incubation with conditioned media from breast cancer cells, followed by studying endothelial expression of αB-crystallin by western blot and migration ability by wound healing assays.

2.11.1 Preparation of conditioned media for co-culture experiments

MDA-MB-231/WT, MDA-MB-468 and MDA-MB-231/*CRYAB* cells were plated at a density of $2x10^6$ cells in T75 flasks in DMEM complete media for 48 h. After 48 h, when they reached 80% confluence, they were washed with serum-free endothelial cell growth medium MV to remove any residual serum, and then 15 ml of serum-free endothelial cell growth medium was added to the flasks. The conditioned media were collected after 48 h and spun down at 3000 rpm for 10 min to remove cell debris. The conditioned media were aliquoted and stored at 80 °C until used in the subsequent experiments.

2.11.2 Testing the expression of αB-crystallin in endothelial cells in co-culture with breast cancer cells

HDBEC were plated at a density of 96,000 cells per well in 6-well plates in a complete endothelial cell growth medium MV and allowed to grow for 48 h. Cells were then incubated with 50% complete endothelial cell growth medium MV media and 50% conditioned media prepared as described previously (Section 2.11.1). As a control, the cells were incubated with 50% complete growth media and 50% serum-free media which had not been in contact with breast cancer cells. After 48 h, the cells were lysed and spun down at 13,000 rpm for 10 min. The supernatant was collected and tested by western blot for αB-crystallin expression.

2.11.3 Wound healing assay

Two-well silicone cell culture inserts were placed centrally in the wells of a 12-well cell culture dish (1 insert per well, 3 wells per cell line). A suspension of 500,000 HDBECs per ml was prepared and 70 µl of this suspension was plated per well. Cells were incubated for 24 h before the cell culture inserts were removed to leave a gap/wound of 500 µm for cells to migrate across. Each well then was filled with 50% complete endothelial cell growth medium MV media and 50% conditioned media prepared as described above. As a control, the cells

were incubated with half complete growth media and half serum-free media which has not been in contact with breast cancer cells. Six images of each well were taken immediately after creating the wound and then again at intervals from 4 to 24 hours. Images were taken with a 10X objective phase contrast camera using the EVOS® Cell Imaging System. Image J was used to calculate the remaining open area in pixels. The percentage of the closed area was calculated using the following equation:

$$\text{Wound closure (\%)} = \frac{\text{(Area of initial scratch - Area of scratch at 4, 8 or 24h)}}{\text{Area of initial scratch}} \times 100$$

These steps were repeated for each experiment for endothelial cells incubated with conditioned media from MB-MDA-231/WT, MB-MDA-468 and MB-MDA-231/*CRYAB* cells.

2.12 Western Blotting

Western blotting is an analytical technique that can be used to identify the presence and relative levels of expression of desired proteins from a cell/tissue lysate. This is achieved by preparing a cell extract in an appropriate sample lysis buffer and loading a sample into a polymerised polyacrylamide gel and the protein is separated based on their molecular weight. The sample buffer contains sodium dodecyl sulphate (SDS) detergent which is negatively charged and coats the proteins. An electric current is applied to enhance the movement of the proteins according to their molecular size before being transferred to a membrane and detected with a specific antibody to the protein of interest. Proteins are then visualised using a range of different detection methods. One of the most widely employed, and the one used here, is chemiluminescence detection. The density of the band is calculated and used to determine the amount of protein present in the samples.

2.12.1 Protein extraction from cells

Cells were lysed and harvested in one of two different lysis buffers, depending on whether protein quantification was required or not:

1- 1X NuPAGE LDS sample buffer consisted of Coomassie G250 and phenol red dyes with 0.1M dithiothreitol (DTT). The buffer mixed with protease inhibitor cocktail diluted at 1:100. Cell lysates were heated at 70˚C for 10 min before being passed through a 27G x 3/4" microlance needle and stored at -20˚C. Proteins extracted in this buffer were analysed without quantification.

2- RIPA lysis buffer consisted of 250 mM Tris-HCl, 5 mM EDTA, 750 mM NaCl, SDS (0.5% Lauryl sulfate, sodium salt in deionized water), DOC (2.5% Deoxycholic acid, sodium salt in deionized water), and Igepal CA-630 (5% Igepal CA-630 in deionized water). These components were mixed together equally with protease inhibitor cocktail diluted at 1:100. Cell lysates were incubated with lysis buffer for 10 min on ice before being spun down at 13,000 rpm for 10 min at 4 °C centrifuge. The supernatant was collected and stored at – 80 ˚C.

2.12.2 Protein quantification

Bicinchoninic acid assay (BCA) is colorimetric assay used to quantify protein concentration in a test sample. This was used to ensure equal loading of proteins onto the gels. The BCA Assay combines the well-known reduction of Cu2+ to Cu1+ by protein in an alkaline medium with the highly sensitive and selective colorimetric detection of the cuprous cation (Cu1+) by bicinchoninic acid). The principle of this technique involves two steps, starting with reduction of Cu2+ to Cu1+ by protein in an alkaline medium, this reaction forms a light blue complex. In the second step, the chelation of two molecules of BCA with one cuprous molecule results in purple-coloured reaction. The BCA/copper complex is water soluble and emits a strong absorbance at 562 nm. By creating a standard curve, the protein concentration of an unknown sample can be estimated by the equation of a straight line (y=mx+c).

2.12.3 Preparation of polyacrylamide gels

The molecular weight of the desired protein to be separated and detected by electrophoresis, determines the percentage of polyacrylamide gel that needs to be prepared. As the molecular size of the protein decreases, the percentage of gel should be increased. For example, smaller proteins (<20 kDa in size) are best resolved using a high percentage gel ($\geqslant$12%) as the higher density of the gel matrix will stop the proteins from migrating too fast during electrophoresis and aid with separation. A high molecular weight protein will separate properly with a small percentage gel ($\leqslant$8%) that gives a gel mixture that has larger pores. For example, for the separation of α B-crystallin which has a molecular weight around 20 kDa, 10% polyacrylamide gels were prepared as detailed in table 2.3. The 10% ammonium persulphate (APS) and

tetramethylethylenediamine (TEMED) solutions were both added last as they are the responsible for the polymerisation of acrylamide. The gel mixture then was poured into 1.5 mm gel cassettes, which were used for the gel casting, in order to fill approximately 2/3 of the cassette. Isopropanol was gently layered onto the surface of the gel to aid complete polymerisation and ensure a smooth, level edge was obtained. Gels were allowed to set for 30 minutes at RT. After setting, the isopropanol was gently rinsed away with water, excess water was then blotted off. The 4% stacking gel was prepared according to table 2.3, by adding 10% APS and TEMED just prior to pouring. The stacking gel was then poured over the polymerised resolving gel. Sample wells were formed using a 10 well comb fitted onto the cassettes. The gel was allowed to set for 30 minutes. The gel was used immediately for protein separation. In addition, 10% precast polyacrylamide gels were also used in some experiments.

Table 2-3 Polyacrylamide gel composites. Volumes of gel composites for casting 10% polyacrylamide gel. Volumes are also shown for the 4% stacking gel. Volumes are shown per gel.

Gel composition	Resolving gel 10%	Stacking gel (4%)
Protogel 30% (National Diagnostics; EC-890)	3.3 ml	1.4 ml
Distilled Water	4.1 ml	6.1 ml
10% Glycerol	100 µl	50 µl
Resolving Buffer x4 (National Diagnostics; EC-892)	2.5 ml	-
Stacking Gel Buffer x4 (National Diagnostics; EC-893	-	2.5 ml
10% APS (Sigma; A3678)	50 µl	50 µl
TEMED (Invitrogen; 15524-010)	5 µl	10 µl

2.12.4 Electrophoresis of protein samples

After the stacking gel was polymerised, the comb was removed gently and the gel was washed with distilled water to remove any unpolymerised traces. The cassette(s) and tank were assembled, and the inner chamber of the tank was completely filled with 1x Tris-Glycine-SDS running buffer (Table 2.4) whilst the outer chamber was only filled to 1/3 of its total volume. Protein samples were re-heated at 95°C for 5 min in the heating block to denature the proteins, allowing separation of the individual protein. 20 µg of the protein in 20 µl total

volume was pipetted into the middle wells of the gel. Molecular weight marker (Precision Plus Protein Dual Color Standards, 25 and 75 kD) was loaded at a volume of 5-10 µl per well. The gel tank was connected to an electrophoresis power supply (Pharmacia Biotech EPS601) and run at 150V (constant voltage) until the bromophenol blue tracking dye had reached the bottom of the gel. This took approximately 50-60 minutes.

2.12.5 Electrophoretic transfer of proteins onto nitrocellulose membrane

The gel was removed from the cassette and the stacking gel was cut from the resolving gel. The gel was immersed in cold 1x transfer buffer (Table 2.4) along with 2 pieces of blotting paper per gel. In addition, a piece of nitrocellulose membrane was cut to size and placed in 1x transfer buffer solution. A nitrocellulose membrane was placed on the top of the blotting paper. The gel was laid on the top of the membrane and the sandwich was completed with the second piece of blotting paper. The transfer was performed using the Biorad Trans-blot Turbo on a pre-programmed setting, up to 25V and 1A, for 30 minutes.

Table 2-4 Western blot buffers. Table showing components of running and transfer buffers used in western blotting experiments.

Western blotting Buffer Composites	1x Running Buffer	1x Transfer Buffer
Tris Glycine SDS PAGE Buffer 10x (National Diagnostics; EC-870)	100ml	-
Tris Glycine Electroblotting Buffer 10x (National Diagnostics; EC-880)	-	100ml
Distilled Water	900ml	700ml
Methanol	-	200m

2.12.6 Antibody incubations

Once the electrophoretic transfer was completed, the membrane was placed immediately, protein side up, in a blocking solution (Table 2.5) and the membrane was incubated for 1 h at room temperature on an orbital shaker. During the blocking stage, the antibodies were made up at the required dilution (Table 2.5). At the end of the incubation period, the blocking buffer was replaced, and the membrane was incubated with diluted primary antibody overnight at 4^{o}C. The membrane then was washed with the TBS-T for 15 minutes, followed by a series of 4 x 5 minutes washes. In order to avoid damaging the membrane, the washing buffer was not poured directly onto the membrane. The membrane was then incubated with secondary

antibody. The incubation period for the secondary antibody was 1h at RT on the orbital shaker. The membrane was washed in PBST buffer for 15 minutes, followed by 4 x 5 minutes washes. The membrane was then ready for chemiluminescent detection of the desired protein.

Table 2-5 Antibodies used for western blotting.

Primary antibodies	Dilution	Blocking solution	Secondary antibodies	Supplier
αB-crystallin	1:1000	5% non-fat dried milk in tris buffered saline 0.1% tween-20 (TBST)	Anti-mouse	Santa Cruz, Biotechnology, 137129
β-tubulin	1:3000	5% non-fat dried milk in TBST	Anti-mouse	Sigma,T40426
β -actin	1:2000	5% non-fat dried milk in TBST	Anti-rabbit	Cell signalling,4967
GAPDH	1:5000	5% non-fat dried milk in TBST	Anti-mouse	Proteintech, 60004-1-Ig

2.12.7 Enhanced chemiluminescence (ECL) Detection

ECL reagents (Biological Industries; 20-500-500) A and B were mixed in equal quantities (3ml of each solution). The mixture was applied to the membrane for three minutes after the washing buffer was discarded. The reverse side of the membrane was dried using blotting paper and covered with cling film. The membrane was placed inside the universal hood in the dark room. The Chemidoc imaging system (Biorad) was used to detect the protein bands. For detection of the bands, the plot chemi option was selected and densitometric analysis of the protein bands was carried out using the 'Lane and Bands' analysis tool within Image Lab™ (version 6). The software then determines the density of signal in each band.

2.13 Analysis of VEGF expression by enzyme-linked immunosorbent assay (ELISA)

ELISA is an analytical biochemical assay used to detect the presence and concentration of a ligand in a sample. The assay was used to measure human VEGF in breast cancer cell lines, following treatment with hypoxia (0.1% O_2) or heat shock. In addition, human and mouse VEGF was measured in the serum and tumour tissues from the mouse model after the

treatment with the anti VEGF antibody (bevacizumab), the chemotherapeutic agent (doxorubicin) or the combination of both agents.

2.13.1 Preparation of breast cancer cell conditioned media and cell lysates.

MDA-MB-231 cells were grown in 75 cm^2 flasks at a density of $2x10^6$/flask or plated at a density of 50,000 cells per well in 6-well plates for 48 h in full growth medium. After 48 h, the medium was removed and cells were washed twice with serum free medium and then serum free medium was added to cells. Cells were exposed for 24 h to either heat shock (42^oC), hypoxia (0.1 % O_2, 37^oC) or normal oxygen at 37^oC as a control as described in section 2.4. Cells in hypoxia and heat shock were placed in the normal incubator at 37 ^oC for a further 24 h. Control cells were maintained at normal oxygen at 37^oC. At the end of the conditioning period, the medium was collected and spun down at 3000 rpm for 10 min. The conditioned medium was aliquoted in 5 ml tubes and stored at -80^oC prior to analysis by an ELISA assay. The cells in each flask or well were trypsinised and counted, so the concentration of VEGF in pg per 10^6 cells could be determined in the ELISA assay (see section 2.13.3). Cells were spun down at 1000 rpm for 5 min and resuspended in 100 µl lysis buffer. The lysed cells were then placed in Eppendorf tubes and spun down at 13,000 rpm for 10 min. The supernatant was collected for VEGF analysis.

For collection of CM following αB-crystallin knockdown with siRNA, MB-MDA-468 cells were plated at a density of 350,000 cells/well in full media in 6-well plates and incubated for 24 h. After 24 h, αB-crystallin siRNA or scrambled sequence negative control siRNA were added to cells (described in Section 2.9.2). After 48 h, the medium was removed, cells were washed twice with serum free medium and 2 ml serum-free medium was then added and cells were exposed to heat shock or hypoxia prior to collection of conditioned media and preparation of cell lysates as described above for MDA-MB-231 cells.

2.13.2 Preparation of tumour tissues extracts and serum for ELISA analysis.

The mouse blood was allowed to clot for 2 hours at room temperature before being spun down at 16,000 rpm for 10 min. The serum then aliquoted and stored in -80^oC until used undiluted in the ELISA assay. For protein extraction from tissues, small amounts of tumour tissues were placed into tubes with 400 µl of 1X RIPPA lysis buffer and one protease inhibitor tablet for each 10 ml of RIPPA lysis buffer. The tissues then placed inside metal bead mill tubes and homogenised with the bead mill homogenizer. The homogenized tissues then were spun

down at 13,000 rpm for 10 min. The supernatant was collected and the protein concentration was measured by BCA assay. For the ELISA assay 0.5 µg/µl total protein was loaded per well in a total volume of 100 µl .

2.13.3 Human VEGF ELISA assay

Human VEGF ELISA kit (Human VEGF Duoset ELISA, DY293B) was used to analyse human VEGF in breast cancer cell lines, serum and tumour tissues. On the first day, the capture antibody was diluted from the stock supplied in the kit (120 µg/ml) to 1 µg /ml. 100 µl of capture antibody was then added to each well. The plate was sealed and was stored at RT overnight. On the following day, the capture antibody was aspirated from all wells, and each well was washed three times using 400 µl per well of X1 wash buffer. Reagent diluent supplied in the kit was used as block solution after it was diluted 1:10 from the stock into the desired volume using distilled water. The plate was blocked by adding 300 µl of diluted reagent diluent to each well for 1 h. At the end of the blocking time, the reagent diluent was aspirated from all wells, and all wells were washed three times with 400 µl wash buffer. A series of standards of recombinant VEGF was prepared from 2000 pg/ml to 31 pg/ml. The dilutions were prepared from a 120 ng/ml stock solution. 100 µl of standard or samples was added to the wells. The plate was incubated for 2 hours at room temperature. The samples and standards were aspirated from all wells and every well was washed three times using 400 µl of wash buffer per well. The detection antibody was diluted from a 6000 ng/ml stock using reagent diluent to a working concentration of 100 ng/ml. 100 µl of 100 ng/ml detection antibody was added to each well and incubated for 2 hours at RT. The detection antibody was aspirated from all wells, and each well was washed three times using 400 µl wash buffer per well. Streptavidin-HRP was diluted by 40-fold using reagent diluent into the desired amount of solution and 100 µl of the solution was added to each well and incubated for 20 min at RT in the dark. At the end of the incubation period, the HRP solution was aspirated from all wells and each well was washed three times using 400 µl of wash buffer per well. Two colour reagents A and B were mixed at equal volumes and 100 µl was added to each well and incubated for 20 min in the dark. This solution was mixed just before use. 50 µl of stop solution was added to each well and mixed gently. The absorbance then was read at 450 nm and 540 nm for background correction. The concentration of unknown VEGF in each sample was calculated from the standard curve of known concentrations and expressed as pg/ml.

2.13.4 Mouse VEGF ELISA assay

Mouse VEGF was measured in mouse serum by ELISA (R&D systems, MMV00) to assess the inhibitory effect of bevacizumab on mouse VEGF concentrations in the in vivo experiments. A polyclonal antibody specific for mouse VEGF was pre-coated onto a microplate. 50 µl of 1X assay diluent was added to each well. A series of standards of recombinant VEGF was prepared from 500 pg/ml to 7.8 pg/ml. The dilutions were prepared from the stock solution 500 pg/ml after being reconstituted with calibrator diluent. A known concentration of recombinant mouse VEGF was used as control. All serum was diluted 5-fold with calibrator diluent. 50 µl of standard, control or serum was added to each well. The plate was mixed by tapping gently for 1 min and incubated for 2 h at room temperature. The samples and standards were aspirated from all wells and every well was washed four times with 400 µl of 1X wash buffer per well. 100 µl of mouse conjugate antibody was added to each well and incubated for 2 h at room temperature. The mouse conjugate antibody was aspirated from each well and each well was washed four times 400 µl per well. Two colour reagents A and B were mixed at equal volumes and 100 µl was added to each well and incubated for 30 min in the dark. 100 µl of stop solution was added to each well and mixed gently. The absorbance then was read at 450 nm and 540 nm for background correction. The concentration of unknown VEGF in each sample was calculated from the standard curve of known concentrations and given in pg/ml.

2.14 *In vivo* experiments: Ethical approval and animal husbandry

All experiments using mouse models were conducted in accordance with the United Kingdom Home Office Animals (Scientific Procedures Act) 1986, Under the Personal Project Licence number P99922A2E (Dr. Penelope Ottewell). 12-week-old female BALB/c nude mice were used for all *in vivo* experiments. Mice were housed in the Biological Services Unit at no more than 4 animals per cage. Ventilated cages were kept in a temperature (22 ± 2°C) and humidity (55% ± 10%) controlled environment with a 12 hrs light/ dark cycle. Pelleted mouse food and water were provided *ad libitum*.

2.14.1 Orthotopic injection of breast cancer cells

MB-MDA-231/WT and MB-MDA-231/*CRYAB* cells were cultured under standard conditions in multiple T175 flasks in order to achieve the number of cells required for tumour implantation in groups of mice. On the day of implantation, cells were trypsinised and resuspended at $2x10^6$

cells in 40 µl suspension of 20% matrigel, 80% PBS and 1% trypan blue per mouse. Matrigel is useful in the development of xenograft tumours from cell lines. This is because it is composed of extracellular matrix proteins such as laminin, collagen IV, heparan sulphate, proteoglycans that help in the attachment and differentiation of anchorage-dependent cell types. Under normal physiological conditions, matrigel polymerizes to produce a stable biologically active matrix, which facilitates establishment of tumours (Mullen 2004). Trypan blue was added as tracking dye to ensure that we inject inside the fat pad. Mice were anaesthetised using 2-3% isoflurane in O_2 and cancer cells were injected with a 30G Insulin syringe into the fourth mammary ducts of the left and right mammary glands. Once tumours had established, tumour volume was measured using digital callipers and mouse body weight was recorded three days/week. Tumour volume was calculated from the formula of the sphere $V = 4/3\ \pi r^3$, where r is the radius of the sphere and calculated from the average of the average the orthogonal tumour diameters.

2.14.2 Determining optimal dose of bevacizumab for use in combination studies *in vivo*

In vivo experiments were carried out to study the effects of *CRYAB* expression on tumour growth and VEGF concentration after treatment with the chemotherapeutic agent (doxorubicin) and anti-VEGF treatment (bevacizumab, which is also known with its brand name (Avastin). A pilot study with MB-MDA-231/WT cells was first performed to determine the lowest inhibitory concentration of bevacizumab on tumour growth. 12-week-old BALB/c nude were injected with $1X10^6$ MDA-MB-231/WT cells in 80% PBS/20%matrigel/1%trypan blue into right and left fourth mammary ducts (n=3/group). 7-days after tumour cell injection, mice were randomly divided into four groups of equal tumour size and treated with saline (control), 5mg/kg, 7.5mg/kg or 10mg/kg bevacizumab via Intraperitoneal (IP) three times a week and mice were culled at day 30 after initial injection of tumour cells. At the end of the procedure, the serum and primary tumours were collected for VEGF detection by ELISA assay. The lowest concentration that inhibited VEGF concentration was used for the subsequent *in vivo* combination treatment study.

2.14.3 Determining effects of doxorubicin, bevacizumab and combination of both on growth of *CRYAB* expressing and non-expressing MDA-MB-231 cells, *in vivo*

7 days after tumour cell injection, mice were randomised into groups of equal tumour size. Each group contained 4 mice per treatment/cell line and the experiment was repeated twice

to give a total of 8 mice per treatment/cell line. The sample size was determined based on Le Morte-Power calculations. For the treatment group compared to the control group, a minimum of 4 mice per group would provide statistical power of 80% with a significance level (alpha) of 0.05. For comparing the effects of doxorubicin alone versus the combination of doxorubicin and bevacizumab, 8 mice per group would achieve the same statistical power. These sample sizes were chosen to ensure that the experiments would have enough statistical power to detect differences of 30% or more in tumour growth between the groups using an analysis of variance (ANOVA) statistical test. At this point treatment commenced and animals received 100 µl of saline (control), 4 mg/kg in 100 µl doxorubicin via intra-venous injection (i.v) (Ottewell *et al.* 2008), 7.5 mg/kg in 100 µl bevacizumab via IP injection or combination of doxorubicin and bevacizumab. All drugs were made up in saline solution (NaCl 0.9%) and delivered using a 30 G insulin needle. The volume administered was calculated based on animal weight. The treatment efficacy was determined by measuring the tumour diameters throughout the growth period and tumour volumes were calculated as described in section 2.14.1 and animals were culled 40 days after initial injection of tumour cells. Figure 2.4 showing the outline of study protocol.

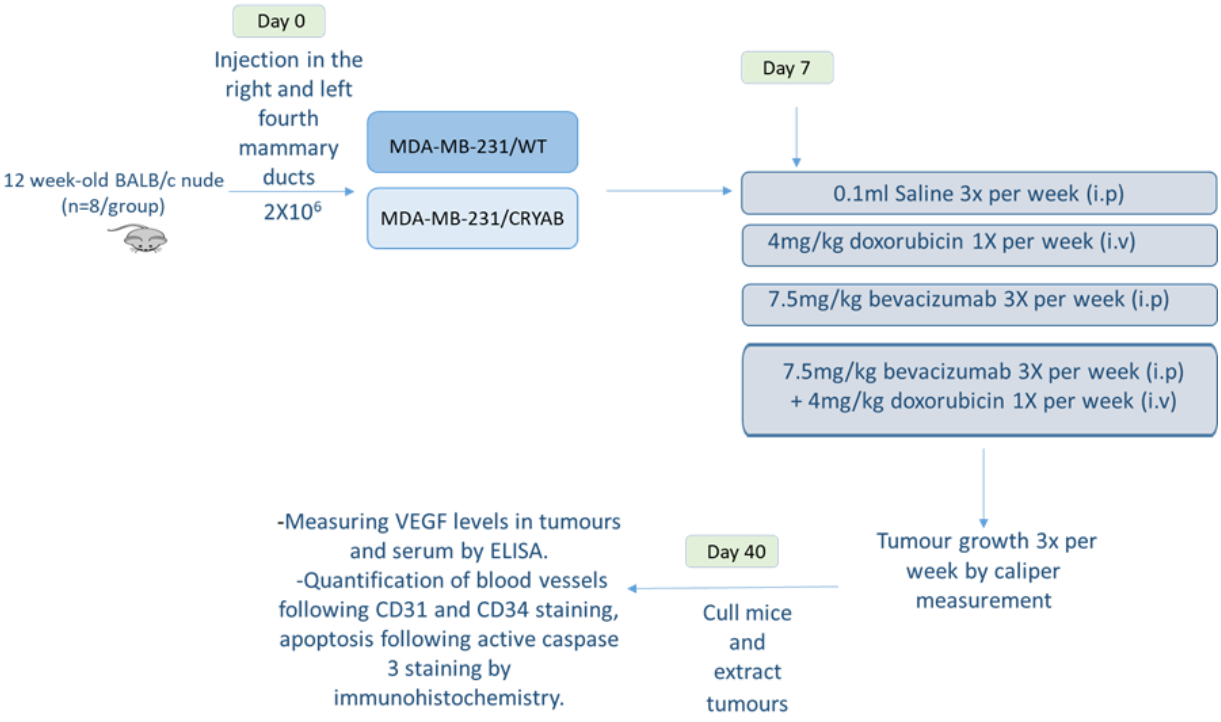

Figure 2.4 The outline of study the effects of doxorubicin, bevacizumab and combination of both in *CRYAB* expressing and non-expressing MDA-MB-231 cells, in vivo. Adminstration doxorubicin, bevacizumab and combination of doxorubicin and bevacizumab following injection of MDA-MB-231/WT and MDA-MB-231/*CRYAB* cells into fourth mammary glands of BALB/c nude mice. 40 days after the inoculation of cancer cells, mice were sacrificed and tumoures were extracted for further analysis.

2.15 Tumour excision

At the end of the procedure, the animals were culled using the Schedule 1 method of overdose with anaesthesia (Isoflourane) followed by cervical dislocation to ensure complete euthanasia. Tumours were excised and weighed before one tumour being fixed in 4% paraformaldehyde and the other was cryopreserved for ELISA analysis at later date.

2.15.1 Paraformaldehyde (PFA) fixation of tumour tissue

One excised tumour per mouse was immersed in 4% paraformaldehyde. After 24 h, the PFA was discarded and replaced with 70% EtOH, following which tissues were placed in tissue processing/embedding cassettes and returned to 70% EtOH. Tumours were then processed, embedded and sectioned by Mrs Maggie Glover (histology core facility).

2.15.2 Tissue sections

Formalin fixed paraffin embedded (FFPE) tumour sections were cut to a thickness of 5 µm and mounted on Superfrost® Plus microscope slides by Mrs Maggie Glover. Between 5 and 10 sections were cut per tumour for subsequent haematoxylin and eosin staining and IHC for endothelial cell markers (CD31, CD34) to assess the vasculture in tumours. Moreover, active caspase 3 was scored in tumour sections to assess the effect of treatments on apoptosis.

2.15.3 Immunohistochemistry (IHC)

The IHC is a powerful technique used to identify a specific antigen in a tissue section by utilising the principle of antibody-antigen binding. First, wax embedded sections were de-waxed in Xylene twice for 10 min each before being rehydrated in a series of Ethanol baths (100%, 100%, 95%, 70%) for 3-5 min each. Sections were placed in dH_2O for 1 min and rinsed in PBS before heat-induced epitope retrieval (HIER) was carried out. Fixation of sections preserves tissue structure within the section, however, fixative solutions such as formalin causes crosslinking among the tissues and that prevents antibody from binding to antigen. HIER aims to recover antigen reactivity and restore secondary or tertiary epitope structure to allow antibody binding. Sections were submerged in Target Retrieval Solution, a modified citrate buffer pH 6.1, and placed in a pressure cooker on a 2-hour programme which heated to 121˚C for 20 minutes before cooling for the remainder of the programme. Following this, sections were rinsed in PBS twice.

2.15.4 Immunostaining of tumour sections

To quench endogenous peroxidase activity, sections were incubated with 3% hydrogen peroxide (H_2O_2)/Methanol for 30 min RT; they were then washed for 5 min in PBS before incubation with the appropriate blocking solution for 1 hour at RT to prevent non-specific antibody binding. Excess blocking solution was removed, and sections were incubated overnight at 4˚C with the primary antibody (see table 2.7). Negative controls were left in blocking solution. All sections were washed 3 times in PBS for 5 min before addition of the secondary antibody at 1:200 for 1 hour RT. Following 3 x 5 min washes, horseradish peroxidase-conjugated avidin-biotin complex (ABC-HRP) reagent was prepared as per the manufacturer's protocol and applied to the sections for 30 min RT. A further 3 x 5 min PBS washes were carried out before the application of 3,3'-diaminobenzidine (Rakha *et al.*) peroxidase reagent, prepared following the manufacturer's protocol. DAB signal was left to develop between 3-10 min before the reaction was stopped by rinsing in tap water. Sections were counterstained with Gill's Haematoxylin for 20 sec; rinsed in tap water for 2 min. Sections were then dehydrated in graded Ethanol (70%, 90%, 95%, 100%, and 100%) for 3 min each, and in xylene two times for 3 min. Sections were mounted using DPX mounting media and glass coverslips.

Table 2-6 Antibodies that used for Immunhistochemistry

Primary antibody	Supplier	Antibody concentrations	Blocking Serum	Biotinylated secondary antibody
Rat anti-CD31	Dianova DIA-310	1:100	10% normal rabbit serum (Vectorlabs, S-5000)	Rabbit anti-rat (Vectorlabs, BA-4001)
Rat anti-CD34	Abcam, [MEC 14.7] (ab8158)	1:100	1:10 casein/PBS	Rabbit anti-rat (Vectorlabs, BA-4001)
Rabbit anti-Caspase 3 polyclonal anti-active caspase 3	VectorLabs (AF835)	1:400	1:10 casein/PBS	Anti rabbit-biotin, Vector BA-1000

2.15.5 Tumour vasculature analysis

Vascular density in tumour tissues can be assessed using staining against endothelial cell markers such as CD31 (platelet endothelial cell adhesion molecule-1, PECAM-1) and CD34 (also known with human hematopoietic progenitor cell antigen). CD31 is transmembrane expressed on the surface of endothelial cells. It mediates cell-to-cell adhesion of endothelial cells, which increase the contact between the cells. CD31 is highly used as specific immunohistochemical marker for the identification of endothelial differentiation, although it is also expressed by some of haematopoietic cells such as myeloid cells (Ordóñez 2012). CD34 is well recognised marker of endothelial cells and hematopoietic progenitor cells. Both markers are used to evaluate tumour angiogenesis (Kim *et al.* 2002, Vieira *et al.* 2005, Yilmazer *et al.* 2007). The analysis of data was done by quantifying positive CD31 or CD34 stained area as a percentage of positive pixels in viable tumour, avoiding the necrotic area and normal tissues. Using the annotation tool in Qupath software, viable areas of tumour tissues were surrounded. The 'positive pixel count' command was then run to give the percentage of DAB positive staining in the area of interest. Figure 2.5 is an example of analysed data.

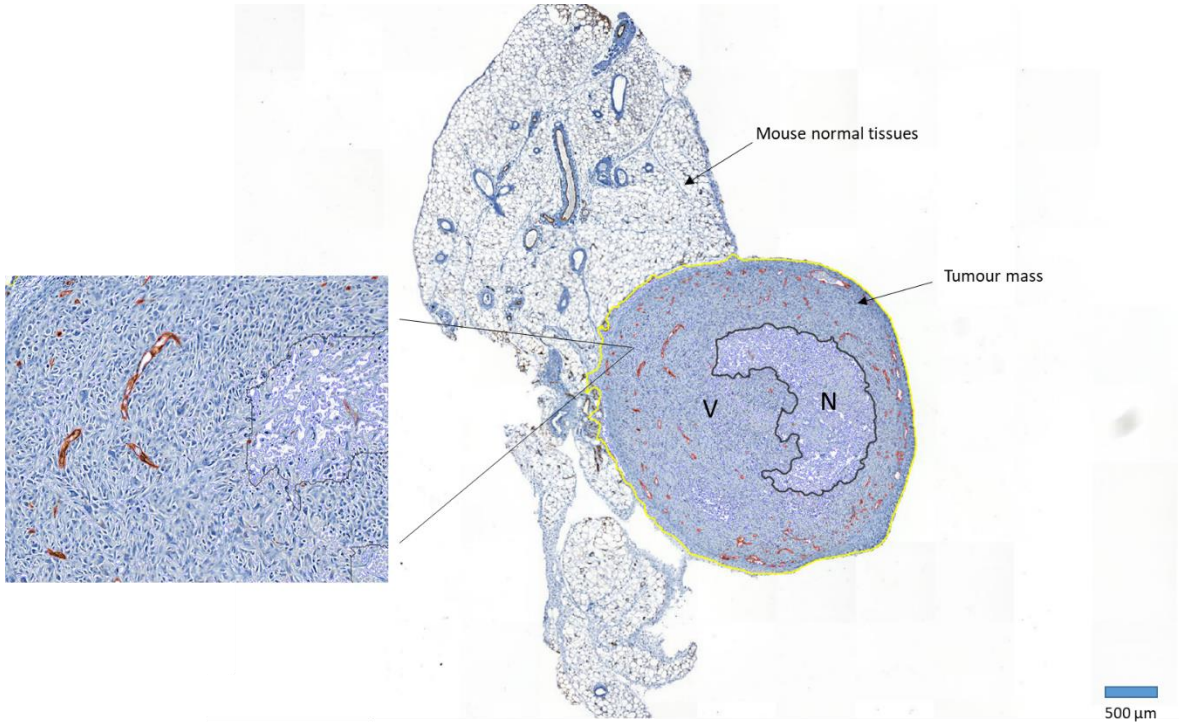

Figure 2.5 the analysis of positive CD31 stained area. The vascularised area was quantified as the percentage of positive pixel area in viable tumours, avoiding the necrotic area and normal tissues. V: viable tumours, N: necrotic area. The CD31 positive area (red). Representative images from viable tumour regions at 10x magnification from whole slide scanning.

2.15.6 Cleaved caspase 3 scoring

Apoptosis in tumour tissues can be determined by IHC detection of active caspase-3 (cleaved form), which is the main executioner of apoptosis (Bressenot *et al.* 2009). Cleaved caspase 3 analysis was used to assess the apoptosis in tumour tissues and to compare the apoptosis between MDA-MB-231/WT tumours and MDA-MB-231/*CRYAB* tumours. Cleaved caspase 3 was scored by counting the DAB positive cells in viable tumour tissues, avoiding necrosis and normal tissues. The number of detected positive pixels cells then was obtained in percentage using Qupath. Figure 2.6 is an example of analysed data.

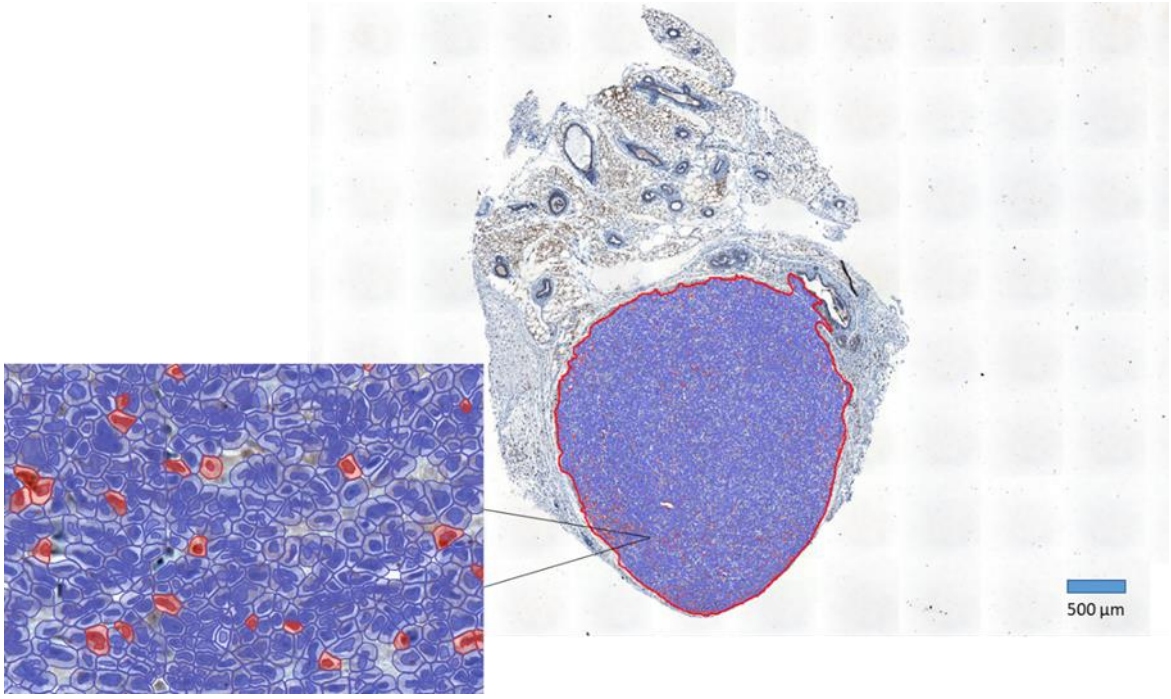

Figure 2.6 The analysis of apoptotic cells in tumour tissues. The positive cells were counted as the percentage of positively detected pixels in the viable tumours, avoiding the necrotic area and normal tissues.

2.16 Statistical analysis

Statistical analyses were carried out using GraphPad Prism software 8.0.2. Pairwise analysis was carried out by unpaired t-test under the assumption that data was parametric. For comparing the means between groups where data were perceived to be non-parametric, one-way or two-way ANOVA followed by Tukeys test for multiple comparison were used, depending on the number of independent variables. The specific analyses used to analyse data for each experiment are detailed in the figure legends. In all plotted data, n denotes the number of independent biological repeats.

Chapter3 **Effects of high levels of αB-crystallin expression on proliferation, response to therapy and VEGF production in TNBC**

3.1 Introduction

αB-crystallin is a member of the small heat shock protein family, whose members function as molecular chaperones that prevent the aggregation of misfolded proteins. It is overexpressed in many cancer types, including the aggressive types of breast cancer such as basal-like breast cancer (Moyano *et al.* 2006). The overexpression of αB-crystallin in breast cancer has been correlated with poor prognosis, lymph node involvement and invasive phenotypes (Chelouche-Lev *et al.* 2004, Ivanov *et al.* 2008, Malin *et al.* 2014, Voduc *et al.* 2015). It is thought that cancer cells may exploit the protective role of αB-crystallin for their survival, proliferation, and metastasis. For example, it has been suggested that αB-crystallin may be an oncoprotein that promotes the proliferation of breast cancer cells (Moyano *et al.* 2006). In colorectal cancer, αB-crystallin over-expression was shown to stimulate the ability of tumour cells to proliferate and invade (Li *et al.* 2017). αB-crystallin has also been shown to prevent protein degradation by binding polypeptides that are accumulated during cellular stress, such as during heat shock. Moreover, αB-crystallin acts as an anti-apoptotic protein, inhibiting the activation of caspase-3 and preventing the translocation of the pro-apoptotic proteins to the mitochondria (Mao *et al.* 2004, Liu *et al.* 2007, Shin *et al.* 2009). In addition, αB-crystallin is associated with resistance to neoadjuvant chemotherapy in TNBC (Ivanov *et al.* 2008). The association of αB-crystallin with the most aggressive types of breast cancer and its role as an anti-apoptotic protein makes it necessary to elucidate its role in breast cancer further. The influence of αB-crystallin on the proliferation and induction of apoptosis after treatment with the chemotherapeutic drug, doxorubicin in TNBC cells, will be investigated in this chapter.

αB-crystallin has been shown to interact with proteins involved in critical cellular pathways such as those involved in tumour growth and angiogenesis (Aalders *et al.* 2017). For example, growth factors such as FGF-2 and VEGF were shown to be protected by αB-crystallin against aggregation induced under stress conditions (Aalders *et al.* 2017). Ruan *et al* studied the

chaperoning function of αB-crystallin to VEGF. These authors demonstrated that breast cancer cells were able to induce αB-crystallin expression in endothelial cells in a paracrine manner and it is believed that this may serve to protect tumour-induced autocrine VEGF in endothelial cells and promote angiogenesis. Moreover, both breast cancer and endothelial cells induced αB-crystallin expression after anti-VEGF treatment in *in vivo* models suggesting that drug treatment may contribute to drug resistance via αB-crystallin related pathway (Ruan *et al.* 2011). VEGF is a prognostic factor in several malignancies and high levels of VEGF are associated with the progression of the disease and poor survival (Bando *et al.* 2005, Hsu *et al.* 2009) The protective role of αB-crystallin on VEGF is a possible mechanism by which this chaperone protein enhances disease progression in TNBC. Therefore, the interaction between αB-crystallin and VEGF under stress conditions was investigated in this chapter.

3.2 Aims

This chapter aims to investigate the influence of αB-crystallin on proliferation, response to a chemotherapeutic agent (doxorubicin) and on the production/secretion of VEGF in TNBC cells. To achieve this:

1- Two TNBC cell lines (MDA-MB-231 and MDA-MB-468) were first screened for αB-crystallin expression.
2- αB-crystallin was stably overexpressed in αB-crystallin null cells using a plasmid containing *CRYAB*; clones overexpressing αB-crystallin were isolated
3- The regulation of αB-crystallin expression under normal versus stress conditions (heat shock and hypoxia) was studied by western blotting.
4- The growth of the cells was studied by counting the cells and calculating the doubling time of overexpressing cells versus their wild type counterparts.
5- Sensitivity to doxorubicin was studied by measuring cell proliferation as in point 4 above.
6- Apoptosis induction was analysed by flow cytometry after treatment with different concentrations of doxorubicin in αB-crystallin overexpressing versus wild type cells.
7- VEGF protein expression under normal cell culture conditions, as well as stress conditions (heat shock, hypoxia) was measured in overexpressing cells and their wild type counterparts by ELISA.

3.3 Results

3.3.1 Screening of TNBC cells for αB-crystallin expression

In order to investigate the role of αB-crystallin and its expression, two TNBC cell lines, MDA-MB-468 and MDA-MB-231 were tested for expression of αB-crystallin and for potential induction of the protein by heat shock.

The cells were plated at a density of 1 x 10^5 cells/well in 12 well plates until they were confluent and then exposed to heat shock (42°C) for 2 h before being transferred to 37 °C for a further 17 h or were continuously exposed to heat shock for 19 h. Protein was extracted and analysed for αB-crystallin by western blotting. As shown in Figure 3.1, MDA-MB-468 cells expressed low levels of αB-crystallin when cultured under normal cell culture conditions (5% CO_2, 37 °C) and this protein was upregulated when cells were exposed to heat shock for 2 hours and further increased after 19 hours. MDA-MB-231 cells did not express αB-crystallin and no induction was seen following heat shock exposure. The results demonstrate that these two TNBC cell lines have differential αB-crystallin expression. In addition, the results indicate that αB-crystallin expression increases in response to heat shock.

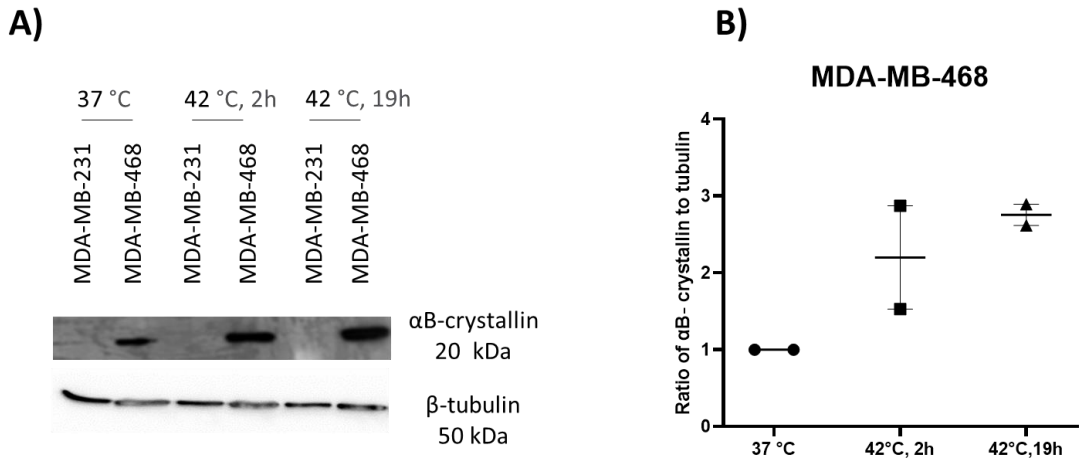

Figure 3.1 Western blot analysis of αB-crystallin protein expression in breast cancer cells. Confluent cultures of MDA-MB-468 and MDA-MB-231 cells were exposed to either 37°C or 42°C for 2 h followed by a further 17 h at 37 °C or 42 °C for 19 h. **A**) Proteins extracts were then analysed by western blotting. As a loading control, blots were probed with an antibody to β-tubulin . **B)** Blots were scanned and the band density of αB-crystallin was expressed as fold increase normalised to control cells at 37 °C. Blot is mean ± SEM from n=2 wells from two independent experiments.

3.3.2 Overexpression of αB-crystallin in MDA-MB-213 cells

In order to study the effect of altered levels of αB-crystallin on cellular functions, αB-crystallin was overexpressed in MDA-MB-231 cells that do not express αB-crystallin using a cDNA expression plasmid that contains the *CRYAB* gene and a neomycin resistance gene that confers resistance to the antibiotic G418 (see plasmid map Figure 2.2).

3.3.3 Determining optimal conditions for G418 selection of transfected cells

Initially, cells were plated and treated with different concentrations of G418 to select the lowest concentration of G418 that kills untransfected cells. The cells were plated in 24 well plates at a density of 50,000 per well in 1 ml full growth medium. 24 h after plating, the full growth medium was replaced with medium containing 0 or 100 – 1000 µg/ml G418. The lowest concentration of G418 that killed all the cells, following culture for two weeks was determined to be 750 µg/ml.

3.3.4 Transfection with *CRYAB* plasmid

The transfection efficiency of MDA-MB-231 cells was assessed using a GFP DNA plasmid since the *CRYAB* plasmid used did not contain a fluorescent tag. The cells were plated in 12 well plates at a density of 50,000/well. On the following day, the medium was replaced with 1 ml of DMEM/10% FCS medium without antibiotics. The transfection mixture (GFP plasmid and TransIT-X2 transfection reagent) (Materials and Methods, Table 2.5) was added to the cells. Potential TransIT-X2 reagent toxicity was tested in one well. The plate was incubated overnight at 37°C. The presence of green cells indicated that the cells were transfected. The cells were observed under a fluorescence microscope and many green cells were seen (data not shown), indicating successful transfection. Following this, TransIT-X2 was used to transfect *CRYAB* plasmid into MDA-MB-231 cells. Cells were treated with a medium containing 750 µg/ml G418 and after two weeks, resistant colonies were observed (Figure 3.2 A), and while G418 killed all cells in un-transfected (control) wells. In order to expand the colonies, they were trypsinised and plated into a 6 well plate in 2 ml medium containing G418. Cells were tested for expression of αB-crystallin and in parallel were expanded and moved into a T25 flask. Cell lysates from transfected MDA-MB-213 cells were screened by western blotting for αB-crystallin expression. Transfected cells were positive for αB-crystallin expression (Figure 3.2 C).

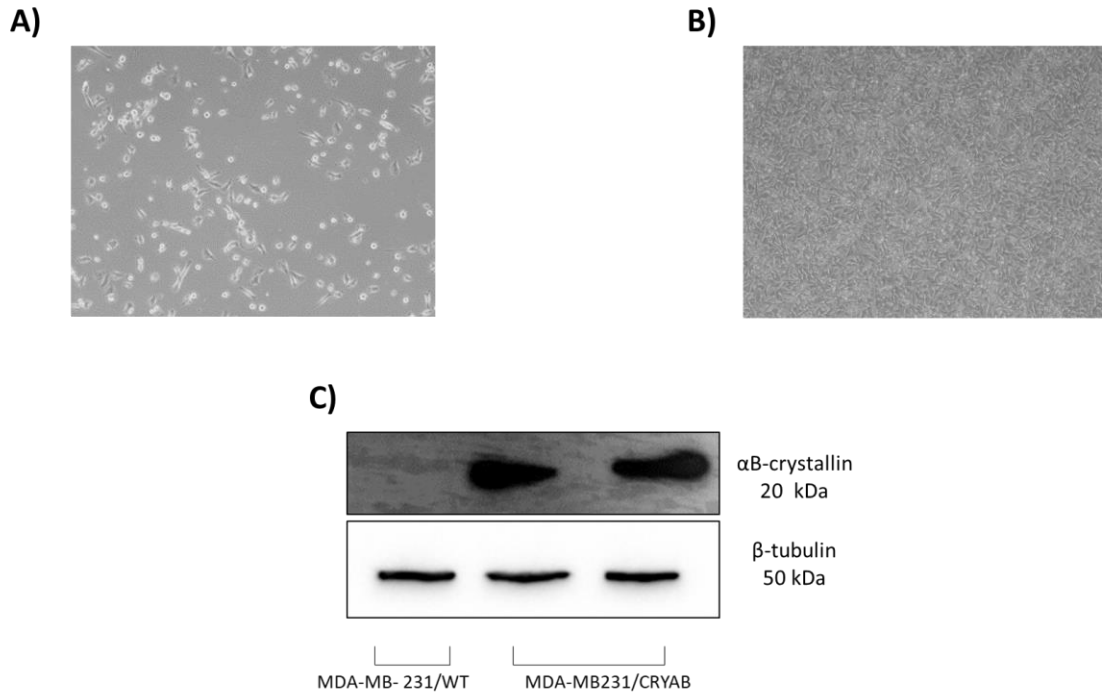

Figure 3.2 Selection of G418 resistant MDA-MB-231 cells transfected with a *CRYAB* plasmid. Images of cells two weeks **(A)** and one month **(B)** after transfection using the *CRAYB* plasmid and TransIT-X2 transfection reagent. The G418 medium was replaced every 2-3 days. **C)** Protein extracts from two MDA-MB-231 transfectant cell pools were analysed by western blotting. β-tubulin was used as a loading control. Blots shown are from one experiment.

3.3.5 Testing different stress related stimuli on the expression of αB-crystallin in *CRYAB* expressing and control cells

αB-crystallin is a chaperone protein that prevents the aggregation of misfolded or unfolded proteins in response to stress (Horwitz 1992). Therefore, changes in expression of this protein in response to hypoxia and exposure to heat shock were studied. MDA-MB-468, MDA-MB-231 *CRYAB* transfected cells (MDA-MB-231 /*CRYAB*) and MDA-MB-231 wild type cells (MDA-MB-231 /WT) were plated in four 12 well plates and allowed to grow. After 48 h, one plate was left in the 37°C incubator for 24 h as a control. The second plate was exposed to low oxygen (0.1 % O_2 for 24 h; hypoxia). Two plates of cells were exposed to heat shock; one placed in a 42°C incubator for 2 h and transferred to a 37^{o}C incubator for 22 h and the second plate was placed in a 42^{o}C incubator for 24 h. After 24 h, all cells exposed to hypoxia or heat shock were placed in the normal incubator at 37^{o}C for a further 24 h, cells were then lysed and tested for αB-crystallin expression by western blot (band density of αB-crystallin was expressed as fold increase of αB-crystallin normalised to control cells at 37^{o}C). The results showed that hypoxia had no effect on αB-crystallin levels in either MDA-MB-468 (Figure 3.3 A and C) or MDA-MB-231 /*CRYAB* cells (Figure 3.3 A and B). Short exposure to heat shock resulted in a trend towards increased αB-crystallin expression in both MDA-MB-468 and MDA-MB-231/*CRYAB* cells but this did not reach significance. However, longer exposure to heat shock (24 h) caused a trend towards increased αB-crystallin protein in MDA-MB-468 cells and a significant increase in αB-crystallin expression in MDA-MB-231 /*CRYAB* cells (P=0.0018). MDA-MB-231/WT that do not express detectable levels of αB-crystallin at 37^{0}C and normal atmospheric oxygen did not express this protein following exposure to either hypoxia or heat shock. These results indicate that hypoxic stress does not increase the αB-crystallin levels in the cell lines tested. However, the induction of αB-crystallin is directly proportional to the duration of heat shock especially in MDA-MB-231/*CRYAB* cells (Figure 3.3).

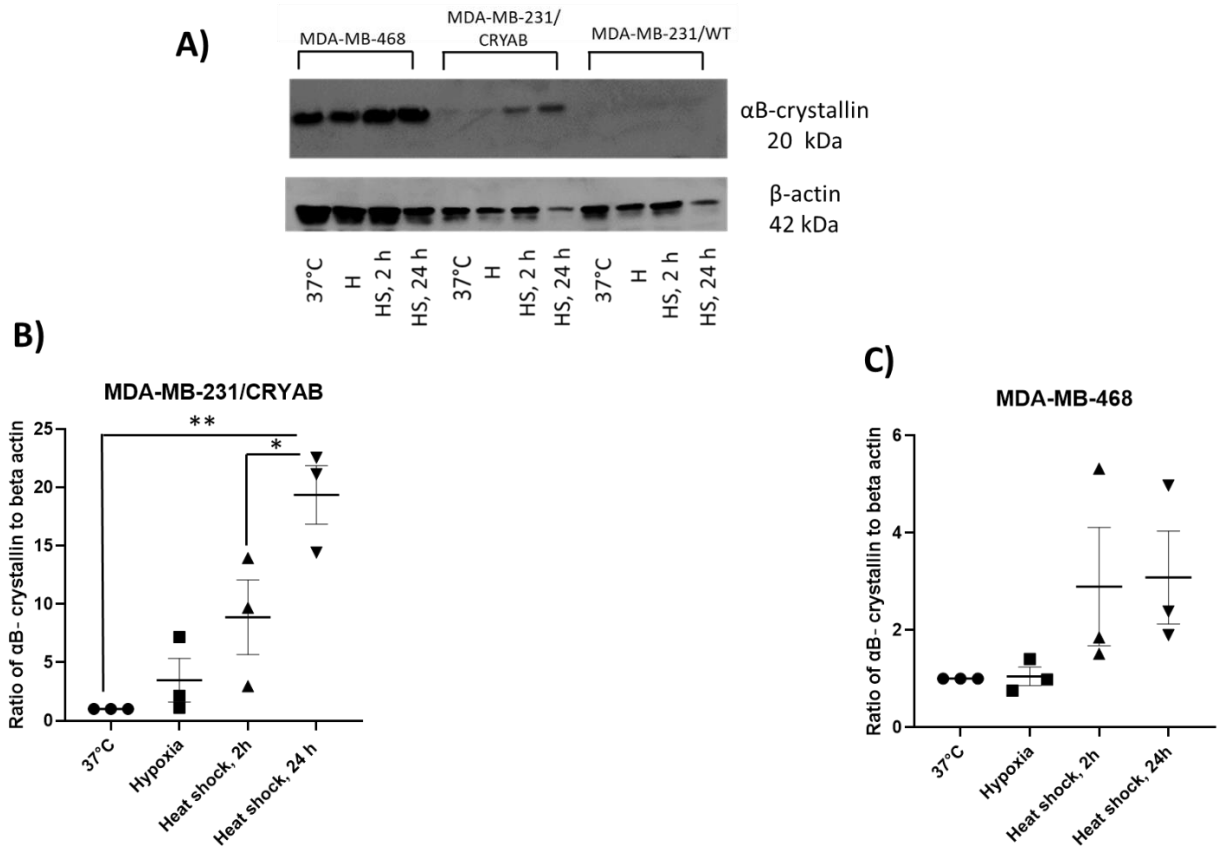

Figure 3.3 αB-crystallin expression in MDA-MB-468, MDA-MB-231/WT and MDA-MB-231/*CRYAB* cells. A) Confluent cultures of cells were exposed to 37°C for 24 h, hypoxia (H) for 24 h, heat shock (HS) at 42°C for 2 h followed by a further 22 h at 37°C or HS at 42°C for 24 h. **(B &C)** Blots were scanned and the band density of αB-crystallin was expressed as fold increase normalised to control cells at 37°C. Plots are mean ± SEM in MDA-MB-231/*CRYAB* **B)** and MDA-MB-468 cells **C).** Data was analysed by ordinary one-way ANOVA with Tukey's multiple comparisons test (n=3 independent experiments; *p=0.0425,**p=0.0018).

3.3.6 Assessment of the effects of doxorubicin on cell viability using alamar blue

Alamar blue is used to quantitatively measure cell viability. The assay depends on the reduction of alamar blue by viable cells (Al-Nasiry *et al.* 2007). Cell viability was tested in MDA-MB-231/WT and MDA-MB-231/*CRYAB* cells using alamar blue. The cells were plated in 96 well plates and allowed to adhere overnight. On the following day, the cells were treated with increasing concentrations (5-100 nM) of doxorubicin. The drug doses were prepared x4 concentrated than the stocks to avoid the dilution of the drugs when they are added to the final volume of 200 µl per well. The drug was incubated for 48 h, then 20 µl of alamar blue was added to each well, and the plates were left in a 37°C incubator for 24 h. The absorbance was read at wavelengths of 570 nm and 600 nm. The percent difference in alamar blue reduction between treated and control cells was measured using the equation in section (2.6). The results showed that there were no significant differences between control and drug-treated cells (Figure 3.4), indicating that the drug doses were not enough to induce cell death, or the cells did not show drug sensitivity using the alamar blue assay.

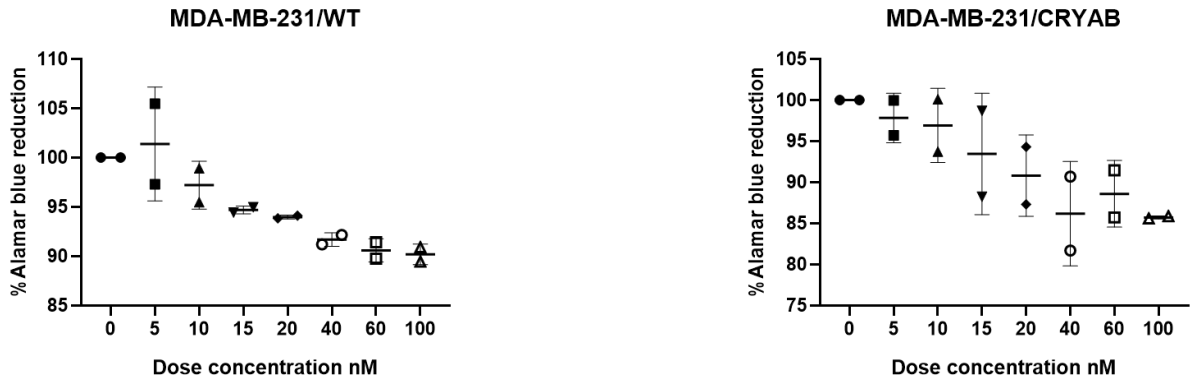

Figure 3.4 MDA-MB-231 /WT and MDA-MB-231 /*CRYAB* cell response to doxorubicin. MDA-MB-231/WT and MDA-MB-231/*CRYAB* were treated with increasing concentrations of doxorubicin (5-100 nM) for 48 h. 20 µl of alamar blue was added and incubated for 24 h at 37°C. The effect on cell viability of doxorubicin was calculated as a decrease in the percentage of alamar blue reduction and compared to the control with no drug. Data were analysed by ordinary one-way ANOVA. Values are mean ± SD from two independent experiments; average values in each experiment were from n=8 wells.

3.3.7 Cloning *CRYAB* transfected MDA-MB-231 cells

Within a polyclonal population individual cells are likely to vary in their expression of αB-crystallin. Furthermore, the transgene expression in a polyclonal population may decrease over time. Therefore, generating a monoclonal cell line by limiting dilution is expected to result in cell populations that are more likely to retain stable transgene expression. To do this, trypsinised cells were counted twice using a hemocytometer and serial dilutions were prepared of 10 cells/ml, 5 cells/ml, and 2.5 cells/ml. 200 µl of each dilution was added to wells of 96-well plates, to give wells containing two cells per well, one cell per well and 0.5 cells per well respectively to increase the likelihood of obtaining single colonies growing in wells. The plates were incubated in the 37^{o}C incubator. After 10 days, the plates were observed under the microscope. Wells containing one single colony were marked and allowed to become confluent, which was approximately a month after the cells were initially plated.

3.3.7.1 Testing the colonies for αB-crystallin expression

The colonies were harvested, and each was plated into two wells of two separate 12 well plates. One plate was kept for expanding the cells, while the other one was used for testing the cells for αB-crystallin expression. Western blotting showed that several colonies expressed αB-crystallin but at different levels (Figure 3.5). Some colonies expressed αB-crystallin at very high levels and others did not express the protein at all while others expressed low levels of protein. The colonies that expressed high and low levels of αB-crystallin were expanded and frozen down. The results demonstrated that the transfected MDA-MB-231 polyclonal cells were heterogeneous and expressed different level of αB-crystallin. Two clones (16 and 19 in Figure 3.5) that expressed low and high levels of αB-crystallin respectively were chosen for future experiments.

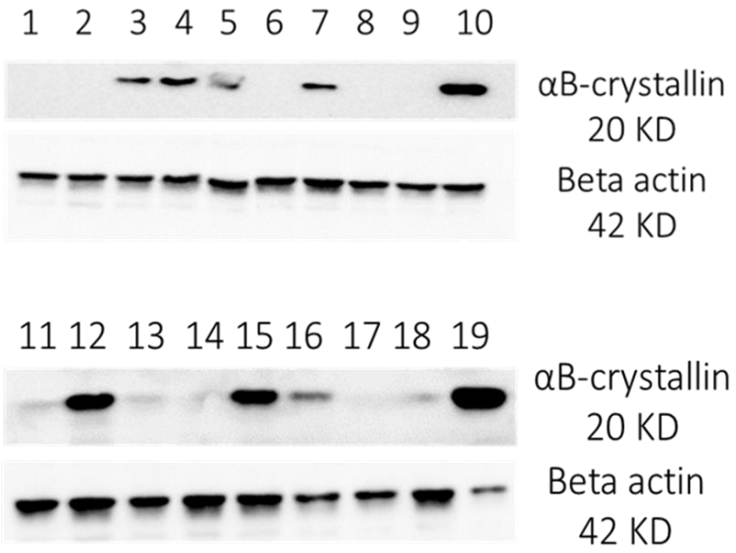

Figure 3.5 Colonies isolated from *CRYAB* transfected MDA-MB-231 cells. Monoclonal cell populations were isolated by limited dilution and protein extracts were analysed by western blotting for αB-crystalline. Beta actin was used as loading control. Blots are from one experiment.

3.3.8 Determining the IC_{50} of doxorubicin in MDA-MB-231/WT and MDA-MB-231/*CRYAB* cells

As described in section 3.3.6, the alamar blue assay was initially used to assess the sensitivity of cells after treatment with doxorubicin. However, this test did not detect significant changes in viability following exposure to 5-100 nM doxorubicin, therefore in the next experiments the concentration of doxorubicin was increased in order to establish a suitable IC_{50}. Cell viability was measured by directly counting the cells after treatment with doxorubicin. In addition, since the alamar blue assay was performed with *CRYAB* transfected polyclonal cell lines, which might be different in their expression of αB-crystallin, here, I used the clone that expressed high levels of αB-crystallin (clone 19, Figure 3.5) and compared it to wild type un-transfected cells.

The cells were plated at a density of 50,000 cells/well in 6-well plates. After 48 h, the cells were treated with different concentrations of doxorubicin, ranging from 400 to 900 nM. After 24 h, the cells were trypsinised and counted using a hemocytometer. Death curves produced for MDA-MB-231/WT and MDA-MB-231/*CRYAB* clone 19 cells (Figure 3.6) demonstrated an IC_{50} for doxorubicin of 200.7 nM for MDA-MB-231/WT and 273 nM for MDA-MB-231/*CRYAB* cells. This may indicate that MDA-MB-231/WT cells are more responsive to doxorubicin than MDA-MB-231/*CRYAB* cells.

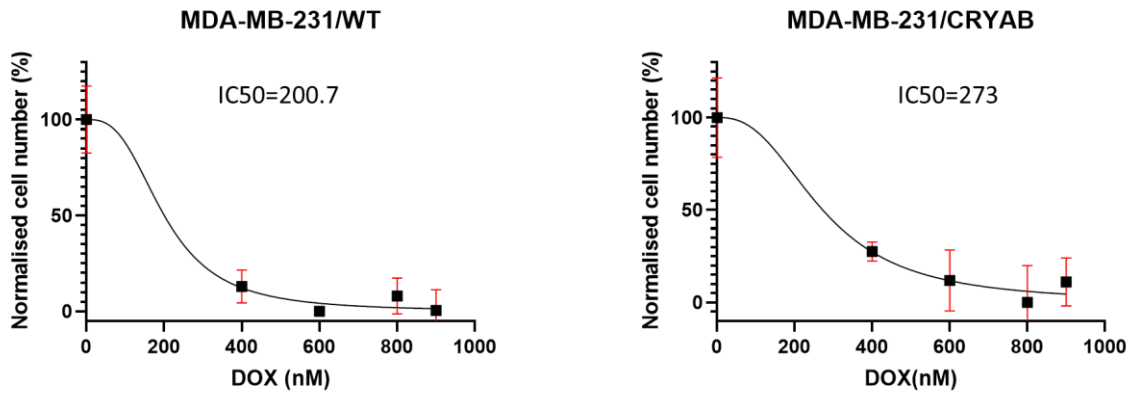

Figure 3.6 Doxorubicin dose response curves of MDA-MB-231/WT & MDA-MB-231/*CRYAB* cells. The cells were plated at a density of 50,000 cells/well in 6-well plates. After 48 h, the cells were treated with increasing concentration of doxorubicin, ranging from 400 to 900 nM. After 24 h, the cells were trypsinised and counted. The IC_{50} of doxorubicin was calculated from the dose response curves and determined using GraphPad prism. Results are from three independent experiments. Data shown is mean ± SEM. Cell numbers are expressed as a percentage normalised to control untreated cultures (100%)

3.3.9 Effects of *CRYAB* overexpression on proliferation of MDA-MB-231 cells

Growth rates of MDA-MB-231/WT and MDA-MB-231/*CRYAB* cells were measured to investigate the effect of CRYAB on proliferation of MDA-MB-231 cells. MB-MDA-231/WT and MB-MDA-231/*CRYAB* clone 19 were plated at a cell density of 50,000 cells/well in 6-well plates and incubated at 37˚C, 5% CO_2. Viable cells from three wells per cell line were counted every 24 h over 4 days using the TC20 Automated Cell Counter. No significant differences in proliferation were observed between MDA-MB-231/WT cells and MDA-MB-231/*CRYAB* cells (Figure 3.7 A). In addition, the doubling time of both cells was calculated. Doubling time of MDA-MB-231/WT was 22.5 h and the doubling time of MDA-MB231/CRAB was 24h (Figure 3.7 B). The results indicated that *CRYAB* overexpression had no significant effect on the proliferation rate of MDA-MB-231 cells.

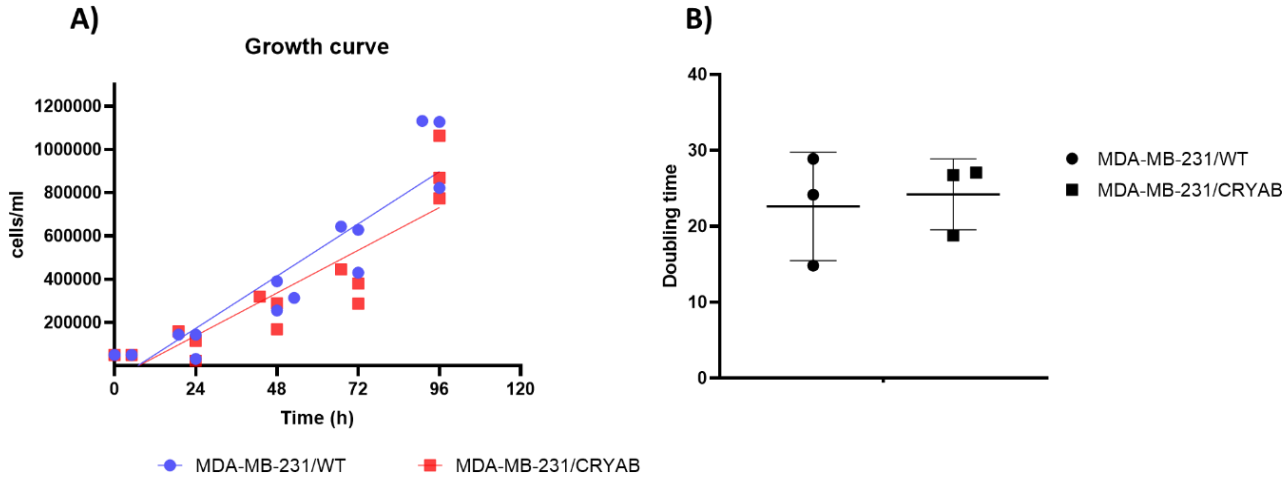

Figure 3.7 The proliferation of MDA-MB-231/WT and MDA-MB-231/*CRYAB* cells. Cells were plated at a cell density of 50,000 cells/well in 6-well plates. At 24, 48, 72 and 96 hours after plating, viable cells from three wells per cell line were counted to establish growth curves. Doubling times were calculated by plotting the log2 of initial average end-point cell number/initial cell number (N/N0) and calculating the inverse slope at the linear part of the curve. **A)** The growth rate of MDA-MB-231/WT and MDA-MB-231/*CRYAB* clone 19. Each data point represents the mean number of live cells from three independent experiments. Each experiment was performed in triplicate wells. The data were analysed by 2-way ANOVA test. **B)** The doubling time of MDA-MB-231/WT and MDA-MB-231/CRYAB. The data was analysed by unpaired t test, plot is mean ± SD from three independent experiments.

3.3.10 Effects of *CRYAB* overexpression on doxorubicin-induced apoptosis in MDA-MB-231 cells

αB-crystallin is an anti-apoptotic protein that is thought to counteract the function of proapoptotic proteins during the initiation and execution phases of apoptosis. Therefore, the effects of this protein on induction of apoptosis were investigated by flow cytometry in MDA-MB-231/WT and *CRYAB* overexpressing cells (clone 19) after treatment with doxorubicin.

Cells were plated at a density of 50,000 cells/well in 6-well plates. After 48 h, the cells were treated with different concentrations of doxorubicin (200 nM , 400 nM and 600 nM). The cells were incubated with the drug for 24 and 48 h. Cells were washed and harvested before being resuspended in 250 µl annexin binding buffer. Annexin V/FITC and Topro3 were added to each sample. Untreated cells were used as a control to adjust the voltage and amp gate and ensure that the cell population was visible on the SSC/FSC plot. A gate was drawn around the main cell population of the SSC/FSC plot to exclude debris from being analysed. Annexin V positive cells were detected by blue 530-30A channel, while TOPRO3 positive cells were detected by red 660-20-A channel.

The flow cytometric analysis of treated cells revealed an increase in the percentage of apoptotic cells in a dose and time-dependent manner in both cell lines. However, doxorubicin induced increased levels of apoptosis in MDA-MB-231/*CRYAB* cells when compared to MDA-MB-231/WT cells although the difference was not statistically significant (Figure 3.8). Apoptosis was not increased in MDA-MB-231/WT cells 24 h following exposure to any of the concentrations of doxorubicin tested compared to untreated cells (Figure 3.8 C). In contrast, MDA-MB-231/*CRYAB* showed an approximate 15% increase in apoptosis with 400 nM and 600 nM doxorubicin when compared to untreated cells (Figure 3.8 C).

After 48 h, a dose-dependent increase in apoptosis was observed in both cell lines. MDA-MB-231/*CRYAB* cells responded more to doxorubicin compared to MDA-MB-231/WT cells (Figure 3.8 F). The difference in apoptotic cell numbers between MDA-MB-231/WT and MDA-MB-231/*CRYAB* was not significant. The results indicate that rather than inhibiting apoptosis, αB-crystallin over-expression tended to make cells more sensitive to doxorubicin induced apoptosis especially at earlier time points.

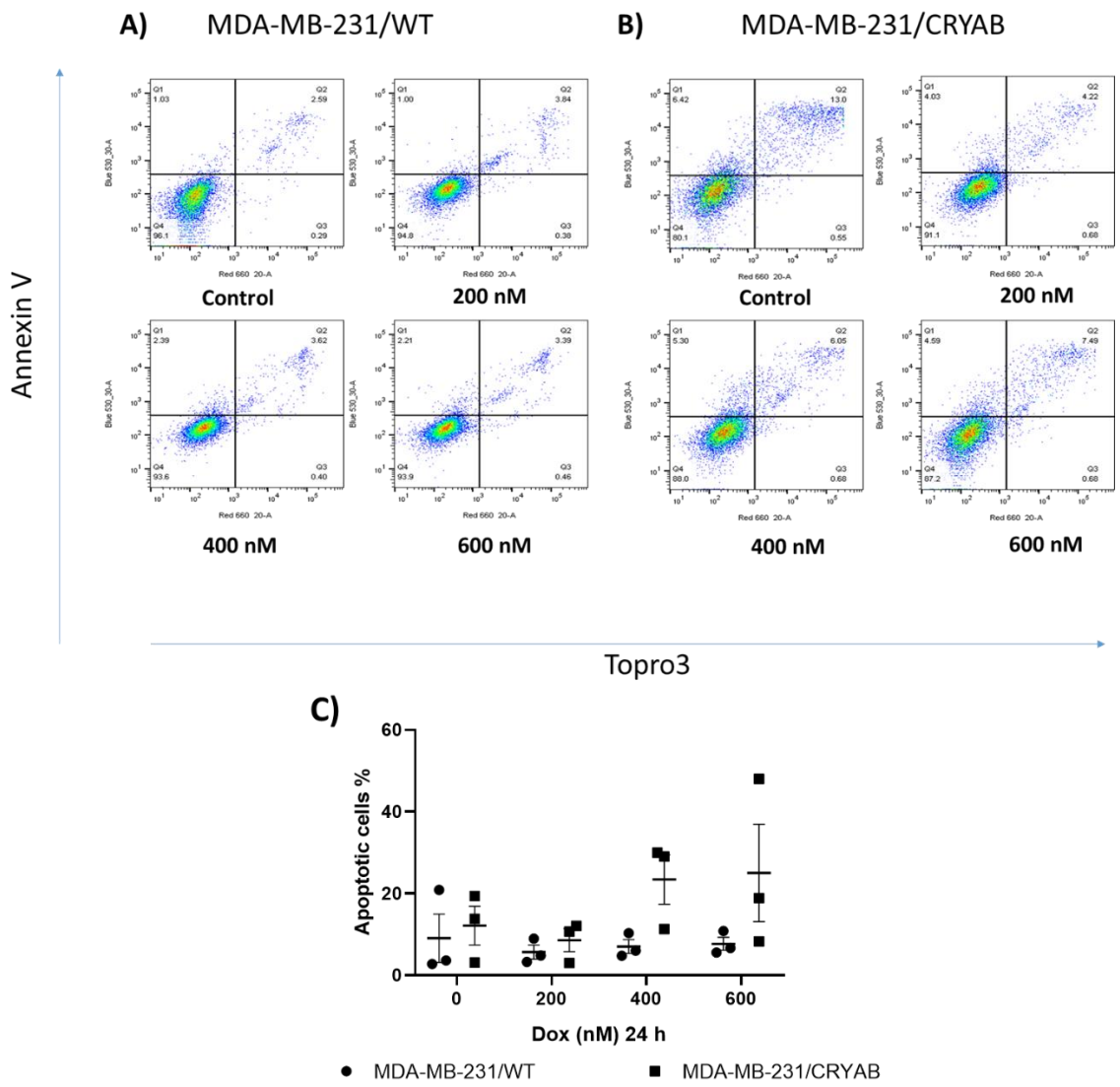

Figure 3.8 Apoptosis induction of MDA-MB-231/WT and MDA-MB-231/*CRYAB* cells after 24 h of doxorubicin treatment. MDA-MB-231/WT and MDA-MB-231/*CRYAB* cells (clone 19) were plated at density of 50,000 cells/well in 6-well plates. After 48 h, the cells were treated with doxorubicin (200 nM , 400 nM and 600 nM). The cells were incubated with the drug for 24 h. Annexin V/FITC and TOPRO3 were added to each sample and the samples were analysed on an LSRII flow cytometer. Representative flow cytometry plots using Annexin V-FITC/TOPRO3 staining for apoptosis in MDA-MB-231/WT cells, **A)** and MDA-MB-231/*CRYAB* cells, **B)**. Lower left quadrants show viable cells (Annexin V-FITC and TOPRO3 negative); lower right quadrants are necrotic cells (TOPRO3 positive and Annexin V negative); upper left quadrants, early apoptotic cells (Annexin V-FITC positive and TOPRO3 negative); upper right quadrants dead cells (Late apoptosis) (TOPRO3 positive and Annexin V-FITC negative). **C)** Apoptosis percentage was calculated by adding the percentage of upper left quadrant and upper right quadrant (early and late apoptosis percentages)**.** Data was analysed by 2-way ANOVA test, plot in **C** is mean ± SEM from three independent experiments.

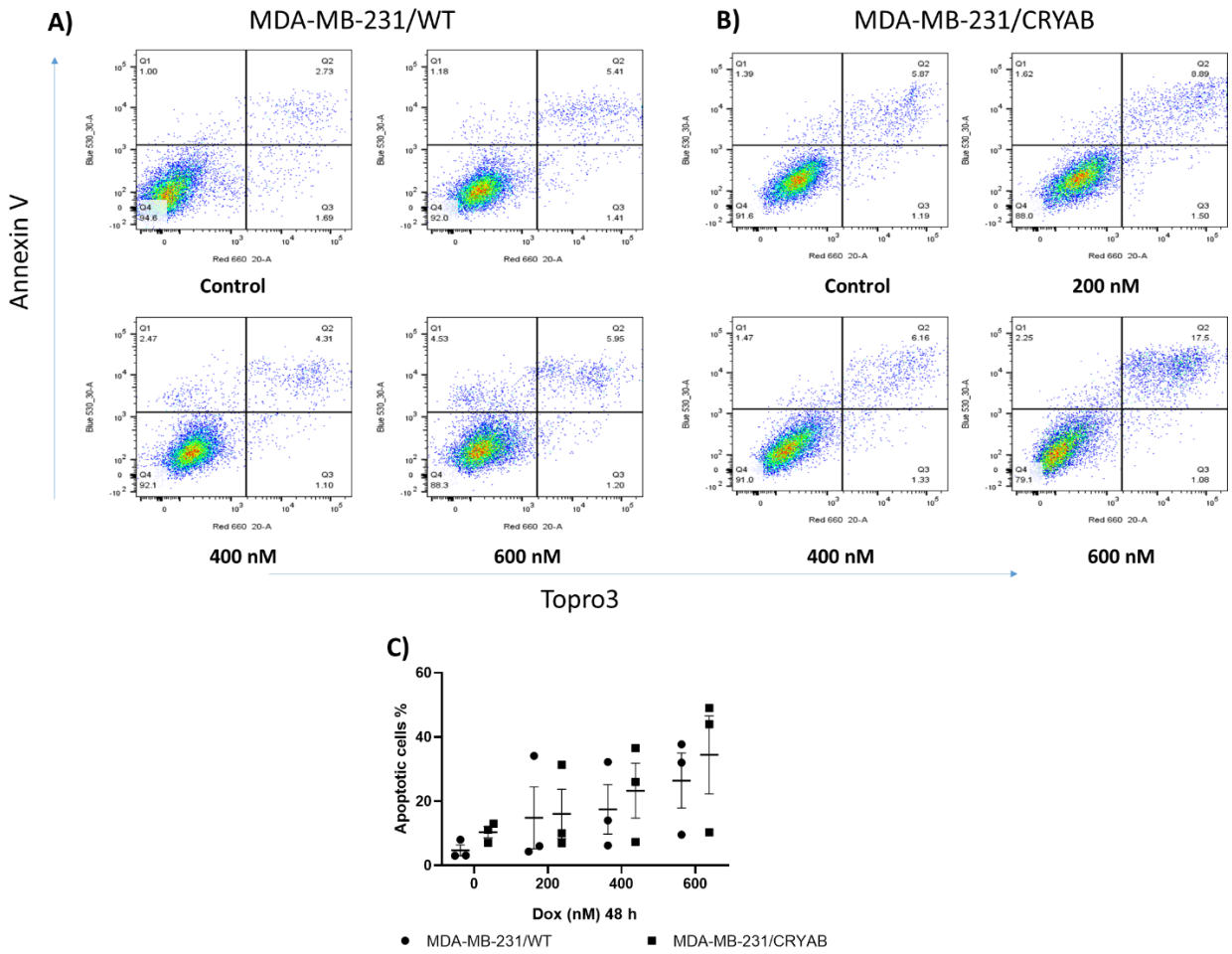

Figure 3.9 Apoptosis induction of MDA-MB-231/WT and MDA-MB-231/*CRYAB* cells after 48 h of doxorubicin treatment. MDA-MB-231/WT and MDA-MB-231/*CRYAB* cells (clone 19) were plated at density of 50,000 cells/well in 6-well plates. After 48 h, the cells were treated with doxorubicin (200 nM , 400 nM and 600 nM). The cells were incubated with the drug for either 48 h. Annexin V/FITC and TOPRO3 were added to each sample and the samples were analysed on an LSRII flow cytometer. Representative flow cytometry plots using Annexin V-FITC/TOPRO3 staining for apoptosis in MDA-MB-231/WT cells, A) and MDA-MB-231/CRYAB cells, B). Lower left quadrants show viable cells (Annexin V-FITC and TOPRO3 negative); lower right quadrants are necrotic cells (TOPRO3 positive and Annexin V negative); upper left quadrants, early apoptotic cells (Annexin V-FITC positive and TOPRO3 negative); upper right quadrants dead cells (Late apoptosis) (TOPRO3 positive and Annexin V-FITC negative). C) Apoptosis percentage was calculated by adding the percentage of upper left quadrant and upper right quadrant (early and late apoptosis percentages). Data was analysed by 2-way ANOVA test, plot is mean ± SEM from three independent experiments.

3.3.11 VEGF secretion by breast cancer cells at 37°C, hypoxia and 42°C heat shock.

αB-crystallin has been previously shown to stabilise and protect endogenous VEGF from degradation in endothelial cells (Dimberg *et al.* 2008, Kase *et al.* 2010, Ruan *et al.* 2011). αB-crystallin has sequences that are thought to interact with VEGF but also other important regulatory proteins and protect against unfolding and aggregation (Ghosh *et al.* 2007). To assess whether αB-crystallin leads to increased VEGF production and hence potential protection of the protein from degradation, the levels of VEGF secreted by MDA-MB-231/WT and MDA-MB-231/*CRYAB* cells was assessed. Two different clones of MDA-MB-231/*CRYAB* cells, one expressing high levels of αB-crystallin (clone 19) and one expressing lower levels of αB-crystallin (Clone 16) (see Figure 3.5) were tested to assess any difference between clones. VEGF levels were measured in conditioned media and cell lysates by ELISA. Since αB-crystallin is a stress induced protein, and VEGF is induced by hypoxia, VEGF produced during both hypoxia and heat shock was measured to assess whether αB-crystallin acts to protect VEGF also under these stress conditions.

The cells were grown in 75 cm^2 flasks or 6-well plates for 48 h in full growth medium. After 48 h, the medium was removed, and cells were washed twice with serum free medium (SFM). Cells were exposed to three different conditions; the first group was placed in a 37°C incubator as a control; the second group was exposed to heat shock at 42 °C in a humidified CO_2 incubator for 24 h and the third group was exposed to low oxygen levels of 0.1 % (hypoxia) at 37°C for 24 h. After 24 h, the cells in hypoxia and heat shock were placed in the normal incubator at 37 °C for a further 24 h. At the end of the 48 h conditioning period, media and cell lysates were collected and analysed for VEGF by ELISA. VEGF concentrations were interpolated from the standard curve of VEGF of known standards, according to the manufacturer's instructions. The number of cells in each sample was counted, so the concentration of VEGF in pg per 10^6 cells could be obtained.

The data showed that under control conditions (37°C), MDA-MB-231/WT cells demonstrated a strong trend towards increased secreted and intra-cellular VEGF compared to MDA-MB 231/*CRYAB* high and low expressing clones (Figure 3.10). Hypoxia enhanced the production of VEGF in all cells compared to VEGF production at 37°C; however, this did not reach significance in all groups. Interestingly, hypoxia led to a significant increase in VEGF secretion

in MDA-MB-231/WT cells compared to that secreted from MDA-MB-231/*CRYAB* (high) cells ($p=0.01$) (Figure 3.10 A), whereas heat shock only induced VEGF expression in MDA-MB-231/*CRYAB* cells but not in wild-type cells when compared to cells at 37 ^{o}C (Figure 3.10 B).

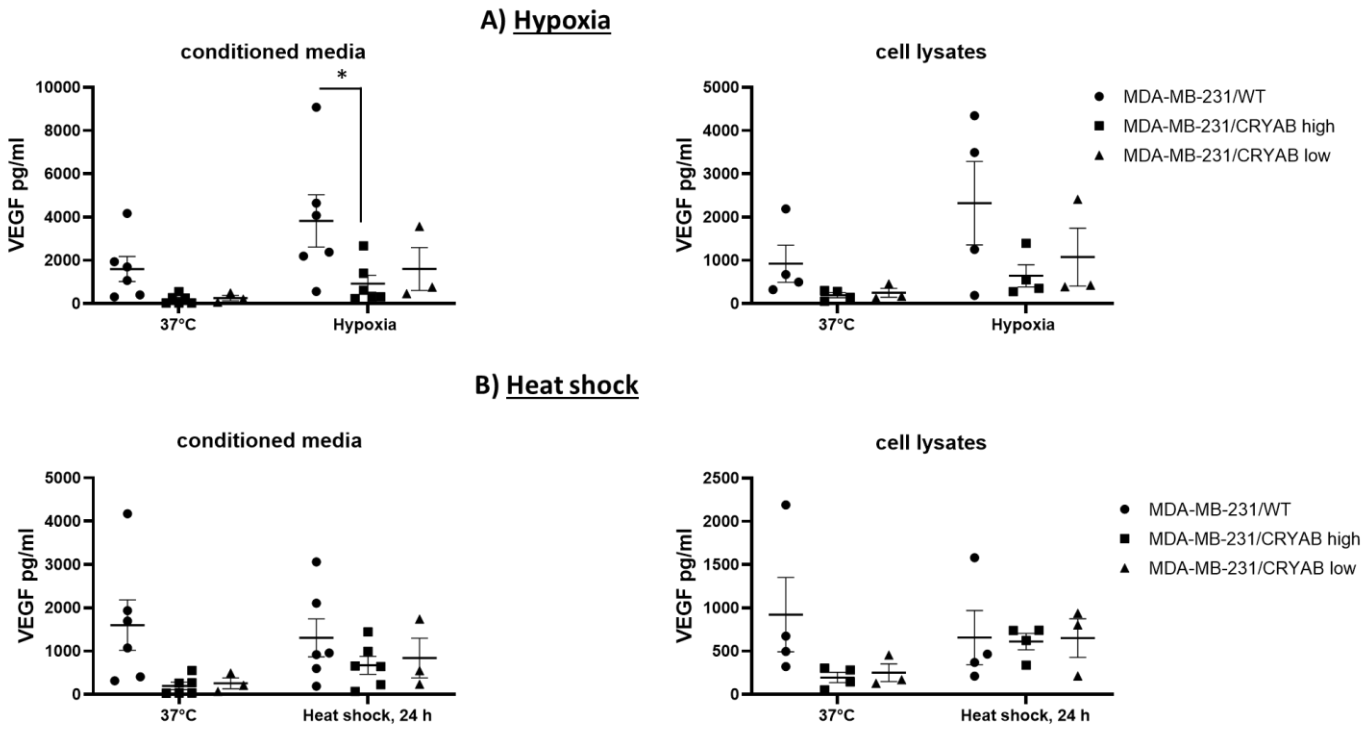

Figure 3.10 VEGF production by MDA-MB-231/WT cells MDAMB-231/*CRYAB* high (clone 19) and low (clone 12) expressing clones. Cells were grown in 75 cm^2 flasks or 6-well plates for 48 h in full growth medium. After 48 h, the medium was removed and replaced with SFM. Cells were exposed to three different conditions; the first set was set in the 37^{o}C incubator as the control; the second set was exposed to heat shock at 42^{o}C in a humidified CO_2 incubator for 24 h and the third set was exposed to low oxygen level of 0.1 % (hypoxia) for 24 h. Cells in hypoxia or heat shock were then incubated for a further 24 h in a 37^{o}C incubator at normal atmospheric oxygen. Conditioned media and cell lysates were collected from all samples and analysed by ELISA assay. VEGF level (pg/ml) was calculated per 10^6 cells in conditioned media and cell lysates in hypoxia **A),** and heat shock **B)**. Data was analysed by 2-way ANOVA with Tukey's multiple comparisons test. Plots are means ± SEM (*$p<0.05$) from 3-6 independent experiments.

3.4 Discussion

Cells express heat shock proteins such as αB-crystallin in order to act as stress-induced molecular chaperones to inhibit apoptosis and prevent the accumulation of denatured proteins, therefore stimulating cell survival (Horwitz 1992, Arrigo *et al.* 2007, Acunzo *et al.* 2012). In addition to cancer cells, *CRYAB* protein expression is also seen in tumour endothelial cells and this is thought to stimulate angiogenesis via autocrine mechanisms and protect VEGF from degradation as shown in co-culture models of breast cancer cells and endothelial cells (Ruan *et al.* 2011). Interestingly, these events correlate with the tumourigenic metastatic states of breast cancer cell lines (Ruan *et al.* 2011). The same study showed that αB-crystallin upregulated in endothelial cells after treatment with anti-VEGF treatment (Ruan *et al.* 2011). Hence, breast cancer cells induce αB-crystallin in endothelial cells to stimulate their survival.

The aim of this chapter was to examine whether upregulated αB-crystallin in breast cancer cells acts to stimulate their own survival and prevent their apoptosis after treatment with drugs such as doxorubicin, which is often used in the treatment of breast cancer. In addition, as αB-crystallin is known to be upregulated under stress conditions, such as heat shock and hypoxia, these stress stimuli were used to test the effect of αB-crystallin on VEGF protection. To achieve these aims, αB-crystallin was overexpressed in MDA-MB-231 cell lines their proliferation rate and apoptosis induction post overexpression and after doxorubicin treatment was tested. In addition, VEGF levels were compared between MDA-MB-231/*CRYAB* cells versus MDA-MB-231/WT cells.

Initially, αB-crystallin expression was examined in two different TNBC cell lines (MDA-MB-231 and MDA-MB-468). The results showed that MDA-MB-468 cells expressed αB-crystallin, while MDA-MB-231 cells did not express this protein, even after exposure to heat shock. It is important to mention that there are variabilities of αB-crystallin band density of MDA-MB-468 at 37 °C between figure 3.1 and figure 3.3. This is because the difference of imaging system that was used to capture western blot images. In figure 3.1, X-ray film was used, whereas in figure 3.3 digital imaging system was used (Chemidoc MP system, Bio-Rad).

Although, both are metastatic TNBC cell-lines, only MDA-MB-468 expressed the protein constitutively. The differences in the level of αB-crystallin expression between these two breast cancer cells agree with data previously published by Chelouche-Lev *et al.* (2004) who

found that αB-crystallin was not detected in MDA-MB-231 cells. In addition, the induction of αB-crystallin by heat shock in both MDA-MB-468 and MDA-MB-231 cells was tested. The protein was induced in response to stress (heat shock) but only in MDA-MB-468 cells. The effect of heat shock on the induction of αB-crystallin in other breast cancer cells was also observed by Chelouche-Lev *et al*. with increased levels of αB-crystallin in GI101A and GILM2 (human breast cancer cell lines). Both cells are metastatic breast cancer cells and in both αB-crystallin was induced in response to heat shock. These findings are similar to the data in this study that showed induction of αB-crystallin post exposure to heat shock in metastatic breast cancer MDA-MB-468 cells. Cells express heat shock proteins such as αB-crystallin as a means to survive under conditions of stress. αB-crystallin performs a chaperone function that helps to protect cell proteins from degradation, refolds unfolded proteins and prevents apoptosis in response to stress (Koletsa *et al.* 2014). Therefore, αB-crystallin may contribute to the resistance to apoptosis which is defined as one of the hallmarks of cancer (Hanahan 2022).

Hypoxia induced stress effects on the induction of αB-crystallin was investigated in the current study. In this study, the cells were incubated at 0.1% O_2. which represents radiobiological hypoxia (<0.13%), in which tumours no longer respond to radiation therapy (Hammond *et al.* 2014, West and Slevin 2019). Therefore, it enables to study the effect of this stress condition on the induction of αB-crystallin. However, hypoxia-induced stress did not increase the expression of αB-crystallin in MDA-MB-231/WT, MDA-MB-468 and MDA-MB-231/*CRYAB* cells. A study by Van Schootbrugge *et al* (2014) using head and neck squamous cell carcinoma (HNSCC) cells observed that αB-crystallin expression in cells exposed to hypoxia (0.1% O_2) for 48 hours was not detected. However, they found that reoxygenation of the cells for 24 h increased the level of αB-crystallin expression. The upregulation of αB-crystallin after the reoxygenation was partially due to the formation of reactive oxygen species (ROS). The induction of αB-crystallin after the hypoxia/reoxygenation phase was also demonstrated in an independent study (Yu *et al.* 2007). This study showed that the process of hypoxia/reoxygenation in cultured human astrocytes from the optic nerve head (ONH), increased αB-crystallin mRNA expression and αB-crystallin protein level. The explanation for this finding was that hypoxia/reoxygenation increased the expression of TGF-β1 and TGF-β2, which stimulated αB-crystallin in cultured human astrocytes of the ONH (Yu *et al.* 2007). However, in this study, the reoxygenation phase of 24 h did not result in the induction of the

protein. The results are restricted to protein expression whereas αB-crystallin mRNA expression may show different results. In addition, it seems that the upregulation of αB-crystallin hypoxia/reoxygenation may not be a general mechanism in all cell types (tumour and normal).

Alamar blue is a sensitive viability assay used as an oxidation-reduction (REDOX) indicator to assess cellular metabolic reduction (Al-Nasiry *et al.* 2007). The response to doxorubicin was assessed in both MDA-MB-231/WT and MDA-MMB-231/*CRYAB* cells using alamar blue. Results using this assay showed that cells did not show significant response to low doses of doxorubicin, indicating that the lower drug doses were ineffective.

αB-crystallin overexpressing cells were expected to be a polyclonal population with cells expressing different levels of the protein. Consequently, the overexpressing αB-crystallin cells were cloned, which was important to produce homogenous cell lines that expressed high or low levels of the protein for use in the current study and retain the transgene selection. The results revealed variable expression of αB-crystallin among the developed monoclonal cell lines.

In the current study, the growth kinetics of overexpressed αB-crystallin monoclonal cells was not statistically different when compared to wild type cells. In contrast, previous studies have shown that αB-crystallin overexpression in MCF-10A cells and MCF-12A, led to increased proliferation and other abnormalities such as enlarged acini, loss of polarity and filled lumen in mammary acini (Moyano *et al.* 2006). It should be noted that MCF-10A and MCF-12A are normal breast cells which may explain the difference between the findings. In addition, it was reported that αB-crystallin promoted the proliferation and invasion of colorectal cancer (CRC) cells through the activation of ERK signalling pathway (Li *et al.* 2017). However, this is not a general mechanism as αB-crystallin overexpression in bladder cancer cells reduced phosphorylated ERK and AKT (Ruan *et al.* 2020).

The effect of αB-crystallin overexpression on the population doubling time was also tested. αB-crystallin had no significant effect on the population doubling time and hence the proliferation of MDA-MB-231 cells. In agreement with this finding, αB-crystallin overexpression in bladder cancer cell lines had a marginal effect on the cell proliferation (Ruan *et al.* 2020).

The cell viability/ proliferation then was measured by counting viable cells using the hemocytometer after treatment with higher doses of doxorubicin, as a more accurate method for assessing proliferation. In addition, the monoclonal overexpressing cells instead of the polyclonal cells were used to assess any differences. The cells were treated with increasing doses of doxorubicin, ranging from 400 to 900 nM. A range of (0-1000 nM) doxorubicin was previously tested in a study to assess cytotoxic activity of doxorubicin using MDA-MB-231 cells (Lee *et al.* 2020). Based on this, concentrations within this range were selected for testing in the current study. The results showed clear dose response curves. The IC_{50} of doxorubicin in MDA-MB-231/WT and MDA-MB-231/*CRYAB* cells was determined from these experiments. The doxorubicin IC_{50} in MDA-MB-231/WT cells was lower than in MDA-MB-231/*CRYAB* cells (200 nM versus 270 nM). Although the results were not statistically different, this suggests a trend towards more sensitivity to doxorubicin by the wild type cells.

Doxorubicin is a widely used chemotherapeutic agent with anticancer activity that results from induction of DNA strand breaks by inhibition of topoisomerase II, interference with DNA unwinding, production of growth arrest (Tewey *et al.* 1984, Fornari Jr *et al.* 1994, Gewirtz 1999), generation of reactive oxygen species such as H_2O_2 (Sinha *et al.* 1987) and induction of apoptosis (Skladanowski and Konopa 1993). In the current study, the influence of αB-crystallin on apoptosis induction after treatment with doxorubicin was studied by flow cytometry analysis. The results showed an increase in the percentage of apoptotic cells from a dose and time-dependent aspect in both studied cell lines. Contrary to expectations, the percentage of MDA-MB-231/*CRYAB* apoptotic cells was higher than that of MDA-MB-231/WT cells. Multiple studies have revealed an antiapoptotic function of αB-crystallin (Mao *et al.* 2004, Shin *et al.* 2009, Launay *et al.* 2010). For example, it has been reported that αB-crystallin protects against oxidative stress-induced cell death by H_2O_2 in astrocytes. The mechanism of this protection was via that αB-crystallin binding to procaspase-3 and inhibiting caspase-3 activation (Shin *et al.* 2009). As previously mentioned, doxorubicin generates H_2O_2, however, αB-crystallin overexpression has no effect on inhibition of apoptosis which may result from H_2O_2 generation. In addition, αB-crystallin prevents the translocation of proapoptotic proteins such as Bax and Bcl-XS to the mitochondria during staurosporine-induced apoptosis (Mao *et al.* 2004). It is not clear why αB -crystallin overexpressing MDA-MB-231 cells are more sensitive to apoptosis induction by doxorubicin in this study. It could be that the levels of αB-

crystallin in the transfected cells are not appropriate (or too high or too low) to confer protection against apoptosis. Further studies are needed to examine whether apoptotic caspases such as caspase 3 are more resistant to cleavage and activation or whether the translocation of pro-apoptotic proteins such as Bax and Bcl-XS to mitochondria is different in wild type versus αB-crystallin overexpressing TNBC cells. Such information would be useful to help explain the data in this thesis.

The interaction between apoptosis regulatory proteins and αB-crystallin in breast cancer cells has been studied by Launay *et al.* (2010). They demonstrated that αB-crystallin overexpression lowered apoptosis levels in MCF7 cells in response to inhibitors of microtubule polymerization (vinblastine), used as anti-cancer agents. Interestingly, phosphorylation of αB-crystallin at serine 59, sensitised the cells to treatment and increased apoptosis (Launay *et al.* 2010). The molecular mechanism was shown to involve αB-crystallin interaction with the anti-apoptotic protein BCL-2 which prevented its translocation to mitochondria, and hence decreased resistance to treatment (Launay *et al.* 2010). In contrast, the phosphorylation of αB-crystallin is essential to exert a protective role in different cells. For example, it was reported that αB-crystallin was upregulated and phosphorylated at serine 59 during the tubular morphogensis in endothelial cells, suggesting a regulatory role for phoshorylated αB-crystallin. Notably, the siRNA-mediated knockdown of αB-crystallin led to attenuation in tubular morphogenesis and activation of caspase 3 (Dimberg *et al.* 2008). In accordance with this finding, the phosphorylation of αB-crystallin in cardiac myocytes exposed to osmotic or ischemic stress conferred a protective function in these cells (Morrison *et al.* 2003). Phosphorylation of αB-crystallin occurred at serines 19, 45, and 59 in response to stress. The phosphorylation is thought to modulate the oligimerization structure of the protein and its chaperone-like function (Thornell and Aquilina 2015). As demonstrated by these studies, there are conflicting findings, and it is not clear yet what the effect of αB-crystallin serine phosphorylation is on its chaperone function. It appears that the target protein and/or the type of cells play roles on the influence of αB-crystallin serine phosphorylation. In this study, the phosphorylation of αB-crystallin was not tested and it is not known whether the increased apoptosis that is seen in MDA-MB-231/*CRYAB* cells was associated with the phosphorylated status of αB-crystallin in these cells.

It has been reported that αB-crystallin serves as a protector for VEGF and prevents its degradation upon exposure to anti-VEGF therapy (Dimberg *et al.* 2008, Kase *et al.* 2010, Ruan *et al.* 2011). In addition, αB-crystallin expression is upregulated during angiogenesis, *in vitro,* suggesting a regulatory function (Dimberg *et al.* 2008). Secreted (in conditioned media) and intracellular (in cell lysates) VEGF was assessed by ELISA to investigate the effect of αB-crystallin on secretion of this pro-angiogenic protein. Conditions of normal oxygen and hypoxia were compared. In addition, VEGF levels were compared between cells in a normal 37^{o}C incubator and cells exposed to heat shock to upregulate αB-crystallin expression and hence potentially also VEGF. As expected, in hypoxia, VEGF levels were higher in conditioned media of all cell lines compared to cells maintained in a normal incubator. Hypoxia is the main regulator of angiogenesis and cancer cells trigger VEGF production to survive the low oxygen environment. The results showed this stimulation and activation of VEGF in cells exposed to low oxygen levels. However, MDA-MB-231/WT cells secreted higher levels of VEGF compared to MDA-MB-231/*CRYAB* cells. The results were not expected MDA-MB-231/*CRYAB* cells produced substantially lower VEGF levels. Results therefore suggest that VEGF expression and/or stability of the protein were negatively affected by αB-crystallin. Further investigations are warranted to establish the stability of VEGF and/or test the level of mRNA to determine whether the gene expression was affected by *CRYAB* overexpression. In contrast, many studies showed that the knockdown of αB -crystallin resulted in low VEGF levels, attenuated endothelial cell activation of caspase 3 and increased apoptosis in endothelial cells (Dimberg *et al.* 2008, Kase *et al.* 2010). Specifically, Kase *et al* used chemical hypoxia to stimulate VEGF as Hif-1α triggers the gene expression of VEGF. They compared VEGF levels produced from retinal pigment epithelial (RPE) cells derived from mice with αB -crystallin knockdown versus wild type mice and measured VEGF by ELISA. αB-crystallin knockdown led to significantly lower concentrations of VEGF-A compared to wild type mice (Kase *et al.* 2010). It is possible that αB-crystallin acts differently depending on the cell type or the method of altering the protein expression.

VEGF secretion was upregulated in response to heat shock in MDA-MB-231/*CRYAB* cells compared to cells in 37 ^{o}C. The chaperone function of αB-crystallin may explain these results. This upregulation was not seen in MDA-MB-231/WT cells, suggesting that αB-crystallin plays a role in protecting VEGF under heat shock.

In summary, the overexpression of αB-crystallin in TNBC cell lines did not show a significant effect on protecting VEGF, hence increasing its expression. It is possible that altering the protein levels by the overexpression is not sufficient to demonstrate a difference in VEGF concentrations. Therefore, in the next chapter, transient knockdown of αB-crystallin was performed to further investigate the role of αB-crystallin in protecting VEGF.

Chapter4 **The effect of transient knockdown of αB-crystallin on VEGF production in breast cancer cells**

4.1 Introduction

αB-crystallin is associated with a poor prognosis in breast cancer patients and has been suggested as a biomarker for TNBC. (Travis *et al.* 2011, Tsang *et al.* 2012, Malin *et al.* 2014). Molecular chaperoning, which prevents protein aggregation, is a well-known activity of αB-crystallin. In addition, it has been demonstrated that αB-crystallin chaperones hypoxia-induced VEGF and leads to proper folding of VEGF and thus efficient angiogenesis (Kase *et al.* 2010, Kerr and Byzova 2010).

Downregulation of αB-crystallin has previously been shown to cause degradation of VEGF in endothelial cells, and weak and leaky blood vessels in *in vivo* models (Dimberg *et al.* 2008, Ruan *et al.* 2011). siRNA-mediated knock-down of αB-crystallin in head and neck squamous cell carcinoma decreased the levels of VEGF produced under normoxic and hypoxic conditions (van de Schootbrugge *et al.* 2013), indicating that αB-crystallin also plays a critical role in protecting VEGF in cancer cells, hence increases its secretion.

In the previous chapter, I showed that *CRYAB* overexpression in MDA-MB-231 cells had no effect on increasing VEGF production. To the contrary, the data showed that *CRYAB* overexpression reduced VEGF secretion; under hypoxic conditions, *CRYAB* overexpressing cells secreted significantly less VEGF compared with wild-type cells, and *CRYAB* overexpressing cells produced more VEGF compared to normal conditions at 37^{o}C, only when exposed to heat shock. In order to investigate further whether these data were due to altered *CRYAB* expression, a second approach was used to silence it using short interfering RNA (siRNA) to reduce αB-crystallin expression in MDA-MB-468 cells that naturally express high levels of this protein.

4.2 Aim

To investigate the effect of αB-crystallin knockdown on the secretion of VEGF. To achieve this, siRNA transient knockdown of αB-crystallin was generated in MDA-MB-468 cells, which has been shown to express high levels of αB-crystallin (chapter 3). The effect of αB-crystallin

knockdown on VEGF production under normal conditions (37^{o}C), hypoxia and following heat shock was investigated.

4.3 Results

4.3.1 Establishing stability and longevity of αB-crystallin knockdown by siRNA in MDA-MB-468 cells

Although siRNA effectively reduces protein expression, the effect is transient and typically lasts for 3-5 days. Initial experiments were performed to establish the optimal transfection conditions and assess how long the transfection will last. MDA-MB-468 cells transfected with either a scrambled siRNA or an individual siRNA targeting the *CRYAB* gene (*CRYAB* siRNA 1). After 48 h, whole cell protein extracts were analysed by western blotting. Extracts were also analysed at 72 h and 96 h following transfection. Results showed the *CRYAB* siRNA resulted in knockdown αB-crystallin, and the knockdown of the protein was sustained for a minimum of 96 hours (Figure 4.1). αB-crystallin was expressed in cells transfected with the scrambled siRNA.

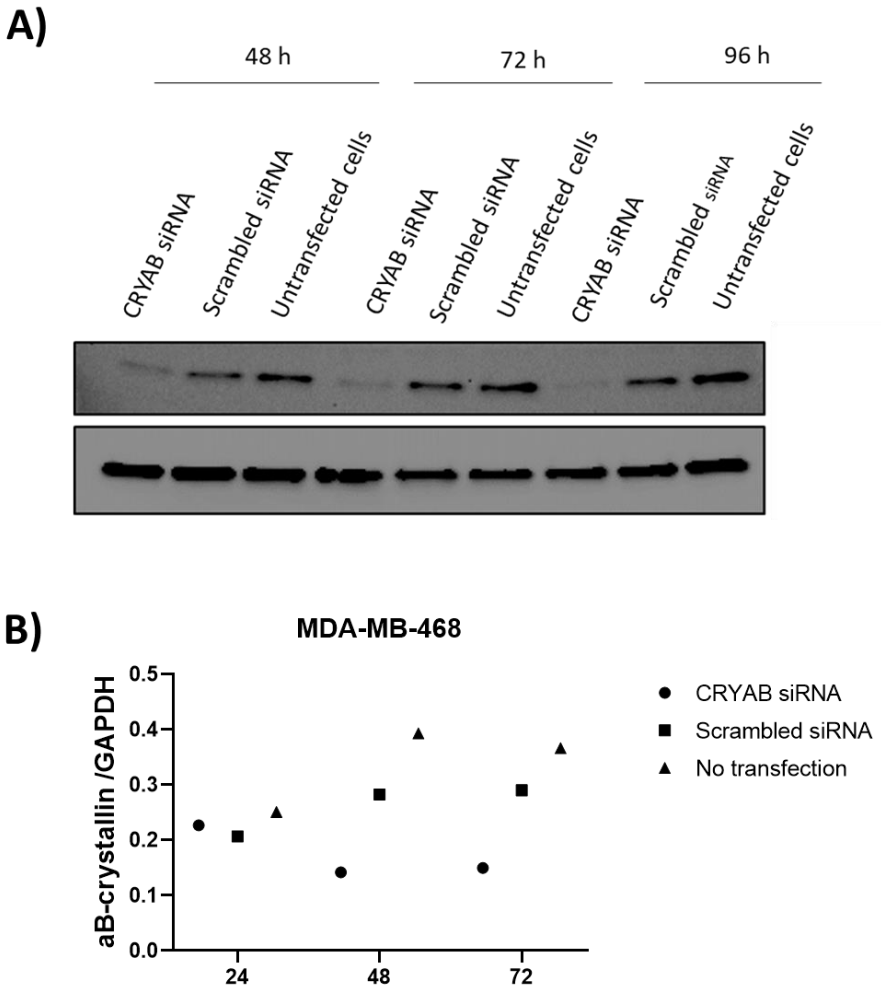

Figure 4.1 Knockdown of αB-crystallin in MB-MDA-468 cells transfected with *CRYAB* siRNA. MDA-MB-468 cells were seeded and transfected with either individual *CRYAB* siRNAs or scrambled siRNA (negative control). A) After 48, 72 and 96 h, protein extracts were analysed by western blotting to check the efficacy of transfection. The membrane was re-probed for GAPDH as an internal control. B) Blots were scanned and the band density of αB-crystallin was expressed as a ratio of GAPDH. Results are from one experiment.

4.3.2 αB-crystallin knockdown did not alter VEGF levels in MDA-MB-468 cells

After successful knockdown of αB-crystallin had been achieved, an experiment to determine the influence of reduced protein expression on VEGF production was set up. Because hypoxia causes an increase in VEGF secretion, the consequences of αB-crystallin knockdown on VEGF levels in MDA-MB-468 cells under hypoxic conditions was investigated. Since results from the previous chapter demonstrated that αB-crystallin was induced in MDA-MB-468 cells in response to heat shock. VEGF levels under heat shock conditions were also evaluated.

MDA-MB-468 cells were transfected with three individual *CRYAB* siRNAs including the original siRNA 1 construct used in Figure 4.1 (*CRYAB* siRNA 1, *CRYAB* siRNA 2 and *CRYAB* siRNA 3) or scrambled siRNA as a negative control. After 48 h, the medium was removed, and SFM was added to the cells. Cells were exposed to three different conditions; the first group was placed in a 37^{o}C incubator as control; the second group was exposed to heat shock at 42^{o}C in a humidified CO_2 incubator for 24 h and the third group was exposed to low oxygen level of 0.1 % (hypoxia) at 37^{o}C for 24 h. After 24 h, the sets of cells in hypoxia and heat shock were placed in the normal incubator 37^{0}C for a further 24 h. At the end of the 48 h conditioning period, media and cell lysates were collected and analysed for VEGF by ELISA. The number of cells in each sample was counted, so the concentration of VEGF pg per 10^6 cells was obtained. Equal amounts of total protein from cell lysates were analysed by western blotting for αB-crystallin expression.

All three different *CRYAB* siRNA, resulted in reduction of αB-crystallin expression. (Figure 4.2) Exposure to heat shock increased αB-crystallin expression in control MDA-MB-468 cells, but hypoxia has no or little influence on the induction of αB-crystallin in control MDA-MB-468 cells. αB-crystallin was not induced by heat shock or hypoxia of following siRNA knockdown compared to control cells.

Analysis of the effects of *CRYAB* siRNA knockdown of VEGF demonstrated that in control conditions (37 ^{0}C), MDA-MB-468 cells transfected with *CRYAB* siRNAs secreted more VEGF compared to negative control (scrambled siRNA) in both conditioned media and cell lysates, however this did not reach significance (Figure 4.3 A, B. Hypoxia increased the production of VEGF in all cells compared to the VEGF produced at normal oxygen and 37 ^{o}C. Nevertheless,

reducing *CRYAB* led to increased VEGF levels compared with VEGF levels from the negative controls (Figure 4.3 A, B). Heat shock stimulated VEGF secretion in all cells; however, in comparison to negative controls, *CRYAB* siRNA transfected cells secreted more VEGF into the media (Figure 4.3 A). In cell lysates, however, negative control cells produced more VEGF compared to cells transfected with *CRYAB* siRNA. Silencing *CRYAB* with three different siRNA led to lower or no change in the intra-cellular levels of VEGF compared to VEGF produced at 37^0C (Figure 4.3 B). The results demonstrated that inhibition of αB-crystallin in MDA-MB-468 cells increased VEGF secretion. The results suggest that αB-crystallin may downregulate VEGF in MDA-MB-468 cells.

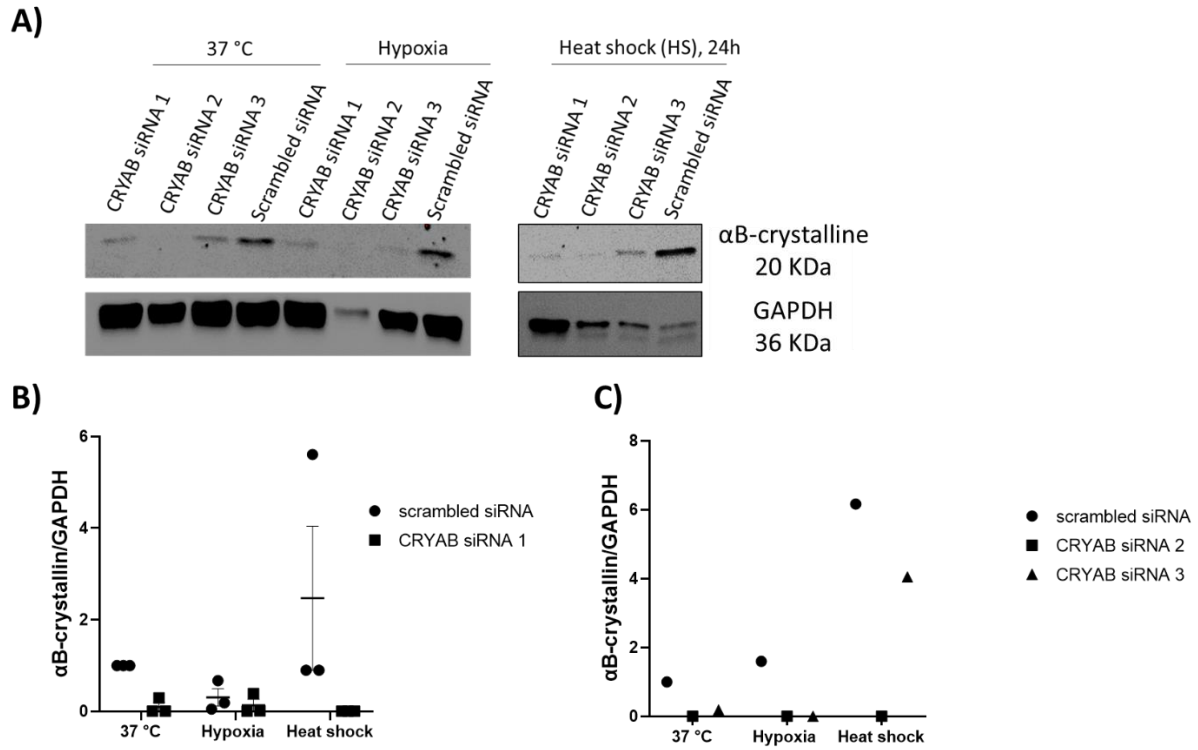

Figure 4.2 Fold increase of αB-crystallin normalised to control cells at 37 °C in *CRYAB* siRNA knockdown MDA-MB-468 cells. Equal amount of cell lysates (20 µg) prepared from MDA-MB-468 transfected with three individual siRNA targeting *CRYAB* or scrambled siRNA (negative control) were analysed by western blotting for αB-crystallin expression. Cells were exposed to three different conditions; the first group was placed in a 37 °C incubator as control; the second group was exposed to low oxygen level of 0.1% (hypoxia) for 24 h and the third group was exposed to heat shock at 42 °C in a humidified CO_2 incubator for 24 h. At the end of the 48 h conditioning period, proteins extracts were then analysed by western blotting to check the efficacy of transfection **A)**. The membranes were re-probed for GAPDH as an internal control. The data blotted are for siRNA 1 **B)** and siRNA 2 & siRNA 3 **C)**. The data plotted are mean± SEM of n=3 for CRYAB siRNA 1 transfected cells and n=1 for CRYAB siRNA 2&3 transfected cells.

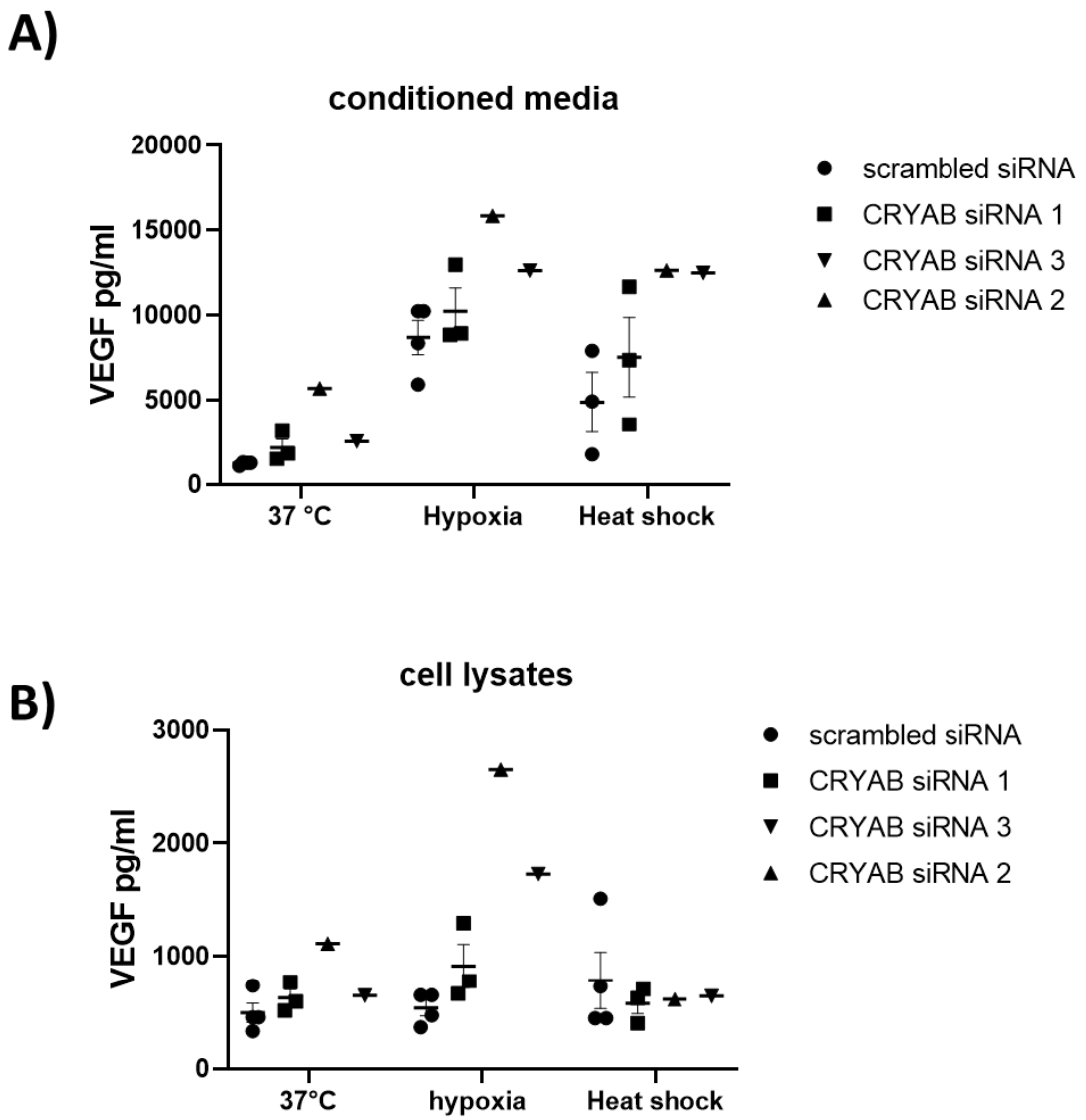

Figure 4.2 Effect of *CRYAB* knockdown on secreted and intracellular VEGF in MDA-MB-468 cells. MDA-MB-468 cells transfected either with three different *CRYAB* siRNA or scrambled siRNA (negative control). After 48 h, cells were exposed to three different conditions; the first group was placed in a 37 ^{o}C incubator as control, the second group was exposed to low oxygen level of 0.1% (hypoxia) at 37^{o}C for 24 h followed by a further 24 h at normal oxygen and the third group was exposed to heat shock at 42 ^{o}C for 24 h followed by a further 24 h at 37^{o}C. At the end of the 48 h conditioning period the medium and cell lysates were collected from all samples and analysed by ELISA assay. The VEGF concentration of all samples was interpolated from the standard curve of known concentration samples. VEGF (pg/ml) was calculated per 10^{6} cells in conditioned media **A)** and cell lysates **B)**. Data were analysed by 2-way ANOVA, plots are mean ± SEM of n=3-4 independent experiments for CRYAB siRNA 1 transfected cells, and n=1 for CRYAB siRNA 2&3 transfected cells.

4.4 Discussion

This chapter has addressed whether the downregulation of αB-crystallin has an effect on VEGF secretion. siRNA was used to silence the protein in MDA-MB-468 cells. The level of VEGF was measured by ELISA under normal conditions (37^0C), hypoxia and heat shock in conditioned media and cell lysates.

The results revealed that silencing *CRYAB* in MDA-MB-468 had no statistically significant effect on VEGF secretion in all tested conditions, although more VEGF was produced by the *CRYAB* silenced cells compared to those transfected with the scrambled control. It should be noted that this result is consistent with the results in chapter 3 showing that αB-crystallin overexpression in MDA-MB-231 reduced VEGF secretion.

Hypoxia is the main regulator of VEGF and as expected, stressing the cells under hypoxia stimulates VEGF secretion as seen here in control cells. However, silencing *CRYAB* led to more VEGF production even though the results did not reach significance. This finding is contrary to previous studies, which have shown that αB-crystallin binds to misfolded VEGF and enhances its secretion in hypoxia-induced conditions in retinal pigment epithelium (RPE) cells (Kerr and Byzova 2010). In addition, after treating the RPE with chemical hypoxia (cobalt chloride), VEGF and αB-crystallin induced in RPE cells in response to hypoxic conditions. The authors demonstrated strong binding between αB-crystallin and VEGF under these hypoxic conditions. Interestingly, the study found that the induction of αB-crystallin increased in the retinal cells of mice at the time of active ocular angiogenesis and then downregulated later in the retina of developed mice. The study demonstrated that αB-crystallin acts to chaperone VEGF during the ocular angiogenesis (Kase *et al.* 2010). It seems that the induction of αB-crystallin and its function as chaperone molecule to VEGF depends on the time of active angiogenesis. This was shown by other study in which the induction of αB-crystallin increased during the formation of new tumour blood vessels *in vitro* (Dimberg *et al.* 2008). Additionally, the types of hypoxia may explain the difference in findings between the results in this study and the study of Kase *et al*. The authors used chemical induced hypoxia, whereas in our studies the cells were incubated in the hypoxic chamber at 0.1 % oxygen. Taken together, the induction of αB-crystallin and its chaperone function is timing and context dependent.

Furthermore, under normoxic and hypoxic conditions, αB-crystallin knockdown reduced VEGF secretion in head and neck squamous cell carcinoma (HNSCC) (van de Schootbrugge *et al.* 2013). This inconsistency between this published data and results presented here may be due to the difference in cell type between breast cancer cells and HNSCC.

Cancer cells produce VEGF as a survival factor to stimulate angiogenesis. Proper folding and secretion of VEGF may ensure efficient angiogenesis and support cancer cell growth. Several reports have linked αB-crystallin with VEGF-dependent angiogenesis (Dimberg *et al.* 2008, Kase *et al.* 2010, Dong *et al.* 2016). For example, siRNA–mediated knockdown of αB-crystallin in tumour vasculature led to high apoptosis in endothelial cells and thinner and disrupted vasculature in mouse model (Dimberg *et al.* 2008). Furthermore, the same effect was found in ocular tissues in αB-crystallin- deficient mice (Kase *et al.* 2010). αB-crystallin was found to play a key role during the intraocular angiogenesis and considers as an essential chaperone for VEGF. αB-crystallin-deficient mice expressed low levels of VEGF proteins compared to wild-type mice during the hypoxic-induced angiogenesis (Kase *et al.* 2010). As a result, the newly developed vessels were attenuated. Importantly, this study demonstrated that the binding between αB-crystallin and VEGF was specific as they did not find interaction between αB-crystallin and TGF-β (Kase *et al.* 2010). The affinity between αB-crystallin and VEGF and other proangiogenic factor FGF was demonstrated in another study by (Ghosh *et al.*). The authors identified the interaction sequences of αB-crystallin with VEGF and FGF. Interestingly, these interactive sequences were found to overlap with the interactive sequences, which are specific for binding with misfolded proteins. αB-crystallin is a chaperone molecule and its binding with proangiogenic proteins through theses interactive sequences indicates that acts to protect these misfolded proteins from aggregation. The chaperone assay from the same study confirmed that αB-crystallin protected FGF from heat aggregation and VEGF from reducing agent aggregation (Ghosh *et al.* 2007). αB-crystallin upregulated in response to heat shock (chapter 3); however, it seems that αB-crystallin may negatively regulate VEGF in this cell line (MDA-MB-468). It is established that cancer cells express various angiogenic factors (Aspriţoiu *et al.* 2021). The relationship between αB-crystallin and other angiogenic factors such as FGF is needed to be determined in future experiments to investigate the relationship between αB-crystallin and other angiogenic factors.

The results from the previous chapter showed that αB-crystallin was induced in response to heat shock. Under heat shock, all cells also produced more VEGF compared to normal conditions at 37^0C. However, silencing αB-crystallin resulted in more VEGF compared to negative scrambled siRNA-transfected cells. This is difficult to explain since it was expected that *CRYAB* would protect VEGF. It is possible that silencing αB-crystallin increases stress and apoptosis in MDA-MB-468 cells and the cells may produce more VEGF to act against apoptosis. It should be noted that only in heat shock condition in the lysates of cells transfected with *CRYAB* siRNA, VEGF levels were lower (but not significantly different) than those in lysates of cells transfected with negative control. VEGF is a growth factor that is mainly produced and secreted to support angiogenesis and cancer cell growth (Goel and Mercurio 2013) and therefore lower levels of VEGF in cell lysates may indicate efficient secretion. In contrast, VEGF accumulation in cell lysates may indicate a problem with secretion.

Phosphorylation of αB-crystallin is induced in response to stress conditions and it is thought to be essential for its chaperoning function (Launay *et al.* 2006). Although this is not a general mechanism in all cells types. However, various studies showed clearly that phosphorylation at serine 59 (ser 59) of αB-crystallin is correlated with increased interaction with VEGF and was associated with increased survival of endothelial cells. For example, phosphorylated αB-crystallin colocalised with VEGF in neovascular endothelial cells of diabetic retinopathy (Dong *et al.* 2016). Moreover, ser 59 phosphorylation of αB-crystallin was upregulated during tubular formation (Dimberg *et al.* 2008). Under hypoxia phosphorylated of αB-crystallin was induced during ocular angiogenesis and was associated with increased levels of VEGF (Kase *et al.* 2010). These data suggested that phosphorylation of αB-crystallin is essential to protect VEGF from stress-induced aggregation. Nevertheless, phosphorylation inhibited the chaperone function of αB-crystallin in breast cancer cells by binding to BCL2 and hence prevents apoptosis (Launay *et al.* 2010). Testing the phosphorylation of αB-crystallin in the cell lines used in this study may help to understand the conflicting of results between this study and those previously published studies. In addition, it will help in revealing whether phosphorylation of αB-crystallin was induced under the stress conditions used in this study (hypoxia and heat shock).

The results demonstrated that silencing CRYAB by siRNA did not result in a significant change in levels of VEGF in MDA-MB-468 cells although there was a trend for an increase. The results

are compatible with the results in the previous chapter where overexpressing CRYAB in MDA-MB-231 cells led to less VEGF. The reason for this is not clear but it is possible that altering CRYAB in the used cells has made the cells independent to VEGF. It is also important to check the levels of VEGF mRNA to see whether increased levels of VEGF were a consequence of more transcription and differences in gene expression. It may be speculated from these findings that αB-crystallin is a negative regulator of VEGF in the cell lines used in this study. However, additional experimental replicates of αB-crystallin silencing utilizing siRNA2 and siRNA3, coupled with an assessment of their effects on VEGF production, are required to substantiate this conclusion.

Chapter5 **The influence of breast cancer cells that express different levels of αB-crystallin on endothelial cell responses**

5.1 Introduction

The role of αB-crystallin in endothelial cell function has been revealed by many studies. αB-crystallin increased endothelial cell survival, protected endothelial cells against apoptosis and stabilised their endogenous autocrine and intracrine VEGF production (Liu *et al.* 2004, Dimberg *et al.* 2008, Kase *et al.* 2010, Ruan *et al.* 2011). Its expression in endothelial cells is induced in response to stress such as osmotic stress and sodium arsenite stress (Golenhofen *et al.* 2002). αB-crystallin was expressed in a subset of tumour vessels such as kidney and lung tumours whereas it was not detected in endothelial cells of normal human lung tissue or healthy human or mouse kidney tissue (Dimberg *et al.* 2008).

αB-crystallin confers different functions to stimulate angiogenesis in the tumour microenvironment. For instance, the conditioned media from trastuzumab-resistant HER2-positive breast cancer cells , which highly expressed αB-crystallin compared to their parental cells, increased tube formation by endothelial cells that were incubated with conditioned media from these cells (Yang *et al.* 2022). Highly tumourgenic and metastatic cells (SK-BR-3, Hs-578T, and MDA-MB-23) induced higher levels of αB-crystallin expression in endothelial cells than non-metastatic (MCF-7, T47D) breast cancer cell lines (Ruan *et al.* 2011). Induction of αB -crystallin in endothelial cells was paralleled with an increase in tubule formation and VEGF levels, whereas αB-crystallin knockdown led to a decrease in VEGF and tubule formation (Ruan *et al.* 2011). αB-crystallin protects breast cancer-induced VEGF from proteolytic degradation and ensures proper folding of VEGF, hence increases their secretion. The mechanism of this function suggested by Kase et al, is that αB-crystallin binds to misfolded VEGF which is transferred to endoplasmic reticulum to be refolded and secreted (Kase *et al.* 2010). These data suggest that αB-crystallin is essential in supporting tumour angiogenesis. It has been reported previously that αB-crystallin expression predicts poor survival in breast cancer and is suggested to be an oncogene (Moyano *et al.* 2006). Thus, breast cancer cells may upregulate αB-crystallin to support tumour angiogenesis.

5.2 Aim

This chapter aimed to test whether breast cancer cells that express different levels of αB-crystallin influence endothelial cell responses. To achieve this:

conditioned media from breast cancer cells with different levels of αB-crystallin were incubated with HDBECs. αB-crystallin expression in HDBECs was then determined by western blot. In addition, the migration of HDBECs exposed to conditioned media derived from the breast cancer cells was assessed by the scratch wound assay.

5.3 Results

5.3.1 Expression of αB-crystallin in HDBECs after incubation with conditioned media from breast cancer cells

To examine whether αB-crystallin is upregulated in HDBECs after incubation with conditioned media from breast cancer cells that express different levels of αB-crystallin, HDBEC were plated at a density of 96,000 cells per well in 6-well plates in a complete endothelial cell growth medium MV and allowed to grow for 48 h. After 48 h, they were incubated with 50% complete endothelial cell growth medium and 50% conditioned media prepared as described in section 2.11.1. As a control, the cells were incubated with 50% complete growth media and 50% serum-free media which had not been in contact with breast cancer cells. After 48 h, proteins extracts were then analysed by western blotting for αB-crystallin expression.

The results showed that there was no induction of αB-crystallin in endothelial cells above basal levels by any of the conditioned media tested. As shown in Figure 5.1, endothelial cells expressed αB-crystallin but levels were not altered by incubation with conditioned media from the breast cancer cells. αB-crystallin levels in the breast cancer cells themselves are also shown on the blot for comparison.

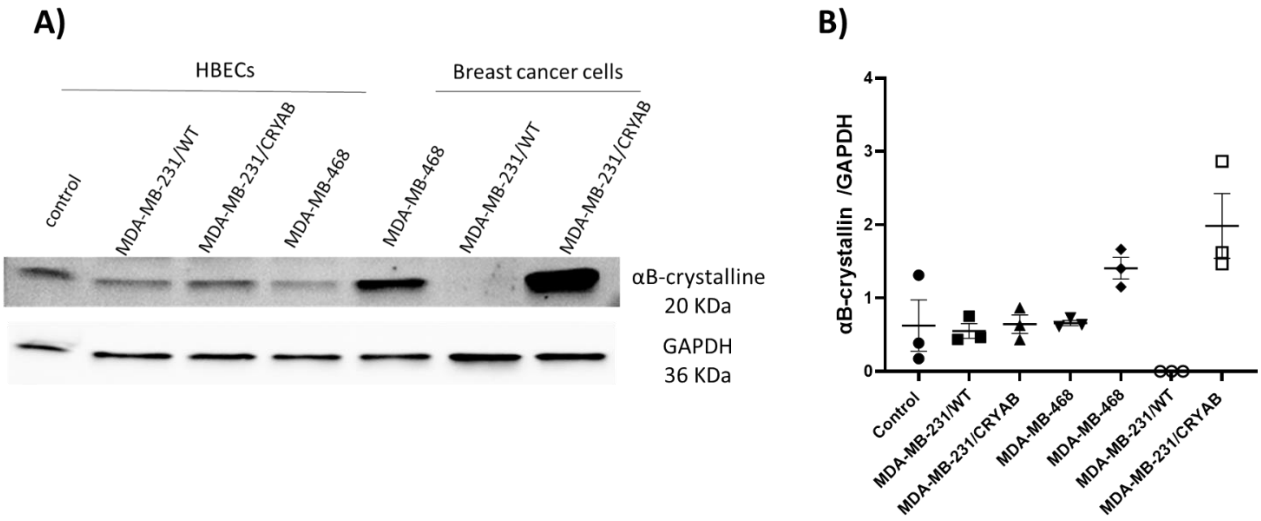

Figure 5.1 Western blot analysis of αB-crystallin protein expression in HDBECs. HDBECs were plated at a density of 96,000 cells per well in 6-well plates in a complete endothelial cell growth medium and allowed to grow for 48 h. After 48 h, they were incubated with 50% complete endothelial cell growth media and 50% conditioned media from MDA-MB-231/WT, MDA-MB-231/*CRYAB* and MDA-MB-468 cells as described in section 2.11.1. As a control, the cells were incubated with 50% complete growth media and 50% serum-free media (SFM) which has not been in contact with breast cancer cells. After 48 h, the cells were lysed and proteins extracts were then analysed by western blotting and for comparison, western blots of extracts from the breast cancer cells are also shown **A)**. Blots were scanned and the band density of αB-crystallin was expressed as a ratio of GAPDH **B)**. The data plotted are mean ± SEM of n=3 independent experiments.

5.3.2 Proliferation of HDBECs with different conditioned media

Before establishing effects of breast cancer cell conditioned media on endothelial migration, it was important to first optimise the conditions of the scratch wound assay and ensure that the proliferation rate of HDBECs was not significantly affected by the conditioned media for the duration of the assay. Differences in proliferation could mask potential effects on migration.

The cells were plated at a density of 96,000 cells per well in 6-well plates. After 48 h, the full growth media was replaced by 50% conditioned media and 50% full complete media or 50% SFM. After 24 h, the media was aspirated, and the cells were counted. Briefly, the conditioned media was prepared by plating MDA-MB-231/WT, MDA-MB-468 and MDA-MB-231/*CRYAB* cells (high expressing clone) at a density of $2x10^6$ cells in DMEM complete media for 48 h. After 48 h, when they reached 80% confluence, the media was replaced with 15 ml of serum-

free endothelial cell growth medium. The conditioned media were collected after 48 h and used in the subsequent experiments.

The results demonstrated that there was no significant effect on the proliferation of HDBECs by different conditioned media during the 24-hour period (Figure 5.2)

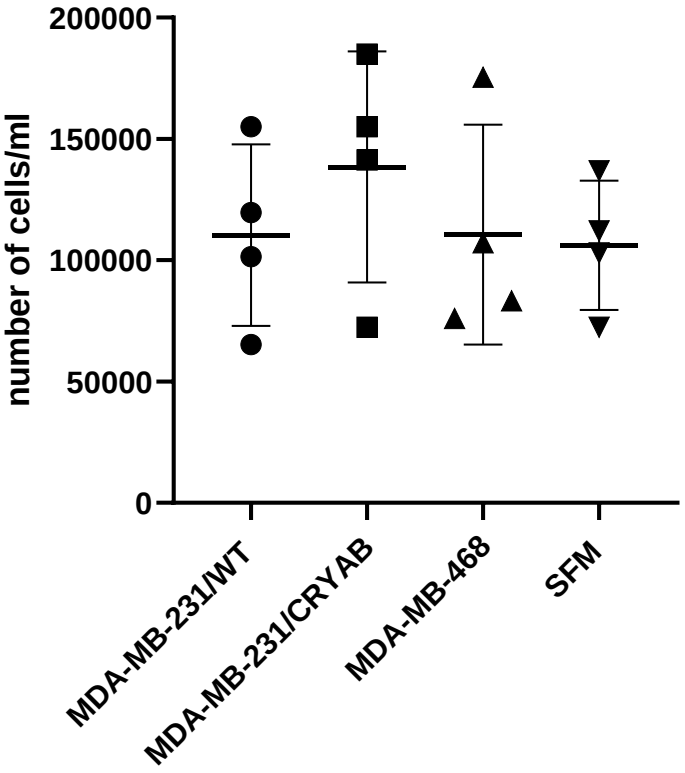

Figure 5.2 Proliferation assay of HBECs. HDBECs were plated at a density of 96,000 cells per well in 6-well plates in complete endothelial cell growth medium and allowed to grow for 48 h. After 48 h, cells were incubated with 50% complete endothelial cell growth medium and 50% conditioned media from either MDA-MB-231/WT, MDA-MB-231/*CRYAB* or MDA-MB-468 cells. As a control, the HDBECs cells were also incubated with 50% complete growth media and 50% SMF which had not been in contact with breast cancer cells. After 24h, the cells were trypsinised and counted. Data was analysed by ordinary one-way ANOVA test, plot is mean ± SEM of n=4 independent experiments.

5.3.3 Effects of conditioned media from breast cancer cells with different levels of αB-crystallin on the migration of HDBECs

To establish whether breast cancer cells with varying levels of αB-crystallin have an effect on the migration of HDBECs, the migration of HDBECs was assessed by a scratch wound assay. Two-well silicone cell culture inserts were placed centrally in the wells of a 12-well cell culture dish (1 insert per well, 3 wells per cell line). A suspension of 500,000 HDBECs per ml was prepared and 70 ul of this suspension was plated per well. Cells were incubated with complete endothelial cell growth media for 24 h before the cell culture inserts were removed to leave a gap/wound of 500 µm for cells to migrate across. Each well was then filled with 50% complete endothelial cell growth medium and 50% conditioned media from breast cancer cells prepared as described in section 2.11.1 . As a control, the cells were incubated with 50% complete growth media and 50% SFM that has not been in contact with breast cancer cells. Six images of each well were taken immediately after creating the wound and then again at 4 h, 8 h and 24 hours. Image J was used to calculate the remaining open area in pixels. The percentage of the closed area was calculated using the equation in 2.11.3.

The results showed that at 4 h, all cells incubated with the various conditioned media closed the wound gap by approximately 15%. At 8 h, there was a further reduction in the wound gap by approximately 30% under all conditions (Figure 5.3). The results showed that there was no significant effect on migration of conditioned media obtained from cells expressing different levels of αB-crystallin or SFM on the migration of HDBECs under the conditions of this assay.

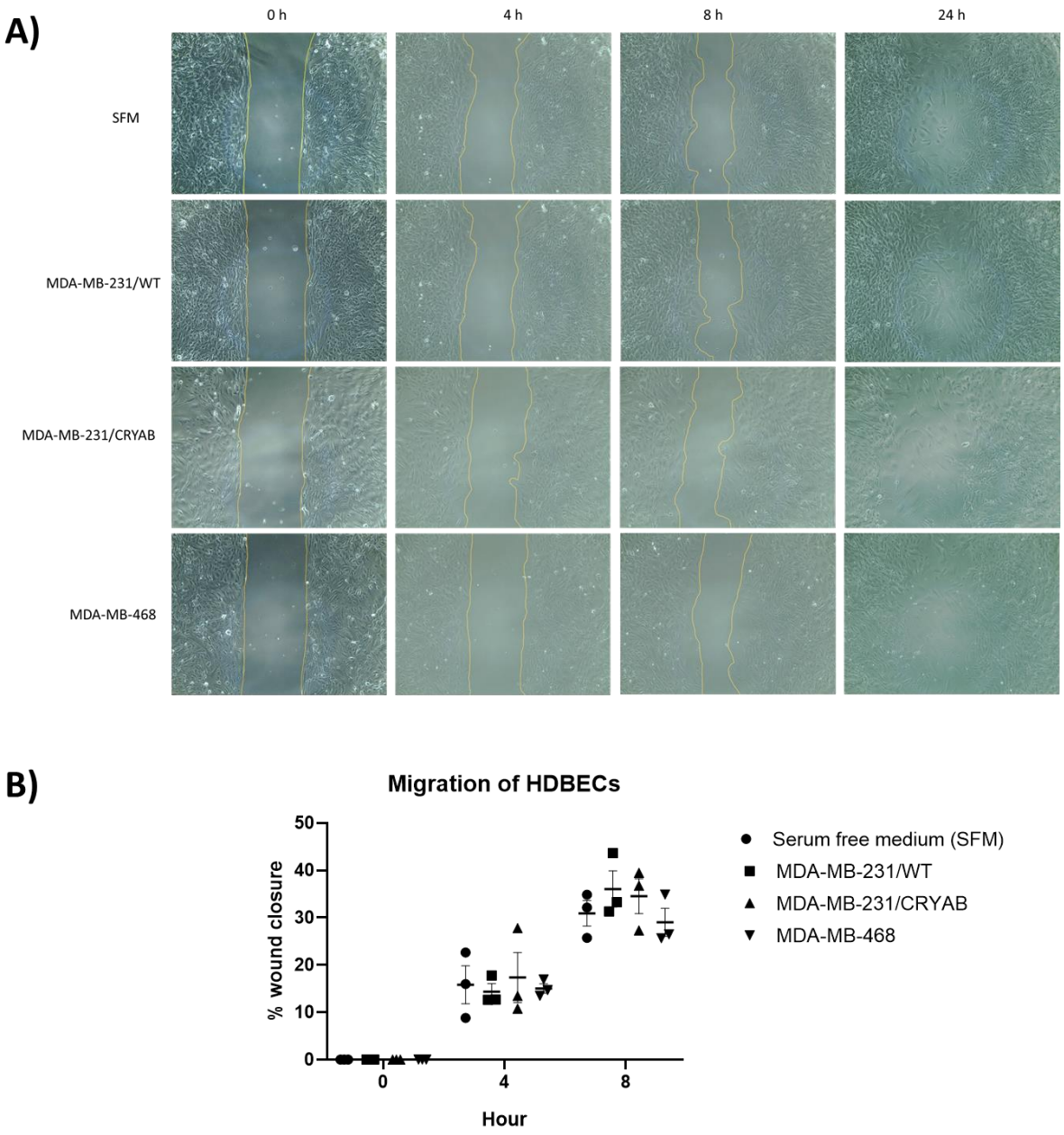

Figure 5.3 Migration of HDBEC after treatment with conditioned media with different levels of αB-crystalline. A suspension of 500,000 HDBECs cells per ml was plated per well in two-well silicone cell culture inserts. Cells were incubated for 24 h before the cell culture inserts were removed. Each well was then filled with half complete endothelial cell growth medium and half conditioned media from breast cancer with different levels of αB-crystalline. As a control, the cells were incubated with half complete growth media and half SFM which has not been in contact with breast cancer cells. Six images per well (three wells per cell line) of each well were taken immediately after creating the wound and then again, at 4 h, 8 h and 24 h. Images were taken with a 10X objective phase contrast camera. Image J was used to calculate the free gap area and % wound closure area was calculated for each time point. The data were analysed by 2-way ANOVA, plot is mean ± SEM of n=3

5.4 Discussion

This chapter aimed to establish whether the breast cancer cells expressing different levels of αB-crystallin have an influence on endothelial cell expression of αB-crystallin and on endothelial angiogenic response. Conditioned media from MDA-MB-231/WT cells, which do not express αB-crystallin, MDA-MB-231/*CRYAB* a clone of the over expressing cells and MDA-MB-468 cells that have endogenous αB-crystallin expression, were incubated with HDBECs. The levels of αB-crystallin expressed by HDBECs and their migration after incubation with conditioned media was assessed by western blotting and scratch wound assay, respectively.

It has been suggested previously that breast cancer cell-induced αB-crystallin in endothelial cells correlated with the malignancy of breast cancer cells such as MDA-MB-231 cells (Ruan *et al.* 2011). This does not appear to be the case in our study even though MDA-MB-231/WT and MDA-MB-468 are both tumourgenic metastatic lines. There were no differences in the expression of αB-crystallin in endothelial cells incubated with conditioned media from these cells. As for the migration assay, it may be that the growth factors present in CM are too dilute to have an effect on endothelial cell expression of αB-crystallin. The different results here and those by previous studies could also be explained by the fact that previous authors used a co-culture model whereas here conditioned media was used. The growth factors produced from breast cancer cells in the co-culture model involve transfer through pores in transwell inserts to endothelial cells directly. Whereas in the model of this study, endothelial cells were incubated with conditioned media from breast cancer cells. It is possible to speculate that the close contact between two cells might be needed to create a positive feedback loop between cells. The co-culture model might facilitate the delivery of growth factors between cells more efficiently than the conditioned media.

αB-crystallin is a chaperone molecule stimulated in response to different stimuli such as osmotic stress, sodium arsenite stress and heat shock (Golenhofen *et al.* 2002, Chelouche-Lev *et al.* 2004). In chapter 3 we also demonstrated that αB-crystallin is upregulated in breast cancer cells in response to heat shock and MDA-MB-231/*CRYAB* cells produces more VEGF in heat shock when compared to normal conditions. Moreover, hypoxia is reported to induce αB-crystallin which is associated with stabilisation of VEGF in retinal pigment epithelial cells and in head and neck squamous cell carcinoma (Kase *et al.* 2010, van de Schootbrugge *et al.* 2013). In addition, it has been reported that αB-crystallin chaperones VEGF in hypoxic

condition and redirects it to endoplasmic reticulum, resulting in proper folding and secretion (Kase *et al.* 2010). VEGF is the main stimulation of angiogenesis, survival and migration of endothelial cells (Abhinand *et al.* 2016). Here the effect of heat shock and hypoxia on the expression of αB-crystallin in endothelial cells have not been tested. Further research is needed to investigate the effect of heat shock and hypoxia stress conditions on the expression of αB-crystallin in endothelial cells and their function.

The migration of endothelial cells by the scratch assay was performed to investigate whether the level of αB-crystallin in breast cancer cells could potentially influence production and secretion of factors by the cells that could in turn alter the migration ability of endothelial cells. The migration assay is dependent on the ability of cells to migrate across a gap/wound and heal the gap but to assess this correctly, effects on proliferation need to be taken into account when comparing different factors produced by different cells. Mitomycin c is usually used to inhibit proliferation of cells and ensure that the scratch is closed only by migration and not cell proliferation. Since HDBECs are primary endothelial cells and tend to be fragile, we avoided treating the cells with the drug. Instead, the cells were counted to confirm that there was no difference in their proliferation when incubated with different conditioned media so the conditions of the assay were optimised. The results showed that there was no significant difference in the proliferation between the different conditions (Figure 5.2), suggesting that if any differences in HDBEC migration were determined it was unlikely to be due to differences in proliferation. The scratch assay data showed that the HDBEC migrated as expected but there was no significant difference in the migration between any of the cells that were incubated with conditioned media from breast cancer cells with different levels of αB-crystallin. Furthermore, conditioned media itself had no effect on the migration, since endothelial cells incubated with SFM migrated in a similar manner to endothelial cells incubated with conditioned media. In chapter three, the results showed that MDA-MB-231/WT cells produce more VEGF than MDA-MB-231/*CRYAB* cells in the serum starved media. Since VEGF is known to induce endothelial cell migration (Soga *et al.* 2001), it was expected that effects on migration would be observed. However, when we tested the same conditioned media on the endothelial cell migration ability, there was no significant difference seen between MDA-MB-231/WT cells and MDA-MB-231/*CRYAB* cells. It is not known why the observed difference in VEGF levels between two cells reported in Chapter 3 did not modulate

endothelial cell migration, but potentially the concentration of VEGF and other growth factors were too low. It may be necessary to concentrate conditioned media in future experiments and expose the endothelial cells to more of the factors that are produced by the breast cancer cells. Yang *et al* demonstrated that the conditioned media from SKBR3 trastuzumab-resistant cell line, which was derived from SKBR3 HER2-positive breast cancer cells, induced the sprouting of human aortic endothelial cells (HAECs) compared to parental trastuzumab-sensitive SKBR3 cells. Interestingly, the group demonstrated that αB-crystallin was significantly greater in SKBR3-trastuzumab-resistant cells than trastuzumab-sensitive SKBR3 parental cells. Importantly, treating HAECs with conditioned medium from SKBR3-trastuzumab-resistant cells after αB-crystallin expression had been knocked down led to a significant decrease in the tubule formation (Yang *et al.* 2022). In contrast, conditioned media from αB-crystallin high expressing cells MDA-MB-231/*CRYAB* or MDA-MB-468 cells did not result in an increase in migration as tested by the scratch assay. The fact that the assay for testing the endothelial cell response is different may explain the contradictory results. In addition, the difference in molecular characteristics between triple negative breast cancer cells and HER2-positive breast cancer cells possibly has an influence. Moreover, the endothelial cells that were used are microvascular endothelial cells derived from the dermis of juvenile foreskin and adult skin, whereas in the Yang *et al* study the human aortic endothelial cells are cardiac endothelial cells. A previous study investigating the effect of αB-crystallin on endothelial tubule formation found that αB-crystallin was upregulated during tubular morphogenesis in bovine capillary endothelial cells and telomerase-immortalized human microvascular endothelial cells. As a result, the total length and area of formed blood vessels were significantly increased compare to the cells with low αB-crystallin (Dimberg *et al.* 2008). Therefore, it appears that the effect of αB-crystallin on endothelial cell response is dependent of cell-type and/or the performed assay.

In summary, the data demonstrated that conditioned media from MDA-MB-231/WT, MDA-MB-231/*CRYAB* and MDA-MB-468 cells under the conditions tested here has no influence on the migration and αB-crystallin expression in HDBECs. More investigations are needed to confirm this result by using other models than the conditioned media.

Chapter6 **Establishing whether αB-crystallin alters the response to treatment**

6.1 Introduction

In this chapter, the effects of the neutralizing anti-VEGF antibody, bevacizumab, on the growth kinetics of MDA-MB-231/WT and MDA-MB-231/*CRYAB* cells orthotopically implanted into nude mice have been evaluated. Furthermore, the effects of doxorubicin, bevacizumab alone or in combination were assessed in mice bearing MDA-MB-231/*CRYAB* and MDA-MB-231/WT tumours. To determine if *CRYAB* alters the response to treatments. Following resection, angiogenesis and apoptosis were evaluated using IHC. VEGF levels from tumour tissues and blood serum were also measured to evaluate any difference between MDA-MB-231/WT and MDA-MB-231/*CRYAB* tumours.

One high *CRYAB* expressing clone of MDA-MB-231/*CRYAB* cells and the wild-type counterpart cells were injected into BALB/C mice. Initially, a pilot study was performed to determine the optimal dose of bevacizumab that resulted in inhibition of tumour derived VEGF. Following this, the same clone of MDA-MB-231/*CRYAB* cells and their wild type counterpart cells were used to establish primary tumours in BALB/C mice through orthotopic injection into the fourth mammary fat pads. Once the primary tumours were established, the mice then were randomised into 8 animals per group of equal tumour size before treating with doxorubicin, bevacizumab, or a combination of both treatments. The resulting tumours were measured three times per week to check the effect of the treatments on tumour growth. At the end of the experiment, blood was collected to measure VEGF in serum and tumours were excised for subsequent analysis of VEGF levels by ELISA. In addition, vascular cell markers and apoptosis was assessed via immunohistochemistry for CD31 CD34 and active-caspase 3. Figure 2.4 showing the outline of the study protocol.

6.2 Aim

The aim of this chapter is assessment of the *in vivo* efficacy of bevacizumab, doxorubicin and the combination of both drugs on the growth and the vasculture of high versus null αB-crystallin breast cancer cells. To achieve this,

1- Evaluate the influence of *CRYAB* overexpression on tumour growth and production of VEGF by measuring the tumour volume and VEGF levels.
2- Evaluate the response of established tumours to bevacizumab, doxorubicin and the combination of both treatments by measuring the tumour volume and VEGF levels.
3- Quantify CD31 and CD34 endothelial markers by IHC to assess the effect of treatments on tumour microvascular density.
4- Determine whether *CRYAB* alters the level of apoptosis *in vivo*, by quantification of active caspase-3 using IHC.

6.3 Results

6.3.1 Establish the optimal dose of bevacizumab for reducing tumour derived VEGF *in vivo*

First, a pilot study was performed to establish the optimal concentration of bevacizumab for reducing VEGF production by MDA-MB-231 breast cancer cells *in vivo*. $1X10^6$ MDA-MB-231/WT cells were injected into the right and left fourth mammary ducts of 12-week BALB C/ mice (n=3/group). 7-days after tumour cell injection, mice were randomly divided into four groups of equal tumour size and treated with 5mg/kg, 7.5mg/kg, 10mg/kg bevacizumab or saline as a control three times a week. The mice were culled at day 30 after initial injection of tumour cells. At the end of the procedure, the serum and primary tumours were collected for VEGF analysis by ELISA assay. The lowest concentration that inhibited VEGF concentration was used for the subsequent *in vivo* combination treatment study.

The results showed that 7.5 mg/kg and 10 mg/kg bevacizumab resulted in inhibition of the tumour VEGF (Figure 6.1). The lowest concentration (7.5 mg/kg) was chosen for the subsequent experiments. The human VEGF was not detected in the serum via ELISA (data not shown). Pilot studies to determine the optimal doses of doxorubicin were not required since previous studies from our laboratories use the concentration of 4 mg/kg doxorubicin and resulted in tumour growth inhibition.

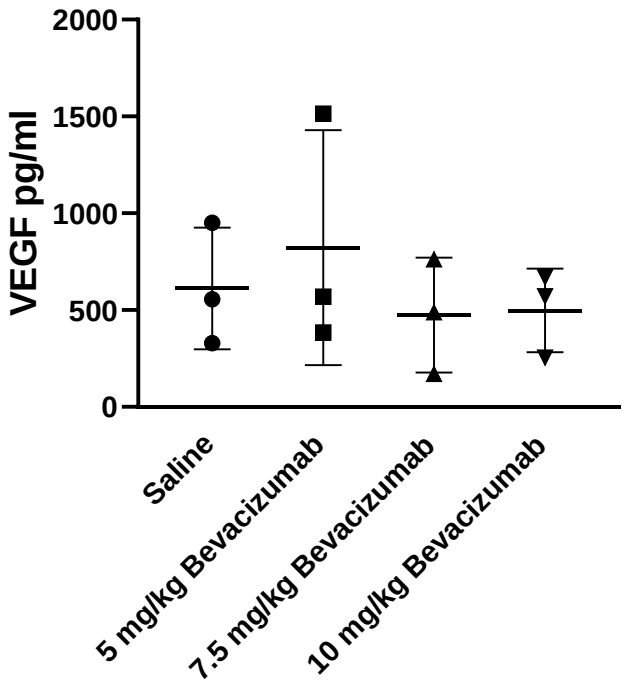

Figure 6.1 Effect of bevacizumab on VEGF concentration in MDA-MB-231/WT tumours +/- bevacizumab. 12-week-old BALB/c nude mice (n=3/group) were injected with $1X10^6$ MDA-MB-231 cells into the 4th left and right mammary glands. After primary tumours were established, mice were treated with three different concentrations of Bevacizumab (5 mg/kg, 7.5 mg/kg and 10 mg/kg) three times before the cull day. One group acted as control and received saline solution three times per week. Tumours were collected for VEGF analysis by ELISA. The VEGF concentration (pg/ml) of all samples was interpolated from the standard curve of known concentration samples. The plot represents mean ± SEM, n=3 mice per groups.

6.3.2 Effect of *CRYAB* on tumour growth and response to different treatment protocols

$1X10^6$ MDA-MB-231/WT or MDA-MB-231/*CRYAB* cells were injected into each of fourth mammary gland in 12-week-old BALB/C mice. Once the tumours had established, the mice were randomly divided into four groups and treated with 4 mg/kg doxorubicin once a week, 7.5mg/kg bevacizumab three times a week, or a combination of bevacizumab and doxorubicin or saline (control). Tumour volumes were measured three times a week by digital calipers, to investigate whether *CRYAB* had an effect on the growth of tumours, *in vivo*, and to evaluate the response to doxorubicin, bevacizumab or the combination of both treatments. At the end point (day 40), the mice were sacrificed, and tumours were excised and weighed.

The data demonstrated that MDA-MB-231/WT grew faster resulting in significant larger tumours compared with MDA-MB-231/*CRYAB* tumours (p=0.0499) (Figure 6.2 A&B). In MDA-MB-231/WT tumours, doxorubicin alone and bevacizumab alone significantly inhibited tumour growth compared with saline (p= <0.0001 and p= 0.0011 respectively). The combination of both treatments reduced tumour growth significantly (P= <0.0001); however, the addition of bevacizumab did not potentiate the effect of doxorubicin (Figure 6.2 C). In MDA-MB-231/*CRYAB* tumours, doxorubicin inhibited the tumour growth significantly (P= <0.0001) whereas bevacizumab did not reduce the tumour volume. In contrast to MDA-MB-231/WT cells doxorubicin and bevacizumab together resulted in more effect than each drug alone; significantly reducing tumour growth compared with the control group (Figure 6.2 D) (P= <0.0001).

At the end point (day 40), the weight of the tumours in all groups were measured (Figure 6.3). The average weight of MDA-MB-231/WT tumours treated with doxorubicin decreased significantly compared to saline (average weight 0.8 g vs 0.3 g, SEM=0.1719, p= 0.03). The combination of both doxorubicin and bevacizumab resulted in a significant decrease in tumour weight (average weight=0.8050 g vs 0.1617 g, SEM=0.1783, p= 0.0075). The tumour weight in bevacizumab treated group also decreased compared to control group, however, this was not significant (average weight= 0.8050 g vs 0.3925, SEM = 0.1668, p=0.0913). The weight of MDA-MB-231/*CRYAB* tumours followed the trend seen in tumour volume with smaller tumour weight. The tumours that were dissected from the doxorubicin treated mice decreased in weight when compared to the control, however, did not reach statistical significance (average weight= 0.2233 g vs 0.07667 g, SEM= 0.07460, p= 0.2391). No

differences were observed between tumour weights in the bevacizumab group compared to control. The tumour weight in the combination group decreased compared to the saline group, but was not significant (tumour weight = 0.2233 g vs 0.01475 g, SEM= 0.08341, p= 0.0957). These results indicate that doxorubicin inhibited tumour growth in MDA-MB-231/WT tumours independent of bevacizumab, whereas the combination of the drugs had more inhibitory effect on MDA-MB-231/*CRYAB* tumour growth than each drug alone.

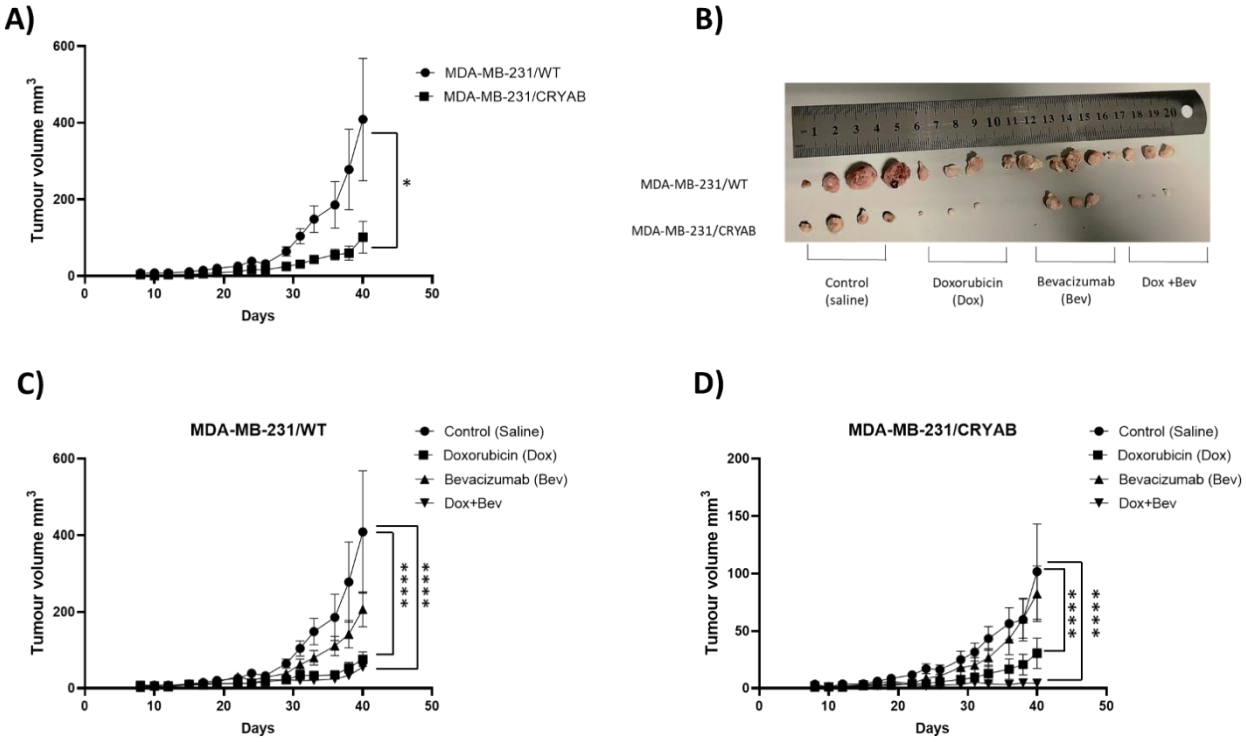

Figure 6.2 Effect of doxorubicin and bevacizumab, alone and in combination on MDA-MB-231/WT and MDA-MB-231/*CRYAB* on tumour growth, *in vivo*. 12-week old BALB/c nude mice were injected into the 4th left and right mammary glands with 1 x 10^{6} MDA-MB-231/WT and MDA-MB-231/*CRYAB* cells. Once primary tumours had established, mice were randomised into groups of equal tumour volume before being treated with either 4 mg/kg doxorubicin, 7.5 mg/kg bevacizumab, combination of doxorubicin and bevacizumab or saline. Tumour volume was measured with digital callipers three times per week until cull day. The results presented are combined from two studies; in each study, 32 mice were divided into 8 groups. **A)** The plot represents the tumour volume of MDA-MB-231/WT and MDA-MB-231/*CRYAB* in control group only (saline). The data analysed by Unpaired t-test. **B)** Appearance of different groups at the end of one experiment. Tumour volume of MDA-MB-231/WT, **C)** and MDA-MB-231/*CRYAB*, **D).** The Data was analysed by two way Anova with Tukey's multiple comparisons test (**** p= <0.0001, * p= 0.0499, mean ± SEM, n=6-8 animals per group.

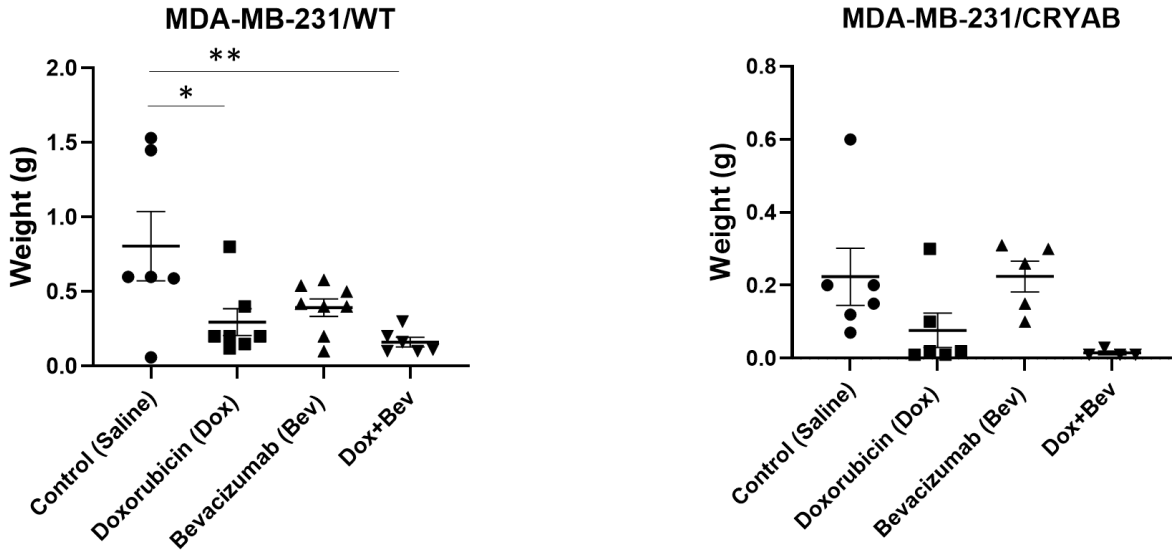

Figure 6.3 Weight of MDA-MB-231/WT and MDA-MB-231/*CRYAB* tumours after treatment with doxorubicin and bevacizumab, alone or in combination. Mice were injected into the 4th left and right mammary glands with 1 x 10^6 of MDA-MB-231/WT and MDA-MB-231/*CRYAB* cells. Once primary tumours had established, mice were treated with either 4 mg/kg doxorubicin, 7.5 mg/kg bevacizumab, the combination of doxorubicin and bevacizumab or saline. Tumour were excised and weighted at the end point (day 40). The results presented are combined data from two studies, in each study 32 mice were divided into 8 groups. Data was analysed by Ordinary one-way ANOVA with Tukey's multiple comparisons test (*P = 0.03, **p = 0.007, ± SEM, n=6-8 animals per group).

6.3.3 The effect of bevacizumab and doxorubicin alone or in combination on VEGF levels

To establish whether *CRYAB* alters the ability of bevacizumab to inhibit VEGF, ELISA was used to determine VEGF concentration in both tumour tissues and blood serum. Mice were treated prior the end point (Day 40) with 4 mg/kg doxorubicin once a week, 7.5 mg/kg bevacizumab three times a week, or combination of both treatments or saline. At the end, blood serum and tumours were collected for VEGF analysis by ELISA.

The results showed that MDA-MB-231/WT tumours produced significantly more VEGF compared to MDA-MB-231/*CRYAB* tumours (P= 0.0021) (Figure 6.4 A), which is consistent with *in vitro* results. Bevacizumab and the combination of both doxorubicin and bevacizumab decreased the concentration of VEGF significantly in MDA-MB-231/WT tumours (P=0.001), whereas in MDA-MB-231/*CRYAB* tumours, only the combination of both doxorubicin and bevacizumab inhibited the production of VEGF significantly (P= 0.03) (Figure 6.4 B,C). These results suggest that tumours derived from *CRYAB* transfected cells are less sensitive to bevacizumab due to the lower levels of VEGF produced. However, the combination of both treatments decreased VEGF significantly. The results suggest that the inhibition of tumour volume seen in this group is due to the decrease in VEGF levels after treatment with combination of bevacizumab and doxorubicin. Human VEGF was not detected in serum in any group possibly due to very low levels secreted into the circulation from human tumour cells (data not shown).

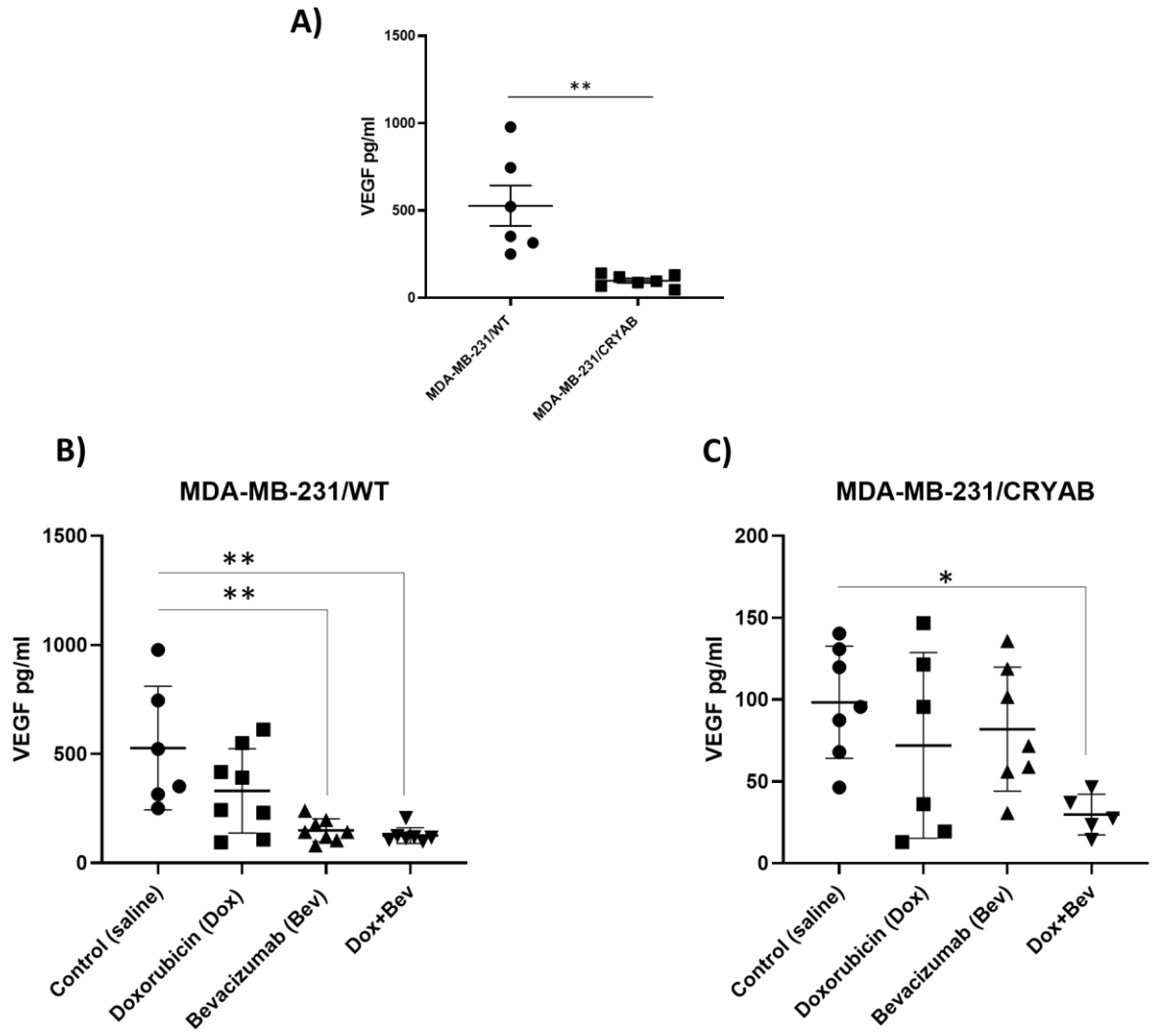

Figure 6.4 Human VEGF concentrations (pg/ml) in MDA-MB-231/WT and MDA-MB-231/*CRYAB* tumours following treatment with doxorubicin, bevacizumab, or a combination of the two treatments. 12-week-old BALB/c nude mice were injected into the 4th left and right mammary glands with 1 x 10^6 of MDA-MB-231/WT and MDA-MB-231/*CRYAB* cells. Once primary tumours had established, mice were selected randomly to be treated with either 4 mg/kg doxorubicin, 7.5 mg/kg bevacizumab, combination of doxorubicin and bevacizumab or saline. At the end point (day 40), tumours were collected and analysed by ELISA for human VEGF expression. 0.5 µg /µL of total protein in total volume of 100 µl were analysed. The optical density was measured at 450 nm and 540 nm for background correction. The VEGF concentration of all samples was interpolated from the standard curve of known concentration samples. **A)** The plot represents the VEGF levels of MDA-MB-231/WT and MDA-MB-231/*CRYAB* in control group only (saline). The data analysed by Unpaired t-test (**p= 0.0021, ± SEM; n =6-7 animals per group. VEGF levels from MDA-MB-231/WT tumours, **B)** and MDA-MB-231/*CRYAB*, **C).** Data were analysed by ordinary one-way ANOVA with Tukey's multiple comparisons test (**p= 0.001, *p = 0.03, ± SEM; n =6-8 animals per group).

6.3.4 Murine-VEGF levels after treatment with bevacizumab and doxorubicin alone or in combination.

Mouse VEGF levels were measured to check the specificity of bevacizumab for human VEGF. Mice were injected into each of the fourth mammary glands with $1x10^6$ cells of MDA-MB-231/WT and MDA-MB-231/*CRYAB* cells. Once the tumours had established, the mice were randomly divided into four groups and treated with 4 mg/kg doxorubicin once a week, 7.5mg/kg bevacizumab three times a week, the combination of bevacizumab and doxorubicin or saline (control). At the end point (day 40), serum and tumours were collected for murine VEGF analysis by ELISA. The results demonstrate that there are no differences between the concentrations of murine VEGF in serum between MDA-MB-231/WT bearing mice and MDA-MB-231/*CRYAB* bearing mice (Figure 6.5), suggesting that the presence of different sized tumours (large WT vs small CRYAB) does not influence host VEGF.

In tumours, there is no significant difference between treated tumours and controls in MDA-MB-231/WT tumours. In MDA-MB-231/*CRYAB* tumours, the treatment combination led to significant inhibition of VEGF compared to bevacizumab alone. This could potentially be linked to the substantially smaller size of tumours within this particular group.

The results indicate that the treatments have no effect on the host VEGF in all groups, suggesting that the treatments were specific for the tumour-derived human VEGF (Figure 6.6).

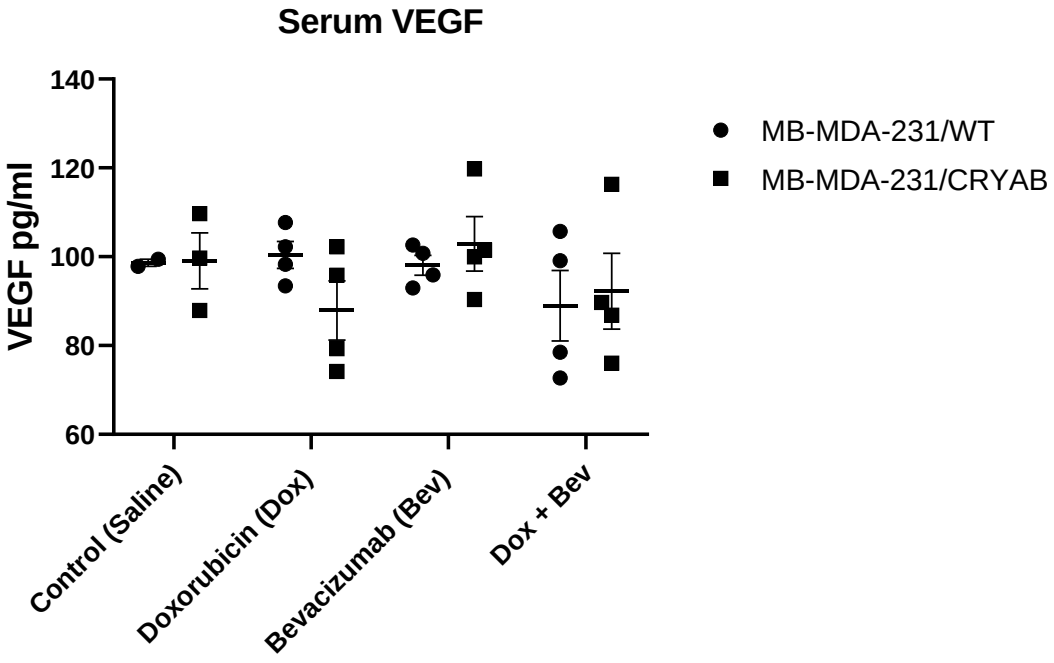

Figure 6.5 Murine VEGF in serum (pg/ml). Mice were injected into the 4th left and right mammary glands with 1 x 10^6 MDA-MB-231/WT and MDA-MB-231/*CRYAB* cells. Once primary tumours had established, mice were treated with either 4 mg/kg doxorubicin, 7.5 mg/kg bevacizumab, a combination of doxorubicin and bevacizumab or saline. At the end point (day 40), blood serum was collected and analysed by ELISA for mouse VEGF expression. The optical density was measured at 450 nm and 540 nm for background correction. The VEGF concentration of all samples was interpolated from the standard curve of known concentration samples. The data plotted are mean ±SEM; n =3-4 animals per group.

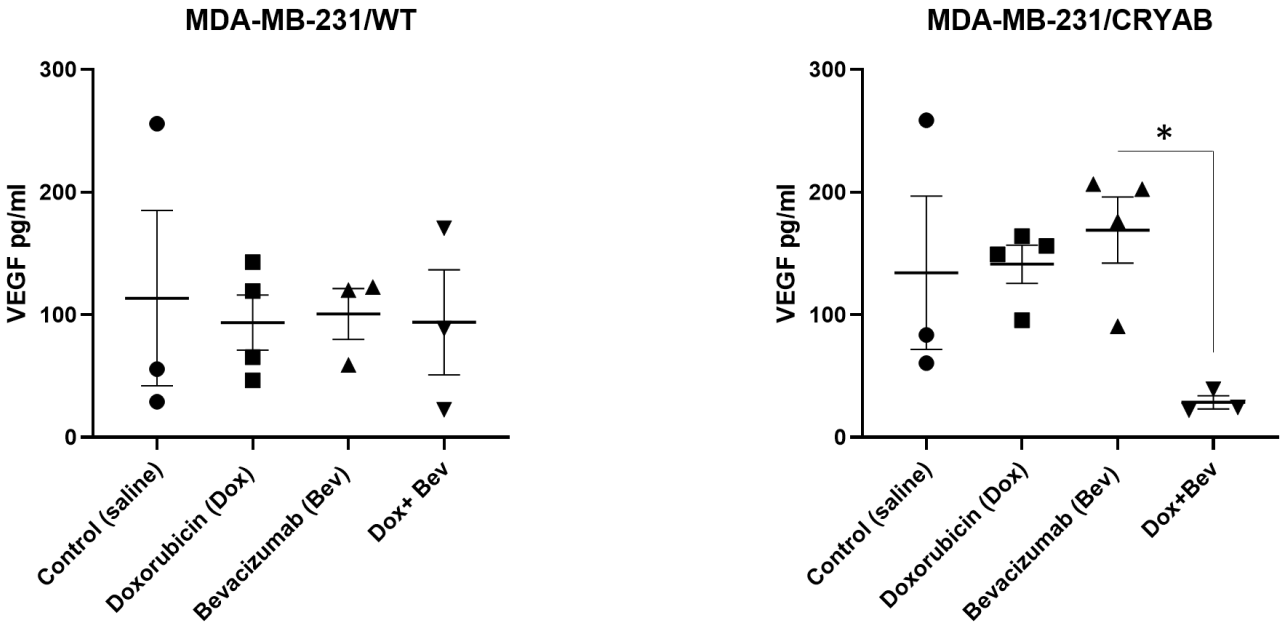

Figure 6.6 Mouse VEGF concentration (pg/ml) in MDA-MB-231/WT and MDA-MB-231/*CRYAB* tumours following treatment with doxorubicin, bevacizumab or combination of the two treatments. 12-week-old BALB/c nude mice were injected into the 4th left and right mammary glands with 1 x 10^{6} cells of MDA-MB-231/WT and MDA-MB-231/*CRYAB* cells. Once primary tumours had established, mice were treated with either 4 mg/kg doxorubicin, 7.5 mg/kg bevacizumab, combination of doxorubicin and bevacizumab or saline. At the end point (day 40), tumours were collected and analysed by ELISA for mouse VEGF expression. 0.5 µg /µL of total protein in total volume of 100 µl were analysed. The optical density was measured at 450 nm and 540 nm for background correction. The VEGF concentration of all samples was interpolated from the standard curve of known concentration samples. Data were analysed by ordinary one-way ANOVA with Tukey's multiple comparisons test (*p = 0.04, mean ± SEM; n =3-4 animals per group.

6.3.5 MDA-MB-231/WT and MDA-MB-231/*CRYAB* tumour microvascular density following treatment with doxorubicin, bevacizumab or combination of both.

To establish whether *CRYAB* has an influence on host vasculature, two endothelial cell markers, platelet-endothelial cell adhesion molecule (PECAM-1/CD31) and CD34 were scored by IHC. CD31 is an adhesion molecule expressed mainly by endothelial cells and other hematpoetic cells (Sapino *et al.* 2001). It is a well described marker of endothelial cells and is used to assess the vascularity of tumours in both mouse models and human (Horak *et al.* 1992, Qiao *et al.* 2022). CD34 is a marker of newly developed vessels and proliferating endothelial cells (Vizio *et al.* 2013). In addition, CD34 is expressed by hematopoietic and endothelial progenitor cells (Vizio *et al.* 2013).

The vascular area was assessed in tumours by quantifying the positive CD31 or CD34 stainined area as a percentage of positive pixels in viable tumour, avoiding the necrotic area and normal tissues, Figure 2.5 is an example of analysed area. This was done separately for each endothelial marker.

Staining with CD31 showed that MDA-MB-231/WT tumours were more vascularised than MDA-MB-231/CRYAB tumours (Figure 6.7, 6.8). The combination of bevacizumab and doxorubicin significantly decreased the vascular area compared with control and doxorubicin alone (p= 0.0288 and 0.0187, respectively). There was no significant difference between bevacizumab alone and the combination of doxorubicin and bevacizumab (Figure 6.7, 6.8). In MDA-MB-231/*CRYAB* tumours there was no significant difference in vascular area between all groups (Figure 6.7, 6.8). The data demonstrate that MDA-MB-231/WT vascularity was affected more than MDA-MB-231/*CRYAB* as evidenced by active angiogenesis through high concentrations of VEGF and more blood vessels in MDA-MB-231/WT tumours compared with MDA-MB-231/*CRYAB* tumours.

CD34 is widely considerded as a marker of endothelial progenitor cells, which mediate neovasculogenesis in the tumour microenvironment. The expression of CD34 is low in both MDA-MB-231/WT and MDA-MB-231/*CRYAB* tumours (Figure 6.9, 6.10). No significant difference was seen in the treated groups compared to the control group for both MDA-MB-231/WT and MDA-MB-231/*CRYAB* tumours.

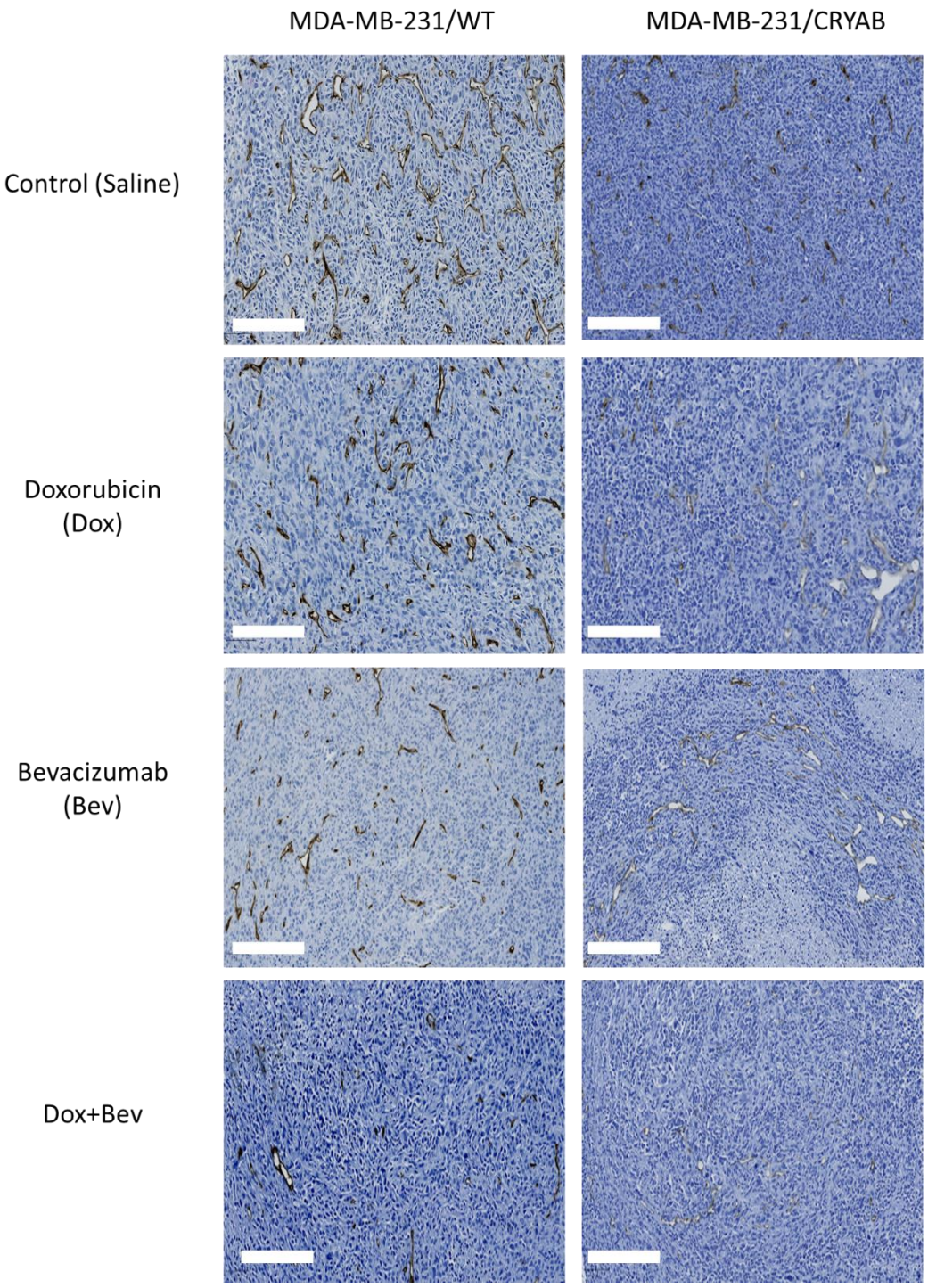

Figure 6.7 Tumour vascularity of MDA-MB-231/WT and MDA-MB-231/CRYAB tumours following treatment with doxorubicin, bevacizumab and combination of both: CD31 staining. Mice were injected into the 4th left and right mammary glands with 1 x 10^6 of MDA-MB-231/WT and MDA-MB-231/CRYAB cells. Once primary tumours had established, mice were treated with either 4 mg/kg doxorubicin ,7.5 mg/kg bevacizumab, combination of doxorubicin and bevacizumab or saline. FFPE tumours sections were stained for CD31 and counterstained with haematoxylin. Representative images of MDA-MB-231/WT and MDA-MB-231/CRYAB tumour vessels captured at 10x magnification from whole slide scanning (scale bar=100 µm).

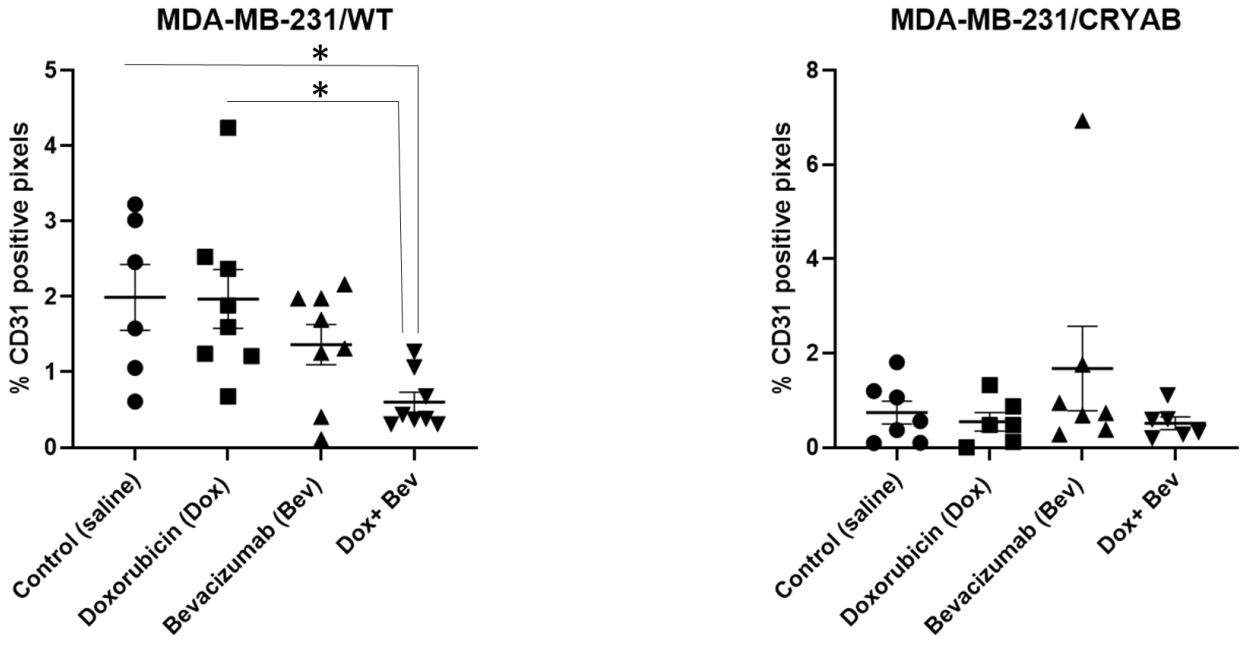

Figure 6.8 Tumour vascularity of MDA-MB-231/WT and MDA-MB-231/CRYAB tumours following treatment with doxorubicin, bevacizumab and combination of both: CD31 staining. Mice were injected into the 4th left and right mammary glands with 1 x 10^6 of MDA-MB-231/WT and MDA-MB-231/CRYAB cells. Once primary tumours had established, mice were treated with either 4 mg/kg doxorubicin ,7.5 mg/kg bevacizumab, combination of doxorubicin and Bevacizumab or saline. FFPE tumours sections were stained for CD31 and counterstained with haematoxylin. Vascular area was quantified by calculating the mean percentage of DAB positive staining (% CD31 positive pixels) from whole scanned viable tumour tissue using QuPath in MDA-MB-231/WT and MDA-MB-231/CRYAB. Data were analysed by Ordinary one-way ANOVA with Tukey's multiple comparisons test (*p= 0.0288 for Control (saline) vs. Dox+ Bev), *p=0.0187 for Doxorubicin (Dox) vs. Dox+ Bev), mean ± SEM; n = 6-8 animals per group.

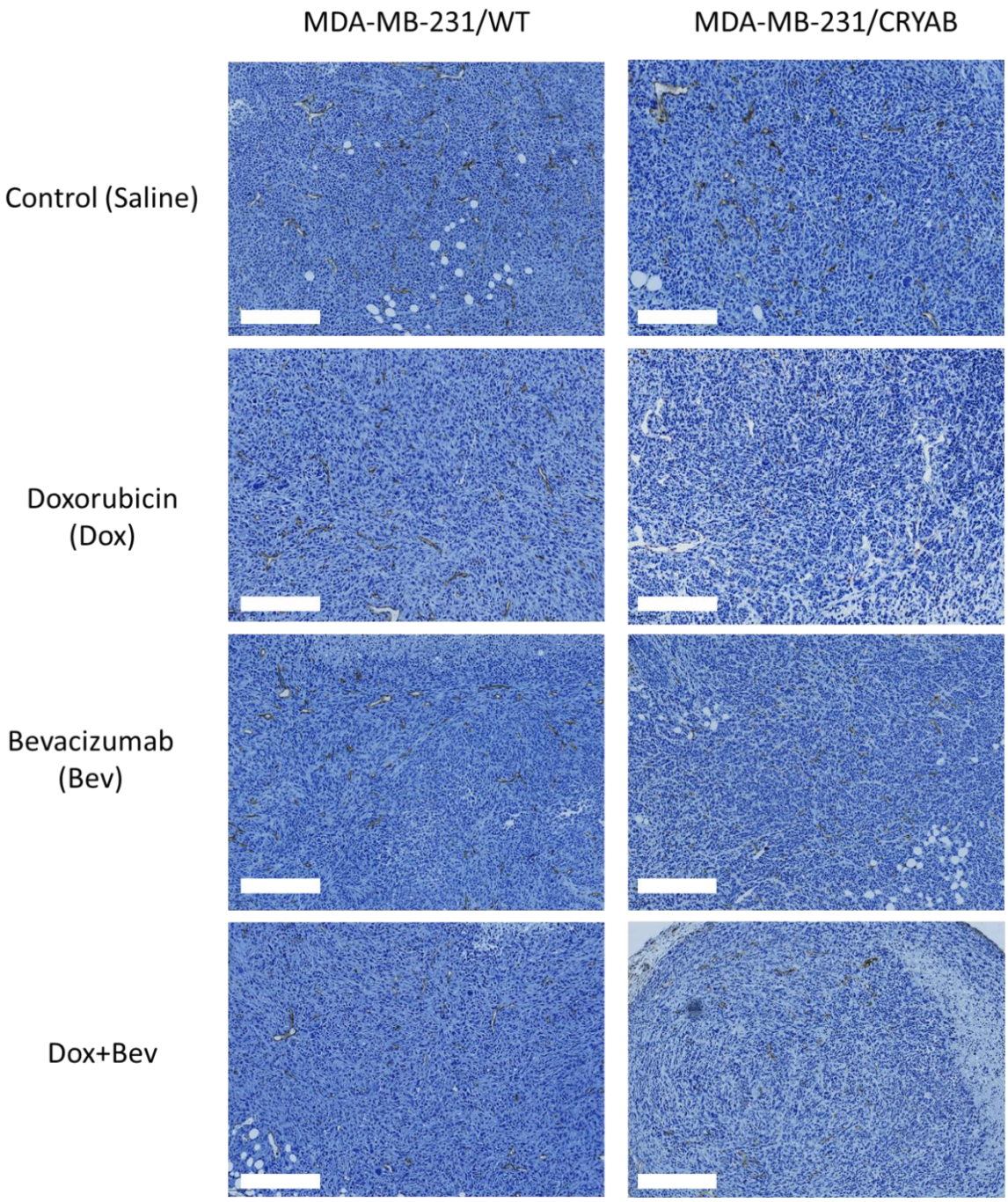

Figure 6.9 Tumour vascularity of MDA-MB-231/WT and MDA-MB-231/*CRYAB* tumours following treatment with doxorubicin, bevacizumab and combination of both: CD34 staining. Mice were injected into the 4th left and right mammary glands with 1 x 10^6 of MDA-MB-231/WT and MDA-MB-231/*CRYAB* cells. Once primary tumours had established, mice were treated with either 4 mg/kg doxorubicin, 7.5 mg/kg bevacizumab, combination of doxorubicin and bevacizumab or saline. FFPE tumours sections were stained for CD34 and counterstained with haematoxylin. Representative images of MDA-MB-231/WT and MDA-MB-231/*CRYAB* tumour vessels captured at 10x magnification from whole slide scanning (scale bar=100 µm).

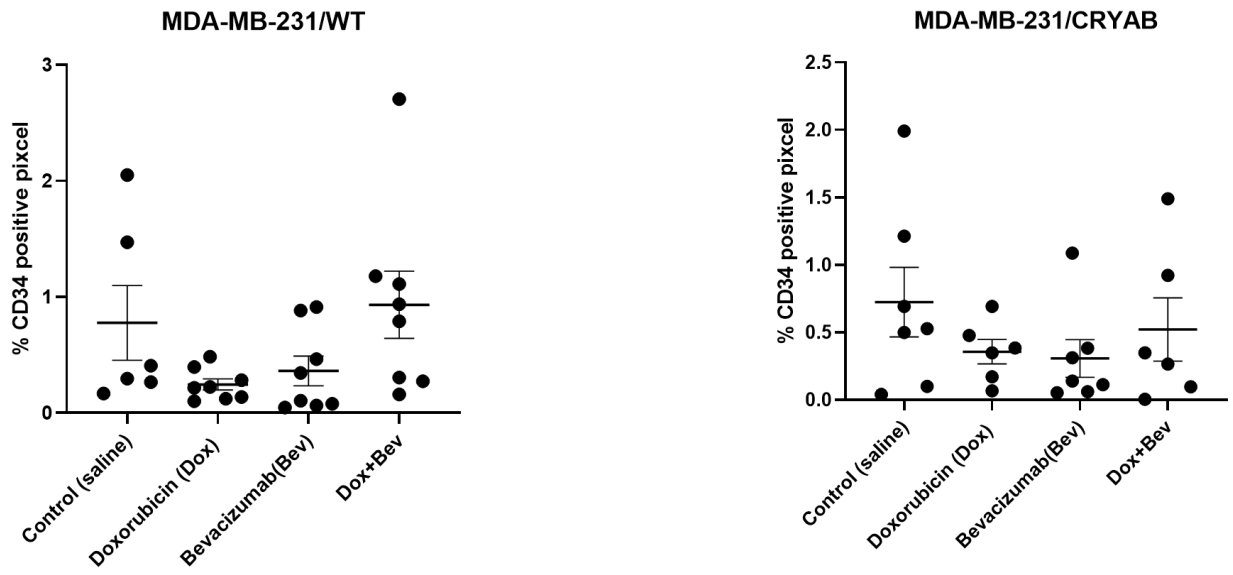

Figure 6.10 Tumour vascularity of MDA-MB-231/WT and MDA-MB-231/*CRYAB* tumours following treatment with doxorubicin, bevacizumab and combination of both: CD34 staining. Mice were injected into the 4th left and right mammary glands with 1 x 10^6 of MDA-MB-231/WT and MDA-MB-231/*CRYAB* cells. Once primary tumours had established, mice were treated with either 4 mg/kg doxorubicin, 7.5 mg/kg bevacizumab, combination of doxorubicin and bevacizumab or saline. FFPE tumours sections were stained for CD34 and counterstained with haematoxylin. Vascular area was quantified by calculating the mean percentage of DAB positive staining (% CD34 positive pixels) from whole scanned tumour tissue using QuPath in MDA-MB-231/WT and MDA-MB-231/*CRYAB*. Data were analysed by ordinary one-way ANOVA with Tukey's multiple comparisons test, mean ± SEM; n= 6-8 animals per group.

6.3.6 Expression of active caspase-3 following treatment with doxorubicin, bevacizumab or combination of both

The combination of doxorubicin and bevacizumab inhibited tumour volume in *CRYAB* expressing tumours was likely due to in part because of the decreased VEGF levels in this group. Apoptosis induction in this group was also assessed by staining the tumour tissues with an antibody to cleaved and therefore active caspase-3, which is the executioner of apoptosis. The number of caspase-3 positive cells were counted as a percentage of positive pixels on histological sections of scanned tumour tissues, avoiding areas of necrosis and normal tissues (Figure 2.6 is an example of the analysed area). The results showed that the percentage of cleaved caspase 3 positive cells was higher in MDA-MB-231/WT control saline treated tumours compared with MDA-MB-231/*CRYAB* treated with saline. In MDA-MB-231/WT tumours, a combination of doxorubicin and bevacizumab significantly increased cleaved caspase 3 expression compared with doxorubicin alone and the control group (p= 0.0104, 0.0241, respectively) (Figure 6.11, 6.12). In MDA-MB-231/*CRYAB* tumours, there was no significant difference between any of the groups (Figure 6.11, 6.12). The results indicate that combining doxorubicin and bevacizumab increased apoptosis in wild-type MDA-MB-231 tumours but not in *CRYAB* overexpressing tumours. Either apoptosis is not induced in *CRYAB* overexpressing tumours and/or the expression of caspase-3 is not detected in these tumours.

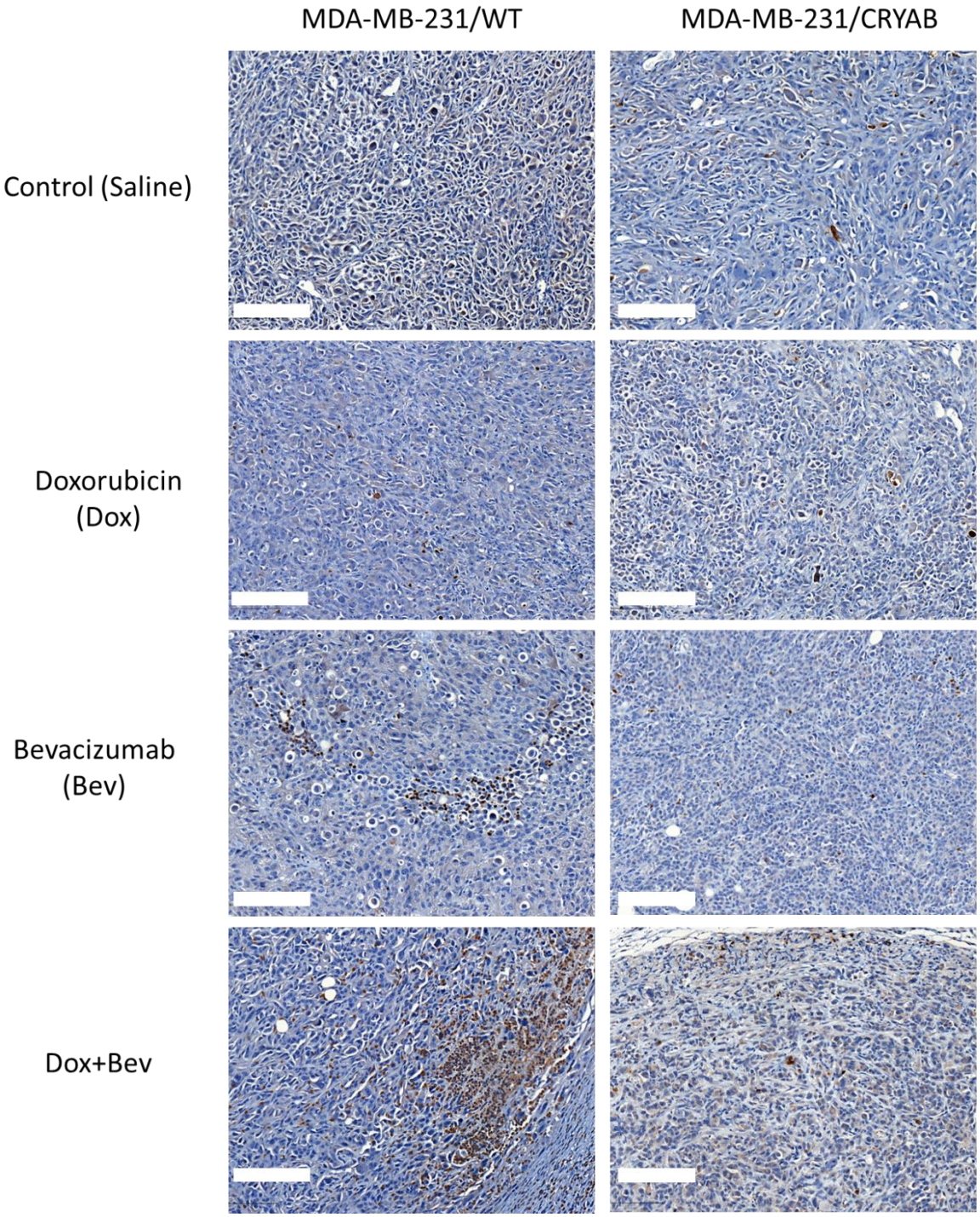

Figure 6.11 Cleaved caspase 3 staining in MDA-MB-231/WT and MDA-MB-231/*CRYAB* tumours following treatment with doxorubicin, bevacizumab and combination of both. Mice were injected into the 4th left and right mammary glands with 1 x 10^6 of MDA-MB-231/WT and MDA-MB-231/*CRYAB* cells. Once primary tumours had established, mice were treated with either 4 mg/kg doxorubicin, 7.5 mg/kg bevacizumab, combination of doxorubicin and bevacizumab or saline. FFPE tumours sections were stained for cleaved caspase 3 and counterstained with haematoxylin. The positive DAB cells were counted, and the percentage of positive cells was calculated from whole scanned tumour tissues in the viable areas in MDA-MB-231/WT and MDA-MB-231/*CRYAB*. Images were captured at 10x magnification from whole slide scanning (scale bar=100 µm).

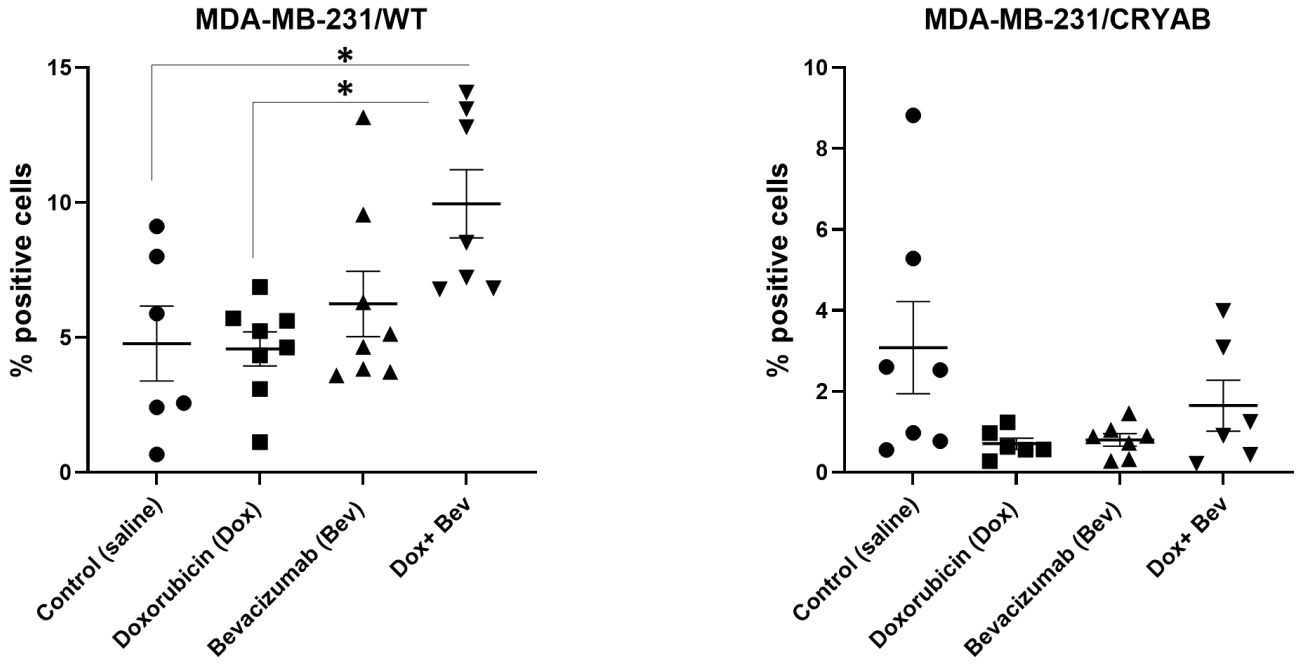

Figure 6.12 Cleaved caspase 3 staining in MDA-MB-231/WT and MDA-MB-231/*CRYAB* tumours following treatment with doxorubicin, bevacizumab and combination of both. Mice were injected into the 4th left and right mammary glands with 1 x 106 of MDA-MB-231/WT and MDA-MB-231/*CRYAB* cells. Once primary tumours had established, mice were treated with either 4 mg/kg doxorubicin, 7.5 mg/kg bevacizumab, combination of doxorubicin and bevacizumab or saline. FFPE tumours sections were stained for cleaved caspase 3 and counterstained with haematoxylin. The positive DAB cells were counted, and the percentage of positive cells was calculated from whole scanned tumour tissues in the viable areas in MDA-MB-231/WT and MDA-MB-231/*CRYAB*. Data were analysed by ordinary one-way ANOVA with Tukey's multiple comparisons test, mean ± SEM; n = 6-8 animals per group.

6.4 Discussion

The aim of this chapter was to investigate the influence of *CRYAB* on tumour growth in a mouse model and the efficacy of bevacizumab in *CRYAB* overexpressing tumours compared to non-*CRYAB* expressing ones. Tumour-secreated VEGF was measured to assess the influence of treatment. The effect on vasculature and apoptosis induction after treatment were tested to assess any difference in the tumour microenvironment between MDA-MB-231/WT and MDA-MB-231/*CRYAB* overexpressing tumours.

Bevacizumab was the first anti-angiogenic therapy when used in combination with a chemotherapeutic agent (paclitaxel) to treat metastatic breast cancer in patients, showed improvement in progression-free survival compared to chemotherapy alone (Miller *et al.* 2007). Bevacizumab monotherapy demonstrated modest therapeutic benefits, whereas multiple preclinical investigations revealed a synergistic relationship between anti-angiogenic treatment and chemotherapeutic agents (Miles *et al.* 2010, Goldfarb *et al.* 2011). Bevacizumab was therefore investigated in combination with a variety of chemotherapy drugs in multiple phase III clinical trials (Miles *et al.* 2010, Goldfarb *et al.* 2011). Doxorubicin is a widely used chemotherapeutic agent and herein, was used in combination with bevacizumab to establish any synergy. Herein, a pilot study was performed first to select the minimum concentration of bevacizumab that inhibits VEGF levels. Different concentrations were tested (5, 7.5 and 10 mg/k), based on published papers that showed an inhibitory effect of blocked VEGF by these concentrations, using tumour models and patients peripheral blood (Cao *et al.* 2011, Heskamp *et al.* 2013, Hodi *et al.* 2014). Although, the result in the current study showed that there was no significant difference in the levels of VEGF between these concentrations compared to the control, 7.5 and 10 mg/kg of bevacizumab showed a reduction in VEGF levels compared to 5 mg/kg (Figure 6.1). 7.5 mg/kg of bevacizumab was selected in the subsequent experiments. However, further investigations could be done to evaluate the effect of the selected concentrations on the downstream signalling activated by VEGF. The experiments into downstream signalling pathways may give significant information about the downstream implications of the chosen concentrations, unravelling the intricate network of signalling events that contribute to the observed decrease in VEGF levels. For example, western blot analysis of the VEGF-mediated signalling pathways.

Overexpression of *CRAYB* in MDA-MB-231 cells implanted into the fourth mammary fat pads, reduced tumour growth in the mouse model (P = 0.0499) compared with the wild type tumours (Figure 6.2 A). Under control conditions (saline treated mice). *CRYAB* overexpresing tumours displayed lower levels of apoptosis than wild type tumours (Figure 6.11) and hence apoptosis could not account for differences in growth. It has previously been reported that stable expression of *CRYAB* in MDA-MB-231 cells promoted xenograft tumour growth and this tumourgenic effect was partially due to resistence to tumor necrosis factor-related apoptosis-inducing apoptosis (Kamradt *et al.* 2005). These authors showed that the growth rate of αB-crystallin overexpressing cells *in vitro* was not different to that of the control cell, but nevertheless tumour growth *in vivo* was enhanced by αB-crystallin overexpression. Our *in vitro* data are in agreement with Kamradt *et al* but in our hands αB-crystallin overexpressing cells formed smaller tumours.

In this study, doxorubicin and the combination of doxorubicin and bevacizumab inhibited tumour growth of MDA-MB-231/WT cells significantly compared with saline. Furthermore, although bevacizumab alone had no affect on tumour growth, simultaneous administration of both doxorubicin and bevacizumab resulted in a significant tumour regression compared with bevacizumab alone (p= <0.0001). In addition, bevacizumab and doxorubicin together increased apoptosis in these tumours compared with either drug alone. The high reduction in tumour volume and increased apoptosis in tumours treated with the combination of both drugs was also associated with high reduction in VEGF levels. It should be noted that bevacizumab alone did not result in tumour regression in MDA-MB-231/*CRYAB* cells. This could be due to the fact that MDA-MB-231/CRYAB tumours were not actively producing VEGF compared to MDA-MB-231/WT tumours, making their growth less dependent on VEGF. However, the addition of doxorubicin sensitised tumours to bevacizumab treatment. It needs to be established why VEGF secretion is so substantially reduced in *CRYAB* overexpressing tumours. MDA-MB-231/*CRYAB* tumours produced less VEGF compared to MDA-MB-231/WT tumours. The *in vivo* findings confirmed what it had been previously shown *in vitro* (chapter 3, which showed that MDA-MB-231/*CRYAB* cells produced less VEGF compared to MDA-MB-231/WT cells. Bevacizumab alone and in combination with doxorubicin were effctive in reducing VEGF concentrations in MDA-MB-231/WT tumours compared with saline group (p= 0.0016 & 0.0011, respectively). Whilest, only the combination of both treatments decreased

VEGF levels in MDA-MB-231/*CRYAB* tumours compared with saline (p= 0.0330). It could be argued that bevacizumab has more effect on secreted VEGF and that the VEGF in the circulation was decreased after treatment with bevacizumab alone. Nevertheless, human VEGF was not detected in the serum of any of the mice analysed (not shown). This migh be that the concentration was vey low to be detected by ELISA.

It is thought that anti-VEGF treatments have cytostatic rather than cytotoxic effects, therefore, they are usually combined with cytotoxic agents such as chemotherapies to maximise their anti-tumour effects (Gasparini *et al.* 2005). Bevacizumab neutralises human VEGF and interferes with its ability to bind to VEGF receptors (VEGFR), primarly VEGR2 on endothelial cells (Kazazi-Hyseni *et al.* 2010) . Consequently, inhibiting VEGF prevents the downstraem signalling such as proliferation and survival of endothelial cells. Two mechanisms of action have been identified for bevacizumab; starvation of the tumour and limiting the blood supply to tumours and/or normalisation of the vasculture. Hence, these effects lead to partial normalisation of the vasculature and a decreased interstitial fluid pressure, resulting in better oxygenation to the tumour and hence an improved distribution of chemotheraputic treatments (Kazazi-Hyseni *et al.* 2010). It is unlikely that the normalisation of blood vessels was the mechanism of the synergistic effect observed in the MDA-MB-231/*CRYAB* tumours because the tumours produced low levels of VEGF and showed low expression of endothelial cell markers CD31 and CD34, although this warrants further investigation. In addition, mouse VEGF decreased significantly after the combination of treatments, demonstrating a direct effect on development of mouse vasculture in these tumours.

Efficacy of antiangiogenic therapies in pre-clinical and clinical studies are commonly monitored by observing changes in variables such microvessel density (MVD), vessel diameter and tortuosity, vascular partial pressure of oxygen, and interstitial pressure (Shih and Lindley 2006, Batchelor *et al.* 2007, Wang *et al.* 2008, Barral *et al.* 2016, Rojas *et al.* 2018). These parameteters can be assessed by different techniques including imaging tools such as CT, MRI and/or measuring the microvascular density by immunohistochemistry staining for endothelial cell markers such as CD31, CD34 (Batchelor *et al.* 2007, Cyran *et al.* 2013). For instance, a pre clinical study investigated the response to regorafenib a multi-kinase inhibitor with antiangiogenic effect by measuring endothelial cells permeability using dynamic contrast-enhanced computed tomography. The authors observed a significant decrease in

endothelila cell permeability, suggesting that the dynamic contrast-enhanced computed tomography can be used to monitor the response to treatment (Cyran *et al.* 2013). In addition, Measuring the micrvascular density by immunohistochemistry staining of endothelial cell markers such as CD31 is also used to assess the benefit from bevacizumab in ovarian cancer (Bais *et al.* 2017). The results showed that there is association between the microvascular density measured by CD31 and the effect of bavacizumab (Bais *et al.* 2017). Furthermore, MVD by CD31 were significant predictive factors for overall survival in colorectal cancer patients (Mohamed *et al.* 2019). To assess microvessel denisty to determine effects of bevacizumab with and without doxorubicin in the experiments, immunohistochemical staining for CD31 and CD34 were used. Assessing the microvascular density by quantifying the expression of the endothelial cell markers is considerded challenging as some of these markers are expressed by other hematopoitic cells. The optimal marker for micovascular density has not been identified due to the lack of specificity of these markers. The most widely used endothelial cell markers are CD31,CD34, von Willebrand factor and CD105 (Müller *et al.* 2002, Moreira *et al.* 2011). CD34 has a significant role in the development of newly devloped blood vessels as its expression increased during the wound healing and tumour growth (Ito *et al.* 1995). In addition, a general increase in the expression of CD34 is seen in newly generated blood vessels in the stroma of malignancies and the expression was correlated with tumour cell differentiation, suggesting that CD34 is an indicator not only for neovascularization but also for tumour progression (Tanigawa *et al.* 1997). CD34 has been utilised to assess tumour neovascularization and microvessel density in a spectrum of carcinomas (Tanigawa *et al.* 1997, Moreira *et al.* 2011). CD31 is an adhesion molecule involved in interactions between leucocytes and endothelial cells, as well as being diffusely expressed in natural killer cells (Moreira *et al.* 2011). In the current study, both CD31 and CD34 were used in addition to measurement of VEGF levels, parameters that may help to report the angiogenic status of tumours and the response to anti-VEGF treatment. CD34 expression was less than CD31 expression in both MDA-MB-231/WT and MDA-MB-231/*CRYAB* tumours. In addition, MDA-MB-231/WT tumours were more vascularised than MDA-MB-231/*CRYAB* tumours which may explain why MDA-MB-231/WT tumours were larger. The simultaneous administration of both bevacizumab and doxorubicin suppressed tumour vascularisation significantly compared to saline in MDA-MB-231/WT tumours. This is was associated with low levels of VEGF seen in this group. There was no significant difference seen in either CD31 or CD34 in MDA-MB-

231/*CRYAB* tumours between any groups compared to control, suggesting that reduced vascularization may not be the mechanism by which combined bevacizumab and doxorubicin exert their anti-tumour effects in *CRYAB* overexpressing tumours.

The addition of both doxorubicin and bevaciazumab resulted in an anti-tumour effect in MDA-MB-231/*CRYAB* tumours. This was associated with decreased VEGF levels in this group. Nevertheless, other mechanism such as increased apoptosis or decrease in the proliferation may be involved. Therefore, it was examined whether the combination of doxorubicin and bevacizumab induced more tumour apoptosis in MDA-MB-231/*CRYAB* tumours compared to MDA-MB-231/WT tumors. The results showed that the rate of apoptosis was very low in MDA-MB-231/*CRYAB* tumours compared to MDA-MB-231/WT tumours. It is difficult to explain this result, but it may be related to apoptosis not being activated or due to the smaller size of tumours it was difficult to score the cleaved caspase 3. Whether proliferation is different between MDA-MB-231/WT and MDA-MB-231/*CRYAB* tumours is still an unanswered question. Investigating the proliferation rate of cancer cells in tumour sections by staining for proliferation markers Ki67 will help to determine the effect of treatments and to assess any differences between MDA-MB-231/WT and MDA-MB-231/*CRYAB* tumours. In addition, the expression of αB-crystallin in tumour tissues needs to be established to ensure that the differences between MDA-MB-231/WT and MDA-MB-231/*CRYAB* are associated with levels of αB-crystallin.

This study is the first to show that *CRYAB* overexpression in tumours overcomes the inhibitory effect of bevacizumab by inactivating the VEGF pathway, supporting tumour growth. Importantly, this tumour protective effect can be reversed by adding doxorubicin to bevacizumab, however the mechanism for this remains to be determined.

Chapter7 **General Discussion**

7.1 αB-crystallin as a potential biomarker for resistance to antiangiogenic treatments

Angiogenesis plays a critical role in tumour growth and metastasis (Folkman 1971), a hypothesis that led to development of numerous antiangiogenic treatments. These treatments have been used widely in treating various malignancies. Despite the promising outcome of these treatments, the benefit in breast cancer is modest. Many patients do not respond to antiangiogenic treatments and some of them show an initial response that is eventually followed by resistance. For this reason and due to the toxicity, which is often associated with antiangiogenic agents, these treatments are discontinued in some settings. Therefore, understanding the causes of resistance may help in two ways. First, by identifying biomarkers that cause resistance so they can be targeted, and hence improve the outcome of these treatments. Second, by selecting the patients who are more likely to benefit from these treatments. Today, even after wide exploring of many potential biomarkers, there are no reliable and validated biomarkers that would enable to select more responsive patients. This is one of the challenges in using antiangiogenic treatments. There is urgent need to identify more biomarkers to improve these treatments. αB-crystallin, a heat shock protein that was associated with aggressive types of breast cancer, including basal like and triple negative breast cancer was studied in this thesis.

αB-crystallin acts as a chaperone molecule, an anti-apoptotic protein and prevents the aggregation of misfolded proteins under several stress conditions (Horwitz 1992). Importantly, it is suggested to be a main regulator of endothelial cell survival during tumour angiogenesis (Dimberg *et al.* 2008). Endothelial cells developed in mice lacking αB-crystallin were disrupted and showed signs of apoptosis, suggesting that the protein acts as a regulatory factor in endothelial cells (Dimberg *et al.* 2008, Kase *et al.* 2010). αB-crystallin was found to protect VEGF from proteolytic degradation and transfer it to the endoplasmic reticulum for refolding and secretion (Kase *et al.* 2010). In *in vivo* models, tumours grown in *CRYAB*-deficient mice were less vascularized and showed signs of apoptosis in contrast to tumours from wild-type mice (Dimberg *et al.* 2008). Moreover, αB-crystallin was shown to co-localise with endothelial cells in breast cancer xenograft tissues, and particularly after treatment with anti-VEGF agents

(Ruan *et al.* 2011). These data points to αB-crystallin as a main regulator of VEGF and tumour angiogenesis. VEGF is the most potent angiogenic factor that stimulates migration and survival of endothelial cells (Shibuya 2011). Several malignancies overexpress VEGF and that associates with poor prognosis (Apte *et al.* 2019). It is thought that αB-crystallin stimulates tumour angiogenesis by enhancing the stability of VEGF and increasing the survival of endothelial cells. Therefore, the protective function of αB-crystallin to tumour angiogenesis may contribute to resistance to antiangiogenic treatments. The aim of this thesis is to test whether αB-crystallin contributes to resistance to antiangiogenic treatments in breast cancer. To elucidate the functional role of αB-crystallin in breast cancer cells, a comprehensive approach was employed, encompassing two distinct methodologies: overexpression and transient knockdown via siRNA interference. αB-crystallin was systematically overexpressed by integrating cDNA containing the *CRYAB* gene into MDA-MB-231 cell lines. Generating stably transfected cell lines ensures sustained expression of the protein over extended periods. Given the extended time required for the *in vivo* experiments, involving the cultivation of primary tumours and the evaluation of the treatment's efficacy, the generated stable cell lines were used. The *CRYAB* overexpressing cells were also used to study the effect of overexpression on growth dynamics, apoptosis induction following doxorubicin treatment, and VEGF production. Conversely, a complementary approach involving transient knockdown using siRNA was employed to reduce the αB-crystallin protein levels in MDA-MB-468 cells. This model was used to study the influence of knockdown on VEGF production only *in vitro* since the knockdown is transient. It is important to acknowledge the potential of CRISPR/Cas9-mediated gene deletion as an alternative method. This method offers the potential of generate stable cell lines, enabling the study of the influence of protein deletion *in vivo*.

7.2 The effect of αB-crystallin overexpression on the proliferation and apoptosis *in vitro*

αB-crystallin was found overexpressed by numerous malignancies, including basal like breast cancer and triple negative breast cancer (Moyano *et al.* 2006, Sitterding *et al.* 2008, Kim *et al.* 2011). Triple negative breast cancer is one of the most aggressive types of breast cancer and is considered as a negative prognostic factor (Yin *et al.* 2020). Chelouche-Lev *et al.* (2004) demonstrated that αB-crystallin was associated with lymph node involvement in metastatic breast cancer in immune deficient mice. In addition, αB-crystallin was linked with brain

metastasis and suggested to be a biomarker for selecting breast cancer patients with high risk of brain metastasis (Malin *et al.* 2014, Voduc *et al.* 2015). The association of αB-crystallin with triple-negative breast cancer, brain and lymph node metastasis indicates that αB-crystallin may be considered as a poor prognostic factor in breast cancer patients. Herein, we confirmed that αB-crystallin is expressed in MDA-MB-468 but not in MDA-MB-231 cells. Both are metastatic triple negative breast cancer cells. In accordance with our finding, αB-crystallin expression was detected in metastatic breast cancer cell lines, including MDA-MB-468, and GILM2 but was not detected in MDA-MB-231 cells (Chelouche-Lev *et al.* 2004). Kamradt *et al* also showed that MDA-MB-231 cells do not express αB-crystallin (Kamradt et al. 2005). These studies indicate that αB-crystallin may not always be expressed in metastatic breast cancer cells.

αB-crystallin acts as a cytoprotective and anti-apoptotic protein and was suggested to be an oncogene (Moyano *et al.* 2006, Bakthisaran *et al.* 2015). This anti-apoptotic function is thought to increase the proliferation rate of αB-crystallin overexpressing cells. Contrary to expectations, the growth of αB-crystallin overexpressing MA-MB-231 cells did not demonstrate a significant difference compared to their wild type counterpart cells. Kamradt *et al.* (2005) also found that overexpression of a wild type αB-crystallin construct into MDA-MB-231 cells, the same cell line used in our study, had no effect on the proliferation of the cells *in vitro* and therefore the results of this study are in agreement with their study. Interestingly, these authors found that overexpression of a mutant construct that mimics phosphorylated αB-crystallin at ser19, ser45 and ser59 in MDA-MDA-231 cells inhibited their proliferation. This study suggests that phosphorylation status of αB -crystallin is important for regulating proliferation. The findings of this study are also consistent with a previously published report showing that overexpression wild type αB-crystallin in bladder cancer cells had no significant effect on their proliferation compared to control cells (Ruan *et al.* 2020). In contrast, αB-crystallin overexpression promoted the proliferation and invasion of colorectal cancer cells (Li *et al.* 2017). Similarly, other groups showed that overexpression of αB-crystallin in human mammary epithelial cells induced malignant-like properties such as luminal filling and increased proliferation. Similar to the MDA-MB-231 cells, overexpression of the phosphorylated αB-crystallin mutant (at ser19, ser45 and ser59) in mammary epithelial failed to induce development of malignant-like properties (Moyano *et al.* 2006).

One of the most known functions of αB-crystallin is its anti-apoptotic function. The data of this study showed that treating αB-crystallin overexpressing cells with doxorubicin, induced apoptosis more than in wild type cells. It has been reported that the chaperone function of αB-crystallin is dependent on its phosphorylation (Bakthisaran *et al.* 2016). We do not have any information on the phosphorylation status of the αB-crystallin that we overexpressed and whether it might have influenced its function as an anti-apoptotic protein. Due to the conflicting findings about the role of αB-crystallin phosphorylation and the possibility that its functions may be highly context-dependent, it is unclear whether phosphorylation and at which specific residues is essential for its chaperone function. αB-crystallin phosphorylation at ser-59 was found to be essential to act as a cytoprotective protein in cardiac myocytes and endothelial cells (Morrison *et al.* 2003, Dimberg *et al.* 2008). Specifically in breast epithelial carcinoma MCF7 cells, it was reported that αB-crystallin overexpression lowered apoptosis levels in response to inhibitors of microtubule polymerization (vinblastine), used as anti-cancer agents (Launay *et al.* 2010). However, expression of ser-59 constitutive phosphorylated αB-crystallin mutant induced apoptosis in vinblastine treated cells, suggesting that phosphorylation of αB-crystallin at this specific site can drive apoptosis (Launay *et al.* 2010). Our data showed that of αB-crystallin overexpression did not influence proliferation while overexpression had a negative influence on apoptosis. It seems that testing for phosphorylated αB-crystallin in the cells used in this study will be essential in order to understand the negative effects that were observed on apoptosis induction by overexpressing αB-crystallin. Although it is not clear which kinases mediate phosphorylation of various residues in αB-crystallin in cells, it is thought that members of the MAPK pathway which are highly activated in cancer are involved (Muranova *et al.* 2018). Understanding pathways that lead to phosphorylation of αB-crystallin and establishing the effects of each phosphorylation site on the chaperone activity of the protein will be important to determine its function in breast cancer.

7.3 The influence of αB-crystallin overexpression and knockdown on VEGF production

As stated above, the protective function of αB-crystallin has been linked with VEGF in several studies. Kase *et al.* (2010) reported that αB-crystallin protects VEGF from proteosomal degradation under hypoxic stress and redirects VEGF to endoplasmic reticulum to be refolded and secreted. Growing number of evidence showed that αB-crystallin stimulates the survival

of endothelial cells and that was correlated with protection of VEGF. This specifically has been shown in the retinal pigment cells that derived from αB-crystallin deficient mice after hypoxia (Kase *et al.* 2010). The cells secreted low levels of VEGF compared to cells from wild-type mice. In addition, αB-crystallin has been shown to interact with important regulatory proteins, in addition to VEGF such as FGF, insulin and β-catenin and protected them from aggregation and unfolding (Ghosh *et al.* 2007). One of the main objectives of this thesis was to assess whether αB-crystallin protects VEGF and increases its secretion under stress conditions (heat shock, hypoxia) in breast cancer cells. First, the results in chapter 3 confirmed that αB-crystallin was induced in response to heat shock in both αB-crystallin overexpressing MDA-MB-231 cells and wild type MDA-MB-468 cells. Although αB-crystallin was not induced in response to hypoxia, the expression of VEGF in the cells was tested since hypoxia is the main regulator of VEGF pathway with more VEGF being produced during hypoxia (Harris 2002, Ruan *et al.* 2009). Therefore, production of VEGF in αB-crystallin overexpressing MDA-MB-231 cells and siRNA mediated knockdown in MDA-MB-468 cells was tested by ELISA. As expected, hypoxia induced VEGF production in all cells. However, MDA-MB-231/WT cells significantly induced more VEGF in conditioned media than MDA-MB-231/*CRYAB* cells. In heat shock, although αB-crystallin overexpressing cells produced less VEGF than wild-type cells, VEGF produced in heat shock was more than VEGF from cells in normal conditions (37 C°) only in αB-crystallin overexpressing cells not in wild-type cells. Moreover, αB-crystallin knockdown cells showed the same trend. The knockdown cells produced higher levels of VEGF than the wild type cells in all conditions. It was indeed envisaged that αB-crystallin would protect VEGF from degradation and increase its production. The findings were unexpected and contrary to previous studies that showed that αB-crystallin increased VEGF in normal conditions and in hypoxia (van de Schootbrugge *et al.* 2013). In the literature, lack of αB-crystallin in retinal pigment cells reduced VEGF secretion compared to wild-type cells (Kase *et al.* 2010). In chapter 6, we found the same trend in our *in vivo* model; tumours derived from αB-crystallin overexpressing cells produced less VEGF than wild-type tumours. Collectively *in vitro* and *in vivo* data suggest that VEGF expression and/ or stability is negatively regulated by αB-crystallin in the system used in this study. Further experiments are warranted to investigate the stability of VEGF protein itself and/or test levels of mRNA to determine whether gene expression was affected or protein stability or both. miRNAs are responsible for regulating gene expression and their distribution and expression in cancer is deregulated (Peng and

Croce 2016). miRNA is non-coding RNA that regulates the gene expression of various genes by inhibiting their translation or regulating the cleavage of mRNA (Cai *et al.* 2009). It may be useful to consider the expression of various miRNAs, for example, those responsible for regulating VEGF (Soheilifar *et al.* 2022) in the cell system of this study to see whether overexpression of αB-crystallin plays a role in regulating miRNAs that are directed against the VEGF gene.

7.4 αB-crystallin may act as a tumour suppressor

The less tumourgenic features of the αB-crystallin overexpressing cells may be due to αB-crystallin acting as a tumour suppressor. There is some literature that demonstrated that αB-crystallin acts as tumour suppressor through different signalling mechanisms. For instance, αB-crystallin was found to be one of the p53-targeted gene and is essential for p53-induced apoptosis (Watanabe et al. 2009). In nasopharyngeal carcinoma, overexpression of *CRYAB* inhibited E-cadhenin translocation and internalisation from the membrane and reduced cell invasiveness (Huang *et al.* 2012). αB-crystallin prevented disruption of cadherin/catenin adherens junctions, which is a key EMT initiation step. The authors found that αB-crystallin localised to junctions prevented cancer cell invasion and migration and the protein was acting as an anti-oncogene. In addition, through regulation of EMT proteins, αB-crystallin was found to inhibit metastasis of nasopharyngeal carcinoma (Huang *et al.* 2012). Beta-catenin also remained membrane associated, and reduced b-catenin signalling led to a reduction in spheroid formation and proliferation *in vitro*. It will be interesting to see if how E-cadherin and b-catenin are affected by αB-crystallin overexpression in the breast cancer cells of this study and whether this is associated with the reduced tumour growth that was observed *in vivo*.

Similarly, it is suggested that αB-crystallin inhibited the migration and invasion of bladder cancer cells (Ruan *et al.* 2020). Overexpression of αB-crystallin in bladder cancer cells reduced phosphorylated ERK and AKT (Ruan *et al.* 2020). Activation of MAPK/ERK and PI3K/AKT signalling pathways through RAS activate transcription factors involved in tumour proliferation and invasion and hence inhibition of this pathway can lead to a reduction in proliferation (Pearlman *et al.* 2017). These data suggest that αB-crystallin could act as tumour suppressor protein via this mechanism. However, this is not a general mechanism as αB-crystallin increased the EMT and proliferation of colorectal cancer cells through activation of

the MAPK/ERK pathway (Li *et al.* 2017). Similarly, αB-crystallin overexpression in human breast epithelial cells initiated the invasive phenotype through the MAPK/ERK pathway. Contrary to the aforementioned study about the inhibitory function of αB-crystallin in nasopharyngeal cancer, Mao *et al*. reported that αB-crystallin is associated with aggressive phenotype of laryngeal squamous cell carcinoma (Mao *et al.* 2012). These data collectively indicate a dual role of αB-crystallin as an oncogene or tumour suppressor. This, in some cases, can be due to the different cancer types. The *in vitro* and *in vivo* data indicate that αB-crystallin may act as tumour suppressor protein. As VEGF acts as mitogenic factor for both endothelial cells and cancer cells (Mercurio *et al.* 2005). However, more research is needed in order to reveal the relationship between αB-crystallin and oncogenic-related pathways such as the MAPK pathway.

7.5 The efficacy of bevacizumab, doxorubicin and the combination of both treatments on αB-crystallin-overexpressing tumours

Bevacizumab decreased VEGF levels in MDA-MB-231/WT tumours significantly. However, it did not decrease VEGF levels in MDA-MB-231/*CRYAB* tumours. It may be that because the significantly smaller MDA-MB-231/*CRYAB* tumours did not actively produce VEGF compared to MDA-MB-231/WT tumours, their growth was less dependent on VEGF. Nevertheless, the combination of bevacizumab and doxorubicin significantly decreased VEGF levels in MDA-MB-231/*CRYAB* tumours. Bevacizumab is the first antiangiogenic therapy that used in combination with a chemotherapeutic agents (paclitaxel) to treat metastatic breast cancer and showed improvement in PFS compared to chemotherapy alone (Miller *et al.* 2007). Our results suggest that the combination of bevacizumab and doxorubicin is a good strategy to make the tumours more sensitive to bevacizumab.

Moreover, to determine the efficacy of bevacizumab and to assess whether *CRYAB* alters its efficacy, endothelial cell markers were analysed by IHC. As discussed in chapter 6, selecting reliable markers of endothelial cells is challenging due to the lack of specificity as most of these markers are expressed by endothelial cells and other hematopoietic cells. Here, we used two of the widely used endothelial markers CD31 and CD34 for estimation of tumour vasculature along with measuring VEGF. CD31 staining showed that MDA-MB-231/WT tumours are more vascularised than MDA-MB-231/*CRYAB* tumours (Figure 6.7). That may explain the bigger size of MDA-MB-231/WT tumours and smaller size of MDA-MB-231/*CRYAB*

tumours and correlates with the levels of VEGF produced by the cells. The simultaneous administration of both bevacizumab and doxorubicin supressed tumour vascularization significantly compared to saline in MDA-MB-231/WT tumours. This was associated with significant low levels of VEGF seen in this group. There was no significant difference in CD31 expression in MDA-MB-231/*CRYAB* tumours in all treatment groups compared to control.

Quantification of CD34 by IHC showed no significant difference between treated and untreated groups in both MDA-MB-231/WT and MDA-MB-231/*CRYAB* tumours. Taken together, the vascular marker expression was very low in MDA-MB-231/*CRYAB* tumours. This could be as a result of low VEGF levels produced by these tumours.

Treatment with combination doxorubicin and bevacizumab resulted in a significant inhibition in tumour growth in MDA-MB-231/*CRYAB* tumours. The data of IHC vascular markers indicate that the inhibition was not due to inhibition in the vasculature. In seeking a mechanism by which the coadministration of doxorubicin and bevacizumab caused growth inhibition in MDA-MB-231/*CRYAB* tumours, IHC for cleaved caspase 3 was performed. The results showed that the expression of cleaved caspase 3 was very low in the group that was treated with a combination of doxorubicin and bevacizumab, showing very little apoptosis levels in this group. This finding also suggests that due to the smaller size of these tumours, apoptosis was low and cleaved caspase 3 was not detected. Alternatively, proliferation rate by IHC staining for proliferation markers such as ki67 needs to be determined to assess if the inhibition effect seen after treatment with doxorubicin and bevacizumab was due to a decrease in proliferation.

7.6 Influence of breast cancer cells that express different levels of αB-crystallin on endothelial cell responses

Conditioned media from breast cancer cells expressing different levels of αB-crystallin did not upregulate the protein in endothelial cells. It was hypothesized that breast cancer cells would induce αB-crystallin in endothelial cells and promote their cell survival. This was hypothesised based on several studies showing that αB-crystallin promoted tumour vascularisation and that was associated with endothelial cell survival and proangiogenic properties (Dimberg *et al.* 2008, Kase *et al.* 2010, Ruan *et al.* 2011). For instance, in co-culture model, breast cancer cells induced the expression of αB-crystallin in endothelial cells. The increase of αB-crystallin in endothelial cells was correlated with the malignancy of breast cancer cells used in the co-

culture model (Ruan *et al.* 2011). This was in contrast to our data, as conditioned media from MDA-MB-231 and MDA-MB-468 cells that are both highly tumorigenic cells failed to induce the expression of αB-crystallin in endothelial cells. It may be that the growth factors in our conditioned media were too dilute to influence endothelial cell expression of αB-crystallin. In addition, the conditioned media were harvested from breast cancer cells after a 48 h starvation period before they were collected and incubated with endothelial cells. It might be that some of growth factors were degraded during this process. More experiments are needed to establish the effect of conditioned media isolated from breast cancer at different time points. In addition, differences between the model of the present study and those presented in previous published data may explain the difference of outcome. The conditioned media was used in this study, whereas previous authors used co-culture models. The co-culture model may ensure the transfer of growth factors through transwell inserts to endothelial cells directly. Herein, endothelial cells were incubated directly with conditioned media from breast cancer. The model of co-culture may facilitate the delivery of growth factors between cells more efficiently than conditioned media.

The migration of endothelial cells might be influenced by the production and secretion of various factors from breast cancer cells with different levels of αB-crystallin. These factors might include VEGF but also other growth factors that can support endothelial cells migration. It was hypothesised that since αB-crystallin overexpression led to changes in VEGF production and potentially production of other factors that might influence migration, conditioned media from the breast cancer cells would influence endothelial migration. No significant difference was found between any of the cells that were incubated with conditioned media from breast cancer cells expressing different levels of αB-crystallin. The conditioned media from MDA-MB-231/WT was confirmed to have more VEGF than that from MDA-MB-231/*CRYAB* cells (chapter 3). It is well established that VEGF acts to stimulate migration of endothelial cells (Soga *et al.* 2001). However, the higher amount of VEGF produced from MDA-MB-231/WT did not enhance endothelial cell migration compared to MDA-MB-231/*CRYAB* in our experiments. In contrast to a previously published study, conditioned media from SKBR3 HER2-positive breast cancer cells induced tubular formation of endothelial cells compared to control cells. The induction of angiogenesis was substantially dependent on αB-crystallin (Yang *et al.* 2022). Another study by Dimberg *et al.* (2008) who also performed the tubular formation assay and

found that αB-crystallin was significantly induced in endothelial cells during the formation of blood vessels. The tubular formation is an assay that is used to assess *in vitro* angiogenesis and could be an additional method for testing the effects of CM from breast cancer cells in the model system of the present study. Collectively, it appears that the effect of αB-crystallin on endothelial cell response is dependent on cell-type and/or specific assay conditions. In addition, it could be that the levels of factors in conditioned media were not sufficiently high to influence migration.

7.7 The interaction between αB-crystallin and VEGF

High levels of VEGF indicate poor prognosis in various malignancies (Poon *et al.* 2001). VEGF is a mitogenic factor that increases proliferation, survival and migration of endothelial cells (Apte *et al.* 2019). Both clinical and animal studies demonstrated that VEGF is a mitogenic factor also for malignant cells. For instance, in breast cancer cells, both VEGF and VEGFR were found to be expressed, suggesting that breast cancer cell progression depends on both autocrine and paracrine signalling (De Jong *et al.* 1998, Mercurio *et al.* 2005). On the level of gene expression, both VEGFR1 and VEGFR2 were found expressed in breast cancer cell lines including MDA-MB-231, T-47D, and MCF7 (Price *et al.* 2001). It should be noted that the expression of VEGF and VEGFR was associated with survival and invasion of breast cancer cells (De Jong *et al.* 1998, Price *et al.* 2001). The low levels of VEGF produced from αB-crystallin overexpressing cells *in vitro* were compatible with *in vivo* results. Indeed, low levels of VEGF correlated with low tumour VEGF and low tumour volumes seen in the tumours derived from these cells. Tumour growth is dependent on the ability of tumour cells to induce angiogenesis. Therefore, a probable explanation for slow tumour growth is lack of VEGF-dependent angiogenesis. It is also possible that growth of MDA-MB-231/*CRYAB* cells was dependent at least in part on VEGF signalling potentially acting in an autocrine manner. However, *in vitro* the proliferation of cells appeared to be independent on αB-crystallin expression and VEGF since no differences in proliferastion were observed. However, to confirm that VEGF plays no role in autocrine signalling to proliferation, VEGF or VEGFR inhibitor experiments would need to be performed.

A main aim of this thesis was to reveal whether αB-crystallin levels in breast cancer cells contribute to resistance to anti-angiogenic therapies by refolding and protecting VEGF from degradation hence increase in its production. However, this relationship between αB-

crystallin and VEGF from the data presented in this thesis contradicts data in the literature. Beside the reasons of differences between the data of this study and those published data that were discussed in each chapter, the validity of some published data may be questioned. For example, in July 2022, the article by Ruan *et al*, 2011 where they described co-culture experiments between breast cancer cell lines and endothelial cells on which the conditioned media experiments were based , was retracted by the journal due to the reuse of an image in this article from another journal (Ruan *et al.* 2022). This should be borne in mind when discussing data from that study and comparing it with the data in this thesis.

Because of the importance of αB-crystallin as a VEGF regulator and angiogenesis, effort has been made to develop inhibitors of αB-crystallin and VEGF interactions. Chen *et al* showed that the interaction between αB-crystallin and VEGF165 could be targeted by small molecule inhibitor (NCI-41356) in TNB cells. They tested this compound using MDA-MB-231 cells and demonstrated that this compound led to significant decrease of VEGF165 and reduction of proliferation and invasiveness of MDA-MB-231 cells *in vitro*. They also showed a significant reduction in tumour growth *in vivo*. However, MDA-MB-231 cells do not express αB-crystallin, as was observed in this study and other studies (Chelouche-Lev *et al.* 2004, Kamradt *et al.* 2005). The authors do not demonstrate αB-crystallin levels in their cells and therefore it is difficult to interpret their data. More studies are needed to establish the interaction between αB-crystallin and VEGF in a wide spectrum of breast cancer cells that express the protein. This will help to reveal the role of αB-crystallin in breast cancer and identify ways through which it can be targeted. It should be noted that αB-crystallin could be targeted by specific miRNAs that target *CRYAB* gene (Wang *et al.* 2017). For example, overexpression of miR-491 in osteosarcoma (OS) inhibited the OS cell lung metastasis, and increased the chemotherapeutic effect *in vivo* and *in vitro* models. This anti-cancer effect was found due to miR-491 targeting the *CRYAB* gene in OS (Wang *et al.* 2017).

7.8 Limitations and future work

The results presented in this thesis agree only with a part of the literature on αB-crystallin. The majority of published studies reported a tumour promoting, antiapoptotic and proinvasive role for αB-crystallin in cancer in general but also specifically in breast cancer (Chelouche‐Lev *et al.* 2004, Moyano *et al.* 2006, van de Schootbrugge *et al.* 2013). It will be important to establish the mechanisms through which in the current study αB-crystallin was

not protective against apoptosis and was associated with a reduced VEGF production and smaller tumour growth. The data of this study point to αB-crystallin as a potential tumour suppressor. There are also other studies that linked αB-crystallin with non-tumourgenic properties (Watanabe *et al.* 2009, Huang *et al.* 2012). Therefore, it is important to establish the mechanisms through which it may promote tumorigenesis or inhibit it. Indeed, identifying its specific role in the context of diverse malignancies will help to determine its role as a prognostic biomarker or/and a therapeutic target. αB-crystallin binds to misfolded proteins and prevents their aggregation (Koletsa *et al.* 2014). Its interaction with specific substrates and molecular systems that may drive proliferation, apoptosis or invasion in different cancer cells plays a crucial role in disease progression. It is important to understand this interaction with each particular substrate and system. Therefore, interactions that promote tumour growth could be targeted through drug intervention to influencing the advancement of a particular disease type.

Furthermore, an important aspect that requires more investigation is confirming the results in this study. Using advanced methods like mass spectrometry to study changes in how various proteins are expressed is important for understanding the detailed molecular processes that cause the observed traits in αB-crystallin-altered cells. This validation approach will help to reveal possible protein patterns that could be responsible for the complex interactions between αB-crystallin and VEGF.

Several studies showed that in some cell types αB-crystallin chaperone function is phosphorylation-dependent (Ecroyd *et al.* 2007). It therefore needs to be determined whether the phosphorylation of αB-crystallin is essential for its activity as a regulator of apoptosis and VEGF production in the breast cancer. Phosphorylation is known to influence the formation of oligomeric structures of αB-crystallin molecules (Ito *et al.* 2001). It is not clear how oligomerization influences chaperone activity. Phosphorylation is thought to alter the distribution of αB-crystallin within different cell compartments. For example, αB-crystallin localizes to the cytoskeleton in response to stress stimuli (Launay *et al.* 2006). It is possible that in the system of this study, overexpression of the protein led to subcellular localization which in way that it interfered with its chaperone activity. It will also be important to analyse signalling pathway that might be responsible for the effects seen by overexpressing αB-crystallin in this study. For example, investigating the activation of MAPK/ERK and PI3/AKT

pathways would reveal whether a relationship exists between αB-crystallin and these dominant oncogenic pathways in these cells. In addition, checking the markers of EMT to check whether αB-crystallin is involved in regulating EMT markers.

7.9 Conclusion

The aim of this thesis is to determine the role of αB-crystallin as a potential biomarker of resistance to anti-VEGF treatments. The *in vitro* and *in vivo* results suggest that αB-crystallin negatively regulates VEGF and breast cancer growth and angiogenesis, which contrasts with previous literature, suggesting that in breast cancer and other cancers αB-crystallin was protective of VEGF and promoted tumour growth. Additionally, αB-crystallin overexpression tended to induce more apoptosis in response to doxorubicin compared to wild-type cells. Although bevacizumab showed no efficacy in αB-crystallin overexpressing tumours, nevertheless, the combination of doxorubicin and bevacizumab increased the efficacy of bevacizumab. Overall, αB-crystallin may acts as tumour suppressor protein in the system of this study by inactivating VEGF production. This needs further investigation to reveal its role in oncogenic-related pathways. Additionally, the interaction of αB-crystallin and VEGF in other breast cancer types could reveal additional information of its role in the disease.

Chapter8 **Bibliography**

Aalders, K. C., K. Tryfonidis, E. Senkus and F. Cardoso (2017). "Anti-angiogenic treatment in breast cancer: Facts, successes, failures and future perspectives." Cancer Treat Rev **53**: 98-110.

Abhinand, C. S., R. Raju, S. J. Soumya, P. S. Arya and P. R. Sudhakaran (2016). "VEGF-A/VEGFR2 signaling network in endothelial cells relevant to angiogenesis." Journal of cell communication and signaling **10**(4): 347-354.

Abou-Elkacem, L., S. Arns, G. Brix, F. Gremse, D. Zopf, F. Kiessling and W. Lederle (2013). "Regorafenib Inhibits Growth, Angiogenesis, and Metastasis in a Highly Aggressive, Orthotopic Colon Cancer Model Regorafenib Inhibits Tumor Progression of Colon Cancer." Molecular cancer therapeutics **12**(7): 1322-1331.

Acunzo, J., M. Katsogiannou and P. Rocchi (2012). "Small heat shock proteins HSP27 (HspB1), αB-crystallin (HspB5) and HSP22 (HspB8) as regulators of cell death." The international journal of biochemistry & cell biology **44**(10): 1622-1631.

Adams, V. R. and M. Leggas (2007). "Sunitinib malate for the treatment of metastatic renal cell carcinoma and gastrointestinal stromal tumors." Clinical therapeutics **29**(7): 1338-1353.

Ahmad, A. and M. I. Nawaz (2022). "Molecular mechanism of VEGF and its role in pathological angiogenesis." Journal of Cellular Biochemistry **123**(12): 1938-1965.

Ahmad, M. F., B. Raman, T. Ramakrishna and C. M. Rao (2008). "Effect of phosphorylation on αB-crystallin: differences in stability, subunit exchange and chaperone activity of homo and mixed oligomers of αB-crystallin and its phosphorylation-mimicking mutant." Journal of molecular biology **375**(4): 1040-1051.

Akinleye, A. and Z. Rasool (2019). "Immune checkpoint inhibitors of PD-L1 as cancer therapeutics." Journal of hematology & oncology **12**(1): 1-13.

Al-Nasiry, S., N. Geusens, M. Hanssens, C. Luyten and R. Pijnenborg (2007). "The use of Alamar Blue assay for quantitative analysis of viability, migration and invasion of choriocarcinoma cells." Human reproduction **22**(5): 1304-1309.

Amaral, J. D., J. M. Xavier, C. J. Steer and C. M. Rodrigues (2010). "The role of p53 in apoptosis." Discovery medicine **9**(45): 145-152.

Aoyagi, Y., H. Iinuma, A. Horiuchi, R. Shimada and T. Watanabe (2010). "Association of plasma VEGF-A, soluble VEGFR-1 and VEGFR-2 levels and clinical response and survival in advanced colorectal cancer patients receiving bevacizumab with modified FOLFOX6." Oncology letters **1**(2): 253-259.

Apte, R. S., D. S. Chen and N. Ferrara (2019). "VEGF in Signaling and Disease: Beyond Discovery and Development." Cell **176**(6): 1248-1264.

Arrigo, A.-P., S. Simon, B. Gibert, C. Kretz-Remy, M. Nivon, A. Czekalla, D. Guillet, M. Moulin, C. Diaz-Latoud and P. Vicart (2007). "Hsp27 (HspB1) and αB-crystallin (HspB5) as therapeutic targets." FEBS letters **581**(19): 3665-3674.

Asahara, T., H. Masuda, T. Takahashi, C. Kalka, C. Pastore, M. Silver, M. Kearne, M. Magner and J. M. Isner (1999). "Bone marrow origin of endothelial progenitor cells responsible for postnatal vasculogenesis in physiological and pathological neovascularization." Circulation research **85**(3): 221-228.

Aspriţoiu, V. M., I. Stoica, C. Bleotu and C. C. Diaconu (2021). "Epigenetic Regulation of Angiogenesis in Development and Tumors Progression: Potential Implications for Cancer Treatment." Frontiers in Cell and Developmental Biology: 2462.

Ayoub, N. M., S. K. Jaradat, K. M. Al-Shami and A. E. Alkhalifa (2022). "Targeting Angiogenesis in Breast Cancer: Current Evidence and Future Perspectives of Novel Anti-Angiogenic Approaches." Frontiers in Pharmacology **13**.

Azzi, S., J. K. Hebda and J. Gavard (2013). "Vascular permeability and drug delivery in cancers." Frontiers in oncology **3**: 211.

Bais, C., B. Mueller, M. F. Brady, R. S. Mannel, R. A. Burger, W. Wei, K. M. Marien, M. M. Kockx, A. Husain and M. J. Birrer (2017). "Tumor microvessel density as a potential predictive marker for bevacizumab benefit: GOG-0218 biomarker analyses." JNCI: Journal of the National Cancer Institute **109**(11).

Bakthisaran, R., K. K. Akula, R. Tangirala and C. M. Rao (2016). "Phosphorylation of αB-crystallin: Role in stress, aging and patho-physiological conditions." Biochimica et Biophysica Acta (BBA)-General Subjects **1860**(1): 167-182.

Bakthisaran, R., R. Tangirala and C. M. Rao (2015). "Small heat shock proteins: role in cellular functions and pathology." Biochimica et Biophysica Acta (BBA)-Proteins and Proteomics **1854**(4): 291-319.

Ballas, M. S. and A. Chachoua (2011). "Rationale for targeting VEGF, FGF, and PDGF for the treatment of NSCLC." OncoTargets and therapy: 43-58.

Bando, H., H. A. Weich, M. Brokelmann, S. Horiguchi, N. Funata, T. Ogawa and M. Toi (2005). "Association between intratumoral free and total VEGF, soluble VEGFR-1, VEGFR-2 and prognosis in breast cancer." Br J Cancer **92**(3): 553-561.

Bang, H. S., M. H. Choi, C. S. Kim and S. J. Choi (2016). "Gene expression profiling in undifferentiated thyroid carcinoma induced by high-dose radiation." Journal of radiation research **57**(3): 238-249.

Barral, M., A. Raballand, A. Dohan, P. Soyer, M. Pocard and P. Bonnin (2016). "Preclinical assessment of the efficacy of anti-angiogenic therapies in hepatocellular carcinoma." Ultrasound in Medicine & Biology **42**(2): 438-446.

Barrios, C. H., M.-C. Liu, S. C. Lee, L. Vanlemmens, J.-M. Ferrero, T. Tabei, X. Pivot, H. Iwata, K. Aogi and R. Lugo-Quintana (2010). "Phase III randomized trial of sunitinib versus capecitabine in patients with previously treated HER2-negative advanced breast cancer." Breast cancer research and treatment **121**(1): 121-131.

Batchelor, T. T., A. G. Sorensen, E. di Tomaso, W.-T. Zhang, D. G. Duda, K. S. Cohen, K. R. Kozak, D. P. Cahill, P.-J. Chen and M. Zhu (2007). "AZD2171, a pan-VEGF receptor tyrosine kinase inhibitor, normalizes tumor vasculature and alleviates edema in glioblastoma patients." Cancer cell **11**(1): 83-95.

Beaudry, P., J. Force, G. N. Naumov, A. Wang, C. H. Baker, A. Ryan, S. Soker, B. E. Johnson, J. Folkman and J. V. Heymach (2005). "Differential effects of vascular endothelial growth factor receptor-2 inhibitor ZD6474 on circulating endothelial progenitors and mature circulating endothelial cells: implications for use as a surrogate marker of antiangiogenic activity." Clinical Cancer Research **11**(9): 3514-3522.

Bergers, G. and L. E. J. N. r. c. Benjamin (2003). "Angiogenesis: tumorigenesis and the angiogenic switch." **3**(6): 401.

Bergers, G. and D. Hanahan (2008). "Modes of resistance to anti-angiogenic therapy." Nat Rev Cancer **8**(8): 592-603.

Bergers, G., S. Song, N. Meyer-Morse, E. Bergsland and D. Hanahan (2003). "Benefits of targeting both pericytes and endothelial cells in the tumor vasculature with kinase inhibitors." The Journal of clinical investigation **111**(9): 1287-1295.

Berra, E., G. Pagès and J. Pouysségur (2000). "MAP kinases and hypoxia in the control of VEGF expression." Cancer and Metastasis reviews **19**: 139-145.

Blanco, R. and H. Gerhardt (2013). "VEGF and Notch in tip and stalk cell selection." Cold Spring Harbor perspectives in medicine **3**(1): a006569.

Brandner, B., R. Kurkela, P. Vihko and A. J. Kungl (2006). "Investigating the effect of VEGF glycosylation on glycosaminoglycan binding and protein unfolding." Biochemical and biophysical research communications **340**(3): 836-839.

Bressenot, A., S. Marchal, L. Bezdetnaya, J. Garrier, F. Guillemin and F. Plénat (2009). "Assessment of apoptosis by immunohistochemistry to active caspase-3, active caspase-7, or cleaved PARP in monolayer cells and spheroid and subcutaneous xenografts of human carcinoma." Journal of Histochemistry & Cytochemistry **57**(4): 289-300.

Cabral-Pacheco, G. A., I. Garza-Veloz, C. Castruita-De la Rosa, J. M. Ramirez-Acuna, B. A. Perez-Romero, J. F. Guerrero-Rodriguez, N. Martinez-Avila and M. L. Martinez-Fierro (2020). "The

roles of matrix metalloproteinases and their inhibitors in human diseases." International journal of molecular sciences **21**(24): 9739.

Cai, M.-H., X.-G. Xu, S.-L. Yan, Z. Sun, Y. Ying, B.-K. Wang and Y.-X. Tu (2018). "Regorafenib suppresses colon tumorigenesis and the generation of drug resistant cancer stem-like cells via modulation of miR-34a associated signaling." Journal of Experimental & Clinical Cancer Research **37**: 1-11.

Cai, Y., X. Yu, S. Hu and J. Yu (2009). "A brief review on the mechanisms of miRNA regulation." Genomics, proteomics & bioinformatics **7**(4): 147-154.

Cao, S., F. A. Durrani, K. Toth, Y. M. Rustum and M. Seshadri (2011). "Bevacizumab enhances the therapeutic efficacy of Irinotecan against human head and neck squamous cell carcinoma xenografts." Oral oncology **47**(6): 459-466.

Carmeliet, P. and R. K. Jain (2011). "Principles and mechanisms of vessel normalization for cancer and other angiogenic diseases." Nature reviews Drug discovery **10**(6): 417-427.

Casak, S. J., I. Fashoyin-Aje, S. J. Lemery, L. Zhang, R. Jin, H. Li, L. Zhao, H. Zhao, H. Zhang and H. Chen (2015). "FDA approval summary: ramucirumab for gastric cancer." Clinical Cancer Research **21**(15): 3372-3376.

Chau, N. G. and R. I. Haddad (2013). "Vandetanib for the treatment of medullary thyroid cancer." Clinical Cancer Research **19**(3): 524-529.

Chelouche‐Lev, D., H. M. Kluger, A. J. Berger, D. L. Rimm and J. E. Price (2004). "αB‐crystallin as a marker of lymph node involvement in breast carcinoma." Cancer **100**(12): 2543-2548.

Chen, D., G. Cao, C. Qiao, G. Liu, H. Zhou and Q. Liu (2018). "Alpha B‐crystallin promotes the invasion and metastasis of gastric cancer via NF‐κB‐induced epithelial‐mesenchymal transition." Journal of Cellular and Molecular Medicine **22**(6): 3215-3222.

Chen, Z., Q. Ruan, S. Han, L. Xi, W. Jiang, H. Jiang, D. A. Ostrov and J. Cai (2014). "Discovery of structure-based small molecular inhibitor of αB-crystallin against basal-like/triple-negative breast cancer development in vitro and in vivo." Breast Cancer Research and Treatment **145**(1): 45-59.

Chin, D., G. M. Boyle, R. M. Williams, K. Ferguson, N. Pandeya, J. Pedley, C. M. Campbell, D. R. Theile, P. G. Parsons and W. B. Coman (2005). "Alpha B‐crystallin, a new independent marker for poor prognosis in head and neck cancer." The Laryngoscope **115**(7): 1239-1242.

Chung, A. S. and N. Ferrara (2011). "Developmental and pathological angiogenesis." Annual review of cell and developmental biology **27**: 563-584.

Cohen, M. H., J. Gootenberg, P. Keegan and R. Pazdur (2007). "FDA drug approval summary: bevacizumab (Avastin®) plus carboplatin and paclitaxel as first-line treatment of

advanced/metastatic recurrent nonsquamous non-small cell lung cancer." The oncologist **12**(6): 713-718.

Cohen, M. H., J. Gootenberg, P. Keegan and R. Pazdur (2007). "FDA drug approval summary: bevacizumab plus FOLFOX4 as second-line treatment of colorectal cancer." The oncologist **12**(3): 356-361.

Crawford, Y. and N. Ferrara (2009). "Tumor and stromal pathways mediating refractoriness/resistance to anti-angiogenic therapies." Trends in pharmacological sciences **30**(12): 624-630.

Crawford, Y., I. Kasman, L. Yu, C. Zhong, X. Wu, Z. Modrusan, J. Kaminker and N. Ferrara (2009). "PDGF-C mediates the angiogenic and tumorigenic properties of fibroblasts associated with tumors refractory to anti-VEGF treatment." Cancer cell **15**(1): 21-34.

Crona, D. J., M. D. Keisler and C. M. Walko (2013). "Regorafenib: a novel multitargeted tyrosine kinase inhibitor for colorectal cancer and gastrointestinal stromal tumors." Annals of Pharmacotherapy **47**(12): 1685-1696.

Cross, M. J., J. Dixelius, T. Matsumoto and L. Claesson-Welsh (2003). "VEGF-receptor signal transduction." Trends in biochemical sciences **28**(9): 488-494.

Cyran, C. C., P. M. Kazmierczak, H. Hirner, M. Moser, M. Ingrisch, L. Havla, A. Michels, R. Eschbach, B. Schwarz and M. F. Reiser (2013). "Regorafenib effects on human colon carcinoma xenografts monitored by dynamic contrast-enhanced computed tomography with immunohistochemical validation." PLoS One **8**(9): e76009.

Das, M. and H. Wakelee (2014). "Angiogenesis and lung cancer: ramucirumab prolongs survival in 2nd-line metastatic NSCLC." Translational Lung Cancer Research **3**(6): 397.

De Jong, J. S., P. J. Van Diest, P. Van Der Valk and J. P. Baak (1998). "Expression of growth factors, growth inhibiting factors, and their receptors in invasive breast cancer. I: An inventory in search of autocrine and paracrine loops." The Journal of Pathology: A Journal of the Pathological Society of Great Britain and Ireland **184**(1): 44-52.

DePrimo, S. E., C. L. Bello, J. Smeraglia, C. M. Baum, D. Spinella, B. I. Rini, M. D. Michaelson and R. J. Motzer (2007). "Circulating protein biomarkers of pharmacodynamic activity of sunitinib in patients with metastatic renal cell carcinoma: modulation of VEGF and VEGF-related proteins." Journal of translational medicine **5**(1): 1-11.

Derham, B. K. and J. J. Harding (1999). "α-Crystallin as a molecular chaperone." Progress in retinal and eye research **18**(4): 463-509.

Déry, M.-A. C., M. D. Michaud and D. E. Richard (2005). "Hypoxia-inducible factor 1: regulation by hypoxic and non-hypoxic activators." The international journal of biochemistry & cell biology **37**(3): 535-540.

Dimberg, A., S. Rylova, L. C. Dieterich, A.-K. Olsson, P. Schiller, C. Wikner, S. Bohman, J. Botling, A. Lukinius and E. F. Wawrousek (2008). "αB-crystallin promotes tumor angiogenesis by increasing vascular survival during tube morphogenesis." Blood **111**(4): 2015-2023.

Dimmeler, S., I. Fleming, B. Fisslthaler, C. Hermann, R. Busse and A. M. Zeiher (1999). "Activation of nitric oxide synthase in endothelial cells by Akt-dependent phosphorylation." Nature **399**(6736): 601-605.

Ding, Y.-t., S. Kumar and D.-c. Yu (2008). "The role of endothelial progenitor cells in tumour vasculogenesis." Pathobiology **75**(5): 265-273.

Döme, B., S. Paku, B. Somlai and J. Tímár (2002). "Vascularization of cutaneous melanoma involves vessel co‐option and has clinical significance." The Journal of pathology **197**(3): 355-362.

Dong, Y., Z. Dong, S. Kase, R. Ando, J. Fukuhara, S. Kinoshita, S. Inafuku, Y. Tagawa, E. T. Ishizuka and W. Saito (2016). "Phosphorylation of alphaB-crystallin in epiretinal membrane of human proliferative diabetic retinopathy." International Journal of Ophthalmology **9**(8): 1100.

Dvorak, H. F. (1986). "Tumors: wounds that do not heal." New England Journal of Medicine **315**(26): 1650-1659.

Dvorak, H. F. (2002). "Vascular permeability factor/vascular endothelial growth factor: a critical cytokine in tumor angiogenesis and a potential target for diagnosis and therapy." Journal of clinical oncology **20**(21): 4368-4380.

Ebos, J. M., C. R. Lee, J. G. Christensen, A. J. Mutsaers and R. S. Kerbel (2007). "Multiple circulating proangiogenic factors induced by sunitinib malate are tumor-independent and correlate with antitumor efficacy." Proceedings of the National Academy of Sciences **104**(43): 17069-17074.

Ecroyd, H., S. Meehan, J. Horwitz, J. A. Aquilina, J. L. Benesch, C. V. Robinson, C. E. Macphee and J. A. Carver (2007). "Mimicking phosphorylation of αB-crystallin affects its chaperone activity." Biochemical Journal **401**(1): 129-141.

El Alaoui-Lasmaili, K. and B. Faivre (2018). "Antiangiogenic therapy: Markers of response,“normalization” and resistance." Critical Reviews in Oncology/Hematology **128**: 118-129.

Eliyatkın, N., E. Yalçın, B. Zengel, S. Aktaş and E. Vardar (2015). "Molecular classification of breast carcinoma: from traditional, old-fashioned way to a new age, and a new way." The journal of breast health **11**(2): 59.

Emblem, K. E., K. Mouridsen, A. Bjornerud, C. T. Farrar, D. Jennings, R. J. Borra, P. Y. Wen, P. Ivy, T. T. Batchelor and B. R. Rosen (2013). "Vessel architectural imaging identifies cancer patient responders to anti-angiogenic therapy." Nature medicine **19**(9): 1178-1183.

Escudier, B., J. Bellmunt, S. Négrier, E. Bajetta, B. Melichar, S. Bracarda, A. Ravaud, S. Golding, S. Jethwa and V. Sneller (2010). "Phase III trial of bevacizumab plus interferon alfa-2a in patients with metastatic renal cell carcinoma (AVOREN): final analysis of overall survival." Journal of Clinical Oncology **28**(13): 2144-2150.

Escudier, B., J. C. Lougheed and L. Albiges (2016). "Cabozantinib for the treatment of renal cell carcinoma." Expert Opinion on Pharmacotherapy **17**(18): 2499-2504.

Ferrara, N. (2005). "VEGF as a therapeutic target in cancer." Oncology **69**(Suppl. 3): 11-16.
Ferrara, N., H.-P. Gerber and J. LeCouter (2003). "The biology of VEGF and its receptors." Nature medicine **9**(6): 669.

Fischer, C., B. Jonckx, M. Mazzone, S. Zacchigna, S. Loges, L. Pattarini, E. Chorianopoulos, L. Liesenborghs, M. Koch and M. De Mol (2007). "Anti-PlGF inhibits growth of VEGF (R)-inhibitor-resistant tumors without affecting healthy vessels." Cell **131**(3): 463-475.

Folkman, J. (2008). History of angiogenesis. Angiogenesis, Springer**:** 1-14.
Folkman, J. J. N. e. j. o. m. (1971). "Tumor angiogenesis: therapeutic implications." The New England Journal of Medicine **285**(21): 1182-1186.

Fong, G.-H., J. Rossant, M. Gertsenstein and M. L. Breitman (1995). "Role of the Flt-1 receptor tyrosine kinase in regulating the assembly of vascular endothelium." Nature **376**(6535): 66-70.

Fornari Jr, F. A., W. D. Jarvis, S. Grant, M. S. Orr, J. K. Randolph, F. K. White, V. R. Mumaw, E. T. Lovings, R. H. Freeman and D. A. Gewirtz (1994). "Induction of differentiation and growth arrest associated with nascent (nonoligosomal) DNA fragmentation and reduced c-myc expression in MCF-7 human breast tumor cells after continuous exposure to a sublethal concentration of doxorubicin." Cell Growth and Differentiation-Publication American Association for Cancer Research **5**(7): 723-734.

Fosu-Mensah, N. A., W. Jiang, A. Brancale, J. Cai and A. D. Westwell (2019). "The discovery of purine-based agents targeting triple-negative breast cancer and the αB-crystallin/VEGF protein–protein interaction." Medicinal Chemistry Research **28**(2): 182-202.

Frentzas, S., E. Simoneau, V. L. Bridgeman, P. B. Vermeulen, S. Foo, E. Kostaras, M. R. Nathan, A. Wotherspoon, Z.-h. Gao and Y. Shi (2016). "Vessel co-option mediates resistance to anti-angiogenic therapy in liver metastases." Nature medicine **22**(11): 1294-1302.

Fridman, J. S. and S. W. Lowe (2003). "Control of apoptosis by p53." Oncogene **22**(56): 9030.

Fukumura, D. and R. K. Jain (2007). "Tumor microenvironment abnormalities: causes, consequences, and strategies to normalize." Journal of cellular biochemistry **101**(4): 937-949.

Garcia, J., H. I. Hurwitz, A. B. Sandler, D. Miles, R. L. Coleman, R. Deurloo and O. L. Chinot (2020). "Bevacizumab (Avastin®) in cancer treatment: A review of 15 years of clinical experience and future outlook." Cancer treatment reviews **86**: 102017.

Gasparini, G., R. Longo, M. Fanelli and B. A. Teicher (2005). "Combination of antiangiogenic therapy with other anticancer therapies: results, challenges, and open questions." Journal of Clinical Oncology **23**(6): 1295-1311.

Gaya, A. and G. Rustin (2005). "Vascular disrupting agents: a new class of drug in cancer therapy." Clinical Oncology **17**(4): 277-290.

George, M. L., M. G. Tutton, F. Janssen, A. Arnaout, A. M. Abulafi, S. A. Eccles and R. I. Swift (2001). "Vegf-a, vegf-c, and vegf-d in colorectal cancer progression." Neoplasia **3**(5): 420-427.

Gerber, H.-P., A. McMurtrey, J. Kowalski, M. Yan, B. A. Keyt, V. Dixit and N. Ferrara (1998). "Vascular endothelial growth factor regulates endothelial cell survival through the phosphatidylinositol 3′-kinase/Akt signal transduction pathway: requirement for Flk-1/KDR activation." Journal of Biological Chemistry **273**(46): 30336-30343.

Gewirtz, D. (1999). "A critical evaluation of the mechanisms of action proposed for the antitumor effects of the anthracycline antibiotics adriamycin and daunorubicin." Biochemical pharmacology **57**(7): 727-741.

Ghosh, J. G., A. K. Shenoy and J. I. Clark (2007). "Interactions between important regulatory proteins and human αB crystallin." Biochemistry **46**(21): 6308-6317.

Gille, H., J. Kowalski, B. Li, J. LeCouter, B. Moffat, T. F. Zioncheck, N. Pelletier and N. J. J. o. B. C. Ferrara (2000). "Analysis of biological effects andsignaling properties of Flt-1 and KDR: A reassessment using novel highlyreceptor-specific VEGF mutants."

Giuliano, S. and G. Pagès (2013). "Mechanisms of resistance to anti-angiogenesis therapies." Biochimie **95**(6): 1110-1119.

Goel, G., A. Chauhan and P. J. Hosein (2016). "Ramucirumab: a novel anti-angiogenic agent in the treatment of metastatic colorectal cancer." Current colorectal cancer reports **12**: 232-240.

Goel, H. L. and A. M. Mercurio (2013). "VEGF targets the tumour cell." Nature Reviews Cancer **13**(12): 871-882.

Goel, S., D. G. Duda, L. Xu, L. L. Munn, Y. Boucher, D. Fukumura and R. K. Jain (2011). "Normalization of the vasculature for treatment of cancer and other diseases." Physiological reviews **91**(3): 1071-1121.

Goldfarb, S. B., C. Hudis and M. N. Dickler (2011). "Bevacizumab in metastatic breast cancer: when may it be used?" Therapeutic Advances in Medical Oncology **3**(2): 85-93.

Golenhofen, N., W. Ness, E. F. Wawrousek and D. Drenckhahn (2002). "Expression and induction of the stress protein alpha-B-crystallin in vascular endothelial cells." Histochemistry and cell biology **117**(3): 203-209.

Grepin, R., M. Guyot, M. Jacquin, J. Durivault, E. Chamorey, A. Sudaka, C. Serdjebi, B. Lacarelle, J. Scoazec and S. Negrier (2012). "Acceleration of clear cell renal cell carcinoma growth in mice following bevacizumab/Avastin treatment: the role of CXCL cytokines." Oncogene **31**(13): 1683.

Hack, S. P., A. X. Zhu and Y. Wang (2020). "Augmenting anticancer immunity through combined targeting of angiogenic and PD-1/PD-L1 pathways: challenges and opportunities." Frontiers in Immunology **11**: 598877.

Hammond, E., M.-C. Asselin, D. Forster, J. P. O'Connor, J. Senra and K. Williams (2014). "The meaning, measurement and modification of hypoxia in the laboratory and the clinic." Clinical oncology **26**(5): 277-288.

Hanahan, D. (2022). "Hallmarks of cancer: new dimensions." Cancer discovery **12**(1): 31-46.
Hao, Z. and P. Wang (2020). "Lenvatinib in management of solid tumors." The oncologist **25**(2): e302-e310.

Harris, A. L. (2002). "Hypoxia--a key regulatory factor in tumour growth." Nat Rev Cancer **2**(1): 38-47.

Harris, L. N., F. You, S. J. Schnitt, A. Witkiewicz, X. Lu, D. Sgroi, P. D. Ryan, S. E. Come, H. J. Burstein, B. A. Lesnikoski, M. Kamma, P. N. Friedman, R. Gelman, J. D. Iglehart and E. P. Winer (2007). "Predictors of resistance to preoperative trastuzumab and vinorelbine for HER2-positive early breast cancer." Clin Cancer Res **13**(4): 1198-1207.

Heldin, C.-H., K. Rubin, K. Pietras and A. Östman (2004). "High interstitial fluid pressure—an obstacle in cancer therapy." Nature Reviews Cancer **4**(10): 806-813.

Hendrix, M. J., E. A. Seftor, A. R. Hess and R. E. Seftor (2003). "Vasculogenic mimicry and tumour-cell plasticity: lessons from melanoma." Nature reviews cancer **3**(6): 411-421.

Heo, Y.-A. and Y. Y. Syed (2018). "Regorafenib: a review in hepatocellular carcinoma." Drugs **78**: 951-958.

Herschkowitz, J. I., K. Simin, V. J. Weigman, I. Mikaelian, J. Usary, Z. Hu, K. E. Rasmussen, L. P. Jones, S. Assefnia, S. Chandrasekharan, M. G. Backlund, Y. Yin, A. I. Khramtsov, R. Bastein, J. Quackenbush, R. I. Glazer, P. H. Brown, J. E. Green, L. Kopelovich, P. A. Furth, J. P. Palazzo, O. I. Olopade, P. S. Bernard, G. A. Churchill, T. Van Dyke and C. M. Perou (2007). "Identification of conserved gene expression features between murine mammary carcinoma models and human breast tumors." Genome Biol **8**(5): R76.

Heskamp, S., O. C. Boerman, J. D. Molkenboer‐Kuenen, W. J. Oyen, W. T. van der Graaf and H. W. van Laarhoven (2013). "Bevacizumab reduces tumor targeting of antiepidermal growth factor and anti‐insulin‐like growth factor 1 receptor antibodies." International journal of cancer **133**(2): 307-314.

Hicklin, D. J. and L. M. Ellis (2005). "Role of the vascular endothelial growth factor pathway in tumor growth and angiogenesis." Journal of clinical oncology **23**(5): 1011-1027.

Hillen, F. and A. W. Griffioen (2007). "Tumour vascularization: sprouting angiogenesis and beyond." Cancer and Metastasis Reviews **26**(3): 489-502.

Hodi, F. S., D. Lawrence, C. Lezcano, X. Wu, J. Zhou, T. Sasada, W. Zeng, A. Giobbie-Hurder, M. B. Atkins and N. Ibrahim (2014). "Bevacizumab plus ipilimumab in patients with metastatic melanoma." Cancer immunology research **2**(7): 632-642.

Holash, J., P. Maisonpierre, D. Compton, P. Boland, C. Alexander, D. Zagzag, G. Yancopoulos and S. Wiegand (1999). "Vessel cooption, regression, and growth in tumors mediated by angiopoietins and VEGF." Science **284**(5422): 1994-1998.

Holmqvist, K., M. J. Cross, C. Rolny, R. Hägerkvist, N. Rahimi, T. Matsumoto, L. Claesson-Welsh and M. Welsh (2004). "The adaptor protein shb binds to tyrosine 1175 in vascular endothelial growth factor (VEGF) receptor-2 and regulates VEGF-dependent cellular migration." Journal of Biological Chemistry **279**(21): 22267-22275.

Horak, E. R., N. Klenk, R. Leek, S. Lejeune, K. Smith, N. Stuart, A. Harris, M. Greenall and K. Stepniewska (1992). "Angiogenesis, assessed by platelet/endothelial cell adhesion molecule antibodies, as indicator of node metastases and survival in breast cancer." The Lancet **340**(8828): 1120-1124.

Horwitz, J. (1992). "Alpha-crystallin can function as a molecular chaperone." Proceedings of the National Academy of Sciences **89**(21): 10449-10453.

Horwitz, J. (2000). The function of alpha-crystallin in vision. Seminars in cell & developmental biology, Elsevier.

Horwitz, J. (2003). "Alpha-crystallin." Experimental eye research **76**(2): 145-153.

Hsu, I.-L., W.-C. Su, J.-J. Yan, J.-M. Chang and W.-W. Lai (2009). "Angiogenetic biomarkers in non-small cell lung cancer with malignant pleural effusion: correlations with patient survival and pleural effusion control." Lung Cancer **65**(3): 371-376.

Huang, H., A. Bhat, G. Woodnutt and R. Lappe (2010). "Targeting the ANGPT–TIE2 pathway in malignancy." Nature Reviews Cancer **10**(8): 575-585.

Huang, X. Y., A. W. Ke, G. M. Shi, X. Zhang, C. Zhang, Y. H. Shi, X. Y. Wang, Z. B. Ding, Y. S. Xiao and J. Yan (2013). "αB‐crystallin complexes with 14‐3‐3ζ to induce epithelial‐mesenchymal transition and resistance to sorafenib in hepatocellular carcinoma." Hepatology **57**(6): 2235-2247.

Huang, Z., Y. Cheng, P. M. Chiu, F. M. Cheung, J. M. Nicholls, D. L. Kwong, A. W. Lee, E. R. Zabarovsky, E. J. Stanbridge, H. L. Lung and M. L. Lung (2012). "Tumor suppressor Alpha B-

crystallin (CRYAB) associates with the cadherin/catenin adherens junction and impairs NPC progression-associated properties." Oncogene **31**(32): 3709-3720.

Huijbers, E. J., J. R. van Beijnum, V. L. Thijssen, S. Sabrkhany, P. Nowak-Sliwinska and A. W. Griffioen (2016). "Role of the tumor stroma in resistance to anti-angiogenic therapy." Drug Resistance Updates **25**: 26-37.

Hurwitz, H., L. Fehrenbacher, W. Novotny, T. Cartwright, J. Hainsworth, W. Heim, J. Berlin, A. Baron, S. Griffing and E. Holmgren (2004). "Bevacizumab plus irinotecan, fluorouracil, and leucovorin for metastatic colorectal cancer." New England journal of medicine **350**(23): 2335-2342.

Ianza, A., F. Giudici, C. Pinello, S. Corona, C. Strina, O. Bernocchi, M. Bortul, M. Milani, M. Sirico and G. Allevi (2020). "ΔKi67 proliferation index as independent predictive and prognostic factor of outcome in luminal breast cancer: data from neoadjuvant letrozole-based treatment." Tumor Biology **42**(6): 1010428320925301.

Isaacs, C., P. Herbolsheimer, M. C. Liu, M. Wilkinson, Y. Ottaviano, G. G. Chung, R. Warren, J. Eng-Wong, P. Cohen and K. L. Smith (2011). "Phase I/II study of sorafenib with anastrozole in patients with hormone receptor positive aromatase inhibitor resistant metastatic breast cancer." Breast cancer research and treatment **125**(1): 137-143.

Ito, A., S. Nomura, S. Hirota, J. Suda, T. Suda and Y. Kitamura (1995). "Enhanced expression of CD34 messenger RNA by developing endothelial cells of mice." Laboratory investigation; a journal of technical methods and pathology **72**(5): 532-538.

Ito, H., K. Kamei, I. Iwamoto, Y. Inaguma, D. Nohara and K. Kato (2001). "Phosphorylation-induced change of the oligomerization state of αB-crystallin." Journal of Biological Chemistry **276**(7): 5346-5352.

Ivanov, O., F. Chen, E. L. Wiley, A. Keswani, L. K. Diaz, H. C. Memmel, A. Rademaker, W. J. Gradishar, M. Morrow and S. A. Khan (2008). "αB-crystallin is a novel predictor of resistance to neoadjuvant chemotherapy in breast cancer." Breast cancer research and treatment **111**(3): 411-417.

Jain, R. K. (2005). "Normalization of tumor vasculature: an emerging concept in antiangiogenic therapy." Science **307**(5706): 58-62.

Jain, R. K., D. G. Duda, C. G. Willett, D. V. Sahani, A. X. Zhu, J. S. Loeffler, T. T. Batchelor and A. G. Sorensen (2009). "Biomarkers of response and resistance to antiangiogenic therapy." Nature reviews Clinical oncology **6**(6): 327-338.

Jászai, J. and M. H. Schmidt (2019). "Trends and challenges in tumor anti-angiogenic therapies." Cells **8**(9): 1102.

Jayson, G. C., R. Kerbel, L. M. Ellis and A. L. Harris (2016). "Antiangiogenic therapy in oncology: current status and future directions." The Lancet **388**(10043): 518-529.

Jayson, G. C., C. Zhou, A. Backen, L. Horsley, K. Marti-Marti, D. Shaw, N. Mescallado, A. Clamp, M. P. Saunders and J. W. Valle (2018). "Plasma Tie2 is a tumor vascular response biomarker for VEGF inhibitors in metastatic colorectal cancer." Nature communications **9**(1): 1-14.

Jubb, A. M., H. I. Hurwitz, W. Bai, E. B. Holmgren, P. Tobin, A. S. Guerrero, F. Kabbinavar, S. N. Holden, W. F. Novotny and G. D. Frantz (2006). "Impact of vascular endothelial growth factor-A expression, thrombospondin-2 expression, and microvessel density on the treatment effect of bevacizumab in metastatic colorectal cancer." Journal of clinical oncology **24**(2): 217-227.

Kabbage, M., M. Trimeche, H. Ben Nasr, P. Hammann, L. Kuhn, B. Hamrita, A. Chaieb, L. Chouchane and K. Chahed (2012). "Expression of the molecular chaperone alphaB-crystallin in infiltrating ductal breast carcinomas and the significance thereof: an immunohistochemical and proteomics-based strategy." Tumour Biol **33**(6): 2279-2288.

Kamradt, M. C., F. Chen and V. L. J. J. o. B. C. Cryns (2001). "The small heat shock protein αB-crystallin negatively regulates cytochrome c-and caspase-8-dependent activation of caspase-3 by inhibiting its autoproteolytic maturation." **276**(19): 16059-16063.

Kamradt, M. C., F. Chen, S. Sam and V. L. Cryns (2002). "The small heat shock protein αB-crystallin negatively regulates apoptosis during myogenic differentiation by inhibiting caspase-3 activation." Journal of Biological Chemistry **277**(41): 38731-38736.

Kamradt, M. C., M. Lu, M. E. Werner, T. Kwan, F. Chen, A. Strohecker, S. Oshita, J. C. Wilkinson, C. Yu and P. G. Oliver (2005). "The small heat shock protein αB-crystallin is a novel inhibitor of TRAIL-induced apoptosis that suppresses the activation of caspase-3." Journal of Biological Chemistry **280**(12): 11059-11066.

Kang, W. K., M. H. Lee, Y. H. Kim, M. Y. Kim and J.-Y. Kim (2013). "Enhanced secretion of biologically active, non-glycosylated VEGF from Saccharomyces cerevisiae." Journal of biotechnology **164**(4): 441-448.

Kanthou, C. and G. Tozer (2018). "Targeting the vasculature of tumours: combining VEGF pathway inhibitors with radiotherapy." The British Journal of Radiology **92**(1093): 20180405.

Kase, S., S. He, S. Sonoda, M. Kitamura, C. Spee, E. Wawrousek, S. J. Ryan, R. Kannan and D. R. Hinton (2010). "αB-crystallin regulation of angiogenesis by modulation of VEGF." Blood, The Journal of the American Society of Hematology **115**(16): 3398-3406.

Kazazi-Hyseni, F., J. H. Beijnen and J. H. Schellens (2010). "Bevacizumab." The oncologist **15**(8): 819.

Kerr, B. A. and T. V. Byzova (2010). "αB-crystallin: a novel VEGF chaperone." Blood, The Journal of the American Society of Hematology **115**(16): 3181-3183.

Khan, K. A. and R. S. Kerbel (2018). "Improving immunotherapy outcomes with anti-angiogenic treatments and vice versa." Nature Reviews Clinical Oncology **15**(5): 310-324.

Kim, H.-S., H.-S. Kang, C. A. Messam, K.-W. Min and C.-S. Park (2002). "Comparative evaluation of angiogenesis in gastric adenocarcinoma by nestin and CD34." Applied Immunohistochemistry & Molecular Morphology **10**(2): 121-127.

Kim, H. S., Y. Lee, Y. A. Lim, H. J. Kang and L. S. Kim (2011). "αB-Crystallin is a novel oncoprotein associated with poor prognosis in breast cancer." Journal of breast cancer **14**(1): 14-19.

Kim, K. J., B. Li, J. Winer, M. Armanini, N. Gillett, H. S. Phillips and N. Ferrara (1993). "Inhibition of vascular endothelial growth factor-induced angiogenesis suppresses tumour growth in vivo." Nature **362**(6423): 841-844.

Kim, M. S., H. W. Lee, S. Y. Jun and E. H. Lee (2015). "Expression of alpha B crystallin and BCL2 in patients with infiltrating ductal carcinoma." Int J Clin Exp Pathol **8**(8): 8842-8856.

Kim, T. S., J. H. Kim, B. hui Kim, Y.-S. Lee, Y. J. Yoo, S. H. Kang, S.-J. Suh, Y. K. Jung, Y. S. Seo and H. J. Yim (2017). "Complete response of advanced hepatocellular carcinoma to sorafenib: another case and a comprehensive review." Clinical and molecular hepatology **23**(4): 340.

Koch, S. and L. J. C. S. H. p. i. m. Claesson-Welsh (2012). "Signal transduction by vascular endothelial growth factor receptors." **2**(7): a006502.

Koletsa, T., F. Stavridi, M. Bobos, I. Kostopoulos, V. Kotoula, A. G. Eleftheraki, I. Konstantopoulou, C. Papadimitriou, A. Batistatou, H. Gogas, A. Koutras, D. V. Skarlos, G. Pentheroudakis, I. Efstratiou, D. Pectasides and G. Fountzilas (2014). "alphaB-crystallin is a marker of aggressive breast cancer behavior but does not independently predict for patient outcome: a combined analysis of two randomized studies." BMC Clin Pathol **14**: 28.

Kolte, D., J. A. McClung and W. S. Aronow (2016). Vasculogenesis and angiogenesis. Translational Research in Coronary Artery Disease, Elsevier**:** 49-65.

Komohara, Y. and M. Takeya (2017). "CAFs and TAMs: maestros of the tumour microenvironment." The Journal of pathology **241**(3): 313-315.

Kowanetz, M. and N. Ferrara (2006). "Vascular endothelial growth factor signaling pathways: therapeutic perspective." Clin Cancer Res **12**(17): 5018-5022.

Kreike, B., M. van Kouwenhove, H. Horlings, B. Weigelt, H. Peterse, H. Bartelink and M. J. van de Vijver (2007). "Gene expression profiling and histopathological characterization of triple-negative/basal-like breast carcinomas." Breast Cancer Research **9**(5): 1-14.

Kristensen, T. B., M. L. Knutsson, M. Wehland, B. E. Laursen, D. Grimm, E. Warnke and N. E. Magnusson (2014). "Anti-vascular endothelial growth factor therapy in breast cancer." Int J Mol Sci **15**(12): 23024-23041.

Launay, N., B. Goudeau, K. Kato, P. Vicart and A. Lilienbaum (2006). "Cell signaling pathways to αB-crystallin following stresses of the cytoskeleton." Experimental cell research **312**(18): 3570-3584.

Launay, N., A. Tarze, P. Vicart and A. Lilienbaum (2010). "Serine 59 phosphorylation of αB-crystallin down-regulates its anti-apoptotic function by binding and sequestering Bcl-2 in breast cancer cells." Journal of Biological Chemistry **285**(48): 37324-37332.

Lee, A. T., R. L. Jones and P. H. Huang (2019). "Pazopanib in advanced soft tissue sarcomas." Signal transduction and targeted therapy **4**(1): 16.

Lee, K.-S., M.-G. Lee, Y.-S. Kwon and K.-S. Nam (2020). "Arctigenin enhances the cytotoxic effect of doxorubicin in MDA-MB-231 breast cancer cells." International Journal of Molecular Sciences **21**(8): 2997.

Lee, M. S., B.-Y. Ryoo, C.-H. Hsu, K. Numata, S. Stein, W. Verret, S. P. Hack, J. Spahn, B. Liu and H. Abdullah (2020). "Atezolizumab with or without bevacizumab in unresectable hepatocellular carcinoma (GO30140): an open-label, multicentre, phase 1b study." The Lancet Oncology **21**(6): 808-820.

Lee, S., S. M. Jilani, G. V. Nikolova, D. Carpizo and M. L. Iruela-Arispe (2005). "Processing of VEGF-A by matrix metalloproteinases regulates bioavailability and vascular patterning in tumors." The Journal of cell biology **169**(4): 681-691.

Li, D., K. Xie, L. Zhang, X. Yao, H. Li, Q. Xu, X. Wang, J. Jiang and J. Fang (2016). "Dual blockade of vascular endothelial growth factor (VEGF) and basic fibroblast growth factor (FGF-2) exhibits potent anti-angiogenic effects." Cancer Letters **377**(2): 164-173.

Li, D. W.-C., J.-P. Liu, Y.-W. Mao, H. Xiang, J. Wang, W.-Y. Ma, Z. Dong, H. M. Pike, R. E. Brown and J. C. Reed (2005). "Calcium-activated RAF/MEK/ERK signaling pathway mediates p53-dependent apoptosis and is abrogated by αB-crystallin through inhibition of RAS activation." Molecular biology of the cell **16**(9): 4437-4453.

Li, L., G. D. Zhao, Z. Shi, L. L. Qi, L. Y. Zhou and Z. X. Fu (2016). "The Ras/Raf/MEK/ERK signaling pathway and its role in the occurrence and development of HCC." Oncol Lett **12**(5): 3045-3050.

Li, Q., Y. Wang, Y. Lai, P. Xu and Z. Yang (2017). "HspB5 correlates with poor prognosis in colorectal cancer and prompts epithelial-mesenchymal transition through ERK signaling." PloS one **12**(8): e0182588.

Li, S., H.-X. Xu, C.-T. Wu, W.-Q. Wang, W. Jin, H.-L. Gao, H. Li, S.-R. Zhang, J.-Z. Xu and Z.-H. Qi (2019). "Angiogenesis in pancreatic cancer: current research status and clinical implications." Angiogenesis **22**(1): 15-36.

Li, W., C. Feng, W. Di, S. Hong, H. Chen, M. Ejaz, Y. Yang and T.-r. Xu (2020). "Clinical use of vascular endothelial growth factor receptor inhibitors for the treatment of renal cell carcinoma." European Journal of Medicinal Chemistry **200**: 112482.

Li, X. and U. Eriksson (2001). "Novel VEGF family members: VEGF-B, VEGF-C and VEGF-D." Int J Biochem Cell Biol **33**(4): 421-426.

Lieu, C. H., H. Tran, Z.-Q. Jiang, M. Mao, M. J. Overman, E. Lin, C. Eng, J. Morris, L. Ellis and J. V. Heymach (2013). "The association of alternate VEGF ligands with resistance to anti-VEGF therapy in metastatic colorectal cancer." PloS one **8**(10): e77117.

Liu, B., M. Bhat and R. H. Nagaraj (2004). "αB-crystallin inhibits glucose-induced apoptosis in vascular endothelial cells." Biochemical and biophysical research communications **321**(1): 254-258.

Liu, J. P., R. Schlosser, W. Y. Ma, Z. Dong, H. Feng, L. Lui, X. Q. Huang, Y. Liu and D. W. Li (2004). "Human alphaA- and alphaB-crystallins prevent UVA-induced apoptosis through regulation of PKCalpha, RAF/MEK/ERK and AKT signaling pathways." Exp Eye Res **79**(6): 393-403.

Liu, S., J. Li, Y. Tao, X. J. B. Xiao and b. r. communications (2007). "Small heat shock protein αB-crystallin binds to p53 to sequester its translocation to mitochondria during hydrogen peroxide-induced apoptosis." **354**(1): 109-114.

Liu, T., W. Ma, H. Xu, M. Huang, D. Zhang, Z. He, L. Zhang, S. Brem, D. M. O'Rourke and Y. Gong (2018). "PDGF-mediated mesenchymal transformation renders endothelial resistance to anti-VEGF treatment in glioblastoma." Nature communications **9**(1): 1-13.

Loges, S., T. Schmidt and P. Carmeliet (2010). "Mechanisms of resistance to anti-angiogenic therapy and development of third-generation anti-angiogenic drug candidates." Genes & cancer **1**(1): 12-25.

Lopes-Coelho, F., F. Martins, S. A. Pereira and J. Serpa (2021). "Anti-angiogenic therapy: current challenges and future perspectives." International Journal of Molecular Sciences **22**(7): 3765.

Loureiro, R. M. and P. A. D'Amore (2005). "Transcriptional regulation of vascular endothelial growth factor in cancer." Cytokine & growth factor reviews **16**(1): 77-89.

Machein, M. R., S. Renninger, E. De Lima‐Hahn and K. H. Plate (2003). "Minor contribution of bone marrow‐derived endothelial progenitors to the vascularization of murine gliomas." Brain pathology **13**(4): 582-597.

Maksimiuk, M., A. Sobiborowicz, A. Tuzimek, A. Deptała, A. Czerw and A. M. Badowska-Kozakiewicz (2020). "αB-crystallin as a promising target in pathological conditions–A review." Annals of Agricultural and Environmental Medicine **27**(3): 326-334.

Malin, D., E. Strekalova, V. Petrovic, A. M. Deal, A. Al Ahmad, B. Adamo, C. R. Miller, A. Ugolkov, C. Livasy, K. Fritchie, E. Hamilton, K. Blackwell, J. Geradts, M. Ewend, L. Carey, E. V. Shusta, C. K. Anders and V. L. Cryns (2014). "alphaB-crystallin: a novel regulator of breast cancer metastasis to the brain." Clin Cancer Res **20**(1): 56-67.

Mancuso, M. R., R. Davis, S. M. Norberg, S. O'Brien, B. Sennino, T. Nakahara, V. J. Yao, T. Inai, P. Brooks and B. Freimark (2006). "Rapid vascular regrowth in tumors after reversal of VEGF inhibition." The Journal of clinical investigation **116**(10): 2610-2621.

Mancuso, P., M. Colleoni, A. Calleri, L. Orlando, P. Maisonneuve, G. Pruneri, A. Agliano, A. Goldhirsch, Y. Shaked and R. S. Kerbel (2006). "Circulating endothelial-cell kinetics and viability predict survival in breast cancer patients receiving metronomic chemotherapy." Blood **108**(2): 452-459.

Maniotis, A. J., R. Folberg, A. Hess, E. A. Seftor, L. M. Gardner, J. Pe'er, J. M. Trent, P. S. Meltzer and M. J. Hendrix (1999). "Vascular channel formation by human melanoma cells in vivo and in vitro: vasculogenic mimicry." The American journal of pathology **155**(3): 739-752.

Mao, Y., J. Liu, H. Xiang and D. W. Li (2004). "Human α A-and α B-crystallins bind to Bax and Bcl-X S to sequester their translocation during staurosporine-induced apoptosis." Cell Death & Differentiation **11**(5): 512-526.

Mao, Y., D. W. Zhang, H. Lin, L. Xiong, Y. Liu, Q. D. Li, J. Ma, Q. Cao, R. J. Chen, J. Zhu and Z. Q. Feng (2012). "Alpha B-crystallin is a new prognostic marker for laryngeal squamous cell carcinoma." J Exp Clin Cancer Res **31**: 101.

Martin, M., S. Loibl, T. Hyslop, J. De la Haba-Rodriguez, B. Aktas, C. Cirrincione, K. Mehta, W. Barry, S. Morales and L. Carey (2019). "Evaluating the addition of bevacizumab to endocrine therapy as first-line treatment for hormone receptor–positive metastatic breast cancer: a pooled analysis from the LEA (GEICAM/2006-11_GBG51) and CALGB 40503 (Alliance) trials." European Journal of Cancer **117**: 91-98.

Matsumoto, T., S. Bohman, J. Dixelius, T. Berge, A. Dimberg, P. Magnusson, L. Wang, C. Wikner, J. H. Qi and C. Wernstedt (2005). "VEGF receptor‐2 Y951 signaling and a role for the adapter molecule TSAd in tumor angiogenesis." The EMBO journal **24**(13): 2342-2353.

Matsumoto, T. and L. Claesson-Welsh (2001). "VEGF receptor signal transduction." Sci. Stke **2001**(112): re21-re21.

Maxwell, P. H., C. W. Pugh and P. J. Ratcliffe (2001). "Activation of the HIF pathway in cancer." Current opinion in genetics & development **11**(3): 293-299.

Maxwell, P. H., M. S. Wiesener, G.-W. Chang, S. C. Clifford, E. C. Vaux, M. E. Cockman, C. C. Wykoff, C. W. Pugh, E. R. Maher and P. J. Ratcliffe (1999). "The tumour suppressor protein VHL targets hypoxia-inducible factors for oxygen-dependent proteolysis." Nature **399**(6733): 271-275.

McFarland, D. C. and K. J. Misiukiewicz (2014). "Sorafenib in radioactive iodine-refractory well-differentiated metastatic thyroid cancer." OncoTargets and therapy: 1291-1299.

Meehan, S., Y. Berry, B. Luisi, C. M. Dobson, J. A. Carver and C. E. MacPhee (2004). "Amyloid fibril formation by lens crystallin proteins and its implications for cataract formation." Journal of Biological Chemistry **279**(5): 3413-3419.

Mercatelli, N., I. Dimauro, S. A. Ciafré, M. G. Farace and D. Caporossi (2010). "αB-crystallin is involved in oxidative stress protection determined by VEGF in skeletal myoblasts." Free Radical Biology and Medicine **49**(3): 374-382.

Mercurio, A. M., E. A. Lipscomb and R. E. Bachelder (2005). "Non-angiogenic functions of VEGF in breast cancer." Journal of mammary gland biology and neoplasia **10**(4): 283-290.

Miles, D., D. Cameron, I. Bondarenko, L. Manzyuk, J. C. Alcedo, R. I. Lopez, S.-A. Im, J.-L. Canon, Y. Shparyk and D. A. Yardley (2017). "Bevacizumab plus paclitaxel versus placebo plus paclitaxel as first-line therapy for HER2-negative metastatic breast cancer (MERiDiAN): A double-blind placebo-controlled randomised phase III trial with prospective biomarker evaluation." European journal of cancer **70**: 146-155.

Miles, D., S. De Haas, L. Dirix, G. Romieu, A. Chan, X. Pivot, P. Tomczak, L. Provencher, J. Cortés and P. Delmar (2013). "Biomarker results from the AVADO phase 3 trial of first-line bevacizumab plus docetaxel for HER2-negative metastatic breast cancer." British journal of cancer **108**(5): 1052-1060.

Miles, D. W., A. Chan, L. Y. Dirix, J. Cortés, X. Pivot, P. Tomczak, T. Delozier, J. H. Sohn, L. Provencher and F. Puglisi (2010). "Phase III study of bevacizumab plus docetaxel compared with placebo plus docetaxel for the first-line treatment of human epidermal growth factor receptor 2–negative metastatic breast cancer." Journal of clinical oncology **28**(20): 3239-3247.

Miles, D. W., A. Chan, L. Y. Dirix, J. Cortes, X. Pivot, P. Tomczak, T. Delozier, J. H. Sohn, L. Provencher, F. Puglisi, N. Harbeck, G. G. Steger, A. Schneeweiss, A. M. Wardley, A. Chlistalla and G. Romieu (2010). "Phase III study of bevacizumab plus docetaxel compared with placebo plus docetaxel for the first-line treatment of human epidermal growth factor receptor 2-negative metastatic breast cancer." J Clin Oncol **28**(20): 3239-3247.

Miller, K., M. Wang, J. Gralow, M. Dickler, M. Cobleigh, E. A. Perez, T. Shenkier, D. Cella and N. E. J. N. E. J. o. M. Davidson (2007). "Paclitaxel plus bevacizumab versus paclitaxel alone for metastatic breast cancer." **357**(26): 2666-2676.

Miyata, T., H. Iizasa, Y. Sai, J. Fujii, T. Terasaki and E. Nakashima (2005). "Platelet‐derived growth factor‐BB (PDGF‐BB) induces differentiation of bone marrow endothelial progenitor cell‐derived cell line TR‐BME2 into mural cells, and changes the phenotype." Journal of cellular physiology **204**(3): 948-955.

Mizukami, Y., W.-S. Jo, E.-M. Duerr, M. Gala, J. Li, X. Zhang, M. A. Zimmer, O. Iliopoulos, L. R. Zukerberg and Y. Kohgo (2005). "Induction of interleukin-8 preserves the angiogenic response in HIF-1α–deficient colon cancer cells." Nature medicine **11**(9): 992-997.

Mohamed, S. Y., H. L. Mohammed, H. M. Ibrahim, E. M. Mohamed and M. Salah (2019). "Role of VEGF, CD105, and CD31 in the prognosis of colorectal cancer cases." Journal of gastrointestinal cancer **50**(1): 23-34.

Moreira, L. R., A. A. Schenka, P. Latuf-Filho, A. L. Penná, C. S. Lima, F. A. Soares, M. A. S. Trevisan and J. Vassallo (2011). "Immunohistochemical analysis of vascular density and area in colorectal carcinoma using different markers and comparison with clinicopathologic prognostic factors." Tumor Biology **32**(3): 527-534.

Morikawa, S., P. Baluk, T. Kaidoh, A. Haskell, R. K. Jain and D. M. McDonald (2002). "Abnormalities in pericytes on blood vessels and endothelial sprouts in tumors." Am J Pathol **160**(3): 985-1000.

Morrison, L. E., H. E. Hoover, D. J. Thuerauf and C. C. Glembotski (2003). "Mimicking phosphorylation of alphaB-crystallin on serine-59 is necessary and sufficient to provide maximal protection of cardiac myocytes from apoptosis." Circ Res **92**(2): 203-211.

Moyano, J. V., J. R. Evans, F. Chen, M. Lu, M. E. Werner, F. Yehiely, L. K. Diaz, D. Turbin, G. Karaca and E. Wiley (2006). "αB-crystallin is a novel oncoprotein that predicts poor clinical outcome in breast cancer." The Journal of clinical investigation **116**(1): 261-270.

Mullen, P. (2004). The use of Matrigel to facilitate the establishment of human cancer cell lines as xenografts. Cancer Cell Culture, Springer**:** 287-292.

Müller, A. M., M. I. Hermanns, C. Skrzynski, M. Nesslinger, K.-M. Müller and C. J. Kirkpatrick (2002). "Expression of the endothelial markers PECAM-1, vWf, and CD34 in vivo and in vitro." Experimental and molecular pathology **72**(3): 221-229.

Muranova, L., M. Sudnitsyna and N. Gusev (2018). "αB-Crystallin phosphorylation: Advances and problems." Biochemistry (Moscow) **83**(10): 1196-1206.

Nair, A., S. J. Lemery, J. Yang, A. Marathe, L. Zhao, H. Zhao, X. Jiang, K. He, G. Ladouceur and A. K. Mitra (2015). "FDA approval summary: Lenvatinib for progressive, radio-iodine–refractory differentiated thyroid cancer." Clinical Cancer Research **21**(23): 5205-5208.

O'connor, J. P., E. O. Aboagye, J. E. Adams, H. J. Aerts, S. F. Barrington, A. J. Beer, R. Boellaard, S. E. Bohndiek, M. Brady and G. Brown (2017). "Imaging biomarker roadmap for cancer studies." Nature reviews Clinical oncology **14**(3): 169-186.

Oguntade, A. S., F. Al-Amodi, A. Alrumayh, M. Alobaida and M. Bwalya (2021). "Anti-angiogenesis in cancer therapeutics: The magic bullet." Journal of the Egyptian National Cancer Institute **33**(1): 1-11.

Ordóñez, N. G. (2012). "Immunohistochemical endothelial markers: a review." Advances in anatomic pathology **19**(5): 281-295.

Orimo, A., P. B. Gupta, D. C. Sgroi, F. Arenzana-Seisdedos, T. Delaunay, R. Naeem, V. J. Carey, A. L. Richardson and R. A. Weinberg (2005). "Stromal fibroblasts present in invasive human breast carcinomas promote tumor growth and angiogenesis through elevated SDF-1/CXCL12 secretion." Cell **121**(3): 335-348.

Ottewell, P. D., H. Mönkkönen, M. Jones, D. V. Lefley, R. E. Coleman and I. Holen (2008). "Antitumor effects of doxorubicin followed by zoledronic acid in a mouse model of breast cancer." Journal of the National Cancer Institute **100**(16): 1167-1178.

Pàez-Ribes, M., E. Allen, J. Hudock, T. Takeda, H. Okuyama, F. Viñals, M. Inoue, G. Bergers, D. Hanahan and O. Casanovas (2009). "Antiangiogenic therapy elicits malignant progression of tumors to increased local invasion and distant metastasis." Cancer cell **15**(3): 220-231.

Pagès, G. and J. Pouysségur (2005). "Transcriptional regulation of the vascular endothelial growth factor gene–a concert of activating factors." Cardiovascular research **65**(3): 564-573.

Pearlman, R. L., M. K. M. de Oca, H. C. Pal and F. Afaq (2017). "Potential therapeutic targets of epithelial–mesenchymal transition in melanoma." Cancer letters **391**: 125-140.

Peng, Y. and C. M. Croce (2016). "The role of MicroRNAs in human cancer." Signal transduction and targeted therapy **1**(1): 1-9.

Perou, C. M., T. Sørlie, M. B. Eisen, M. Van De Rijn, S. S. Jeffrey, C. A. Rees, J. R. Pollack, D. T. Ross, H. Johnsen and L. A. Akslen (2000). "Molecular portraits of human breast tumours." nature **406**(6797): 747.

Personeni, N., L. Rimassa, T. Pressiani, V. Smiroldo and A. Santoro (2019). "Cabozantinib for the treatment of hepatocellular carcinoma." Expert review of anticancer therapy **19**(10): 847-855.

Petit, I., D. Jin and S. Rafii (2007). "The SDF-1–CXCR4 signaling pathway: a molecular hub modulating neo-angiogenesis." Trends in immunology **28**(7): 299-307.

Poon, R. T.-P., S.-T. Fan and J. Wong (2001). "Clinical implications of circulating angiogenic factors in cancer patients." Journal of Clinical Oncology **19**(4): 1207-1225.

Presta, L. G., H. Chen, S. J. O'connor, V. Chisholm, Y. G. Meng, L. Krummen, M. Winkler and N. Ferrara (1997). "Humanization of an anti-vascular endothelial growth factor monoclonal antibody for the therapy of solid tumors and other disorders." Cancer research **57**(20): 4593-4599.

Price, D. J., T. Miralem, S. Jiang, R. Steinberg and H. Avraham (2001). "Role of vascular endothelial growth factor in the stimulation of cellular invasion and signaling of breast cancer cells."

Pujade-Lauraine, E., F. Hilpert, B. Weber, A. Reuss, A. Poveda, G. Kristensen, R. Sorio, I. Vergote, P. Witteveen and A. Bamias (2014). "Bevacizumab combined with chemotherapy for

platinum-resistant recurrent ovarian cancer: the AURELIA open-label randomized phase III trial." Obstetrical & Gynecological Survey **69**(7): 402-404.

Qiao, T., J. Zhao, X. Xin, Y. Xiong, W. Guo, F. Meng, H. Li, Y. Feng, H. Xu and C. Shi (2022). "Combined pembrolizumab and bevacizumab therapy effectively inhibits non-small-cell lung cancer growth and prevents postoperative recurrence and metastasis in humanized mouse model." Cancer Immunology, Immunotherapy: 1-13.

Qin, H., Y. Ni, J. Tong, J. Zhao, X. Zhou, W. Cai, J. Liang and X. Yao (2014). "Elevated expression of CRYAB predicts unfavorable prognosis in non-small cell lung cancer." Med Oncol **31**(8): 142.

Rakha, E. A., J. S. Reis-Filho, F. Baehner, D. J. Dabbs, T. Decker, V. Eusebi, S. B. Fox, S. Ichihara, J. Jacquemier and S. R. Lakhani (2010). "Breast cancer prognostic classification in the molecular era: the role of histological grade." Breast cancer research **12**(4): 1-12.

Raymond, E., L. Dahan, J.-L. Raoul, Y.-J. Bang, I. Borbath, C. Lombard-Bohas, J. Valle, P. Metrakos, D. Smith and A. Vinik (2011). "Sunitinib malate for the treatment of pancreatic neuroendocrine tumors." New England Journal of Medicine **364**(6): 501-513.

Relf, M., S. LeJeune, P. A. Scott, S. Fox, K. Smith, R. Leek, A. Moghaddam, R. Whitehouse, R. Bicknell and A. L. Harris (1997). "Expression of the angiogenic factors vascular endothelial cell growth factor, acidic and basic fibroblast growth factor, tumor growth factor β-1, platelet-derived endothelial cell growth factor, placenta growth factor, and pleiotrophin in human primary breast cancer and its relation to angiogenesis." Cancer research **57**(5): 963-969.

Ribatti, D., T. Annese, S. Ruggieri, R. Tamma and E. Crivellato (2019). "Limitations of anti-angiogenic treatment of tumors." Translational Oncology **12**(7): 981-986.

Ribatti, D. and E. Crivellato (2012). ""“Sprouting angiogenesis”, a reappraisal." Developmental biology **372**(2): 157-165.

Ricci, V., M. Ronzoni and T. Fabozzi (2015). "Aflibercept a new target therapy in cancer treatment: a review." Critical Reviews in Oncology/Hematology **96**(3): 569-576.

Richard, D. E., E. Berra, E. Gothié, D. l. Roux and J. Pouysségur (1999). "p42/p44 mitogen-activated protein kinases phosphorylate hypoxia-inducible factor 1α (HIF-1α) and enhance the transcriptional activity of HIF-1." Journal of Biological Chemistry **274**(46): 32631-32637.

Richard, D. E., E. Berra and J. Pouysségur (1999). "Angiogenesis: how a tumor adapts to hypoxia." Biochemical and biophysical research communications **266**(3): 718-722.

Rini, B. I., T. Powles, M. B. Atkins, B. Escudier, D. F. McDermott, C. Suarez, S. Bracarda, W. M. Stadler, F. Donskov and J. L. Lee (2019). "Atezolizumab plus bevacizumab versus sunitinib in patients with previously untreated metastatic renal cell carcinoma (IMmotion151): a multicentre, open-label, phase 3, randomised controlled trial." The Lancet **393**(10189): 2404-2415.

Risau, W. (1997). "Mechanisms of angiogenesis." Nature **386**(6626): 671.

Risau, W. and I. Flamme (1995). "Vasculogenesis." Annual review of cell and developmental biology **11**(1): 73-91.

Robert, N. J., V. Dieras, J. Glaspy, A. M. Brufsky, I. Bondarenko, O. N. Lipatov, E. A. Perez, D. A. Yardley, S. Y. Chan, X. Zhou, S. C. Phan and J. O'Shaughnessy (2011). "RIBBON-1: randomized, double-blind, placebo-controlled, phase III trial of chemotherapy with or without bevacizumab for first-line treatment of human epidermal growth factor receptor 2-negative, locally recurrent or metastatic breast cancer." J Clin Oncol **29**(10): 1252-1260.

Rojas, J. D., V. Papadopoulou, T. J. Czernuszewicz, R. M. Rajamahendiran, A. Chytil, Y.-C. Chiang, D. C. Chong, V. L. Bautch, W. K. Rathmell and S. Aylward (2018). "Ultrasound measurement of vascular density to evaluate response to anti-angiogenic therapy in renal cell carcinoma." IEEE Transactions on Biomedical Engineering **66**(3): 873-880.

Ruan, H., Y. Li, X. Wang, B. Sun, W. Fang, S. Jiang and C. Liang (2020). "CRYAB inhibits migration and invasion of bladder cancer cells through the PI3K/AKT and ERK pathways." Japanese Journal of Clinical Oncology **50**(3): 254-260.

Ruan, K., G. Song and G. Ouyang (2009). "Role of hypoxia in the hallmarks of human cancer." Journal of cellular biochemistry **107**(6): 1053-1062.

Ruan, Q., S. Han, W. G. Jiang, M. E. Boulton, Z. J. Chen, B. K. Law and J. Cai (2011). "alphaB-crystallin, an effector of unfolded protein response, confers anti-VEGF resistance to breast cancer via maintenance of intracrine VEGF in endothelial cells." Mol Cancer Res **9**(12): 1632-1643.

Ruan, Q., S. Han, W. G. Jiang, M. E. Boulton, Z. J. Chen, B. K. Law and J. Cai (2022). "Retraction: αB-Crystallin, an Effector of Unfolded Protein Response, Confers Anti-VEGF Resistance to Breast Cancer via Maintenance of Intracrine VEGF in Endothelial Cells." Molecular cancer research: MCR **20**(7): 1179.

Ruohola, J. K., E. M. Valve, M. J. Karkkainen, V. Joukov, K. Alitalo and P. L. Härkönen (1999). "Vascular endothelial growth factors are differentially regulated by steroid hormones and antiestrogens in breast cancer cells." Molecular and cellular endocrinology **149**(1-2): 29-40.

Saharinen, P., L. Eklund, K. Pulkki, P. Bono and K. Alitalo (2011). "VEGF and angiopoietin signaling in tumor angiogenesis and metastasis." Trends in molecular medicine **17**(7): 347-362.

Sapino, A., M. Bongiovanni, P. Cassoni, L. Righi, R. Arisio, S. Deaglio and F. Malavasi (2001). "Expression of CD31 by cells of extensive ductal in situ and invasive carcinomas of the breast." The Journal of Pathology: A Journal of the Pathological Society of Great Britain and Ireland **194**(2): 254-261.

Semenza, G. L. (2003). "Targeting HIF-1 for cancer therapy." Nature reviews cancer **3**(10): 721-732.

Shaked, Y., A. Ciarrocchi, M. Franco, C. R. Lee, S. Man, A. M. Cheung, D. J. Hicklin, D. Chaplin, F. S. Foster, R. Benezra and R. S. Kerbel (2006). "Therapy-induced acute recruitment of circulating endothelial progenitor cells to tumors." Science **313**(5794): 1785-1787.

Shalaby, F., J. Rossant, T. P. Yamaguchi, M. Gertsenstein, X.-F. Wu, M. L. Breitman and A. C. J. N. Schuh (1995). "Failure of blood-island formation and vasculogenesis in Flk-1-deficient mice." **376**(6535): 62.

Sharma, G. N., R. Dave, J. Sanadya, P. Sharma and K. Sharma (2010). "Various types and management of breast cancer: an overview." Journal of advanced pharmaceutical technology & research **1**(2): 109.

Shen, Y., S. Li, X. Wang, M. Wang, Q. Tian, J. Yang, J. Wang, B. Wang, P. Liu and J. Yang (2019). "Tumor vasculature remolding by thalidomide increases delivery and efficacy of cisplatin." Journal of Experimental & Clinical Cancer Research **38**(1): 1-16.

Shibuya, M. (2011). "Vascular endothelial growth factor (VEGF) and its receptor (VEGFR) signaling in angiogenesis: a crucial target for anti-and pro-angiogenic therapies." Genes & cancer **2**(12): 1097-1105.

Shibuya, M. and L. Claesson-Welsh (2006). "Signal transduction by VEGF receptors in regulation of angiogenesis and lymphangiogenesis." Experimental cell research **312**(5): 549-560.

Shigeta, K., M. Datta, T. Hato, S. Kitahara, I. X. Chen, A. Matsui, H. Kikuchi, E. Mamessier, S. Aoki and R. R. Ramjiawan (2020). "Dual programmed death receptor ‐ 1 and vascular endothelial growth factor receptor ‐ 2 blockade promotes vascular normalization and enhances antitumor immune responses in hepatocellular carcinoma." Hepatology **71**(4): 1247-1261.

Shih, T. and C. Lindley (2006). "Bevacizumab: an angiogenesis inhibitor for the treatment of solid malignancies." Clinical therapeutics **28**(11): 1779-1802.

Shin, J. H., S. W. Kim, C. M. Lim, J. Y. Jeong, C. S. Piao and J. K. Lee (2009). "alphaB-crystallin suppresses oxidative stress-induced astrocyte apoptosis by inhibiting caspase-3 activation." Neurosci Res **64**(4): 355-361.

Shojaei, F. and N. Ferrara (2008). "Role of the microenvironment in tumor growth and in refractoriness/resistance to anti-angiogenic therapies." Drug Resistance Updates **11**(6): 219-230.

Shojaei, F., B. H. Simmons, J. H. Lee, P. B. Lappin and J. G. Christensen (2012). "HGF/c-Met pathway is one of the mediators of sunitinib-induced tumor cell type-dependent metastasis." Cancer Lett **320**(1): 48-55.

Shojaei, F., X. Wu, A. K. Malik, C. Zhong, M. E. Baldwin, S. Schanz, G. Fuh, H.-P. Gerber and N. Ferrara (2007). "Tumor refractoriness to anti-VEGF treatment is mediated by CD11b+ Gr1+ myeloid cells." Nature biotechnology **25**(8): 911-920.

Sinha, B. K., A. G. Katki, G. Batist, K. H. Cowan and C. E. Myers (1987). "Adriamycin-stimulated hydroxyl radical formation in human breast tumor cells." Biochemical pharmacology **36**(6): 793-796.

Sitterding, S. M., W. R. Wiseman, C. L. Schiller, C. Luan, F. Chen, J. V. Moyano, W. G. Watkin, E. L. Wiley, V. L. Cryns and L. K. Diaz (2008). "αB-crystallin: a novel marker of invasive basal-like and metaplastic breast carcinomas." Annals of diagnostic pathology **12**(1): 33-40.

Skladanowski, A. and J. Konopa (1993). "Adriamycin and daunomycin induce programmed cell death (apoptosis) in tumour cells." Biochemical pharmacology **46**(3): 375-382.

Sledge, G. W. (2015). Anti–vascular endothelial growth factor therapy in breast cancer: game over?, Citeseer. **33:** 133-135.

Socinski, M. A., R. M. Jotte, F. Cappuzzo, F. Orlandi, D. Stroyakovskiy, N. Nogami, D. Rodríguez-Abreu, D. Moro-Sibilot, C. A. Thomas and F. Barlesi (2018). "Atezolizumab for first-line treatment of metastatic nonsquamous NSCLC." New England Journal of Medicine **378**(24): 2288-2301.

Soga, N., J. O. Connolly, M. Chellaiah, J. Kawamura and K. A. Hruska (2001). "Rac regulates vascular endothelial growth factor stimulated motility." Cell communication & adhesion **8**(1): 1-13.

Soheilifar, M. H., N. Masoudi-Khoram, S. Madadi, S. Nobari, H. Maadi, H. K. Neghab, R. Amini and M. Pishnamazi (2022). "Angioregulatory microRNAs in breast cancer: molecular mechanistic basis and implications for therapeutic strategies." Journal of Advanced Research **37**: 235-253.

Sørlie, T. (2004). "Molecular portraits of breast cancer: tumour subtypes as distinct disease entities." European journal of cancer **40**(18): 2667-2675.

Stessels, F., G. Van den Eynden, I. Van der Auwera, R. Salgado, E. Van den Heuvel, A. Harris, D. Jackson, C. Colpaert, E. Van Marck and L. Dirix (2004). "Breast adenocarcinoma liver metastases, in contrast to colorectal cancer liver metastases, display a non-angiogenic growth pattern that preserves the stroma and lacks hypoxia." British journal of cancer **90**(7): 1429-1436.

Styp‐Rekowska, B., R. Hlushchuk, A. Pries and V. Djonov (2011). "Intussusceptive angiogenesis: pillars against the blood flow." Acta physiologica **202**(3): 213-223.

Tamburrino, A., G. Piro, C. Carbone, G. Tortora and D. Melisi (2013). "Mechanisms of resistance to chemotherapeutic and anti-angiogenic drugs as novel targets for pancreatic cancer therapy." Frontiers in pharmacology **4**: 56.

Tanaka, H., M. Yamamoto, N. Hashimoto, M. Miyakoshi, S. Tamakawa, M. Yoshie, Y. Tokusashi, K. Yokoyama, Y. Yaginuma and K. Ogawa (2006). "Hypoxia-independent overexpression of hypoxia-inducible factor 1α as an early change in mouse hepatocarcinogenesis." Cancer research **66**(23): 11263-11270.

Tang, Q., Y.-F. Liu, X.-J. Zhu, Y.-H. Li, J. Zhu, J.-P. Zhang, Z.-Q. Feng and X.-H. Guan (2009). "Expression and prognostic significance of the αB-crystallin gene in human hepatocellular carcinoma." Human pathology **40**(3): 300-305.

Tanigawa, N., C. Lu, T. Mitsui and S. Miura (1997). "Quantitation of sinusoid‐like vessels in hepatocellular carcinoma: its clinical and prognostic significance." Hepatology **26**(5): 1216-1223.

Teicher, B. A. (1996). "A systems approach to cancer therapy." Cancer and Metastasis Reviews **15**(2): 247-272.

Teleanu, R. I., C. Chircov, A. M. Grumezescu and D. M. Teleanu (2019). "Tumor angiogenesis and anti-angiogenic strategies for cancer treatment." Journal of clinical medicine **9**(1): 84.

Tewari, K. S., M. W. Sill, H. J. Long III, R. T. Penson, H. Huang, L. M. Ramondetta, L. M. Landrum, A. Oaknin, T. J. Reid and M. M. Leitao (2014). "Improved survival with bevacizumab in advanced cervical cancer." New England Journal of Medicine **370**(8): 734-743.

Tewey, K., T. Rowe, L. Yang, B. Halligan and L.-F. Liu (1984). "Adriamycin-induced DNA damage mediated by mammalian DNA topoisomerase II." Science **226**(4673): 466-468.

Thornell, E. and A. Aquilina (2015). "Regulation of αA-and αB-crystallins via phosphorylation in cellular homeostasis." Cellular and Molecular Life Sciences **72**(21): 4127-4137.

Thurston, G. and J. Kitajewski (2008). "VEGF and Delta-Notch: interacting signalling pathways in tumour angiogenesis." British Journal of Cancer **99**(8): 1204-1209.

Tozer, G. M., S. Akerman, N. A. Cross, P. R. Barber, M. A. Bjorndahl, O. Greco, S. Harris, S. A. Hill, D. J. Honess, C. R. Ireson, K. L. Pettyjohn, V. E. Prise, C. C. Reyes-Aldasoro, C. Ruhrberg, D. T. Shima and C. Kanthou (2008). "Blood vessel maturation and response to vascular-disrupting therapy in single vascular endothelial growth factor-A isoform-producing tumors." Cancer Res **68**(7): 2301-2311.

Travis, W. D., E. Brambilla, M. Noguchi, A. G. Nicholson, K. R. Geisinger, Y. Yatabe, D. G. Beer, C. A. Powell, G. J. Riely and P. E. Van Schil (2011). "International association for the study of lung cancer/american thoracic society/european respiratory society international multidisciplinary classification of lung adenocarcinoma." Journal of thoracic oncology **6**(2): 244-285.

Tsang, J. Y., M. W. Lai, K. H. Wong, S. K. Chan, C. C. Lam, A. K. Tsang, A. M. Yu, P. H. Tan and G. M. Tse (2012). "alphaB-crystallin is a useful marker for triple negative and basal breast cancers." Histopathology **61**(3): 378-386.

Tyler, T. (2012). "Axitinib: newly approved for renal cell Carcinoma." Journal of the advanced practitioner in oncology **3**(5): 333.

UK, C. R. (2018). "Breast cancer statistics." CANCERRESEARCH UK.

van de Schootbrugge, C., J. Bussink, P. N. Span, F. C. Sweep, R. Grénman, H. Stegeman, G. J. Pruijn, J. H. Kaanders and W. C. Boelens (2013). "αB-crystallin stimulates VEGF secretion and tumor cell migration and correlates with enhanced distant metastasis in head and neck squamous cell carcinoma." BMC cancer **13**(1): 1-8.

van de Schootbrugge, C., F. van Asten, I. D. Nagtegaal, Y. M. Versleijen-Jonkers, H. W. van Laarhoven, M. H. Roeffen, F. C. Sweep, J. Bussink, J. H. Kaanders and G. J. Pruijn (2013). "αB-crystallin expression is correlated with phospho-ERK1/2 expression in human breast cancer." The International journal of biological markers **28**(4): 365-370.

Van Der Graaf, W. T., J.-Y. Blay, S. P. Chawla, D.-W. Kim, B. Bui-Nguyen, P. G. Casali, P. Schöffski, M. Aglietta, A. P. Staddon and Y. Beppu (2012). "Pazopanib for metastatic soft-tissue sarcoma (PALETTE): a randomised, double-blind, placebo-controlled phase 3 trial." The Lancet **379**(9829): 1879-1886.

Van Engeland, M., L. J. Nieland, F. C. Ramaekers, B. Schutte and C. P. Reutelingsperger (1998).

"Annexin V ‐ affinity assay: a review on an apoptosis detection system based on phosphatidylserine exposure." Cytometry: The Journal of the International Society for Analytical Cytology **31**(1): 1-9.

Vempati, P., A. S. Popel and F. Mac Gabhann (2014). "Extracellular regulation of VEGF: isoforms, proteolysis, and vascular patterning." Cytokine & growth factor reviews **25**(1): 1-19.

Verheul, H., E. Voest and R. Schlingemann (2004). "Are tumours angiogenesis ‐ dependent?" The Journal of Pathology: A Journal of the Pathological Society of Great Britain and Ireland **202**(1): 5-13.

Vieira, S. C., B. B. Silva, G. A. Pinto, J. Vassallo, N. G. Moraes, J. O. Santana, L. G. Santos, G. A. Carvasan and L. C. Zeferino (2005). "CD34 as a marker for evaluating angiogenesis in cervical cancer." Pathology-Research and practice **201**(4): 313-318.

Vizio, B., F. Biasi, T. Scirelli, A. Novarino, A. Prati, L. Ciuffreda, G. Montrucchio, G. Poli and G. Bellone (2013). "Pancreatic-carcinoma-cell-derived pro-angiogenic factors can induce endothelial-cell differentiation of a subset of circulating CD34+ progenitors." Journal of Translational Medicine **11**(1): 1-15.

Voduc, K. D., T. O. Nielsen, C. M. Perou, J. C. Harrell, C. Fan, H. Kennecke, A. J. Minn, V. L. Cryns and M. C. Cheang (2015). "αB-crystallin expression in breast cancer is associated with brain metastasis." NPJ Breast Cancer **1**(1): 1-7.

Vuong, D., P. T. Simpson, B. Green, M. C. Cummings and S. R. Lakhani (2014). "Molecular classification of breast cancer." Virchows Archiv **465**(1): 1-14.

Walker, C. A., A. N. Spirtos and D. S. Miller (2023). "Pembrolizumab plus lenvatinib combination therapy for advanced endometrial carcinoma." Expert Review of Anticancer Therapy **23**(4): 361-368.

Wallin, J. J., J. C. Bendell, R. Funke, M. Sznol, K. Korski, S. Jones, G. Hernandez, J. Mier, X. He and F. S. Hodi (2016). "Atezolizumab in combination with bevacizumab enhances antigen-specific T-cell migration in metastatic renal cell carcinoma." Nature communications **7**(1): 1-8.

Wang, D., C. R. Stockard, L. Harkins, P. Lott, C. Salih, K. Yuan, D. Buchsbaum, A. Hashim, M. Zayzafoon and R. Hardy (2008). "Immunohistochemistry in the evaluation of neovascularization in tumor xenografts." Biotechnic & histochemistry **83**(3-4): 179-189.

Wang, S.-N., S. Luo, C. Liu, Z. Piao, W. Gou, Y. Wang, W. Guan, Q. Li, H. Zou and Z.-Z. Yang (2017). "miR-491 inhibits osteosarcoma lung metastasis and chemoresistance by targeting αB-crystallin." Molecular therapy **25**(9): 2140-2149.

Ward, J. E. and W. M. Stadler (2010). "Pazopanib in renal cell carcinoma." Clinical Cancer Research **16**(24): 5923-5927.

Watanabe, G., S. Kato, H. Nakata, T. Ishida, N. Ohuchi and C. Ishioka (2009). "α B‐crystallin: A novel p53‐target gene required for p53‐dependent apoptosis." Cancer science **100**(12): 2368-2375.

Weathers, S.-P. and J. De Groot (2014). "Resistance to antiangiogenic therapy." Current neurology and neuroscience reports **14**(5): 1-8.

Weigelt, B. and J. S. Reis-Filho (2009). "Histological and molecular types of breast cancer: is there a unifying taxonomy?" Nature reviews Clinical oncology **6**(12): 718-730.

Weitzman, S. P. and M. E. Cabanillas (2015). "The treatment landscape in thyroid cancer: a focus on cabozantinib." Cancer management and research: 265-278.

West, C. and F. Slevin (2019). "Tumour hypoxia." Clinical Oncology **31**(9): 595-599.

Wettstein, G., P. S. Bellaye, O. Micheau and P. Bonniaud (2012). "Small heat shock proteins and the cytoskeleton: an essential interplay for cell integrity?" Int J Biochem Cell Biol **44**(10): 1680-1686.

Wilhelm, S., C. Carter, M. Lynch, T. Lowinger, J. Dumas, R. A. Smith, B. Schwartz, R. Simantov and S. Kelley (2006). "Discovery and development of sorafenib: a multikinase inhibitor for treating cancer." Nature reviews Drug discovery **5**(10): 835-844.

Williamson, S. C., R. L. Metcalf, F. Trapani, S. Mohan, J. Antonello, B. Abbott, H. S. Leong, C. P. Chester, N. Simms and R. Polanski (2016). "Vasculogenic mimicry in small cell lung cancer." Nature communications **7**(1): 1-14.

Winkler, F., S. V. Kozin, R. T. Tong, S.-S. Chae, M. F. Booth, I. Garkavtsev, L. Xu, D. J. Hicklin, D. Fukumura and E. di Tomaso (2004). "Kinetics of vascular normalization by VEGFR2 blockade governs brain tumor response to radiation: role of oxygenation, angiopoietin-1, and matrix metalloproteinases." Cancer cell **6**(6): 553-563.

Winkler, F., S. V. Kozin, R. T. Tong, S. S. Chae, M. F. Booth, I. Garkavtsev, L. Xu, D. J. Hicklin, D. Fukumura, E. di Tomaso, L. L. Munn and R. K. Jain (2004). "Kinetics of vascular normalization by VEGFR2 blockade governs brain tumor response to radiation: role of oxygenation, angiopoietin-1, and matrix metalloproteinases." Cancer Cell **6**(6): 553-563.

Yang, L., K. Higashisaka, M. Shimoda, Y. Haga, N. Sekine, H. Tsujino, K. Nagano, K. Shimazu and Y. Tsutsumi (2022). "Alpha-crystallin B chains in trastuzumab-resistant breast cancer cells promote endothelial cell tube formation through activating mTOR." Biochemical and Biophysical Research Communications **588**: 175-181.

Yersal, O. and S. Barutca (2014). "Biological subtypes of breast cancer: Prognostic and therapeutic implications." World journal of clinical oncology **5**(3): 412.

Yilmaz, M., O. F. Karatas, B. Yuceturk, H. Dag, M. Yener and M. Ozen (2015). "Alpha-B-crystallin expression in human laryngeal squamous cell carcinoma tissues." Head Neck **37**(9): 1344-1348.

Yilmazer, D., Ü. Han and B. Önal (2007). "A comparison of the vascular density of VEGF expression with microvascular density determined with CD34 and CD31 staining and conventional prognostic markers in renal cell carcinoma." International urology and nephrology **39**: 691-698.

Yin, L., J.-J. Duan, X.-W. Bian and S.-c. Yu (2020). "Triple-negative breast cancer molecular subtyping and treatment progress." Breast Cancer Research **22**(1): 1-13.

Yoshida, S., M. Ono, T. Shono, H. Izumi, T. Ishibashi, H. Suzuki and M. Kuwano (1997). "Involvement of interleukin-8, vascular endothelial growth factor, and basic fibroblast growth factor in tumor necrosis factor alpha-dependent angiogenesis." Molecular and cellular biology **17**(7): 4015-4023.

Yu, A. L., R. Fuchshofer, M. Birke, S. G. Priglinger, K. H. Eibl, A. Kampik, H. Bloemendal and U. Welge-Lussen (2007). "Hypoxia/reoxygenation and TGF-beta increase alphaB-crystallin expression in human optic nerve head astrocytes." Exp Eye Res **84**(4): 694-706.

Zarrin, B., F. Zarifi, G. Vaseghi and S. H. Javanmard (2017). "Acquired tumor resistance to antiangiogenic therapy: Mechanisms at a glance." Journal of research in medical sciences: the official journal of Isfahan University of Medical Sciences **22**.

Zhang, Y., C. D. Kontos, B. H. Annex and A. S. Popel (2019). "Angiopoietin-Tie signaling pathway in endothelial cells: a computational model." IScience **20**: 497-511.

Zhao, Y. and A. A. Adjei (2015). "Targeting angiogenesis in cancer therapy: moving beyond vascular endothelial growth factor." The oncologist **20**(6): 660-673.

Zhou, C., A. Clamp, A. Backen, C. Berzuini, A. Renehan, R. E. Banks, R. Kaplan, S. J. Scherer, G. B. Kristensen and E. Pujade-Lauraine (2016). "Systematic analysis of circulating soluble angiogenesis-associated proteins in ICON7 identifies Tie2 as a biomarker of vascular progression on bevacizumab." British journal of cancer **115**(2): 228-235.

Zhou, C., J. O'Connor, A. Backen, J. Valle, J. Bridgewater, C. Dive and G. Jayson (2022). "Plasma Tie2 trajectories identify vascular response criteria for VEGF inhibitors across advanced biliary tract, colorectal and ovarian cancers." ESMO open **7**(2): 100417.

Ziello, J. E., I. S. Jovin and Y. Huang (2007). "Hypoxia-Inducible Factor (HIF)-1 regulatory pathway and its potential for therapeutic intervention in malignancy and ischemia." The Yale journal of biology and medicine **80**(2): 51.

Appendix

List of reagents and suppliers detailed in the materials and methods

0.2 µm nitrocellulose membrane	Bio-Rad
10% Mini-PROTEAN® TGX™ Precast Gel	Bio-Rad, #4561033EDU
10% Mini-PROTEAN® TGX™ Precast Protein Gels	Bio-Rad, 4561033
10% precast polyacrylamide gels	Bio-Rad, 4561033
1X NuPAGE LDS sample buffer	ThermoFisher Scientific
3,3-Diaminobenzidine substrate (Rakha *et al.*)	Vector Laboratories
Alpha B Crystallin (*CRYAB*) Human siRNA Oligo Duplex (Locus ID 1410)	Origene, SR300995
Ammonium persulfate (APS)	Sigma, A3678
Annexin binding buffer	Biolegend,422201
Avastin (25 mg/ml)	Roche
BCA protein assay kit	Thermofisher,23250
Clarity™ Western ECL Substrate	Bio-Rad,#1705060
Dimethyl Sulphoxide (DMSO)	Sigma-Aldrich, D5879
Dithiothreitol (DTT)	ThermoFisher Scientific, R0861
Dithiothreitol (DTT)	ThermoFisher Scientific, R0861
Doxorubicin (2mg/ml)	Pfizer
Dulbecco's phosphate buffered saline (DPBS)	Lonza, BE17-512F
DuoSet ELISA Ancillary Reagent Kit 2	R&D systems, DY008
Eosin	Sigma, E4009
Ethanol	Fisher Scientific
Fetal Bovine Serum (FBS)	Invitrogen, 10270
FITC Annexin V	Biolegend,640906
Geneticin G418 sulphate	Gibco, 11811
Gill's haematoxylin	Sigma, GHS116
Human VEGF DuoSet ELISA	R&D systems, DY293B-05
Hydrogen peroxide (30%)	Sigma
Isopropanol	Sigma, 650447
L-Glutamine	Lonza, BE17-605E
Lipofectamine	Invitrogen
Lipofectamine RNAiMAX Transfection Reagent	ThermoFisher Scientific-13778075
Mammalian Cell Lysis Kit (RIPA buffer)	Sigma-Aldrich, MCL1
Marvel dried skimmed milk	
Methanol	Fisher Scientific
Mouse VEGF ELISA	R&D SYSTEMS, MMV00

Mouse VEGF Quantikine ELISA Kit	R&D systems, MMV00
NaCl 0.9% w/v (Saline solution)	
Opti-MEM™	ThermoFisher Scientific
Penicillin and streptomycin	Life Technologies, 15140
Pierce™ BCA Protein Assay Kit	Thermo Scientific, 23227
Precision Plus Protein Dual Color Standards	Bio-Rad, 1610374
protease inhibitor cocktail	Sigmaaldrich, 4693132001
Protogel 30%	National Diagnostics, EC-890
Reagent	Supplier
Resolving Buffer x4	National Diagnostics,EC-892
Stacking Gel Buffer x4	National Diagnostics, EC-893
Superfrost® Plus microscope	Fisher Scientific, 10149870
Target Retrieval Solution (10x)	DAKO,S1699
TEMED	Invitrogen, 15524-010
TOPRO3	Thermo Fisher
Transfer stacks/ filter paper	Bio-Rad
TransIT-Brca	Mirus
TransIT-X2® transfection reagent	Mirus, MIR6000
Tris-glycine electroblotting buffer	National Diagnostics, EC-880
Tris-glycine SDS PAGE buffer	National Diagnostics, EC-870
Trypan Blue	Life Technologies
Trypsin	Lonza,17161F
Tween20	Sigma-Aldrich, UK
Wax pen	Vector
Weigert's iron hematoxylin solution	Sigma, HT1079
Xylene	ThermoFisher Scientific

Equipment detailed in Materials and Methods

Equipment	**Supplier**
ChemiDoc™ MP System	Bio-Rad
Fisherbrand™ Bead Mill 4 Mini Homogenizer	Fisher scientific, 15525799
HIER pressure cooker Aptum	Aptum
LSR II Flow Cytometer	BD Biosciences
Nikon Eclipse TS100 phase contrast microscope	Nikon
Orbital shaker	Stuart, Staffordshire, UK
Pannoramic slide scanner	Sysmex
TC20 Automated Cell Counter	Bio-Rad
Trans-Blot® Turbo™ Blotting system	Bio-Rad

Consumables detailed in the Materials and Methods

Material	Supplier
25 cm2 /75 cm2 filter-cap flasks	ThermoFisher Scientific
5 mL round-bottomed polystyrene tubes	ThermoFisher Scientific
6, 12 & 96 well cell culture plates	ThermoFisher Scientific
Disposable pipets 10 ml	Thermo fisher scientific
Macrosette processing/embedding cassettes	Simport Scientific
Two-well silicone cell culture inserts	Ibidi, 81176
Universal tubes 25-50 ml	Sarstedt

CRYAB cDNA full sequence:

GAAACAAGACCATGACAAGTCACCGGTCAGCTCAGCCCTGCCTGTGTTTCTCTTTTCTTAGCTCAGTG
AGTACCGGAAGCTTCAGAAGACTGCATATATAAGGGGCCGGCTGGAGCTGCTGCTGAAGGAGTTG
ACCAGCCAACCGACTCTGCATTCATCTAGCCACAATGGACATCGCCATCCACCACCCCTGGATCCGGC
GCCCCTTCTTCCCCTTCCACTCCCCAAGCCGCCTCTTCGACCAGTTCTTCGGAGAGCACCTGTTGGAG
TCTGACCTCTTCTCAACAGCCACTTCCCTGAGCCCCTTCTACCTTCGGCCACCCTCCTTCCTGCGGGCA
CCCAGCTGGATTGACACCGGACTCTCAGAGATGCGTTTGGAGAAGGACAGATTCTCTGTGAATCTG
GACGTGAAGCACTTCTCTCCGGAGGAACTCAAAGTCAAGGTTCTGGGGGGACGTGATTGAGGTCCAC
GGCAAGCACGAAGAACGCCAGGACGAACATGGCTTCATCTCCAGGGAGTTCCACAGGAAGTACCG
GATCCCAGCCGATGTGGATCCTCTCACCATCACTTCATCCCTGTCATCTGATGGAGTCCTCACTGTGA
ATGGACCAAGGAAACAGGTGTCTGGCCCTGAGCGCACCATTCCCATCACCCGTGAAGAGAAGCCTG
CTGTCGCCGCAGCCCCTAAGAAGTAGATCCCCTTTCCTCATTGAGTTTTTTTTAAAACAAGGAAGTTT
CCCATCAGTGATTGAAAATCTGTGACTAGTGCTGAAGCTTATTAATGCTAAGGGCTGGCCCAGATTA
TTAAGCTAATAAAAATATCATTCAGCAACAAAAAAA AAAAAAAA

Alpha B Crystallin (CRYAB)g Human siRNA Oligo Duplex

Duplex Sequences:

siRNA 1 (SR300995A): rGrGrArArCrUrCrArArArGrUrUrArArGrGrUrGrUrUrGrGGA

siRNA 2 (SR300995B): rArCrCrArGrUrGrArArUrGrArArArGrUrCrUrUrGrUrGrACT

siRNA 3 (SR300995C): rUrGrArArGrArGrCrGrCrCrArGrGrArUrGrArArCrArUrGGT

Scramble control (SR30004): rCrGrUrUrArArUrCrGrCrGrUrArUrArArUrArCrGrCrGrUAT